From Workshop to Concert Hall: Acoustic Observations on a Grand Piano under Construction

Dissertation zur Erlangung des Grades des Doktors der Philosophie (Dr. phil) an der Fakultät für Geisteswissenschaften der Universität Hamburg im Promotionsfach Systematische Musikwissenschaft, vorgelegt von

Niko Plath

Hamburg, im September 2019

Datum der Disputation: 10. Dezember 2019
1. Gutachter: Prof. Dr. Rolf Bader
2. Gutachter: Prof. Dr. Albrecht Schneider

Abstract

In the scope of a research project, a series of measurements has been taken on two concert grand pianos, starting with the glue-laminated soundboard planks and ending with the completed piano playing in a concert hall. The work is divided in two parts, even though dealing with different questions in detail, the two conducted experiments are interrelated by the overarching questions: How does the piano achieve its sound? What are important influential factors in the building process, as well as in concert business?

For the first experiment, two concert grand pianos have been accompanied with acoustic measurements through their manufacture to investigate the influence of successive production steps on the development of the pianos' final sound. The utilization of a microphone array led to insights about the vibrational behavior of the soundboard with remarkable temporal and spatial resolution, and allowed novel observations in time domain, leading to the following results:

The application of ribs has a crucial impact on the propagation behavior of the initial bending waves. In direction normal to grain the propagation is not circular but rather a traveling plane wave front, as a result of superposition of reflections between the ribs. The ribs act as waveguides for higher frequencies with locally changed stiffness. The influence of the bridge is clearly observable in the initial bending wave pattern: Stiffening increases the wave velocity locally and the propagation seems to follow the bridge direction, even when curved.
It has been possible to estimate the flexural wave velocity ratio between longitudinal and radial direction on the soundboard: Application of ribs nearly compensates the anisotropy to a ratio of 0.9. Overcompensation is not observable. The attached bridge causes a local stiffening, mainly in grain direction, which leads to higher velocities along its direction and thereby a decrease of

v_{RR}/v_{LL}. Gluing the soundboard into the rim changes the system dramatically but, in total, leads back to nearly the general 'isotropic state' it had with only the ribs.
The energy loss could be described not only as a general signal decay, but could also be given exclusively for the initial propagation on the soundboard before any reflections or drain at the boundaries:
The energy loss per traveled distance is twice as large in radial, than in longitudinal direction for the blank soundboard. The greatest portion of the supplied energy is preserved in grain direction. After application of the ribs the majority of the supplied energy is preserved in radial direction between adjacent ribs. After attaching the bridge, the supplied energy seems to be able to distribute more uniformly due to the local stiffness increase by the bridge, acting as a waveguide in mainly longitudinal direction. The bass bridge and the connected lower treble bridge part form a loop in the upper half of the soundboard which confines significant parts of the vibrational energy (*bridge loop effect*).
The spatial distribution of vibrational energy on the soundboard per frequency has been approximated with exponential decays. The model is capable of distinguishing the typical frequency domains for a vibrating piano soundboard: It displays the transition from modal- to driving point dependent domain as a decrease of the standard deviation of exponent κ. Although localization effects can produce deviating vibrational patterns in high frequencies, the directional averaged behavior can be approximated with an exponential decay. For frequencies greater than 2 kHz to 3 kHz, κ has values between 1 and 2. With $\kappa = 1$, the soundboard behaves like a reflection free plate, higher values of κ can be explained with local waveguide effects by ribs and bridge.
The method should be applicable to other structures for the discrimination between modal- and driving point dependent domain.
The observable differences in wood material properties between the two examined soundboards are not reflected in the acoustic measurements. This leads to the assumption, that in this range of variation, the geometry plays a predominant role for the resulting behavior.

An alternative approach to classic modal analysis has been presented for the description of the vibro-acoustical behavior of piano soundboards. Even if the presented physical descriptions might not be relevant for the instrument builder in daily practice, visualizations of the time dependent spatial distribution of vibrational energy on the soundboard should be comprehensible and

hopefully help piano builders to understand the effect of individual production steps for the final behavior of the instrument.

In a second experiment, measurements have been performed on a concert grand piano before and after one year in concert business in order to identify influential factors for a presumed change in tonal quality.
Measurements have been performed on two occasions: First, on a completed instrument prepared for sale. Second, on the same piano after having been played for one year in a concert hall. Single notes have been recorded with dummy-head-microphones in player position in an anechoic chamber. An extended ABX listening test engaging 100 players, tuners, and builders, addressed the questions whether a variation in tonal quality is audible and if so, what sound properties could lead to a perceived difference. Semantic subgrouping allowed for indication on the vocabulary listeners of varying expertise use to verbalize their sensation. The statements gave hints on what could have changed over the year and have been used as a basis for the analysis of corresponding physical properties and psychoacoustic parameters related to the described sensations.

The conducted listening test showed, that a difference in tonal quality is perceivable for a piano after one year in concert usage, even for non-experts.
The most stated properties used to distinguish between similar piano tones were *Timbre* related, followed by *Pitch* and *Temporal* attributes. *Spatial* and *Loudness* related sensations do not seem to have played an important role in discrimination, even when stimuli should have exceeded the just noticeable difference.
Semantic sub-grouping allowed for indication on the vocabulary listeners of varying expertise used to verbalize their sensation. Even experts in piano playing or building used descriptive and metaphoric vocabulary to a high degree in describing their sensations. The vocabularies of non-experts, players, and builders differed far less than presumed.
A disparity has been found between clear perceptibility of tonal differences on the one hand, and insufficient representability with well established psychoacoustic metrics on the other. Although even non-experts seem to perceive small differences in tonal quality of similar piano tones, individual well established psychoacoustic parameters do not seem to be capable of reflecting these differences.
With regard to a change in physical properties, no significant differences could

be observed between states.
Within the bounds, and given the described uncertainties of the study design, it can be stated with confidence that within the time frame of one year, the technician can be expected to have much more impact on the tonal development of the piano than the effects of wood aging or playing. The presented findings give the technician to the same extent the responsibility, but also the opportunity to turn a good concert instrument into an excellent one.

Zusammenfassung

Im Rahmen der vorliegenden Arbeit wurde eine Reihe von Messungen an zwei Konzertflügeln in verschiedenen Baustadien durchgeführt, angefangen bei den verleimten Resonanzbodendielen, bis hin zum fertigen Flügel im Konzertsaal. Die Arbeit gliedert sich in zwei Teile. Auch wenn es sich im Detail um unterschiedliche Forschungsfragen handelt, sind die beiden durchgeführten Studien durch die folgenden übergeordneten Fragen verknüpft: Wie erhält der Flügel seinen Klang? Was sind wichtige Einflussfaktoren für den Klang, sowohl im Bauprozess als auch im klassischen Konzertbetrieb?

Für das erste Experiment wurden zwei Konzertflügel während ihrer Herstellung mit akustischen Messungen begleitet, um den Einfluss aufeinanderfolgender Produktionsschritte auf die Entwicklung des Endklangs der Klaviere zu untersuchen. Die Verwendung eines Mikrofon-Arrays führte zu Erkenntnissen über das Schwingungsverhalten der Decke mit bemerkenswerter zeitlicher und räumlicher Auflösung und ermöglichte neue Beobachtungen im Zeitbereich, die zu den folgenden Ergebnissen führten:

Der Einsatz von Rippen hat einen entscheidenden Einfluss auf das Ausbreitungsverhalten der initialen Biegewellen. In radialer Richtung ist die Ausbreitung nicht kreisförmig, sondern eine sich bewegende ebene Wellenfront, bedingt durch die Überlagerung von Reflexionen zwischen den Rippen. Die Rippen wirken für höhere Frequenzen als Waveguide, bedingt durch lokal erhöhte Steifigkeit. Der Einfluss des Steges ist in der initialen Ausbreitung der Biegewellen deutlich zu erkennen: Die Versteifung erhöht die Wellengeschwindigkeit lokal und die Ausbreitung scheint der Stegrichtung zu folgen, auch wenn sie gekrümmt ist. Es ist gelungen, das Verhältnis der Biegewellengeschwindigkeiten auf der Decke zwischen Longitudinal- und Radialrichtung zu schätzen: Das Aufbringen von Rippen gleicht die Anisotropie zu einem Verhältnis von

0,9 nahezu aus. Eine Überkompensation ist nicht zu beobachten. Der angebrachte Steg bewirkt eine lokale Versteifung, hauptsächlich in Faserrichtung, was zu höheren Geschwindigkeiten entlang ihrer Richtung und damit zu einer Abnahme von v_{RR}/v_{LL} führt. Das Einkleben des Resonanzbodens in den Rahmen verändert das System dramatisch, führt aber insgesamt fast in den im Mittel isotropen Zustand zurück, den es vor Aufbringung des Steges hatte. Der Energieverlust konnte nicht nur als allgemeiner Signalabfall beschrieben werden, sondern auch ausschließlich für die initiale Ausbreitung auf dem Resonanzboden vor Reflexionen oder Abfluss an den Grenzen: Der Energieverlust pro zurückgelegter Wegstrecke ist radial doppelt so groß wie in longitudinaler Richtung für den Resonanzboden ohne Anbringungen. Der größte Teil der zugeführten Energie bleibt in Faserrichtung erhalten. Nach dem Aufbringen der Rippen bleibt der Großteil der zugeführten Energie in radialer Richtung zwischen benachbarten Rippen erhalten. Nach dem Anbringen des Steges scheint sich die zugeführte Energie aufgrund der lokalen Steifigkeitssteigerung durch den Steg, der als Waveguide in Longitudinalrichtung wirkt, gleichmäßiger verteilen zu können. Der Bass-Steg und der damit verbundene untere Hauptsteg bilden in der oberen Hälfte des Resonanzbodens eine Schleife, in der wesentliche Teile der eingekoppelten Schwingungsenergie festgehalten werden (*Bridge Loop Effect*). Die räumliche Verteilung der Schwingungsenergie auf dem Resonanzboden pro Frequenz wurde mit Exponentialfunktionen approximiert. Das Modell ist in der Lage, die typischen Frequenzbereiche für einen vibrierenden Klavierboden zu unterscheiden: Es zeigt den Übergang zwischen modal auflösbarer Domain und eingangsabhängiger Domain als Abnahme der Standardabweichung des Exponenten κ an. Obwohl Lokalisierungseffekte abweichende Schwingungsmuster in hohen Frequenzen erzeugen können, kann das richtungsgemittelte Verhalten mit einer exponentiellen Dämpfung approximiert werden. Für Frequenzen größer als 2 kHz bis 3 kHz hat κ Werte zwischen 1 und 2. Mit $\kappa = 1$ verhält sich der Resonanzboden wie eine reflexionsfreie Platte, höhere Werte von κ lassen sich mit lokalen Waveguide-Effekten durch Rippen und Steg erklären. Das Verfahren sollte auf andere Strukturen zur Unterscheidung zwischen modal- und eingangsabhängiger Domain anwendbar sein. Die beobachtbaren Unterschiede in den Holzwerkstoffeigenschaften zwischen den beiden untersuchten Resonanzdecken spiegeln sich in den akustischen Messungen nicht wider. Dies führt zu der Annahme, dass in diesem Variationsbereich die Geometrie eine vorherrschende Rolle für das resultierende Verhalten spielt.

Ein alternativer Ansatz zur klassischen Modalanalyse wurde für die Beschreibung des vibroakustischen Verhaltens von Klavierböden vorgestellt. Auch wenn die vorgestellten physikalischen Beschreibungen für Instrumentenbauer(innen) in der täglichen Praxis nicht relevant sind, sollten die präsentierten Visualisierungen der zeitabhängigen räumlichen Verteilung der Schwingungsenergie auf der Decke leicht zugänglich sein und Klavierbauer(innen) helfen, den Einfluss einzelner Produktionsschritte auf das Endverhalten des Instruments zu verstehen.

In einem zweiten Experiment wurden vor und nach einem Jahr im Konzertbetrieb Messungen an einem Konzertflügel durchgeführt, um Einflussfaktoren für eine von Konzerttechniker(innen) vermutete Veränderung der Klangqualität zu identifizieren.

Es wurden zu zwei Anlässen Messungen durchgeführt: Erstens, an einem verkaufsfertigen Instrument. Zweitens, auf dem gleichen Flügel, nachdem er ein Jahr lang in einem Konzertsaal gespielt wurde. Einzelne, gespielte Töne wurden mit Kunstkopf-Mikrofonen in Spielerposition in einem reflexionsarmen Raum aufgenommen. Ein erweiterter ABX-Hörtest, an dem 100 Spieler(innen), Techniker(innen) und Klavierbauer(innen) teilnahmen, befasste sich mit der Frage, ob eine Variation der Klangqualität hörbar ist und wenn ja, welche Klangeigenschaften zu einer wahrgenommenen Differenz führen konnten. Eine semantische Gruppierung ermöglichte Annahmen, welches Vokabular Hörer(innen) mit unterschiedlichen Fachkenntnissen zur Verbalisierung der Sinneseindrücke nutzen. Die Aussagen gaben Hinweise darauf, welche Einflussfaktoren relevant gewesen sein könnten und dienten als Grundlage für die Analyse der entsprechenden physikalischen Eigenschaften und psychoakustischen Parameter im Zusammenhang mit den beschriebenen Empfindungen.
Der durchgeführte Hörtest zeigte, dass für einen Konzertflügel nach einem Jahr im Konzertbetrieb ein Unterschied in der Klangqualität selbst für Laien erkennbar ist. Die am häufigsten genannten Eigenschaften zur Unterscheidung ähnlicher Klaviertöne waren der Klangfarbe zuzuordnen, gefolgt von zeitlichen sowie tonhöhenbezogenen Attributen. Auf Lautstärke und Räumlichkeit bezogene Empfindungen scheinen keine wichtige Rolle bei der Diskriminierung gespielt zu haben, auch wenn die Reize die differentielle Wahrnehmbarkeitsschwelle deutlich überschritten.
Selbst Expert(innen), die sich beruflich mit dem Klavierspiel oder dem Kla-

vierbau beschäftigen, nutzten in hohem Maße deskriptives und metaphorisches Vokabular, um ihre Hörempfindungen zu beschreiben. Die Vokabulare von Laien, Spieler(innen) und Klavierbauer(innen) unterschieden sich weitaus weniger als angenommen. Es wurde eine Diskrepanz deutlich zwischen der klaren Wahrnehmbarkeit von Klangunterschieden auf der einen Seite, und der unzureichenden Darstellbarkeit mit etablierten psychoakustischen Parametern auf der anderen Seite. Obwohl selbst Laien kleine Unterschiede in der Klangqualität ähnlicher Klaviertöne wahrnehmen, scheinen einzelne, etablierte psychoakustische Parameter nicht in der Lage zu sein, diese Unterschiede abzubilden. Im Hinblick auf eine Änderung der strukturellen Eigenschaften konnten keine signifikanten Unterschiede zwischen den gemessenen Zuständen beobachtet werden. Innerhalb der Grenzen und angesichts der beschriebenen Unsicherheiten des Studiendesigns kann festgestellt werden, dass Techniker(innen) innerhalb eines Jahres voraussichtlich wesentlich größeren Einfluss auf die klangliche Entwicklung des Flügels haben, als die Auswirkungen der Holzalterung oder des Spielens. Die vorgestellten Erkenntnisse geben Techniker(innen) in gleichem Maße die Verantwortung, aber auch die Möglichkeit, aus einem guten Konzertinstrument ein hervorragendes zu machen.

Acknowledgements

Throughout the writing of this dissertation I have received a great deal of support and assistance. Firstly, I would like to express my sincere gratitude to my advisor Prof. Dr. Rolf Bader for the continuous support of my Ph.D study and related research, for his patience, motivation, and immense knowledge. I would like to express my great appreciation to Prof. Dr. Albrecht Schneider for his valuable and constructive suggestions, especially with regard to the second part of this treatise. I would also like to thank Prof. Dr. Robert Mores for fruitful discussions about the vibrations of plates over the last year and for accepting attendance in the audit committee. I am particularly grateful for the assistance given by Florian and Christian, without whose support during measurements and analysis this work would not have been possible. My sincere thanks also go to Christian, Florian, and Simon for proofreading this work. Furthermore, I would like to thank Jost, Malte, Michael, Orie, Tim, Henning, Anna, and all the others at the institute for providing a great working atmosphere. I sincerely would like to thank the *Deutsche Forschungsgemeinschaft* for supporting me financially during the years 2014-2016.

A heartfelt thank you goes to my wife Mascha and to my parents Marlis & Klaus for all the patience and support.

Contents

1. Introduction 1
   - 1.1. Part 1 . . . 1
   - 1.2. Part 2 . . . 4
   - 1.3. Outline of Thesis Structure . . . 6

2. Main Components of a Piano 9
   - 2.0.1. The Action . . . 11
   - 2.0.2. The Hammer . . . 15
   - 2.0.3. The Strings . . . 20

I. Grand Piano Soundboard Characteristics in Different Stages of Production 29

3. Theory 31
   - 3.1. Soundboard Structure . . . 31
     - 3.1.1. General Overview . . . 31
     - 3.1.2. Ribs . . . 34
     - 3.1.3. Driving Point Mobility . . . 37
     - 3.1.4. Curvature and Internal Stresses . . . 39
     - 3.1.5. Radiation . . . 40
   - 3.2. Soundboard Material . . . 41
     - 3.2.1. Elastic Constants of Wood . . . 41
     - 3.2.2. Wood for Piano Soundboards . . . 45
     - 3.2.3. Influence of Wood Moisture Content . . . 48
     - 3.2.4. Influence of Varnishes . . . 49
     - 3.2.5. Damping in wood . . . 50
     - 3.2.6. Dispersion in wood . . . 53

4. Experimental Arrangement 55
4.1. Production Stages 55
4.2. Utilized Hardware 56
4.2.1. Excitation 56
4.2.2. Response 57
4.3. Climate Conditions 61
4.4. Data Structure 62

5. Methods 63
5.1. Exponential Sine Sweep Technique 63
5.2. Back-Propagation of Radiated Sound Pressure 66
5.2.1. Methodology 66
5.2.2. Single-Array Application 72
5.2.3. Multiple-Array Application 72

6. Results 77
6.1. Structural Properties 77
6.1.1. Number of Wood Stripes / Annual Ring Width 77
6.1.2. Mass and Density 78
6.1.3. Curvature 80
6.2. Harmonic Responses 81
6.3. Driving Point Mobility 86
6.4. Bending Wave Propagation on the Soundboard 91
6.5. Grain Angle dependent Bending Wave Velocity Ratio 96
6.6. Angle Dependent Dispersion 100
6.7. Damping 101
6.7.1. Damping as Reverberation Time T_{60} 102
6.7.2. Damping of Initial Wave Front Propagation 103
6.8. Exponential Model for Spatial Attenuation per Frequency . . . 109

7. Discussion Part 1 115
7.1. Critique of Method 115
7.2. Reflection on Results 117
7.2.1. Development of Structural Properties 117
7.2.2. Development of Vibrational Behavior 117

II. Influence of Playing on the Tonal Characteristics of a Concert Grand Piano - an Observational Study 119

8. Theory 121
8.1. Influential Factors . . . 122
8.1.1. Keys and Action . . . 122
8.1.2. Hammers . . . 123
8.1.3. Strings . . . 124
8.1.4. Soundboard . . . 124
8.2. Disturbances Determined by the Experimental Design . . . 126
8.2.1. Tuning the Instrument . . . 126
8.2.2. Measurement Errors . . . 127
8.3. Study Design Considerations . . . 127

9. Experimental Arrangement 131
9.1. Instrument . . . 131
9.2. Utilized Hardware . . . 132
9.2.1. Excitation . . . 132
9.2.2. Response . . . 133

10. Methods 135
10.1. Listening Test . . . 135
10.1.1. Aim . . . 135
10.1.2. Design . . . 136
10.1.3. Instructions . . . 137
10.1.4. Implementation . . . 138
10.1.5. Participants . . . 139
10.1.6. Statistical Analysis . . . 139

11. Listening Test Results 143
11.1. Participant Variables . . . 143
11.2. ABX Test . . . 144
11.3. Verbalizations . . . 147

12. Comparison with Psychoacoustic and Structural Metrics 155
12.1. Psychoacoustic Features . . . 155
12.1.1. Timbre Domain . . . 155

12.1.2. Pitch Domain 162
12.1.3. Temporal Domain 166
12.1.4. Spatial Domain 168
12.1.5. Loudness Domain 170
12.2. Structural Metrics 172
12.2.1. Driving Point Mobility / Soundboard Crowning 172
12.2.2. Action Timing 174
12.3. Dimensional Reduction by Principal Component Analysis . . 175

13. Discussion Part 2 181
13.1. Critique of Method 181
13.2. Reflection on Results 182

14. Conclusion and Outlook 187
14.1. Part 1 187
14.2. Part 2 189
14.3. Outlook 190

A. Appendix 193
A.1. Climate Conditions during Measurements 194
A.2. Crowning per Production Stage 198
A.3. Bending Wave Shapes 204
A.4. Bending Wave Velocity Ratios 220
A.5. Exponential Fitting for Attenuation per Frequency 231
A.6. Interview Transcriptions 236
A.6.1. Interview with the Technician after Tuning *D1 PROD7* 236
A.6.2. Interview with the Technician after Tuning *D1 PROD8* 238
A.7. Screenshots Listening Test 243
A.8. Listening Test Results per Key 246
A.9. Listening Test Results per Participant 247
A.10. Feature Set for Principal Component Analysis 252

List of Figures

1. Cartesian coordinate system definition xxxiv

2.1. Predecessor of the modern grand piano built by *Steinway & Sons*. 10
2.2. The action of a modern grand piano, from Günther[1] 12
2.3. Action timing diagram, from Askenfelt and Jansson,[2] p. 56 . . 12
2.4. Nonlinearity in the piano action, from Goebl, Bresin, and Galembo,[3] p. 1160 14
2.5. Spectra for a *C4* note produced with three different hammer conditions, from Askenfelt and Jansson,[4] p. 2191 16
2.6. Hammer force F_h vs. compression y_f of the hammer surface during contact, from Giordano and Jiang,[5] p. 928. 17
2.7. Relative hammer string contact duration for different keys in percent of $T_0/2$, from Askenfelt and Jansson,[6] p.47 19

[1] W. Günther (1959). *U.S. Patent No. 2,911,874: Means for adjusting the touch of keys in pianos and like musical instruments*.

[2] Anders Askenfelt and Erik V. Jansson (1990a). "From touch to string vibrations." In: *Five lectures on the Acoustics of the piano*. Ed. by Anders Askenfelt. Stockholm: Royal Swedish Academy of Music.

[3] Werner Goebl, Roberto Bresin, and Alexander Galembo (2005). "Touch and temporal behavior of grand piano actions." In: *The Journal of the Acoustical Society of America* 118.2, pp. 1154–1165. DOI: 10.1121/1.1944648.

[4] Anders Askenfelt and Erik V. Jansson (1993). "From touch to string vibrations. III: String motion and spectra." In: *The Journal of the Acoustical Society of America* 93.4, pp. 2181–2196. DOI: 10.1121/1.406680.

[5] Nicholas Giordano and M. Jiang (2004). "Physical Modeling of the Piano." In: *EURASIP Journal on Advances in Signal Processing* 2004.7, pp. 926–933. DOI: 10.1155/S111086570440105X.

[6] Anders Askenfelt and Erik V. Jansson (1990a). "From touch to string vibrations." In: *Five lectures on the Acoustics of the piano*. Ed. by Anders Askenfelt. Stockholm: Royal Swedish Academy of Music.

2.8. Root mean square of transversal deflection of two adjacent unison strings 22
2.9. Wrapped string, from Conklin,[7] p. 1290 23
2.10. Inharmonicity as a function of n^2, from Schuck and Young,[8] p. 5 25
2.11. Inharmonicity dependence of piano range, from Schuck and Young,[9] p. 6 26
2.12. Deviations from equal temperament in a small piano, from Martin and Ward,[10] p. 583 27

3.1. Model of a concert grand bridge 32
3.2. Mobility as a function of frequency, from Conklin,[11] p. 698 . . 33
3.3. Inter-rib-distances from bass to treble for a modern concert grand piano 35
3.4. Rib configuration for a modern concert grand piano vs. a suggestion by Conklin[12] 36
3.5. Tapering curve for piano ribs 37
3.6. Radial (R), tangential (T), and longitudinal (L) axis in a tree trunk, from Franke and Quenneville,[13] p. 188 45
3.7. Schematic of a dispersion curve for bending waves in an isotropic thin plate 54

4.1. Locations of driving point positions on the soundboard 58

[7] Harold A. Conklin (1996c). "Design and tone in the mechanoacoustic piano. Part III. Piano strings and scale design." In: *The Journal of the Acoustical Society of America* 100.3, pp. 1286–1298. DOI: 10.1121/1.416017.

[8] O. H. Schuck and R. W. Young (1943). "Observations on the Vibrations of Piano Strings." In: *The Journal of the Acoustical Society of America* 15.1, pp. 1–11. DOI: 10.1121/1.1916221.

[9] O. H. Schuck and R. W. Young (1943). "Observations on the Vibrations of Piano Strings." In: *The Journal of the Acoustical Society of America* 15.1, pp. 1–11. DOI: 10.1121/1.1916221.

[10] D. W. Martin and W. D. Ward (1961). "Subjective Evaluation of Musical Scale Temperament in Pianos." In: *The Journal of the Acoustical Society of America* 33.5, pp. 582–585. DOI: 10.1121/1.1908730.

[11] Harold A. Conklin (1996b). "Design and tone in the mechanoacoustic piano. Part II. Piano structure." In: *The Journal of the Acoustical Society of America* 100.2, pp. 695–708. DOI: 10.1121/1.416233.

[12] Harold A. Conklin (1973). *U.S. Patent No. US3866506 A: Soundboard construction for stringed musical instruments*.

[13] Bettina Franke and Pierre Quenneville (Mar. 2011). "Numerical Modeling of the Failure Behavior of Dowel Connections in Wood." In: *Journal of Engineering Mechanics* 137.3, pp. 186–195. DOI: 10.1061/(ASCE)EM.1943-7889.0000217.

4.2. Self-built frame for measurements *PROD1-PROD4* 59
4.3. Self-built frame for measurements *PROD5-PROD6* 60
4.4. Illustration of coverage of the sound board surface 60
4.5. Measured maximum z distance per production stage 61

5.1. Spectrogram of an exemplary output of one of the array microphones 64
5.2. Obtained impulse response after deconvolution 64
5.3. Exemplary reconstruction energy for different α values 68
5.4. Maximum distance from microphone to surface per frequency to be considered as in *near-field* 69
5.5. Real part of pressure field at resonance frequencies, plucked $E2$ string on a guitar 73
5.6. Exemplary differences in force excitation between measurements for *ARRAY1* to *ARRAY18* 75

6.1. X-ray micro computed tomography (CT) of a glued piece of soundboard spruce 78
6.2. Cross section through the curvature profile at $y = 1.22$ m per production stage 81
6.3. Development of soundboard curvature over the production process for *D1* 82
6.4. Modulus of operating deflection shapes for the first three soundboard resonances 84
6.5. Operating deflection shapes of third resonance for *D1 PROD5 POS5-POS14* 85
6.6. Driving point dependency for operating deflection shapes at 2 kHz 86
6.7. Mobility maps for average mobility per production stage . . . 88
6.8. Frequencies of the first three soundboard resonances per production stage 88
6.9. Average mobility 50 Hz to 1000 Hz per production stage 89
6.10. Modulus of mobility for different stages of production before and after the modification is applied 90
6.11. Bending wave propagation for *PROD1 POS8* 92
6.12. Bending wave propagation for *PROD1 POS15* 92
6.13. Bending wave propagation for *PROD2 POS8* 94

6.14. Bending wave propagation for *PROD3 POS4* 94
6.15. Bending wave propagation for *PROD3 POS8* 95
6.16. Bending wave propagation for *PROD4 POS8* 95
6.17. Bending wave propagation for *PROD5 POS9* 96
6.18. Angle dependent wave velocity ratio for *D1 PROD1-PROD5*. . . 98
6.19. Moving average of angle dependent bending wave velocity ratio for *D1 PROD1-PROD5*. Diagonal grid lines depict grain angle (v_{LL}: bottom right to top left). 99
6.20. Modulus of impulse response before and after traveling through the soundboard. 99
6.21. Bending wave velocity ratio of v_{LL} over v_{RR}. 100
6.22. Average attack time of impulse responses per production stage for *D1*. 101
6.23. Spatial distribution of attack time for *D1 PROD3*. 102
6.24. Average impulse response decay as T_{60} per production stage. . 103
6.25. Average decay per input position before and after gluing the soundboard into the rim. 103
6.26. Energy loss on the soundboard for *PROD1 POS9*. 105
6.27. Energy loss on the soundboard for *PROD2 POS11*. 106
6.28. Energy loss on the soundboard for *PROD3 POS12*. 107
6.29. Energy loss on the soundboard for *PROD4 POS8*. 107
6.30. Energy loss on the soundboard for *D4 PROD5 POS2*. 108
6.31. Modeled spatial attenuation on the soundboard for exemplary cases a) $\kappa = 1$, and b) $\kappa = 3$. 110
6.32. Exponential fittings for magnitude per distance from the input position. 112
6.33. κ per frequency for *PROD3*. 112
6.34. Influence of production step on parameter κ. 113

8.1. Influential factors and disturbances for the experimental design 126

9.1. Experimental arrangement. 132
9.2. Time series of measured force for the key / key bed contact of an exemplary keystroke. 133
9.3. Number of matched recording pairs between *PROD7* and *PROD8* per defined maximum F_{key} difference. 133
9.4. Distribution of F_{key} values for *PROD8* of *D1*. 134

10.1. Binomial distribution for 25 trials of a Bernoulli experiment. . 140
10.2. Inverse cumulative binomial distribution for 25 trials of a Bernoulli experiment. 140

11.1. Listening test total number of completions per key. 143
11.2. Histograms for professional background of participants. 145
11.3. Average hit probability per F_{key} difference. 146
11.4. Hit probability per key at 0.6 N maximum F_{key} difference. . . 146
11.5. Histogram for probability per hit ratio. 147
11.6. Word cloud for the 100 most commonly used words 149
11.7. Percentile of words used from each defined perceptual domain per key. 150
11.8. Percentage of terms used per sub-group and category 153

12.1. Spectral centroid of radiated sound for *PROD7* and *PROD8* . . 157
12.2. SC difference between *PROD7* and *PROD8* vs. proportion of used timbre domain related words per key 157
12.3. Average fractal correlation dimension for the transient part of the piano tone per key 159
12.4. One cent f_1 difference in Hz per key. 160
12.5. Average f_1 detuning of unison strings for *PROD7* and *PROD8*. 160
12.6. Perceived roughness per frequency difference $|f_1 - f_2|$. 161
12.7. Perceived roughness per key for *PROD7* and *PROD8*. 162
12.8. f_1 deviation from equal tempered tuning for *PROD7* and *PROD8*. 164
12.9. f_1 differences between *PROD7* and *PROD8* in cent vs. usage percentile of pitch related verbalizations. 165
12.10. Attack time of radiated sound for *PROD7* and *PROD8*. 167
12.11. Damping of radiated sound at player position for *PROD7* and *PROD8* 169
12.12. Inter-aural level difference at player position for played keys in *PROD7* and *PROD8*. 171
12.13. Sound pressure level at player position for played keys in *PROD7* and *PROD8*. 173
12.14. Driving point mobility for *PROD7* and *PROD8* at *POS11*. . . . 174
12.15. Time delay (Δt) between key bed contact and vibrational activation at the bridge for *PROD7* and *PROD8* 175
12.16. Histograms of feature distributions for *PROD7* and *PROD8* . . 176

12.17. Exemplary projection of a two dimensional dataset (Feature 1 and 2) onto two orthogonal principal components (PC 1 and 2) 177
12.18. Scree plots of explained variance per principal components . . 178
12.19. Principal Component 1 179
12.20. Principal Component 2 179
12.21. Principal Component 3 180

A.1. Climate conditions during measurements of *D1 PROD1-PROD3*. 194
A.2. Climate conditions during measurements of *D1 PROD4-PROD5*. 195
A.3. Climate conditions during measurements of *D4 PROD1-PROD3*. 196
A.4. Climate conditions during measurements of *D4 PROD4-PROD5*. 197
A.5. Crowning *D1 PROD1*. 198
A.6. Crowning *D1 PROD2*. 198
A.7. Crowning *D1 PROD3*. 199
A.8. Crowning *D1 PROD4*. 199
A.9. Crowning *D1 PROD5*. 200
A.10. Crowning *D1 PROD6*. 200
A.11. Crowning *D4 PROD1*. 201
A.12. Crowning *D4 PROD2*. 201
A.13. Crowning *D4 PROD3*. 202
A.14. Crowning *D4 PROD4*. 202
A.15. Crowning *D4 PROD5*. 203
A.16. Crowning *D4 PROD6*. 203
A.17. Bending wave distribution for *D1*, *PROD1* vs. *PROD2*. 205
A.18. Bending wave distribution for *D1*, *PROD3* vs. *PROD4*. 206
A.19. Bending wave distribution for *D1*, *PROD5*, *POS04*. 207
A.20. Bending wave distribution for *D1*, *PROD1* vs. *PROD2*. 208
A.21. Bending wave distribution for *D1*, *PROD3* vs. *PROD4*. 209
A.22. Bending wave distribution for *D1*, *PROD5*, *POS08*. 210
A.23. Bending wave distribution for *D1*, *PROD1* vs. *PROD2*. 211
A.24. Bending wave distribution for *D1*, *PROD3* vs. *PROD4*. 212
A.25. Bending wave distribution for *D1*, *PROD5*, *POS09*. 213
A.26. Bending wave distribution for *D1*, *PROD1* vs. *PROD2*. 214
A.27. Bending wave distribution for *D1*, *PROD3* vs. *PROD4*. 215
A.28. Bending wave distribution for *D1*, *PROD5*, *POS12*. 216
A.29. Bending wave distribution for *D1*, *PROD1* vs. *PROD2*. 217
A.30. Bending wave distribution for *D1*, *PROD3* vs. *PROD4*. 218

A.31. Bending wave distribution for *D1*, *PROD5*, *POS14*. 219
A.32. Angle dependent bending wave velocity ratio for *D1 PROD1*. . 221
A.33. Angle dependent bending wave velocity ratio for *D1 PROD2*. . 222
A.34. Angle dependent bending wave velocity ratio for *D1 PROD3*. . 223
A.35. Angle dependent bending wave velocity ratio for *D1 PROD4*. . 224
A.36. Angle dependent bending wave velocity ratio for *D1 PROD5*. . 225
A.37. Angle dependent bending wave velocity ratio for *D4 PROD1*. . 226
A.38. Angle dependent bending wave velocity ratio for *D4 PROD2*. . 227
A.39. Angle dependent bending wave velocity ratio for *D4 PROD3*. . 228
A.40. Angle dependent bending wave velocity ratio for *D4 PROD4*. . 229
A.41. Angle dependent bending wave velocity ratio for *D4 PROD5*. . 230
A.42. Exponential fitting per frequency for *D1 PROD1*. Dashed lines depict the fitting error. 231
A.43. Exponential fitting per frequency for *D1 PROD2*. Dashed lines depict the fitting error. 232
A.44. Exponential fitting per frequency for *D1 PROD3*. Dashed lines depict the fitting error. 233
A.45. Exponential fitting per frequency for *D1 PROD4*. Dashed lines depict the fitting error. 234
A.46. Exponential fitting per frequency for *D1 PROD5*. Dashed lines depict the fitting error. 235
A.47. Front page for the listening test (English and German version). 243
A.48. Exemplary trial page (English and German version). 244
A.49. Conclusive survey page (English and German version). 245

List of Tables

1. Denotation of production stages xxxiii

3.1. Mechanical properties of Sitka spruce and European spruce . . 47

4.1. Denotation of production stages 55
4.2. Driving point positions 57

6.1. Annual ring width per piano 77
6.2. Soundboard mass per production stage in [kg]. 79

9.1. Denotation of production stages 131
9.2. Acceleration sensor position on the bridge per played key. . . . 134

11.1. Number of participants per country 144
11.2. Definition and hit ratio for sub-groups (disjoint sets) 145
11.3. The 15 most frequently used words and their frequency of occurrence 151
11.4. Classification of the 50 most frequent words into perceptual domains and levels of foreknowledge 152

12.1. Feature set for the principal component analysis 178

A.1. Individual results per key. 246
A.2. Individual results per key (continued from previous page). . . 247
A.3. Individual results per participant. 248
A.4. Individual results per participant (continued from previous page). 249
A.5. Individual results per participant (continued from previous page). 250
A.6. Individual results per participant (continued from previous page). 251

A.7. Feature set for principal component analysis. 253
A.8. Feature set for principal component analysis (continued from previous page). 254
A.9. Feature set for principal component analysis (continued from previous page). 255
A.10. Feature set for principal component analysis (continued from previous page). 256
A.11. Feature set for principal component analysis (continued from previous page). 257
A.12. Feature set for principal component analysis (continued from previous page). 258
A.13. Feature set for principal component analysis (continued from previous page). 259

Nomenclature

κ Exponential decay constant, page 109

λ Wavelength [m], page 44

ω Angular frequency [rad s^{-1}], page 44

e Euler's number, page 44

h Plate thickness [m], page 44

i Unit imaginary number, page 44

r Radius, used as distance from input position [m], page 109

α' **Part 2:** Criterion of significance (type 1 error risk), page 141

α **Part 1:** Directivity parameter, page 66

α **Part 2:** Significance level (Probability of c or more events in a sample of size n due to chance alone.), page 141

β' Specified type 2 error risk., page 141

β Probability of type 2 error risk (Accepting H_0 when H_0 is actually false.), page 141

δ Logarithmic decrement, page 52

η Damping factor, page 52

$\Gamma^{ij}(\alpha)$ Amplitude attenuation dependent on directivity parameter α, page 66

$[\sigma]$ Stress Matrix, page 41

$[\varepsilon]$ Strain Matrix, page 41

$[C]$ Stiffness Matrix, page 41

$[S]$ Compliance Matrix, page 41

ν Poisson's Ratio, page 46

π Ratio of a circle's circumference to its diameter, page 28

ρ Density [kg m^{-3}], page 46

σ Standard Deviation, page 46

ξ Felt compression factor, page 28

$_L$ Index for the longitudinal direction of mechanical properties in wood, page 45

$_R$ Index for the radial direction of mechanical properties in wood, page 45

$_T$ Index for the tangential direction of mechanical properties in wood, page 45

A_{max} Maximum amplitude of initial (reflection free) wave front, page 104

B Inharmonicity coefficient for a stiff string, page 28

c' **Part 2:** Critical c. (Minimum value of c which, together with n and p_1, can produce significance level α), page 141

c **Part 1:** Sound Velocity [m s^{-1}], page 46

c **Part 2:** Number of correct responses, page 141

c/n **Part 2:** Correct-response rate, page 141

D Inharmonicity between measured and nominal partial frequency [Cent], page 28

d/L Hammer/string contact position, page 28

E Young's Modulus [GPa], page 46

F Force [N], page 28

f Frequency [Hz], page 63

f_1° Fundamental frequency of an ideal string without stiffness [Hz], page 28

f_1 Fundamental frequency [Hz], page 28

f_n Frequency of nth partial [Hz], page 28

F_{key} Force applied to the key when striking the key bed [N], page 146

G Shear Modulus [GPa], page 46

H_0 Null Hypothesis, page 141

H_1 Alternative Hypothesis, page 141

K Bulk modulus with coefficients λ_{lam} and G, page 41

k Wave vector, page 66

L Speaking length of a string [m], page 28

n Sample size, page 141

p **Part 1:** Sound pressure [Pa], page 41

p^i **Part 1:** Pressure of radiating source point i, page 66

p^j **Part 1:** Pressure of point j in obtained pressure field, page 66

p_1 **Part 2:** Proportion of events in population if chance alone is operating, page 141

p_2 **Part 2:** Effect size. Hypothesized proportion of events in population if a factor other than chance is operating, page 141

R_{ij} Radiation matrix, page 66

r_{ij} distance between p^i and p^j [m], page 66

S Cross sectional area of a string, page 28

T_{60} Reverberation time [s], page 52

V Volume [kg/m³], page 79

Y Mechanical mobility (admittance), page 32

y_B Years of experience as a piano builder, page 147

y_I Years of experience playing other instruments, page 147

y_P Years of experience as a piano player, page 147

y_T Years of experience as a piano tuner, page 147

Z Mechanical Impedance, page 32

ADC Analog-to-digital converter, page 134

CAD Computer-Aided Design, page 79

CT Computed Tomography, page 78

DAW Digital Audio Workstation, page 74

EMC Equilibrium Moisture Content [%], page 48

ESS Exponential Sine Sweep (Technique), page 65

FFT Fast Fourier transform, page 156

FRF Frequency Response Function, page 65

IR Impulse Response, page 65

JND Just noticable difference, page 156

MC Moisture Content [%], page 48

PC Principal Component, page 177

PCA Principal Component Analysis, page 177

RH Relative Humidity [%], page 48

SC Spectral centroid [Hz], page 156

SEA Statistical energy analysis, page 190

SNR Signal-to-noise ratio [dB], page 52

SPL Sound pressure level [dB], page 172

Explanation of Abbreviations

- It was originally planned to accompany four instruments through the production process. Unfortunately, that could not be realized without hindering the company's production flow. Therefore, only two instruments are considered for the study at hand, further denoted as *D1* and *D4*. Part 2 of this work only considers *D1*.

- For the first experiment the soundboards are examined in six stages of production. For the second experiment the finished pianos are examined on two additional dates. Even if manufacture is completed at the last two occasions, they are also denoted as 'production stages' for reasons of consistency. Hereafter, the production stages are denoted as *PROD1 - PROD8* (see Table 1 for a detailed description of the states of manufacture).

- For the first experiment the soundboard is excited at 15 positions corresponding to string termination points at the bridge. The driving point positions are further denoted as *POS1-POS15* (see Table 4.2 for detailed information about the exact locations).

- For the first experiment the radiated sound pressure is recorded with a microphone array from 18 consecutive locations to cover the entire soundboard surface. These array locations are further denoted as *ARRAY1 - ARRAY18*.

- The utilized microphone array consists of 105 microphones arranged in three rows of 35. If individual microphones are referenced they are denoted as *MIC1 - MIC105*.

- Units are given following the metric SI-system (ISO 80000-1:2009).

- The notation of keys follows either the American standard (the lowest note on a modern piano is *A0* and the highest note is *C8*) or the piano keys are numbered from 1 for *A0* up to 88 for *C8*.

- The denotation of construction parts follows the vocabulary given by the *Steinway Service Manual - Leitfaden zur Pflege eines Steinway*.[14]
- A Cartesian coordinate system is defined as illustrated in Figure 1. The origin can be located at the outer, upper left corner of the rim. All denoted coordinates (e.g. microphone positions, driving point positions) refer to this system.
- Wood has orthotropic mechanical properties, hence, three perpendicular spatial directions have to be considered when describing vibrations in wooden structures: the longitudinal axis (L) along the fiber direction, the radial (R) direction along the radius of the cross section of the trunk, and the tangential (T) direction as the tangent on the approximated circle of the cross section (illustrated in Figure 3.6). Note, that for the soundboard T aligns with z in the previously defined coordinate system. R has an angle of 40°, and L has an angle of 130° to x in the x, y plane.

Table 1.: Denotation of production stages.

PROD	
1	blank soundboard (glue-laminated strips of spruce)
2	after the ribs have been attached
3	after the bridge has been attached
4	after the ribs have been notched
5	after the soundboard has been glued to the rim
6	after application of the iron frame and stringing
7	after regulation, voicing and tuning - concert tuned state
8	after being played in a concert hall for one year - concert tuned state

[14] Max Matthias (1990). *Steinway Service Manual: Leitfaden zur Pflege eines Steinway*. Fachbuchre. Frankfurt am Main: Verlag Erwin Bochinsky.

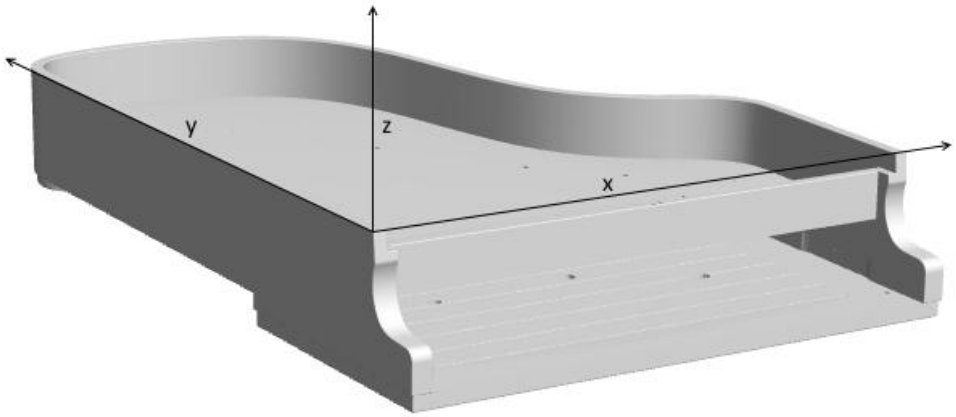

Figure 1.: Cartesian coordinate system definition used for the present work.

1. Introduction

1.1. Part 1

Historically, scientific findings have played an important role in the development and refinement of piano building. In the late 19th century, C. F. Theodore Steinway claimed to have been inspired by Hermann von Helmholtz's research on the perception of higher order harmonics, when inventing the duplex string schematic.[15] In the 1920s, the piano company *Grotrian Steinweg* regularly operated an acoustics lab ("*akustischer Experimentiersaal*") in their factory, where wood samples could be tested for suitability with the help of Chladni patterns.[16] The earliest published systematic experiments on piano soundboards and their influence on the final sound have been conducted by Paul Bilhuber in the 1940s,[17] an excellent wood worker who also attended physics, engineering, and metallurgy classes at Columbia College prior to becoming *Steinway & Sons*' most important developer in the early 20th century.[18] During the 1950s, a few attempts at utilizing new materials like metal for piano soundboards have been made.[19] However, vibrational testing and acoustic measurements have

[15] Niko Plath and Katharina Preller (2018). "Early Development Process of the Steinway & Sons Grand Piano Duplex Scale." In: *Wooden Musical Instruments - Different Forms of Knowledge. Book of End of WoodMusICK COST Action FP1302*. Cité de la Musique - Philharmonie de Paris.

[16] Sonja Petersen (2011). *Vom "Schwachstarktastenkasten" und seinen Fabrikanten - Wissensräume im Klavierbau 1830 bis 1930*. Waxmann Verlag.

[17] Paul H. Bilhuber and C. A. Johnson (1940). "The Influence of the Soundboard on Piano Tone Quality." In: *The Journal of the Acoustical Society of America* 11.3, pp. 311–320. DOI: 10.1121/1.1916039.

[18] Richard K. Lieberman (1995). *Steinway & Sons*. New Haven & London: Yale University Press, pp. 1–374.

[19] S. Hansing (1950). *Das Pianoforte in seinen akustischen Anlagen*. 2. Auflage. Herausgegeben von Freunden Siegfried Hansings.

not been established in modern everyday piano production. This is in contrast to lute and violin family instruments, where the influence of individual production steps on the resulting sound of the finished instrument is well researched,[20] and implemented into the regular building process.[21] Take for example the self-evident application of tap tone testing when producing violin top- and back plates.[22]

The lack of use of acoustic testing methods during piano making can be explained by several circumstances: Since the manufacture of a grand piano takes approx. one year, the feedback on an implemented modification is highly delayed compared to smaller instruments, which can be tested in fast iterations. Mass production methods imply labor division, which means that an instrument is built compartmentalized by numerous employees and nobody individually accompanies the complete emergence of the instrument, compared to as in small guitar or violin workshops. Therefore, the consequences of builders' actions on the sound produced are not directly tangible. Furthermore, the most crucial components for the sound production are irreversibly installed. It is not possible to test several soundboards on one instrument (as compared to changing a top plate of a violin), without effectively assembling a new instrument. It can be assumed, that the resulting long prototyping cycles hinder innovation.

As a consequence, the present ways of building modern grand pianos still rely on findings dated from the late 19th and early 20th century. E.g. the *Steinway & Sons' D-274* concert grand piano is built today for the most part as it was in 1884.

Most recently however, piano companies have regained great interest in understanding the sound producing mechanisms of their instruments in detail. Reasons are, among others, the need to find ways to substitute high quality tone wood with lower qualities or alternative materials due to decreasing availabil-

[20] Erik V. Jansson (2002). *Acoustics for violin and guitar makers*; Eddie Norman (2003). "Innovation in design and technology : the polymer acoustic guitar and the case for the relegation of ' the design process '." In: *DATA International Research Conference*, pp. 91–97.

[21] Martin Schleske (2002). "Empirical Tools in Contemporary Violin Making: Part II. Psychoacoustic Analysis and Use of Acoustical Tools." In: *Catgut Acoustical Society Journal* 4.6, pp. 43–61; Martin Schleske (1996). "Eigenmodes of Vibration in the Working Process of a Violin." In: *J. Catgut Acoust. Soc.* 3.1.

[22] Carleen Maley Hutchins, K. A. Stetson, and P. A. Taylor (1971). "Clarification of "Free Plate Tap Tones" by Hologram Interferometry." In: *J. Catgut Acoust. Soc.* 16.2, pp. 15–23.

ity and increasing prices of high quality spruce. Furthermore, the desire for developing new instruments, like modern reproduction pianos or genre specific models, drive the need to gain knowledge about the influence of material and geometry on the finally produced sound.

Most common methods for the analysis of the vibrational behavior of piano soundboards are Fourier based methods, like the analysis of driving point mobilities[23] and experimental modal analysis.[24] Individual driving point mobilities can be measured without great effort, but the informative value is rather limited since a single mobility measurement only describes the structure's behavior for one specific location and angle. Experimental modal analysis based on Fourier transforms works well for the piano soundboard only within a small frequency range. Due to high modal density and damping, individual modes cannot be distinguished for frequencies higher than approx. 200 Hz.[25] Most recent high-resolution estimation methods are based on the assumption, that the analyzed impulse responses can be modeled with a sum of exponentially damped sinusoids.[26] Ege[27] utilized the *ESPRIT* algorithm to extend the fre-

[23] Harold A. Conklin (1973). *U.S. Patent No. US3866506 A: Soundboard construction for stringed musical instruments*; Klaus Wogram (1979). *Akustische Untersuchungen an Klavieren*. Tech. rep. Braunschweig: Phys.-Techn. Bundesanstalt, pp. 1–45; Isao Nakamura (1983). "The vibrational character of the piano soundboard." In: *Proceedings of the 11th ICA*, pp. 385–388; Nicholas Giordano (1998). "Mechanical impedance of a piano soundboard." In: *The Journal of the Acoustical Society of America* 103.4, pp. 2128–2133. DOI: 10.1121/1.421358.

[24] Hideo Suzuki (1986). "Vibration and sound radiation of a piano soundboard." In: *The Journal of the Acoustical Society of America* 80.6, pp. 1573–1582. DOI: 10.1121/1.394321; Nicholas Giordano (1997). "Simple model of a piano soundboard." In: *The Journal of the Acoustical Society of America* 102.2, pp. 1159–1168. DOI: 10.1121/1.419868; Roberto Corradi, Paolo Fazioli, and S. Marforio (2010). "Modal analysis of a grand piano soundboard." In: *Proceedings of ISMA2010*, pp. 59–72.

[25] J. Berthaut, M. N. Ichchou, and L. Jézéquel (2003). "Piano soundboard: Structural behavior, numerical and experimental study in the modal range." In: *Applied Acoustics* 64, pp. 1113–1136. DOI: 10.1016/S0003-682X(03)00065-3.

[26] Jean Laroche (1993). "The use of the matrix pencil method for the spectrum analysis of musical signals." In: *The Journal of the Acoustical Society of America* 1.4, pp. 1958–1965; Richard Roy and Thomas Kailath (1989). "ESPRIT - Estimation of Signal Parameters via Rotational Invariance Techniques." In: *IEEE Transactions on Acoustics, Speech, and Signal Processing* 37.7, pp. 984–995. DOI: 10.1109/29.32276.

[27] Kerem Ege (2009). "La table d'harmonie du piano-Études modales en basses et moyennes fréquences." PhD thesis.

quency range for modal analysis up to 2.5 kHz.
However, the informative value of modern analysis methods for piano builders is often rather small or too abstract.

Additionally, most existing studies consider just the soundboard with ribs and bridge or the finished piano, eventually with subsequently removed strings. To the author's knowledge, only most recently one piano related study has been published that accompanies the soundboard through the production process.[28]

The main objectives for the first part of this thesis are therefore:

- to trace the impact of individual production steps during manufacture on the behavior of a piano soundboard,
- to present alternative approaches to describe the vibrational behavior of a piano soundboard,
- to help the instrument builder in understanding the effects of his work on the evolving characteristics of the piano,
- in the best case, to derive proposals for structural modifications from the results obtained.

1.2. Part 2

The second part of the present thesis is related to the presumed change of tonal quality for a grand piano when being operated in a concert hall. Well-maintained concert pianos are said to "mature" and to "change for the better" over the first years. When auditioning concert pianos for purchase, technicians often do not choose the best sounding instrument but the one with the greatest potential for future development. When asked, technicians are certain about occurring changes within the instrument, but there is great uncertainty as to what these might be.

[28] Roberto Corradi et al. (2017). "Modal analysis of a grand piano soundboard at successive manufacturing stages." In: *Applied Acoustics* 125, pp. 113–127. DOI: 10.1016/j.apacoust.2017.04.010.

Three factors can contribute to a change in tonal quality for a musical instrument:

Aging: When addressing the long-term development of musical instruments, most published works focus on the time-conditioned degeneration of wood, eventually accelerated by periodic humidity alterations.[29] Aging might be a crucial factor for the preservation of an instrument, particularly when dealing with historical instruments within the museum context. However, since this work attempts to address the possible changes in tonal quality for only the first year of a concert instrument under intensive supervision, other aspects gain in importance.

Playing: The vibrational properties of wood change when it is subject to vibrations for extended periods of time.[30] Thereby, regular playing could cause an audible change in vibrational characteristics of piano soundboards.[31]

Maintenance: A grand piano at a concert hall is intensively monitored by a technician. It is tuned several times a week and prior to each concert, substantial adjustments to keys, action, and hammers might be made in consultation with the player to achieve a certain requested playing feel and tonal character.

The second part of this thesis, therefore, aims to answer the following questions:

With regard to a concert piano being played for one year in a concert hall:

- What are potentially influential factors and what is their contribution to a possible change in tonal quality?
- Are structural changes measurable?

[29] Iris Brémaud and Joseph Gril (2015). "Effect of transitional moisture change on the vibrational properties of violin-making wood." In: *Cost FP1302 WoodMusICK annual conference "Effects of playing on early and modern musical instruments"*; A. Beavitt (1996). "Humidity cycling." In: *Strad* November, pp. 916–920.

[30] D. G. Hunt and E. Balsan (1996). "Why old fiddles sound sweeter." In: *Nature* 379.6567, pp. 681–681. DOI: 10.1038/379681a0; Carleen Maley Hutchins (1998). "A Measurable Effect of Long-term Playing on Violin Family Instruments." In: *Catgut Acoustical Society Journal* 3.5, pp. 38–40.

[31] Gregor Weldert (2017). "Sound Enhancement of Musical Instruments by 'Playing them in': Fact or Fiction?" In: *Europiano* 3, pp. 41–43.

- Is a tonal difference perceivable?
- If so, what sound properties lead to an audible difference?
- How do listeners of various professional backgrounds verbalize these differences?

Even though dealing with different questions in detail, the two conducted experiments are interrelated by the overarching questions:

How does the piano achieve its sound? What are important influential factors in the building process, as well as in concert business?

1.3. Outline of Thesis Structure

This thesis is structured in two parts, covering successive studies. As a prepended chapter, a general overview over the acoustics of the piano is given (**Chapter 2**). Important attributes for the tonal quality of a piano, like the force compression characteristics of hammer felt, or the inharmonicity of a real string are introduced. The chapter should create a basic understanding of the tone production, which will be presupposed in the following main parts.

The first part opens with theoretical considerations about the piano soundboard. **Chapter 3** is divided in two sections, one describing the soundboard as a vibrating structure, the second one discussing the soundboard in terms of material dependent characteristics.

Chapter 4 describes the experimental setup in terms of production stages to be considered, type of excitation and response measurements, chosen driving point positions, and reflections about the climate conditions during measurements.

Chapter 5 reviews the post-processing methods to be applied on the obtained raw data. Impulse responses are calculated using the so-called *exponential sine sweep technique*. The recorded pressure field had been planned to be back-propagated to the soundboard surface, using the so-called *minimum energy*

method. It discusses in detail the challenges posed by the multiple-array application used for the first time and what ultimately led to the decision not to propagate the recorded pressure data.

Chapter 6 begins with a description of the development of structural properties through the production. The analysis of vibrational properties is opened with a description of the development of harmonic responses and driving point mobilities. Based on the remarkable spatial resolution of approx. 1,300 impulse responses per measurement, the propagation of bending waves on the soundboard can be visualized. Based on travel time estimations, grain angle dependent velocity ratios are calculated for bending waves traveling on the soundboard. Influence of attached components on the grain angle dependent degree of bending wave dispersion is estimated. Based on the initial wave propagation, the grain angle dependent energy loss is described. Finally, the frequency dependent spatial energy distribution on the soundboard is modeled with exponential decay functions. For all given measures, the development through the production process can be described.

Chapter 7 discusses the utilized methods and reflects the results obtained.

Chapter 8 opens the second part with a review of the factors potentially responsible for a tonal change of a grand piano in concert business. The issue is approached with regard to three main influences: Aging, playing, and maintenance. Possible disturbances are discussed, leading to considerations about the appropriate study design to choose for the investigation.

Chapter 9 describes the experimental setup in terms of the instrument investigated and the type of excitation and response measurements. Measurements are performed on two occasions: Firstly, on a completed instrument prepared for sale. Secondly, on the same piano after having been played for one year in a concert hall. Single notes are recorded with dummy-head-microphones in player position in an anechoic chamber.

In **Chapter 10**, an extended ABX listening test is proposed, engaging players, tuners, and builders to address the questions whether a variation in tonal quality is audible and if so, what sound properties could lead to a perceived difference. The established ABX comparison scheme is extended with free text input to query the properties, which supposedly allowed for a discrimination of the

presented tones. Participant variables are sampled to allow a subsequent distinction based on professional background.

Chapter 11 presents results of the listening test. Three sub-groups (disjoint sets) are defined regarding their experience as non-experts, players and builders/-tuners. A statistical analysis of the ABX test is presented. The second research question is approached by analyzing the free text input with natural language processing methods. The data is pre-processed with tokenization, stop word removal, stemming, and subsequently analyzed. Semantic sub-grouping allows for indication on the vocabulary listeners of varying expertise use to verbalize their sensation.

In **Chapter 12**, the given statements are used as a basis for the analysis of corresponding physical properties and psychoacoustic parameters related to the described sensations. Subsequently, a principal component analysis is performed on the obtained psychoacoustic features to reduce dimensions, and eventually detect embedded distinctness in the data regarding the target classes.

Chapter 13 discusses the utilized methods, particularly with regard to the study design, and reflects on the results obtained by listening test and subsequent analysis.

The final **Chapter 14** concludes the central achievements of this thesis and gives an outlook on how to continue working on the basis of the goals achieved.

Measurement data used in this work has been obtained from 2014 to 2018 in the scope of the research project *"Real-Time FPGA and GUI-driven Auralization of Geometry and Material Variations of the Piano"*, funded under the project identifier *Deutsche Forschungsgemeinschaft (DFG) - Project number 246374245*.[32]

[32] `https://gepris.dfg.de/gepris/projekt/246374245?language=en`, accessed in September 2019.

2. Main Components of a Piano

The following sections give a general overview over the acoustics of the piano. Suzuki and Nakamura,[33] Fletcher and Rossing[34] and Rossing[35] give summaries of research papers up to the year they were published.

When a piano key is pressed, the action accelerates the hammer toward the string and raises the damper. The jack ensures that the action releases the hammer right before it strikes the string. The hammer moves freely when contacting the string. Energy is induced and the string is set into vibration. The vibration is transferred over the bridge to the soundboard. The soundboard couples to the air and radiates the audible tone.
A modern piano has 88 keys, covering 8+1/3 octaves from *A0* to *C8* (27.5 Hz to 4186.01 Hz in the equal tempered scale). This is four times the range of most other instruments, such as flutes, clarinets or trumpets. The actions' main function is the transfer of energy from the finger to the hammer, and then to the strings. Most of the roughly 10,000 individual parts of a piano are assembled in the action. For the player its complex mechanism is responsible for the haptic feel of the instrument. Depending on the specific model a modern piano has approximately 230 strings. Their lengths vary from about 2 m in the bass range to 0.05 m in the treble range. For the lowest notes a single steel string, wrapped with one or two layers of copper, is struck when a key is pressed. The rest of the bass range has two and three wrapped strings for each note. From the low mid range to the highest notes, each hammer strikes a

[33] Hideo Suzuki and Isao Nakamura (1990). "Acoustics of pianos." In: *Applied Acoustics* 30.2-3, pp. 147–205. DOI: 10.1016/0003-682X(90)90043-T.

[34] Neville H. Fletcher and Thomas D. Rossing (1998). *The Physics of Musical Instruments*. New York, NY: Springer New York, p. 756. DOI: 10.1007/978-0-387-21603-4.

[35] Thomas D. Rossing, ed. (2010). *The Science of String Instruments*. New York, NY: Springer New York. DOI: 10.1007/978-1-4419-7110-4.

Figure 2.1.: Predecessor of the modern grand piano built by *Steinway & Sons*: Prototype grand piano model *Style 3* (Ser. No. 21.460, New York 1871) with retrofitted duplex scale, owned by Hermann von Helmholtz. Since 2009 on display at Deutsches Museum, Inv. No. 2009-0477.

group of three unwrapped unison strings. The strings vibrate mainly in the direction perpendicularly to the soundboard. On one end each string is clamped to a tuning pin, so that the string tension may be varied to adjust the vibration frequency.

On the other end the string is connected to the bridge via two so-called *bridge pins* and then rigidly clamped to the frame with a so-called *hitch pin*. The bridge transfers the string vibration to the soundboard, which couples the vibration to the air and radiates the sound. In terms of tone production, the important parts of the piano are discussed in detail in the following sections.

2.0.1. The Action

The piano action is a complex mechanic construction, but mainly consists of four parts (see Figure 2.2). The pressed key raises the damper of the string and sets the system of levers in motion to accelerate the hammer. Shortly before the hammer hits the string it is released from the action and swings free. The action also catches the hammer when it returns from the string. The damper is lowered back down on the string when the key is released by the player. A detailed illustration of the successive operation steps of a piano action is given by Askenfelt and Jansson[36].[37]

All contact points of moving parts in the action are covered with leather or felt to minimize sound production and backlash. The use of wood, felt and leather implies that the action is highly sensitive to variations in temperature and humidity. Therefore, a correct and well balanced mechanism requires a periodic regulation.

Figure 2.3 shows a diagram for contact times of the different parts in a grand piano action. The tone is a *staccato* played *C4* at *forte* level. Following the processes in the action chronologically, the damper looses contact to the string

[36] Anders Askenfelt and Erik V. Jansson (1990b). "From touch to string vibrations. I: Timing in the grand piano action." In: *The Journal of the Acoustical Society of America* 88.1, pp. 52–63. DOI: 10.1121/1.399933.

[37] Anders Askenfelt and Erik V. Jansson (1990a). "From touch to string vibrations." In: *Five lectures on the Acoustics of the piano*. Ed. by Anders Askenfelt. Stockholm: Royal Swedish Academy of Music.

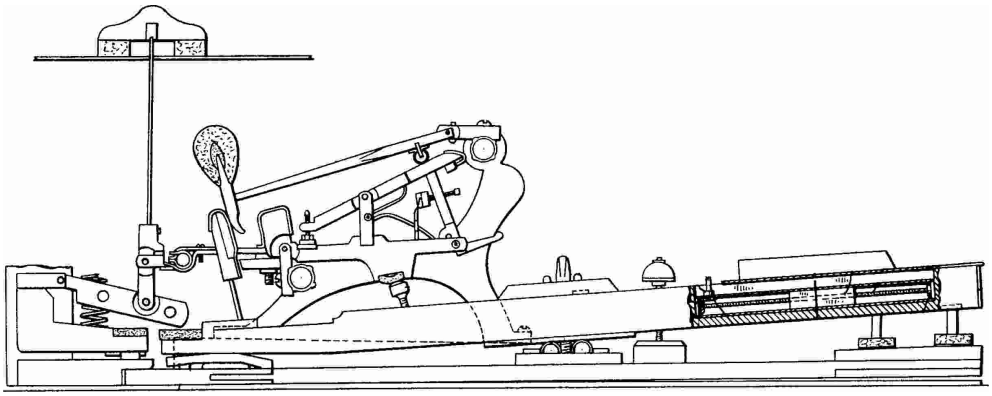

Figure 2.2.: The action of a modern grand piano, from W. Günther (1959). *U.S. Patent No. 2,911,874: Means for adjusting the touch of keys in pianos and like musical instruments.*

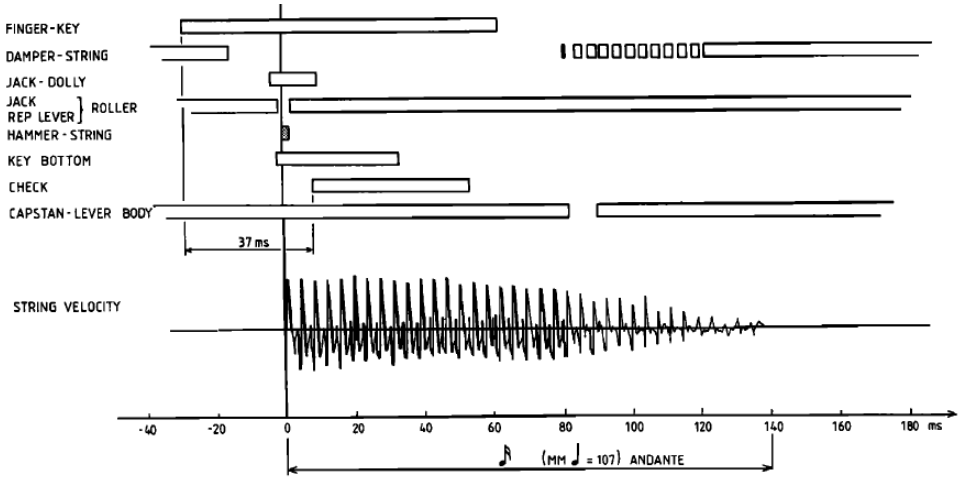

Figure 2.3.: Timing diagram of a grand piano action for a *staccato* played *C4* at *forte* level. Reprinted with permission from Anders Askenfelt and Erik V. Jansson (1990a). "From touch to string vibrations." In: *Five lectures on the Acoustics of the piano*. Ed. by Anders Askenfelt. Stockholm: Royal Swedish Academy of Music, p. 56. Copyright The Royal Swedish Academy of Music 1990.

15 ms before the hammer hits the string. Less than one millisecond before the hammer hits the string, the jack releases the hammer and it swings free. The hammer-string contact lasts for only a few milliseconds; only in this short time span energy can be transferred to the string. For this measurement the hammer-string contact is synchronous with the key-bottom contact. Dependent on the played dynamic level, this relationship can be disturbed. At a *piano* level the hammer-string contact happens before the key reaches the bottom. At louder levels the key-bottom contact can advance the hammer-string contact. As the bottom feeling of a key is an important feedback from the instrument, and these delays can reach about 20 ms, this can affect the playing. An important part of the regulation process is to balance these delays between the keys and minimize variations in key dynamics. 20 ms after the key is released the damper lowers on the string and stops the vibration. Note that the traveling pulses in the string force the damper to bounce; the damper is not capable of stopping the vibration immediately.[38] The use of felt and leather for the contact surfaces and the flexibility of the wooden parts in the action adds a strong non-linearity to the behavior of the system.[39] Figure 2.4 illustrates a non-linear relation between the travel time and the maximum hammer velocity.

The design of an upright piano action is different from that of a grand piano. The hammers and dampers move horizontally and therefore have to be returned to their initial position by a spring force. In a grand piano action a repetition lever enables short note repetitions when the key has only half way returned to its rest position. The upright action has no such mechanism, so that the key must be released before a repetition.[40]

The action even contributes to the characteristic onset of the piano tone when the key hits the stop rail on the key frame. This impact excites the key bed and partly the soundboard[41] and produces a characteristic percussive component

[38] Askenfelt and Jansson, "From touch to string vibrations."

[39] Werner Goebl, Roberto Bresin, and Alexander Galembo (2003). "The piano action as the performer's interface: Timing properties, dynamic behaviour, and the performer's possibilities." In: *Proceedings of the Stockholm Music Acoustics Conference, August 6–9, 2003 (SMAC 03)*. Vol. 2003. Smac 03, pp. 159–162.

[40] Fletcher and Rossing, *The Physics of Musical Instruments*.

[41] Askenfelt and Jansson, "From touch to string vibrations. I: Timing in the grand piano action."

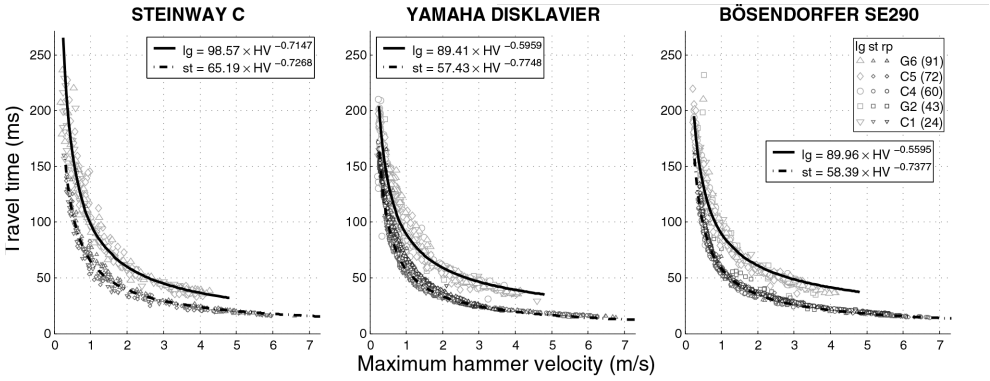

Figure 2.4.: Dependency of travel time (time span between finger-key and hammer-string contact) to maximum hammer velocity for three different grand pianos and different dynamic levels. The relation varies marginally between models, but considerably between keys. Reprinted with permission from Werner Goebl, Roberto Bresin, and Alexander Galembo (2005). "Touch and temporal behavior of grand piano actions." In: *The Journal of the Acoustical Society of America* 118.2, pp. 1154–1165. DOI: 10.1121/1.1944648, p. 1160. Copyright The Journal of the Acoustical Society of America 2005, Acoustic Society of America.

to the piano tone onset. Askenfelt states, that a piano tone produced without the transient component "lacks something of the interesting piano character, resembling a plucked string more closely than a struck one".[42]

2.0.2. The Hammer

The piano hammer and its effects on tone production have been widely investigated. Major early contributions where given by Askenfelt and Jansson, Conklin, and Hall.[43] High resolution measurements of the hammer-string interaction with tracked motion trajectories, obtained from high speed camera recordings, have been carried out by Birkett.[44] Modeling of the hammer-string interaction has been performed in several publications.[45]

[42] Askenfelt and Jansson, "From touch to string vibrations. I: Timing in the grand piano action," p. 52.

[43] Anders Askenfelt and Erik V. Jansson (1991). "From touch to string vibrations. II: The motion of the key and hammer." In: *The Journal of the Acoustical Society of America* 90.5, pp. 2383–2393. DOI: 10.1121/1.402043; Harold A. Conklin (1996b). "Design and tone in the mechanoacoustic piano. Part II. Piano structure." In: *The Journal of the Acoustical Society of America* 100.2, pp. 695–708. DOI: 10.1121/1.416233; Donald E. Hall (1986). "Piano string excitation in the case of small hammer mass." In: *The Journal of the Acoustical Society of America* 79.1, pp. 141–147. DOI: 10.1121/1.393637.

[44] Stephen Birkett (2013). "Experimental investigation of the piano hammer-string interaction." In: *The Journal of the Acoustical Society of America* 133.4, pp. 2467–2478. DOI: 10.1121/1.4792357.

[45] Xavier Boutillon (1988). "Model for piano hammers: Experimental determination and digital simulation." In: *The Journal of the Acoustical Society of America* 83.February, pp. 746–754; Antoine Chaigne and Anders Askenfelt (1994). "Numerical simulations of piano strings. II. Comparisons with measurements and systematic exploration of some hammer-string parameters." In: *The Journal of the Acoustical Society of America* 95.3, pp. 1631–1640. DOI: 10.1121/1.408549; Anatoli Stulov (2003). "Experimental and theoretical studies of piano hammer." In: *Proceedings of the Stockholm Music Acoustics …* 2003.Smac 03, pp. 6–9; Nicholas Giordano and M. Jiang (2004). "Physical Modeling of the Piano." In: *EURASIP Journal on Advances in Signal Processing* 2004.7, pp. 926–933. DOI: 10.1155/S111086570440105X.

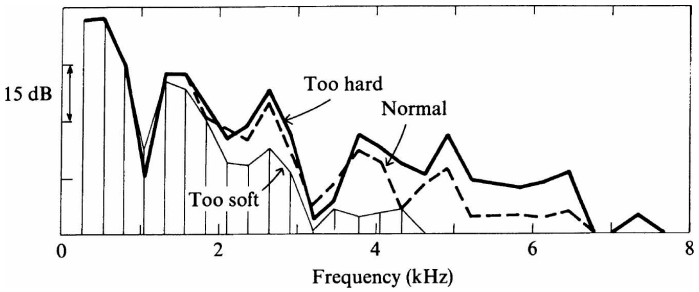

Figure 2.5.: Spectra for a *C4* note produced with three different hammer conditions (too soft, normal, and too hard). Reprinted with permission from Anders Askenfelt and Erik V. Jansson (1993). "From touch to string vibrations. III: String motion and spectra." In: *The Journal of the Acoustical Society of America* 93.4, pp. 2181–2196. DOI: 10.1121/1.406680, p. 2191. Copyright The Journal of the Acoustical Society of America 1993, Acoustic Society of America.

Material Properties

Modern piano hammers are made of wooden mallets with multiple layers of felt wrapped around a hardwood core. The outermost felt layers are the softest. The hammer hardness can be adjusted by the tuner in both directions (so-called *voicing*). Hammers which are too hard produce harsh tones, overly soft hammers produce dull and dark tones[46] (see Figure 2.5).

The total weight and the thickness of the felt vary between bass and treble. A modern high treble hammer has a mass of about 4 g, a lowest bass hammer has a mass of about 11 g.[47] The ratio of hammer mass to string mass varies from 8 for the highest strings to 0.08 for the lowest ones.

Force-Compression Characteristics

The hardness of the hammer implies one of the most important effects that determine the characteristic piano tone. Many materials have linear compression

[46] Fletcher and Rossing, *The Physics of Musical Instruments*.
[47] Conklin, "Design and tone in the mechanoacoustic piano. Part II. Piano structure."

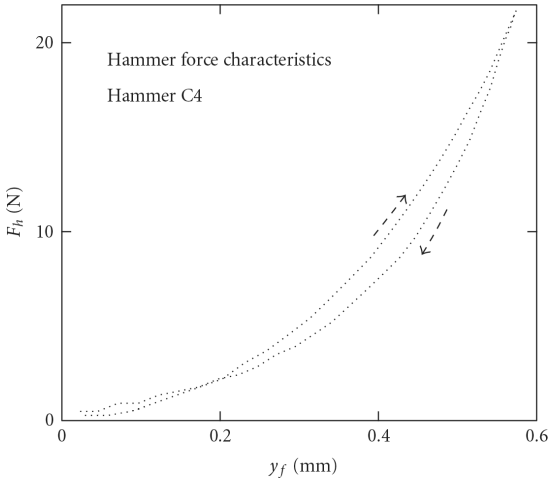

Figure 2.6.: Hammer force F_h vs. compression y_f of the hammer surface during contact. Reprinted by permission from Nicholas Giordano and M. Jiang (2004). "Physical Modeling of the Piano." In: *EURASIP Journal on Advances in Signal Processing* 2004.7, pp. 926–933. DOI: 10.1155/S111086570440105X, p. 928. Copyright Springer Nature 2004.

characteristics. Those materials obey *Hooke's law*. Piano hammers show a nonlinear compression behavior, the force increases faster than the compression.[48] Figure 2.6 shows the hammer force as a function of the felt compression. The hammer force depends linearly on the velocity the hammer has when it strikes the string (for a given hammer mass). Therefore, the hardness of the hammer is different for *piano* and *forte*.

The relationship between the hammer force F and the felt compression ξ can be roughly described as

$$F = K\xi^p, \tag{2.1}$$

where K is a generalized stiffness and p is an exponent to describe the varia-

[48] Nicholas Giordano and J. P. Winans (2000). "Piano hammers and their force compression characteristics: Does a power law make sense?" In: *The Journal of the Acoustical Society of America* 107.4, pp. 2248–2255. DOI: 10.1121/1.428505.

tion of stiffness with force. p varies from 2.2 to 3.5 for used piano hammers.[49] Figure 2.6 also shows hysteresis behavior of the system. K and p each have different values for compression and relaxation. Note that the simple model 2.1 by Hall[50] includes no consideration of the hysteresis effect. Recent models consider the dynamic features such as hysteresis of the force-compression characteristic and their dependence on the hammer speed.[51] A strike with an effectively harder hammer results in a shorter hammer-string contact duration and thus an increased excitation of higher string modes. Therefore, a brighter tone is radiated because the soundboard is excited with more high-frequency partials.[52] The general relationship between collision time and frequency spectrum can be explained with the Fourier theorem. A short pulse in the time domain yields to a broad distribution in the spectral domain and vice versa. Figure 2.7 shows hammer-string contact durations for the *C1-C8* keys as a percentage of $T_0/2$. Horizontal bars indicate the variation in contact time for the different dynamic levels and give implications to the variability in produced tone color. For the bass range the contact duration is only a fraction of a period, for the treble range it reaches several periods length.

In summary, it can be said that the change of the piano tone spectrum with dynamic level is determined by the non-linear behavior of the piano hammers.

Hammer-String Interaction

When a hammer strikes a string two displacement pulses start to travel along the string. One from the hammer to the nearby agraffe, and one from the hammer to the bridge. The first pulse is reflected several times between hammer and agraffe, while the second pulse travels to the bridge and back. Every reflected pulse from the agraffe is inverted and contributes to the release of the

[49] Donald E. Hall (1987). "Piano string excitation II: General solution for a hard narrow hammer." In: *The Journal of the Acoustical Society of America* 81.2, pp. 535–546. DOI: 10.1121/1.394919.

[50] Ibid.

[51] Stulov, "Experimental and theoretical studies of piano hammer"; Anatoli Stulov (1995). "A simple grand piano hammer felt model." In: *Proc. Estonian Acad. Sci. Engin*, pp. 172–182.

[52] Anders Askenfelt and Erik V. Jansson (1993). "From touch to string vibrations. III: String motion and spectra." In: *The Journal of the Acoustical Society of America* 93.4, pp. 2181–2196. DOI: 10.1121/1.406680.

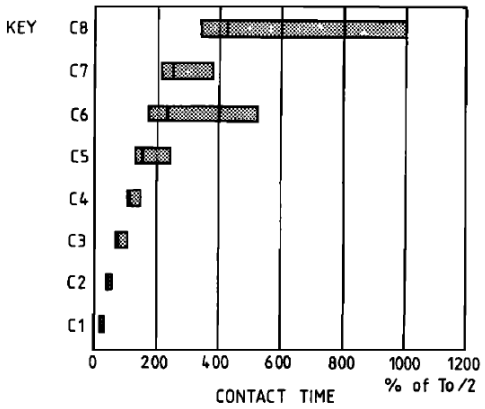

Figure 2.7.: Relative hammer string contact duration for different keys in percent of $T_0/2$. The bar length shows the variation between a *fortissimo* (left end) and a *pianissimo* (right end) played note. Reprinted with permission from Anders Askenfelt and Erik V. Jansson (1990a). "From touch to string vibrations." In: *Five lectures on the Acoustics of the piano*. Ed. by Anders Askenfelt. Stockholm: Royal Swedish Academy of Music, p. 47. Copyright The Royal Swedish Academy of Music 1990.

hammer. Hall[53] states, that gravity can not have a relevant effect to rebound the hammer before the string begins pushing back on the hammer. "At middle *C* a half cycle of string motion takes only about 2 ms, during which gravity can impart only about 2 cm s^{-1} of velocity and can move the object from rest a distance of only 20 µm".[54] For very low ratios of hammer mass to string mass the string may contact the hammer again after release (so-called *second contact*).

Hammer-String Contact Position

The position of the hammer-string contact point d/L directly affects the resulting string motion.[55] A string observed at a certain point shows no energy in a

[53] Hall, "Piano string excitation in the case of small hammer mass."

[54] Ibid., p. 141.

[55] Conklin, "Design and tone in the mechanoacoustic piano. Part II. Piano structure"; Askenfelt and Jansson, "From touch to string vibrations. III: String motion and spectra"; Donald E. Hall and Peter Clark (1987). "Piano string excitation IV: The question of missing modes."

vibration partial which has a node at this point. The string does not move in this partial at this point. Conversely, striking an ideal string at a certain point prevents the string to vibrate in all partials which have a vibrational node at this point. E.g., striking an ideal string at $1/5$ prevents all integer multiples of f_5. For real strings several effects lead to a strong but not absolute attenuation for the d/Lth partial. A real hammer has a finite width so that the hammer-string contact never takes place only at a nodal point. Additionally, the non-rigid boundary conditions of the string at the bridge lead to an amount of energy in the d/Lth partials.[56]

2.0.3. The Strings

Looking at a piano as a generator-resonator model, the strings act as the generator in this system. They contribute the energy to the system and define the pitch of the instrument. The vibrations of the strings determine the frequencies of the produced sound (the amplitudes of the spectral components are greatly influenced by subsequent parts of the tone production). The following section gives an introduction to the basic equations of vibration for the ideal string. Morse and Ingard,[57] Fletcher and Rossing[58] and Rossing[59] give broad overviews to the mathematical descriptions of vibrating bodies. Section 2.0.3 discusses the specific features of real piano strings in comparison to the ideal string.

Piano String Design

As shown above, the motion of an ideal string produces a series of standing waves with frequencies $f_n = nf_1$. For a real string the model of an ideal string provides a good first approximation of the vibrational behavior, but does not

In: *The Journal of the Acoustical Society of America* 82.6, pp. 1913–1918. DOI: 10.1121/1.395686.

[56] Hall and Clark, "Piano string excitation IV: The question of missing modes."

[57] P. M. Morse and K. U. Ingard (1986). *Theoretical Acoustics*. Internatio. Princeton University Press.

[58] Fletcher and Rossing, *The Physics of Musical Instruments*.

[59] Rossing, *The Science of String Instruments*.

reproduce characteristic features of the piano string.[60] The piano string does not exactly fulfill the restrictions for ideal strings. Real instrument strings have a bending stiffness and they have a real positive diameter. The following section describes how this affects the string modes and why string scaling implies a complex challenge for the piano designer.
The pitch is inversely proportional to the speaking length, so that a pitch change of an octave downwards requires doubling of the string length with constant mass per unit length and the same string tension. If a piano designer used strings of the same diameter and tension for all keys and left the highest treble string as long as it typically is ($L_{C8} \approx 0.05\,\mathrm{m}$), they would have to assemble a *C1* string of $L_{C1} \approx 6.4\,\mathrm{m}$ length.

Different possibilities exist to lower the vibration frequency with constant speaking length: Lowering the tension would lower the frequency, but also decrease the restoring force and thus decrease the amplitude of vibration. An increased mass per unit length causes the string to move more slowly and decreases the vibrational frequency for a given tension. To increase the string mass the diameter is increased; a doubled diameter leads to a pitch change of an octave. The more the string diameter is increased, the more the string behaves like a bar than like a string. When the string is displaced, an extra force from bending stiffness has to be added to the tension force. This leads to a greater net restoring force. Therefore, the frequencies of the standing waves are increased. The increase, due to bending stiffness, is frequency dependent. Thus, the standing wave frequencies of a stiff string are not harmonic.

In the initial phase the transversal string vibration is polarized mainly in the vertical direction (orthogonal to the soundboard). Input impedance for energy transfer in this direction is low, therefore, energy loss from string to soundboard is high. Due to rocking motions of the soundboard, energy is coupled at the bridge from vertical to horizontal polarization over time. When the hor-

[60] O. H. Schuck and R. W. Young (1943). "Observations on the Vibrations of Piano Strings." In: *The Journal of the Acoustical Society of America* 15.1, pp. 1–11. DOI: 10.1121/1.1916221; Harvey Fletcher, E. Donnell Blackham, and Richard Stratton (1962). "Quality of Piano Tones." In: *The Journal of the Acoustical Society of America* 34.6, pp. 749–761. DOI: 10.1121/1.1918192; Askenfelt and Jansson, "From touch to string vibrations. III: String motion and spectra"; Harold A. Conklin (1996a). "Design and tone in the mechanoacoustic piano. Part I. Piano hammers and tonal effects." In: *The Journal of the Acoustical Society of America* 99.6, pp. 3286–3296. DOI: 10.1121/1.414947.

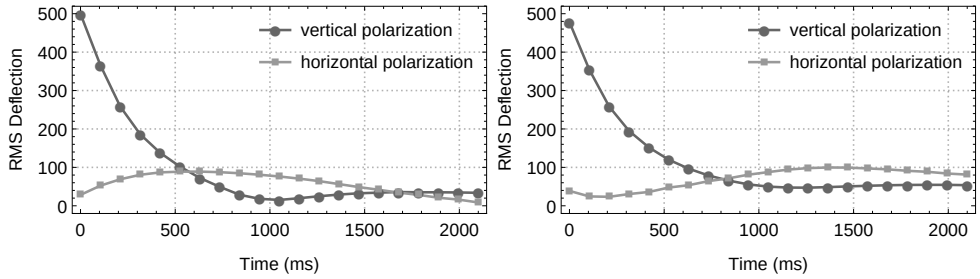

Figure 2.8.: Root mean square of transversal deflection of two adjacent unison strings. Recorded with a high speed camera. The two perpendicular polarizations are captured by utilizing mirrors.

izontal transversal deflection dominates the string vibration, energy loss per time decreases (see Figure 2.8).

Vibrations of a Stiff String

To add stiffness to an ideal string one can modify the basic wave equation with a term corresponding to bending stiffness:

$$\mu \frac{\partial^2 y}{\partial t^2} = T \frac{\partial^2 y}{\partial x^2} \boxed{-ESK^2 \frac{\partial^4 y}{\partial x^4}}, \tag{2.2}$$

where E is the Young's modulus, S is the cross sectional area and K is the radius of gyration. The derivation of the bending term is given in Fletcher and Rossing.[61]
For a string with pinned ends the solution gives mode functions

$$f_n = n f_0^\circ (1 + Bn^2)^{1/2},$$

where f_0° is the fundamental frequency of the string without stiffness and $B = \pi^2 ESK^2/TL^2$.

[61] Fletcher and Rossing, *The Physics of Musical Instruments*, p.58.

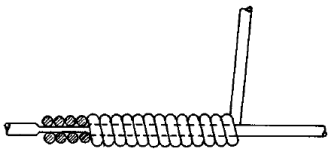

Figure 2.9.: Wrapping of a string. The end of the copper coil is anchored to a flattened portion of the steel wire. Reprinted with permission from Harold A. Conklin (1996c). "Design and tone in the mechanoacoustic piano. Part III. Piano strings and scale design." In: *The Journal of the Acoustical Society of America* 100.3, pp. 1286–1298. DOI: 10.1121/1.416017, p. 1290. Copyright The Journal of the Acoustical Society of America 1996, Acoustic Society of America.

The effect of stiffness becomes larger for increased Young's modulus and diameter, and becomes smaller for an increased speaking length. For a string with clamped ends an approximate solution gives

$$f_n = n f_1^{\circ} (1 + B n^2)^{1/2} \left[1 + \left(\frac{2}{\pi} \right) B^{1/2} + \left(\frac{4}{\pi^2} \right) B \right], \tag{2.3}$$

for $B \ll 1$. Clamping the ends causes an increase of the mode functions.

Wrapped Strings

To reduce the strong inharmonicity due to great string diameters, the bass strings are made of a steel core wire with a coil of copper wire winded around the core[62] (see Figure 2.9). Wrapping increases the mass per unit length with only a small increase of bending stiffness.

[62] Robert W. Young (Jan. 1954). "Inharmonicity of Piano Bass Strings." In: *The Journal of the Acoustical Society of America* 26.1, pp. 144–144. DOI: 10.1121/1.1917803; Conklin, "Design and tone in the mechanoacoustic piano. Part I. Piano hammers and tonal effects"; Alexander Galembo and Anders Askenfelt (2004). "Perceptual relevance of inharmonicity and spectral envelope in the piano bass range." In: *Acta Acustica united with Acustica*, pp. 528–536.

Inharmonicity and Implications for Tuning

Schuck and Young[63] describe the inharmonicity D as the difference in cents between a measured modal frequency f and its nominal value nf_1 with the fundamental frequency f_1 and the mode number n as

$$D = 1200 \log_2(f/nf_1). \tag{2.4}$$

They find a proportionality of the inharmonicity to the square of the mode number for the medium grand piano (See Figure 2.10). The straight curves are all positive, so the partials are always sharp compared to the nominal harmonics. The different slopes illustrate that the inharmonicity changes over the registers of the piano. The sharpening is least between *C2* and *C4* and increasing to the bass- and treble range (see Figure 2.11). For *F1* the 15th partial has the frequency of the 16th nominal harmonic. In the treble range this jump is reached even earlier.

Young[64] shows that rather all inharmonicity of piano strings (wrapped strings excluded) result from their inherent bending stiffness. Fletcher, Blackham, and Stratton[65] synthesize piano tones (additive synthesis of sines) and compare them to real measured tones in order to find objective parameters for the description of piano tone quality. They find the inharmonicity to be the cause for the warmth of the characteristic tone and thus to be an important factor for piano tone quality.[66] Railsback[67] measures 16 pianos tuned by ear. Tuners tend to tune increasingly sharp in the middle and high registers and increasingly flat in the low register (see Figure 2.12). This can be explained by the process of piano tuning:

[63] Schuck and Young, "Observations on the Vibrations of Piano Strings."

[64] Robert W. Young (1952). "Inharmonicity of Plain Wire Piano Strings." In: *The Journal of the Acoustical Society of America* 24.3, pp. 267–273. DOI: 10.1121/1.1906888.

[65] Fletcher, Blackham, and Stratton, "Quality of Piano Tones."

[66] D. W. Martin and W. D. Ward (1961). "Subjective Evaluation of Musical Scale Temperament in Pianos." In: *The Journal of the Acoustical Society of America* 33.5, pp. 582–585. DOI: 10.1121/1.1908730.

[67] O. L. Railsback (Jan. 1938). "Scale Temperament as Applied to Piano Tuning." In: *The Journal of the Acoustical Society of America* 9.3, pp. 274–274. DOI: 10.1121/1.1902056.

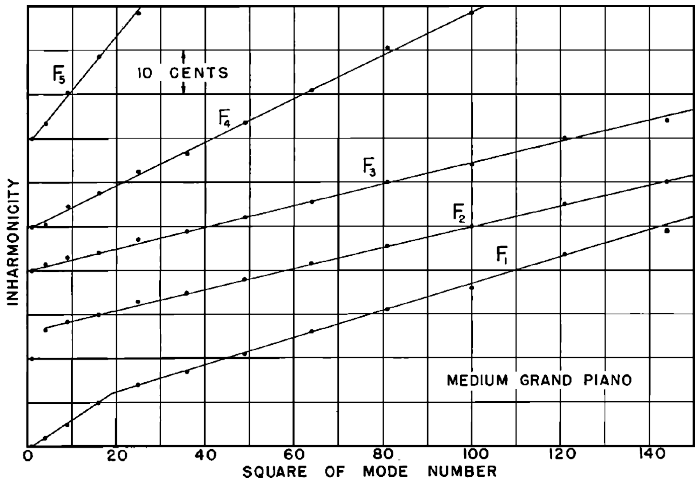

Figure 2.10.: Inharmonicity as a function of n^2. Reprinted with permission from O. H. Schuck and R. W. Young (1943). "Observations on the Vibrations of Piano Strings." In: *The Journal of the Acoustical Society of America* 15.1, pp. 1–11. DOI: 10.1121/1.1916221, p. 5. Copyright The Journal of the Acoustical Society of America 2005, Acoustic Society of America.

> "To tune upward by an octave, one adjusts the tension of the upper string until its fundamental has the same frequency as the second mode of the lower string, as indicated by the absence of beats. If the second mode of the lower string is sharper than a true second harmonic of the fundamental, then the upper string's fundamental will be tuned sharp. The next octave jump will increase the sharpening still further, particularly since the inharmonicity increases toward the high end,..."[68]

Longitudinal Vibrations of Piano Strings

During collision with the hammer the piano string is slightly elongated. This displacement along the axis of the string implies longitudinal vibrations. Their amplitudes are small compared to the transversal vibrations, but they affect the tonal quality of the piano tone. Particularly for the lower notes of the piano they

[68] Schuck and Young, "Observations on the Vibrations of Piano Strings," p. 8-9.

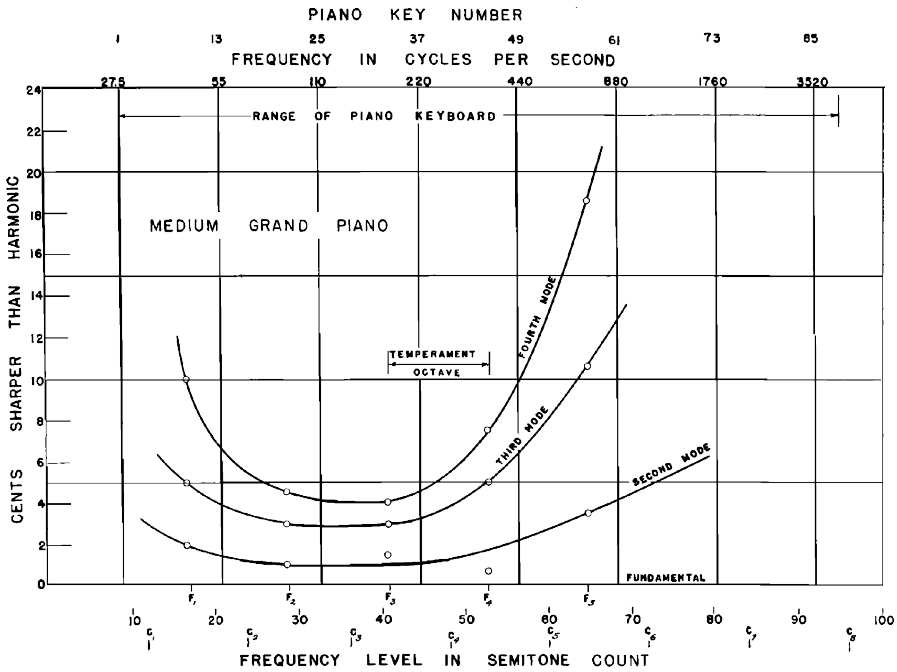

Figure 2.11.: Inharmonicity dependence of piano range. Reprinted with permission from O. H. Schuck and R. W. Young (1943). "Observations on the Vibrations of Piano Strings." In: *The Journal of the Acoustical Society of America* 15.1, pp. 1–11. DOI: 10.1121/1.1916221, p. 6. Copyright The Journal of the Acoustical Society of America 2005, Acoustic Society of America.

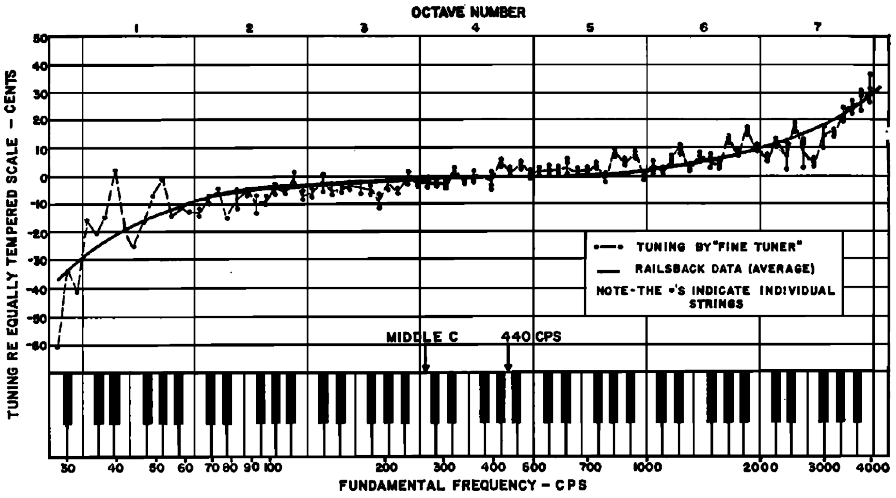

Figure 2.12.: Deviations from equal temperament in a small piano. Reprinted with permission from D. W. Martin and W. D. Ward (1961). "Subjective Evaluation of Musical Scale Temperament in Pianos." In: *The Journal of the Acoustical Society of America* 33.5, pp. 582–585. DOI: 10.1121/1.1908730, p. 583. Copyright The Journal of the Acoustical Society of America 1961, Acoustic Society of America.

contribute significantly to the tonal character.[69] Conklin measured the pitch relation of the transverse and longitudinal modes and showed its influence on the quality of the tone. Listening tests suggest that longitudinal components are audible up to *C5* ($f_1 = 523\,\mathrm{Hz}$).[70]

[69] Conklin, "Design and tone in the mechanoacoustic piano. Part I. Piano hammers and tonal effects"; Askenfelt and Jansson, "From touch to string vibrations. I: Timing in the grand piano action"; Nicholas Giordano and A. J. Korty (1996). "Motion of a piano string: Longitudinal vibrations and the role of the bridge." In: *The Journal of the Acoustical Society of America* 100.6, pp. 3899–3908. DOI: 10.1121/1.417219.

[70] Balázs Bank and Heidi-Maria Lehtonen (2010). "Perception of longitudinal components in piano string vibrations." In: *The Journal of the Acoustical Society of America* 128.3, EL117–23. DOI: 10.1121/1.3453420; Balázs Bank and László Sujbert (2005). "Generation of longitudinal vibrations in piano strings: From physics to sound synthesis." In: *The Journal of the Acoustical Society of America* 117.4, pp. 2268–2278. DOI: 10.1121/1.1868212.

Part I.

Grand Piano Soundboard Characteristics in Different Stages of Production

3. Theory

3.1. Soundboard Structure

3.1.1. General Overview

Modern piano soundboards are assembled from 5 cm to 15 cm wide stripes of spruce. The thickness varies from 9 mm near the soundboard center to 6 mm near the edges. The soundboard is clamped rigidly to the outer rim. The elastic properties along and perpendicular to the wood grain are very different. The Young's modulus E for spruce along the grain is about 12 GPa, perpendicular to the grain it is almost 100 times smaller (0.1 GPa). The density ρ of spruce is roughly 0.4 g/cm^3, which leads to a high factor E/ρ. To reach a balanced relation of stiffness in along- and cross-grain direction and for static purposes, several ribs are glued to the bottom of the soundboard oriented about 90° to the grain direction. The ribs are tapered near the edges to increase the board flexibility especially for low frequencies.[71]

A modern piano has a treble- and a bass bridge, glued to the soundboard (see Figure 3.1). The bass bridge is taller than the treble bridge to allow the bass strings to cross over the higher strings and, thereby, to maximize the speaking length of all strings in the given space of the piano frame. The bridges are made of hardwood; softwood would not resist the mechanical stress at the bridge pins. The driving-point impedance presented to the strings is a function of frequency and position on the soundboard. Measurements of the sound-

[71] Paul H. Bilhuber (1937). *U.S. Patent No. 2,070,391: Soundboard for Pianos.*

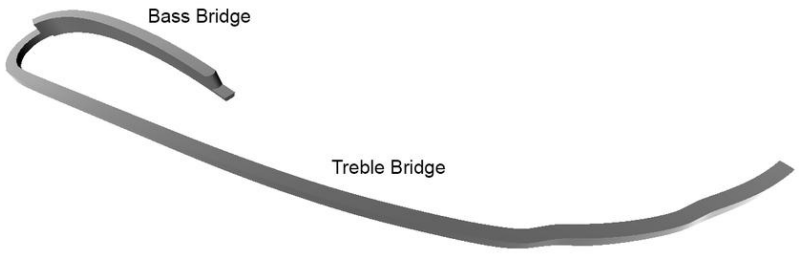

Figure 3.1.: Model of a concert grand bridge. The bass bridge and treble bridge are connected.

board mobility have been performed by Nakamura[72] and Conklin.[73] Wogram[74] and Jiang and Giordano[75] measured the mechanical impedance at the bridge. Moore and Zietlow[76] measured the deflection shapes of an upright piano with electronic speckle pattern interferometry. Figure 3.2 shows mobility plots[77]. The eigenmodes can be observed as local maxima in a Y vs. f plot. A comparison of the mobility plots for the soundboard a) with- and b) without string load shows that the load profoundly affects the behavior of the soundboard. The frequency of the breathing mode increased from 48 Hz to 60 Hz and its maximum decreased about 15 dB.[78] The string load seems to smoothen the mobility curves. For a detailed discussion on the mechanical mobility of piano soundboards see Section 6.3.

The design of the bridges affects the tonal quality drastically. The bridge in-

[72] Nakamura, "The vibrational character of the piano soundboard."

[73] Harold A. Conklin (1996c). "Design and tone in the mechanoacoustic piano. Part III. Piano strings and scale design." In: *The Journal of the Acoustical Society of America* 100.3, pp. 1286–1298. DOI: 10.1121/1.416017.

[74] Wogram, *Akustische Untersuchungen an Klavieren*.

[75] Minghui Jiang and Nicholas Giordano (1999). "Sound production by a vibrating piano soundboard: Theory." In: *The Journal of the Acoustical Society of America* 106.4, pp. 2141–2141. DOI: 10.1121/1.427322.

[76] Thomas R. Moore and Sarah A. Zietlow (2006). "Interferometric studies of a piano soundboard." In: *The Journal of the Acoustical Society of America* 119.3, pp. 1783–1793. DOI: 10.1121/1.2164989.

[77] The *mobility* or *admittance* Y is the reciprocal of the complex mechanical impedance Z.

[78] Conklin, "Design and tone in the mechanoacoustic piano. Part III. Piano strings and scale design."

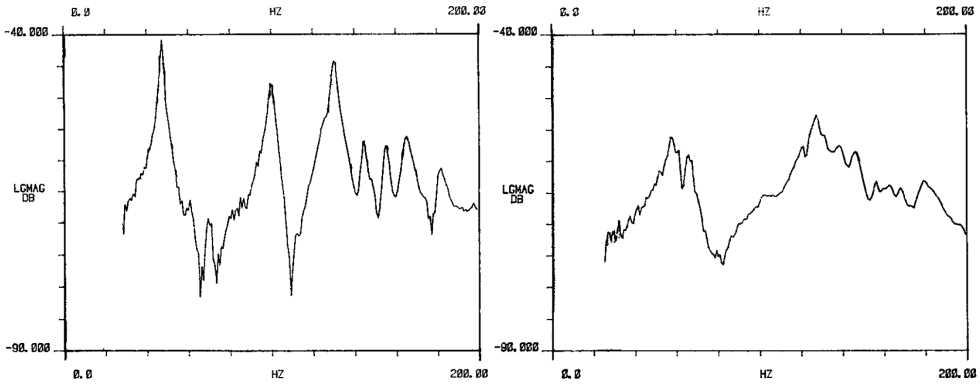

(a) **(b)**

Figure 3.2.: Mobility as a function of frequency for the termination point of the *E2* string on the bridge. Measurements where taken perpendicular to the soundboard plane. **a)** strings and plate removed, **b)** strings assembled and tuned. Reprinted with permission from Harold A. Conklin (1996b). "Design and tone in the mechanoacoustic piano. Part II. Piano structure." In: *The Journal of the Acoustical Society of America* 100.2, pp. 695–708. DOI: 10.1121/1.416233, p. 698. Copyright The Journal of the Acoustical Society of America 1996, Acoustic Society of America.

creases the impedance mismatch between strings and soundboard, and therefore slows the energy transfer from strings to soundboard. Additionally, the bridge acts as a lever to transfer string vibration that is directed parallel to the soundboard (longitudinal-, and horizontal polarized transversal vibrations). The breathing mode f_1 for a typical piano soundboard appears at approx. 50 Hz to 100 Hz. Figure 3.2 shows a rapid decrease in mobility for frequencies below this mode. According to this, the soundboard still vibrates in lower frequencies, but its amplitude is heavily decreased for the same applied force. Even for a concert grand with a breathing mode $f_1 = 50$ Hz, the strings of almost the first octave *A0-G1* have fundamental frequencies below the first soundboard mode.

3.1.2. Ribs

A set of 15-18 wooden ribs is glued to the bottom of the soundboard. The ribs are arranged rectangular to the grain direction of the soundboard strips (130°) with an inter-rib distance of 100 mm to 150 mm (see Figure 3.3). Besides for static reasons, the ribs are applied to compensate the anisotropy of the wood by adding stiffness across the grain and, thereby, strengthening the radial axis. Additionally, the application of ribs reduces the formation of cracks due to variations in climate conditions.[79] After Conklin, "*the cross-grain stiffness of a ribbed solid-wood soundboard comes predominantly from the ribs. For that reason the characteristics of a piano soundboard are relatively independent of variations in the cross-grain properties of the strips themselves.*"[80] Therefore, in contrast to the violin, variation in E_R of the soundboard plate strips will not affect the overall behavior of the soundboard significantly, since the mechanical properties in radial direction are dominated by the ribs.[81]

Above a critical frequency, the soundboard modes fit into the spacing between the ribs with their nodal lines, for lower frequencies the modes distribute in the

[79] Conklin, "Design and tone in the mechanoacoustic piano. Part II. Piano structure."
[80] Ibid.
[81] Ege, "La table d'harmonie du piano-Études modales en basses et moyennes fréquences."

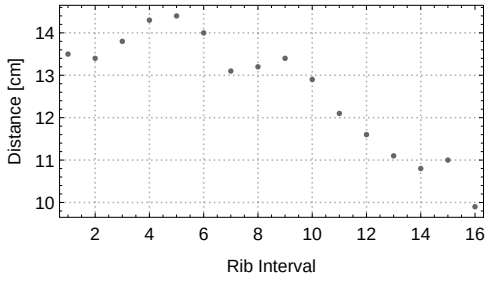

Figure 3.3.: Inter-rib-distances from bass to treble for a modern concert grand piano.

soundboard regardless of the rib spacing.[82] Chaigne, Cotté, and Viggiano[83] describe this critical frequency to be reached when the distance between adjacent ribs is comparable to half the structural wavelength, empirically verified by Moore and Zietlow.[84] The ribs start to play the role of almost rigid boundary conditions. Therefore, the inter-rib distance becomes an important parameter to influence the higher eigenmodes and even small irregularities in the rib spacing can change the piano's tonal quality. In this regard, Conklin[85] suggested a new configuration of ribs for the piano soundboard (compare Figure 3.4): To increase the first cut-off frequency to the range of the fundamental frequency of the highest note ($C8 \approx 4186\,\mathrm{Hz}$), he proposed a configuration with 39 ribs instead of 17. The rib height is unmodified but the rib width is decreased from 25 mm to 11 mm. This way, the total stiffness increase due to application of the ribs is similar but the inter-rib distance is more than halved. According to Conklin, the altered configuration should lead to 'improved tonal quality' and 'increased uniformity of frequency response'. Nevertheless, to the knowledge of the author, the proposed design has not yet been systematically applied.

The ribs, as well as the soundboard, are tapered in the edge area. The concept of

[82] Wogram, *Akustische Untersuchungen an Klavieren*; Nicholas Giordano, Harvey Gould, and Jan Tobochnik (1998). "The physics of vibrating strings." In: *Computers in Physics* 12.2, p. 138. DOI: 10.1063/1.168621.

[83] Antoine Chaigne, Benjamin Cotté, and Roberto Viggiano (2013). "Dynamical properties of piano soundboards." In: *The Journal of the Acoustical Society of America* 133.4, pp. 2456–2466. DOI: 10.1121/1.4794387.

[84] Moore and Zietlow, "Interferometric studies of a piano soundboard."

[85] Conklin, *U.S. Patent No. US3866506 A: Soundboard construction for stringed musical instruments*.

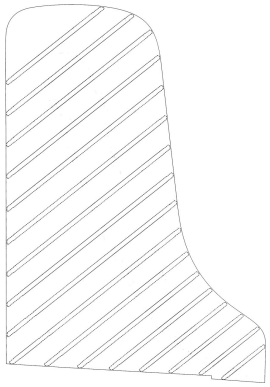

(a) Modern concert grand piano: 17 ribs, average inter-rib distance: 12.65 cm, average rib height: 20 mm, average rib width: 25 mm.

(b) Suggestion by Conklin: 39 ribs, average inter-rib distance: 5.5 cm, average rib height: 20 mm, average rib width: 11 mm.

Figure 3.4.: Rib configuration for a modern concert grand piano vs. a suggestion by Harold A. Conklin (1973). *U.S. Patent No. US3866506 A: Soundboard construction for stringed musical instruments.*

a *diaphragmatic soundboard* is based on the work of Paul Bilhuber, a Steinway family member by marriage, who was responsible for most of the technical innovations at *Steinway & Sons* in the early 20th century. The patented idea[86] is still implemented today in modern pianos. By thinning the outer regions of the soundboard, a stiffness decrease should increase the mobility, which can be favorable for low frequencies.[87]

The ribs of a modern grand piano are tapered at the ends from a height of approx. $h_r \approx 20\,\text{mm}$ down to $h_r \approx 4\,\text{mm}$, which can be approximated for a distance d from the start of the notch with the exponential function $h_r(d)$ [mm]:

$$h_r(d) = 19.55e^{-0.024d} + 4. \tag{3.1}$$

Figure 3.5 shows the measured tapering profile for the concert grand piano at

[86] Paul H. Bilhuber (1936). *U.S. Patent No. 2,051,633: Soundboard for pianos and other instruments or devices using soundboards.*

[87] Bilhuber and Johnson, "The Influence of the Soundboard on Piano Tone Quality."

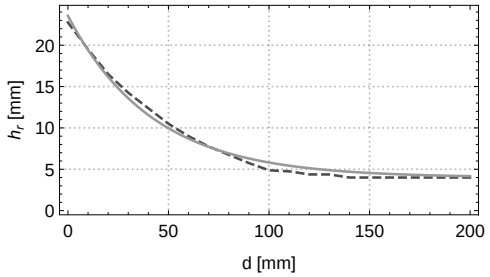

Figure 3.5.: Tapering curve for piano ribs. The dashed line depicts the average of 10 measurements on the concert grand piano at hand, the bright line shows the exponential curve fit as given in Equation 3.1.

hand vs. an exponential curve fit after Equation 3.1.

3.1.3. Driving Point Mobility

The impedance mismatch between strings and soundboard is a crucial factor for the actual sound produced by a piano. If the mismatch is too small the tone is harsh and short, if it is too great the tone becomes long but too soft.[88] Historically, piano manufacturers tried to find the optimum relation by experimenting with the structural design of the soundboard and strings.
The driving point mobility

$$Y(\omega) = \frac{v(\omega)}{F(\omega)}, \tag{3.2}$$

with ω being the angular frequency is a widely accepted parameter to describe the frequency dependent behavior of musical instrument parts as a ratio between a complex velocity response v and a complex excitation force F for one specific point and angle on the vibrating structure. For the present work, only the direction normal to the soundboard is considered. A detailed description

[88] Conklin, "Design and tone in the mechanoacoustic piano. Part II. Piano structure."

of mobility concepts can be found in several textbooks.[89]
Wogram is the first to describe the vibrational behavior of a piano soundboard by means of driving point impedances.[90] He performs measurements on an upright piano soundboard, with and without strings. Subsequent publications question the correctness of his data in the higher frequency range: The impedance falloff above 1 kHz, inversely proportional to frequency, is considered to appear due to decoupling of excitation device and soundboard.[91] Nakamura presents mobility measurements for a completely assembled upright piano.[92] Consistent with Wogram, he observes an increase of mobility above 1 kHz. Even though the resonances of his measurement devices are located in the regarding frequency range, he explains the increase with the ribs becoming fixed edges for high frequency vibrations. Giordano performs impedance measurements on a fully assembled upright piano.[93] He confirms a decrease of impedance above 2.5 kHz for measurements at the bridge. Ege and Boutillon[94] give a synthetic description for the mobility of a fully assembled upright piano based on three parameters: modal density, mean loss factor and structure mass. They explain a rise of mobility in high frequencies to be dependent on the inter-rib effect, to occur when the wavelength equals twice the rib spacing. A transition frequency range between 2 kHz and 3 kHz, from which onward the soundboard motion is governed by the ribs, is also proposed by Berthaut, Ichchou, and Jézéquel[95] and experimentally confirmed by Moore and Zietlow.[96] After Conklin,[97] the attenuation effect due to ribbing

[89] L. Cremer, M. Heckl, and B.A.T. Petersson (2005). *Structure-Borne Sound*. Berlin, Heidelberg: Springer Berlin Heidelberg, pp. 1–607. DOI: 10.1007/b137728; M. P. Norton and D. G. Karczub (2003). *Fundamentals of Noise and Vibration Analysis for Engineers*. Cambridge University Press, pp. 147–155. DOI: 10.3397/1.2721371.

[90] Wogram, *Akustische Untersuchungen an Klavieren*.

[91] Giordano, "Mechanical impedance of a piano soundboard"; Kerem Ege and Xavier Boutillon (2010a). "Synthetic description of the piano soundboard mechanical mobility." In: *arXiv preprint arXiv:1210.5688* August, pp. 25–31.

[92] Nakamura, "The vibrational character of the piano soundboard."

[93] Giordano, "Mechanical impedance of a piano soundboard."

[94] Ege and Boutillon, "Synthetic description of the piano soundboard mechanical mobility."

[95] Berthaut, Ichchou, and Jézéquel, "Piano soundboard: Structural behavior, numerical and experimental study in the modal range."

[96] Moore and Zietlow, "Interferometric studies of a piano soundboard."

[97] Conklin, *U.S. Patent No. US3866506 A: Soundboard construction for stringed musical instruments*.

should occur at 1.2 kHz for conventional rib spacing. Conklin[98] presents mobility measurements of a concert grand piano (with conventional rib spacing) with and without strings. Stringing seems to increase resonance frequencies and to lower peak values. No influence of down-bearing on mobilities is observable above 1 kHz. Contradictory to previous publications, his data does not confirm a mobility increase at high frequencies (he presents mobility functions up to 3.2 kHz). The present work tries to elaborate on some of the issues and questions remaining with regard to these, often contradictory, findings.

3.1.4. Curvature and Internal Stresses

The bridges and the soundboard have to withstand a static load from the string tension as a result of a small angle from the bridge pin downwards to the hitch pin. This down bearing has a strength of about 0.3%-0.5% of the string tension force in direction perpendicular to the soundboard, which adds up to 1800 N.[99] To withstand this constant load, the soundboard is manufactured to a convex shape which is called *crowning* or *curvature*. This shape is the result of a careful treatment through the production process. The development of the final shape is influenced by a) the order in which ribs and bridge are applied and the ribs are tapered, b) combination of varnishing the soundboard surfaces[100] and succession of air conditioning steps, and c) depends on the angles of the rim profile the soundboard is glued into. After gluing the soundboard to the rim but prior to attaching the strings, the curvature has a radius of about 15 m to 50 m. With the strings under full tension the soundboard is said to be only slightly crowned. The static load on the convex shaped soundboard (also called *pre-stress*) contributes essentially to the brightness of the piano sound.[101]

[98] Conklin, "Design and tone in the mechanoacoustic piano. Part II. Piano structure."

[99] Conklin, "Design and tone in the mechanoacoustic piano. Part III. Piano strings and scale design."

[100] As a first step, only the bottom side is sealed. This way, moisture can permeate into the wood only from the topside leading to a dis-balance in water exchange which increases the curvature.

[101] Ege and Boutillon, "Synthetic description of the piano soundboard mechanical mobility"; Adrien Mamou-Mani et al. (2012). "Prestress effects on the eigenfrequencies of the soundboards: Experimental results on a simplified string instrument." In: *The Journal of the Acoustical Society of America* 131.1, pp. 872–877. DOI: 10.1121/1.3651232.

The relationship between tension and increased eigenmode frequencies is nonlinear.[102]

3.1.5. Radiation

For sounds with wavelengths λ much greater than the size of the soundboard, the efficiency of radiation of the soundboard is rather small. When the distance from the top- to the bottom side of the soundboard is smaller than λ, the produced pressure waves of both sides have a disposition to interfere and mutually cancel.[103] Consider for instance that the *E2* string in Figure 3.2 has a fundamental frequency $f_1 = 82.4\,\text{Hz}$. This corresponds to a wavelength $\lambda_0 = 4.16\,\text{m}$ for $c = 343\,\text{m}\,\text{s}^{-1}$, which already exceeds the size of a concert grand. The lowest bass note *A0* has a wavelength $\lambda_0 = 12.5\,\text{m}$. Therefore, the first resonances, especially in the bass range, have suppressed radiated amplitudes relative to the higher resonances. For the lowest bass notes mostly the f_1 octave defines the perceived pitch.
To characterize the sound production of a vibrating soundboard the ratio p/v_b can be used as a ratio between the produced sound pressure p and the velocity of the soundboard v_b. Both p and v_b are functions of the positions where they are measured and applied, and of the exciting frequency. Wogram[104] measures p/v_b for an upright piano and finds a strong decrease above about 1 kHz. Giordano's measurements of p/v_b for an upright piano are consistent with the results of Suzuki,[105] but do not agree with the results of Wogram.[106] All measurements show a decreasing p/v_b at low frequencies. This is due to the wavelength λ becoming larger than the size of the soundboard. Suzuki[107] measures the radiation efficiency as the ratio of radiated power to injected mechanical power for a grand piano. Below 80 Hz radiation efficiency is low due to the

[102] Adrien Mamou-Mani, Joël Frelat, and Charles Besnainou (2008). "Numerical simulation of a piano soundboard under downbearing." In: *The Journal of the Acoustical Society of America* 123.4, pp. 2401–2406. DOI: 10.1121/1.2836787.
[103] Rossing, *The Science of String Instruments*.
[104] Wogram, *Akustische Untersuchungen an Klavieren*.
[105] Suzuki, "Vibration and sound radiation of a piano soundboard."
[106] Jiang and Giordano, "Sound production by a vibrating piano soundboard: Theory."
[107] Suzuki, "Vibration and sound radiation of a piano soundboard."

described short-circuit effect between upper and bottom side of the soundboard. The *critical frequency*, as the transition range where the radiated sound wavelengths become shorter than the flexural wave lengths in the soundboard, is found at 1.2 kHz to 1.6 kHz. For higher frequencies, the radiation becomes very efficient.

3.2. Soundboard Material

3.2.1. Elastic Constants of Wood

In the following section, the elastic constants needed for the description of vibrations in wood are derived after Bucur:[108]
After Hooke's law, the elastic properties of a solid structure can be described as

$$[\sigma] = [C] \times [\varepsilon] \,, \tag{3.3}$$

with the volume average stress matrix $[\sigma]$, the volume average strain matrix $[\varepsilon]$, and the elasticity matrix $[C]$. Or, with compliances $[S]$ instead of stiffnesses:

$$[\varepsilon] = [S] \times [\sigma] \,, \tag{3.4}$$

with $[C] = [S]^{-1}$.

Following Equation 3.3, since strain is dimensionless, stiffness has the same dimensions as stress [N/m² = Pa].

[108] Voichita Bucur (2006). *Acoustics of Wood*. Springer Series in Wood Science. Berlin: Springer-Verlag. DOI: 10.1007/3-540-30594-7, pp. 39–69.

Isotropic Case

For the simplest case of an isotropic material, the elastic symmetry depends on only two independent constants, λ_{lam} and shear modulus G:

$$G = \frac{E}{2(1+\nu)}, \tag{3.5}$$

$$\lambda_{lam} = \frac{E\nu}{(1+\nu)(1-2\nu)}, \tag{3.6}$$

$$K = \frac{E}{3(1-2\nu)} = \lambda_{lam} + \frac{2}{3}G, \tag{3.7}$$

with the Young's modulus E, G, the Poisson's ratio ν, and the bulk modulus K with the Lamé coefficients λ_{lam} and G. The entries in the stiffness matrix $[C]$ are

$$C_{11} = C_{22} = C_{33} = \lambda_{lam} + 2G, \tag{3.8a}$$
$$C_{12} = C_{23} = C_{13} = \lambda_{lam}, \tag{3.8b}$$
$$C_{44} = C_{55} = C_{66} = G, \tag{3.8c}$$

or

$$\begin{bmatrix} C_{11} & C_{12} & C_{12} & 0 & 0 & 0 \\ & C_{11} & C_{12} & 0 & 0 & 0 \\ & & C_{11} & 0 & 0 & 0 \\ & & & (C_{11}-C_{12})/2 & 0 & 0 \\ & & & & (C_{11}-C_{12})/2 & 0 \\ & & & & & (C_{11}-C_{12})/2 \end{bmatrix}. \tag{3.9}$$

The propagation velocity of a longitudinal wave in an infinite solid is

$$c_{long} = \sqrt{\frac{E_{11}}{\rho}} = \sqrt{\frac{\lambda_{lam} + 2G}{\rho}}, \tag{3.10}$$

with the density ρ. The propagation velocity of a transversal wave in an infinite solid is

$$c_{trans} = \sqrt{\frac{G}{\rho}}. \tag{3.11}$$

Orthotropic Case

Wood can be defined as an orthotropic solid, which implies that elastic constants are described in three perpendicular planes of elastic symmetry: the longitudinal axis (L) along the fiber direction, the radial (R) direction along the radius of the cross section of the trunk, and the tangential (T) direction as the tangent on the approximated circle of the cross section (illustrated in Figure 3.6).
In this case, the compliance matrix $[C]$ contains nine independent constants: six diagonal terms and three off-diagonal terms:

$$[S] = \begin{bmatrix} S_{11} & S_{12} & S_{13} & 0 & 0 & 0 \\ S_{21} & S_{22} & S_{23} & 0 & 0 & 0 \\ S_{31} & S_{32} & S_{33} & 0 & 0 & 0 \\ 0 & 0 & 0 & S_{44} & 0 & 0 \\ 0 & 0 & 0 & 0 & S_{55} & 0 \\ 0 & 0 & 0 & 0 & 0 & S_{66} \end{bmatrix}, \tag{3.12}$$

with the following physical significance: S_{11}, S_{22}, and S_{33} relate an extensional stress to an extensional strain in the same direction, which yields the Young's moduli E_L, E_R, and E_T (see Section 3.2). S_{12}, S_{13}, and S_{23} relate an extensional strain to a perpendicular extensional stress, which leads to the six Poisson's ratios. S_{44}, S_{55}, and S_{66} relate a shear strain to a shear stress in the same plane, which leads to the shear ratios, corresponding to planes 23, 13, and 12. The Hooke's law in compliance form for wood is then

$$\begin{bmatrix} \varepsilon_{LL} \\ \varepsilon_{RR} \\ \varepsilon_{TT} \\ \varepsilon_{LR} \\ \varepsilon_{LT} \\ \varepsilon_{RT} \end{bmatrix} = \begin{bmatrix} \frac{1}{E_L} & -\frac{\nu_{LR}}{E_R} & -\frac{\nu_{LT}}{E_T} & 0 & 0 & 0 \\ -\frac{\nu_{RL}}{E_L} & \frac{1}{E_R} & -\frac{\nu_{12}}{E_R} & 0 & 0 & 0 \\ -\frac{\nu_{TL}}{E_L} & -\frac{\nu_{TR}}{E_R} & \frac{1}{E_T} & 0 & 0 & 0 \\ 0 & 0 & 0 & \frac{1}{G_{RT}} & 0 & 0 \\ 0 & 0 & 0 & 0 & \frac{1}{G_{LT}} & 0 \\ 0 & 0 & 0 & 0 & 0 & \frac{1}{G_{LR}} \end{bmatrix} \begin{bmatrix} \sigma_{LL} \\ \sigma_{RR} \\ \sigma_{TT} \\ \sigma_{LR} \\ \sigma_{LT} \\ \sigma_{RT} \end{bmatrix}. \tag{3.13}$$

Rectangular Wood Plates

Since wood can be described as an orthotropic material, the elastic constants are related by

$$\frac{\nu_{ij}}{E_i} = \frac{\nu_{ji}}{E_j}, \tag{3.14}$$

for $i, j = L, R, T$.
For a rectangular wooden thin plate with free boundary conditions and lengths L_L and L_R, the lowest (1,1) mode can be approximated by

$$f_{1,1} = \frac{h}{L_L L_R}\sqrt{\frac{G}{\rho}} \approx \frac{h c_R c_L}{L_L L_R}\sqrt{\frac{1-\sqrt{\nu_{RL}\nu_{LR}}}{2}}, \tag{3.15}$$

with shear module

$$G = \frac{\sqrt{E_L E_R}}{2(1+\sqrt{\nu_L \nu_R})}. \tag{3.16}$$

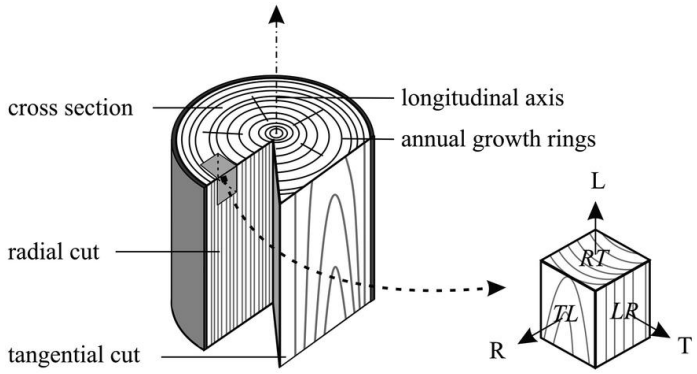

Figure 3.6.: Radial (R), tangential (T), and longitudinal (L) axis in a tree trunk. The radial cut plane corresponds to the surface of a *quarter-sawn* plank. Republished with permission of The American Society of Civil Engineers, from Bettina Franke and Pierre Quenneville (Mar. 2011). "Numerical Modeling of the Failure Behavior of Dowel Connections in Wood." In: *Journal of Engineering Mechanics* 137.3, pp. 186–195. DOI: 10.1061/(ASCE)EM.1943-7889.0000217, p. 188; permission conveyed through Copyright Clearance Center, Inc.

3.2.2. Wood for Piano Soundboards

Two species of spruce are utilized for piano soundboards: *Picea sitchensis* (Sitka spruce) and *Picea excelsa* (Norway/European spruce) with marginal differences in material properties (see Table 3.1). For soundboard manufacture, logs are sawn in *quarter-cut*, a sawing technique which gives predominantly edge-grain strips. The width of a single strip is limited by the radius of the tree trunk. Soundboards are manufactured by glue-laminating approx. 15-20 strips with a width of 5 cm to 15 cm. As shown by Schleske,[109] sound velocity in R direction decreases rapidly for soundboards with smaller annual ring angles (< 90° to the radial plane), hence, 'standing' annual rings (90° to the radial plane) are preferred. For concert grand models, strips from the centerpiece of the quarter cut is preferably used, giving perfect rectangular (90°) annual ring angles. For less expensive instruments annual ring angles can vary widely with minimum values of 45°.

[109] Martin Schleske (1990). "Speed of sound and damping of spruce in relation to the direction of grains and rays." In: *Catgut Acoustical Society Journal* 1.6, pp. 16–20.

The proportion of late wood to early wood is approx. 25 %, the relation of densities between late and early wood is chosen as great as possible, with the transition between them as smooth as possible.[110] Ring widths of 1 mm to 2 mm are acceptable for high quality instruments.[111]
In relation to other species, spruce is characterized by a high degree of anisotropy ($E_L/E_R > 10$), which is particularly beneficial for the low frequency modes.[112]
The sound speed in a bar $c = \sqrt{E/\rho}$ is similar for spruce (in L direction) and aluminum, which implies a high correlation between E_L and ρ.[113]
Mechanical properties for Sitca spruce and European spruce are given in Table 3.1, averaged from data by Haines[114] and Hearmon.[115] After Ono,[116] the requirements for high quality soundboard wood can be summarized as follows:

- high anisotropy,
- low density,
- high sound velocity,
- high acoustic radiation,
- high Young's modulus in L direction,
- low damping coefficient in L direction (see Section 3.2.5).

[110] Ulrike G. K. Wegst (2006). "Wood for sound." In: *American Journal of Botany* 93.10, pp. 1439–1448.
[111] F. Rocaboy and Voichita Bucur (1990). "About the physical properties of wood of twentieth century violins." In: *Catgut Acoustical Society Journal* 1.6.
[112] Chris Waltham and Shigeru Yoshikawa (2018). "Construction of Wooden Musical Instruments." In: *Springer Handbook of Systematic Musicology*. Ed. by Rolf Bader. Springer H. Springer, Berlin, Heidelberg, pp. 63–79. DOI: 10.1007/978-3-662-55004-5_4.
[113] Ibid.
[114] Daniel W. Haines (1980). "On musical instrument wood - part 2." In: *Catgut Acoustical Society Journal* 1.31, pp. 19–23.
[115] Roy F. S. Hearmon (1948). "Elasticity of Wood and Plywood." In: *Nature* 162.4125, pp. 826–826. DOI: 10.1038/162826a0.
[116] Teruaki Ono (1981). "Relationship of the Selection of Wood Used for Piano Soundboards to the Dynamic Mechanical Properties." In: *Journal of the Society of Materials Science, Japan* 30.334, pp. 719–724.

Table 3.1.: Mechanical properties of Sitka spruce and European spruce (standard deviation σ in brackets).

Unit	ρ [kg m^{-3}]	c_L [m s^{-1}]	c_R [m s^{-1}]	E_L [GPa]	E_R [GPa]	E_T [GPa]	G_{LT} [GPa]	G_{RT} [GPa]	G_{LR} [GPa]	ν_{LR}	ν_{LT}	ν_{RT}	η_L	η_R
Picea sitchensis	425	5300	1400	12.3	0.89	0.50	0.85	0.05	0.75	0.37	0.47	0.43	8.30	21.00
(σ)	(50)	(280)	(210)	(2.5)	(0.24)	-	(0.22)	(0.03)	-	-	-	-	(1.00)	(2.90)
Picea excelsa	450	5600	1300	15.4	0.72	0.39	0.80	0.04	0.62	0.44	0.38	0.47	6.70	20.40
(σ)	(51)	(260)	(200)	(2.1)	(0.26)	-	(0.22)	(0.01)	-	-	-	-	(1.00)	(3.20)

3.2.3. Influence of Wood Moisture Content

As a hygroscopic material, wood absorbs and reabsorbs water from the ambient medium. The *equilibrium moisture content* (EMC) of wood is the moisture content (MC), where the material neither gains nor looses moisture to the ambient medium. Its value depends on relative humidity (RH) and temperature. When ambient conditions are changed, the wooden structure will adapt to its environment by absorbing or reabsorbing moisture until the EMC is reached. String instruments in concert hall condition have an EMC of approx. 7 % to 12 %. Temperature changes affect all wood properties in the order of 0.5 %/°C in R direction. The influence of wood moisture content on the mechanical properties is more pronounced with an average order of 4 %/%MC.[117] An example illustrates the importance: A change in relative humidity from 40 % to 70 % will yield a change of moisture content in a wood sample of 7 %. Applying the estimation from above, this would lead to an average change in mechanical properties by 28 %. As a general tendency, a decreased wood moisture content leads to an increase of mechanical and acoustical properties.[118] Dimensional modifications in response to changing moisture content affect the structure, strongly dependent on the orientation: With a decrease of moisture content from 30 % to 0 %, spruce shrinks by 4 % in R direction and by 7 % in T direction.[119] Applied to a grand piano soundboard, this would correspond to a shrinkage of 40 mm in R direction.
Borland[120] finds the effect of a changed wood moisture content (11 % to 7 %) on the modal frequencies of a guitar top plate to be small (< 2 %). The effect on the damping coefficient, however, has been found to be significant with 27 % change of the quality factor Q (see Section 3.2.5) for the first mode.

[117] Bucur, *Acoustics of Wood*.
[118] Ibid.
[119] Voichita Bucur (2016). *Handbook of Materials for String Musical Instruments*. Cham: Springer International Publishing. DOI: 10.1007/978-3-319-32080-9.
[120] M. J. Borland (2014). "The Effect of Humidity and Moisture Content on the Tone of Musical Instruments." PhD thesis, pp. 1–146.

3.2.4. Influence of Varnishes

Besides the effects of beautifying and preserving wooden surfaces, a major reason for applying varnish is to prevent moisture ingress and, thereby, reducing the effects described above. Comprehensive studies have been conducted on the influence of varnishes on the tonal quality of violin family instruments.[121] Varnishing violin top plates has been found to marginally increase plate stiffness and damping losses.[122] Varnishing of spruce plates decreases sound power levels (SPL) in low frequencies (< 300 Hz), and increases or decreases SPL in high frequencies (> 3000 Hz), depending on E_R.[123] For piano soundboards, water-based varnishes, shellac, lacquer, and even epoxy resin have been used.[124] In general, application of varnish increases the internal damping,[125] whereby shellac seems to have less impact on damping and Young's modulus than Polyester varnish.[126] The sealing layer has different mechanical properties compared to the wooden structure, e.g. the density of applied varnish is higher than the density of spruce (early- and late wood averaged) by a factor of 2-3. Therefore, it is preferable to apply coatings as thin as possible to minimize its influence on the E/ρ ratio for the worse.

[121] Morton A. Hutchins (1991). "Effects on spruce test strips of four-year application on four different sealers plus oil varnish." In: *Catgut Acoustical Society Journal* 1.7, pp. 11–16; Martin Schleske (1998). "On the acoustical properties of violin varnish." In: *Catgut Acoustical Society Journal* 3.6, pp. 27–43.

[122] John C. Schelleng (1968). "Acoustical Effects of Violin Varnish." In: *The Journal of the Acoustical Society of America* 44.5, pp. 1175–1183. DOI: 10.1121/1.1911243.

[123] Teruaki Ono (1993). "Effects of varnishing on acoustical characteristics of wood used for musical instrument soundboards." In: *Journal of the Acoustical Society of Japan (E)* 14, pp. 397–407. DOI: 10.1250/ast.14.397.

[124] Edwin M. Good (2001). *Giraffes, Black Dragons, and Other Pianos*. Stanford University Press.

[125] Schelleng, "Acoustical Effects of Violin Varnish"; Ono, "Effects of varnishing on acoustical characteristics of wood used for musical instrument soundboards."

[126] Mohammadreza Ghaznavi et al. (2013). "Traditional Varnishes and Acoustical Properties of Wooden Soundboards." In: *Science International* 1.12, pp. 401–407. DOI: 10.17311/sciintl.2013.401.407.

3.2.5. Damping in wood

When vibrational energy is distributed through a musical instrument[127], three mechanisms of energy loss have to be taken into account: a) damping due to radiation into the surrounding medium, b) energy loss through the boundary conditions between instrument components, and c) loss of vibrational energy due to internal friction. The acquisition of the individual types of damping for a complex vibrating structure like a musical instrument is difficult due to the interrelation between loss types: E.g. when measuring a radiated sound with a microphone, the observed decay is always the sum of the combination of all losses. However, approaches have been performed to deduce loss types from measurements of the total damping[128] or by suppressing one of the losses, e.g. with measurements in vacuum conditions.[129] The reasons for the intrinsic damping are not perfectly clear, thermodynamic losses, viscoelastic losses due to shearing, and even quantum mechanical effects are considered.[130]

In the following, examples of energy loss are given for each loss type related to the piano:

- For a musical instrument energy loss by radiation into the surrounding medium is highly desired as the soundboard is designed specifically for this purpose. However, the radiated piano sound also consists of components produced when the key hits the key bed and by mechanical friction in the action.

- After clamping the soundboard into the rim, it is considered to have fixed boundary conditions, assuming that no vibrational energy can

[127] A simplified transfer path for the piano would be: Key -> Hammer -> String -> Bridge -> Soundboard -> Air.

[128] George Bissinger (n.d.). *Extracting Internal Damping From Total Damping And Radiation Efficiency Measurements*. Tech. rep.

[129] Dietrich Holz (1974). "On some important properties of non-modified coniferous and leaved woods in view of mechanical and acoustical data in piano soundboards." In: *Archiwum Akustyki* 9.1, pp. 37–57.

[130] Allan D. Pierce (2010). "Intrinsic damping, relaxation processes, and internal friction in vibrating systems." In: *Proceedings of Meetings on Acoustics*. Vol. 9. May, pp. 065001–065001. DOI: 10.1121/1.3449319.

drain into the frame. However, frame and lid are actually excited by coupling and show distinct resonances.[131]

- Although being the least understood mechanism, the internal damping is shown to make up the greatest part of the total loss in a piano soundboard.[132] The degree of damping has a crucial impact on the produced sound: On one hand, a too low damping would make a soundboard unusable by causing a too selective radiation. Too much of the soundboard resonance characteristics would be present in the produced sound. This effect also seems to be the major reason for unsuccessful attempts of utilizing metal for piano soundboards.[133] On the other hand, a too high damping would impair the sound quality by extremely shortening the decay of the produced tone.[134]

Several parameters can be used to describe damping of an oscillator:[135]
In frequency domain, the dimensionless *quality factor* Q describes the degree of damping of a resonance as the ratio of the resonance center frequency f_r to its bandwidth Δf:

$$Q = \frac{f_r}{\Delta f}. \tag{3.17}$$

The bandwidth is defined as $\Delta f = f_2 - f_1$, with the frequency range $[f_1, f_2]$ where half of the power is attenuated (*half-power point*). The reciprocal of Q is called *loss-* or *damping factor* and denoted with η.

[131] Martin Keane (2006). "An evaluation of piano sound and vibration leading to improvements through modification of the material properties of the structure." PhD thesis. The University of Auckland.

[132] Holz, "On some important properties of non-modified coniferous and leaved woods in view of mechanical and acoustical data in piano soundboards."

[133] Hansing, *Das Pianoforte in seinen akustischen Anlagen*.

[134] W. Lottermoser and F. J. Meyer (1960). "Impulsmethode zur Messung von Geigenresonanzen." In: *Gravesaner Blätter* 5.19/20, pp. 106–119; E. Lieber (1979). "The influence of the soundboard on piano sound." In: *Das Musikinstrument* 20.

[135] Malte Kob (2017). "Experimental Approaches to the Study of Damping in Musical Instruments." In: *Studies in Musical Acoustics and Psychoacoustics*. Ed. by Albrecht Schneider. Springer International Publishing, pp. 187–200. DOI: 10.1007/978-3-319-47292-8_6.

In time domain, Q is defined as $Q = \pi f_r \tau$, with τ being the time the oscillator takes to decay to $1/e$ of its initial amplitude. The damping of an oscillator can also be described in time domain with the *logarithmic decrement* δ as the natural logarithm of the amplitude ratio of two subsequent maxima A_n and A_{n+1} as

$$\delta = \ln\left(\frac{A_n}{A_{n+1}}\right). \tag{3.18}$$

In room acoustics, damping of a resonating space is described with the *reverberation time* T_{60} [s] as the time interval for the sound pressure level to decrease by 60 dB. When dealing with insufficient signal-to-noise ratios (SNR), T_{60} is often extrapolated from the duration the signal needs for a 30 dB (T_{30}), or 20 dB (T_{20}) decrease.
The described measures are interrelated in the following way:

$$Q = \frac{1}{\eta} = \frac{\pi}{\delta} = \frac{2\pi f_r T_{60}}{6\ln(10)}. \tag{3.19}$$

For wood, Q is mostly given as three constants for L, R, and T direction, however, it is in fact frequency dependent. Fukada[136] found conifer wood samples to have maximum values at approx. 1 kHz, decreasing for frequencies $<$ 200 Hz and $>$ 3 kHz. Based on the frequency dependent damping curves alone they could distinguish between conifers and broad-leafed species. Holz[137] measures the relationship between damping factor and frequency for bars of Rumanian spruce resonant wood: η stays almost constant from 100 Hz to 2000 Hz. Above 2 kHz, η increases nonlinearly with frequency. Regarding the relationship between damping, density, and Young's modulus, Holz reports an increase of E and a decrease of η, when ρ is increasing.

[136] Eiichi Fukada (1950). "The Vibrational Properties of Wood I." in: *Journal of the Physical Society of Japan* 5.5, pp. 321–327. DOI: 10.1143/JPSJ.5.321.

[137] Holz, "On some important properties of non-modified coniferous and leaved woods in view of mechanical and acoustical data in piano soundboards."

3.2.6. Dispersion in wood

The transverse displacement $w(x, y, t)$ in z direction of a thin isotropic plate in the x,y plane with thickness h satisfies the differential equation[138]

$$D\left(\frac{\partial^4 w}{\partial x^4} + \frac{\partial^4 w}{\partial y^4} + 2\frac{\partial^4 w}{\partial x^2 \partial y^2}\right) + \rho h \frac{\partial^2 w}{\partial t^2} = 0, \tag{3.20}$$

with the flexural rigidity $D = \frac{Eh^3}{12(1-\nu^2)}$.

Assuming a harmonic solution

$$w(x, y, t) = W e^{ik_x x} e^{ik_y x} e^{i\omega t}, \tag{3.21}$$

with wavenumbers k_x and k_y. Inserting 3.21 into 3.20 gives the dispersion relation

$$D\left(k_x^2 + k_y^2\right)^2 - \rho h \omega^2 = 0. \tag{3.22}$$

With the wave heading θ,

$$\begin{aligned} k_x &= k\cos\theta, \\ k_y &= k\sin\theta, \\ k^2 &= k_x^2 + k_y^2, \end{aligned} \tag{3.23}$$

the bending wavenumber k is related to frequency in the following way (see Figure 3.7):

$$k = \sqrt{\omega}\left(\frac{\rho h}{D}\right)^{1/4}. \tag{3.24}$$

[138] Fletcher and Rossing, *The Physics of Musical Instruments.*

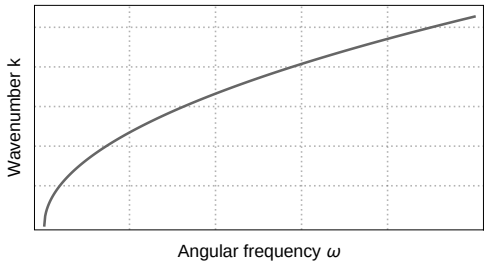

Figure 3.7.: Schematic of a dispersion curve for bending waves in an isotropic thin plate.

Despite the difficulties to transfer the given relation on complex structures like piano soundboards, several general dependencies can be identified for plates:

- With increasing height h or decreasing density ρ of a thin plate k decreases for a given ω.
- An increasing Young's modulus increases the flexural rigidity, which decreases k for a given ω.

4. Experimental Arrangement

4.1. Production Stages

The industrial manufacture of a concert grand piano normally takes approx. one year. Over the time span of 30 months, two instruments are accompanied through their construction with acoustic measurements. The soundboard is inspected for the first time after gluing of the hand selected stripes of spruce (*PROD1*). Table 4.1 shows the stages where measurements are performed. For each measurement the soundboard/piano is transported from the factory to the an-echoic chamber at the Institute for Systematic Musicology in Hamburg.

Table 4.1.: Denotation of production stages.

PROD	Condition
1	blank soundboard (glue-laminated strips of spruce)
2	after the ribs have been attached
3	after the bridge has been attached
4	after the ribs have been notched
5	after the soundboard has been glued to the rim
6	after application of the iron frame and stringing

4.2. Utilized Hardware

4.2.1. Excitation

Shaker

To be able to utilize the exponential sine sweep technique (see Section 5.1) to obtain impulse responses, a shaker (*Brüel & Kjær Vibration Exciter 4809*) is used for excitation of the soundboards. Since the pianos at hand were (unfortunately) not proposed to be 'laboratory instruments' after manufacture but high prized sales objects, a fundamental prerequisite was to strictly avoid any visible modifications of the soundboards. Therefore, the shaker could not be rigidly connected to the structure with the aid of glue or screws. To prevent contact loss during the measurements, the shaker is situated on the soundboard with a static pre-load of approx. 1 kg. As a consequence, the induced pre-stress is known to slightly alter the vibrational behavior of the soundboard (see Section 3.1.4). Nevertheless, a trade-off had to be made between minimum pre-load on the soundboard and maximum amplitude without contact loss.

Impact Hammer

To allow a comparison between sweep excitation and impulse excitation, additional driving point mobility measurements are performed with an impact hammer (*Kistler 9722A500*[139]) in positions similar to the ones mentioned below.

Driving Point Positions

The soundboard is excited in 15 positions corresponding to string termination points on the bridge (see Table 4.2 for detailed information about the driving point locations and Figure 4.1 for an illustration). The distance between input points *POS6-POS10* varies for reasons of accessibility due to the cross-stringing. Until attachment of the bridge, the soundboard is excited at the

[139] `https://www.kistler.com/en/product/type-9722a500/`, accessed in March 2019

Table 4.2.: Driving point positions.

POS	Key	f_1 [Hz]	*ARRAY*	x [cm]	y [cm]	Bridge	Strings
1	1	27.50	16	43.0	220.0	Bass	1
2	10	46.25	14-15	56.5	204.0	Bass	2
3	15	61.73	13	62.5	184.5	Bass	3
4	20	82.41	11	68.0	160.0	Bass	3
5	21	87.31	14-15	30.5	203.0	Treble	3
6	23	98.00	13	35.5	187.0	Treble	3
7	26	116.54	11-12	43.5	167.0	Treble	3
8	30	146.83	9-10	52.0	143.5	Treble	3
9	34	185.00	7-8	62.6	120.5	Treble	3
10	39	246.94	6	71.5	103.0	Treble	3
11	45	349.23	5	81.5	84.5	Treble	3
12	53	554.36	3	93.0	69.5	Treble	3
13	63	987.77	2	109.0	56.5	Treble	3
14	74	1864.66	1	125.5	48.5	Treble	3
15	88	4186.01	1	144.5	41.5	Treble	3

corresponding locations directly (*PROD1-PROD2*). For *PROD3-PROD6* the soundboard is excited on the bridge at the hitch pins normal to the soundboard plane. The measurement error for the shaker placement is in the range of $\pm$ 2.5 mm for x and y directions.

4.2.2. Response

Microphone Array

For the response measurement an array of 128 microphones is utilized. The microphone array and the corresponding analysis methodology are developed at the Institute for Systematic Musicology in Hamburg. Since 2009, it has been successfully utilized for measurements of various musical instruments.[140] 128

[140] Rolf Bader (2012b). "Radiation characteristics of multiple and single sound hole vihuelas and a classical guitar." In: *The Journal of the Acoustical Society of America* 131.1, pp. 819–828. DOI: 10.1121/1.3651096; Florian Pfeifle (2013). "Acoustical measurements and finite

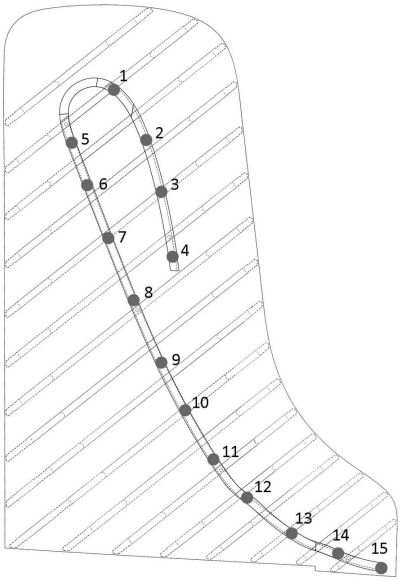

Figure 4.1.: Locations of driving point positions on the soundboard.

omnidirectional measurement microphones (*IsemCon EMM-07D146*[141]) are connected to 16 8-channel audio pre-amps (*RME Micstasy*[142]). Routing and synchronization is done via the *Multi Channel Audio Digital Interface* (MADI). Two synchronized MADI fibre-optical I/O streams with 64 channels (the maximum at 48 kHz sample rate) are accessed with an audio interface (*RME MADIface XT*[143]) which is connected with USB 3.0 to a personal computer. Recordings are performed with the digital audio workstation (DAW) *Samplitude Pro Suite*[144] which allows the handling of a sufficient number of physical audio inputs. A talk-back circuit allows communication between control room and anechoic chamber.

difference simulation of the West-African "talking drum"." In: *The Journal of the Acoustical Society of America* 134.5, pp. 4158–4158. DOI: 10.1121/1.4831238; Tim Ziemer (2014). "Sound Radiation Characteristic of a Shakuhachi with different Playing Techniques." In: *Proceedings of ISMA 2014*, pp. 549–555.

[141] `http://www.isemcon.net/shopus/product_info.php?products_id=51`, accessed in March 2019

[142] `http://www.rme-audio.de/products/micstasy.php`, accessed in March 2019

[143] `http://www.rme-audio.de/products/madiface_xt.php`, accessed in March 2019

[144] `https://www.magix.com/int/music/samplitude/suite/`, accessed in March 2019

(a) **(b)**

Figure 4.2.: a) Self-built frame for measurements *PROD1-PROD4*. b) Exemplary measurement setup for *D1 PROD2 POS4 ARRAY3*.

Figure 4.2 shows the self-built frame for measurements *PROD1-PROD4* and the setup for excitation and response measurement. The soundboard is positioned on foam in the same layout it is later glued into the rim. Brackets hold the array in position and secure an identical arrangement of microphones for each successive measurement step. The microphone array is arranged in a 3 $\times$ 35 grid with 40 mm orthogonal distance between microphones. The image shows an exemplary measurement in the second production stage (*PROD2*), the sound board is excited at an input position corresponding to string termination of note *E2* on the bass bridge (*POS4*). The microphone array is situated in the third position (*ARRAY3*). Note that the distance from the microphone plane to the soundboard surface varies between and within measurements due to the increasing crowning, the attached bridge, and the rim height (See Figure 4.5). The measurement error for the array placement is in the range of $\pm$ 1 mm for x and y directions.

Piezoelectric Transducers

A piezoelectric force sensor (*PCB 208C01*[145]) is attached to the stinger end to measure the dynamic input force. An acceleration sensor (*PCB 352C23*[146]) is

[145] `http://www.pcb.com/products/model/208c01`, accessed in March 2019
[146] `http://www.pcb.com/Products.aspx?m=352C23`, accessed in March 2019

(a) (b)

Figure 4.3.: a) Self-built frame for measurements *PROD5-PROD6*. **b)** Close-up of excitation at string termination point of note *C8* (*POS15*).

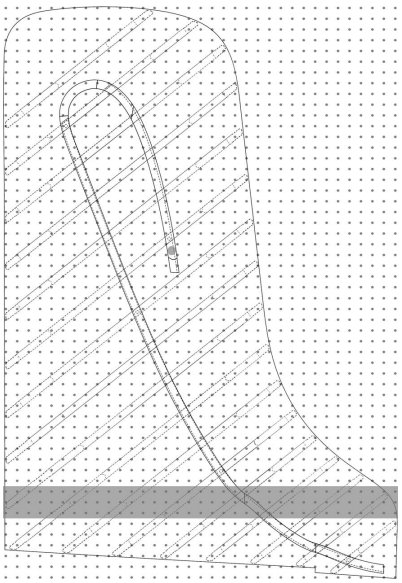

Figure 4.4.: Illustration of coverage of the sound board surface. Dots depict microphone positions, *ARRAY3* is highlighted in grey.

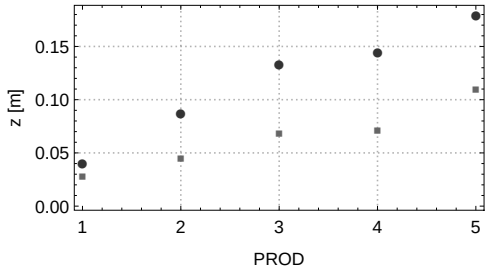

Figure 4.5.: (a) Measured maximum z distance (dark circles), mean z distance (bright squares) per production stage for *D1*.

positioned as close to the input position as possible to allow driving point mobility measurements (see Figure 4.3). To protect the wooden instrument surfaces from adhesive petro wax, piezoelectric transducers are solely attached to the steel hitch pins. The sensors are connected to an IPC pre-amp (*Kistler 4-Channel TEDS Piezotron (IEPE) Coupler*[147]) and then routed to two spare channels of the microphone pre-amps. Thereby, the sensor signals are in sync with the microphone array.

4.3. Climate Conditions

All measurements are performed in an anechoic chamber situated in the Institute for Systematic Musicology in Hamburg. The rectangular room (2 × 4 m) was built in the early 1980s and is located adjacent to the buildings exterior wall on two sides. The room does not have any pre-installed air conditioning, but is connected to the buildings ventilation system at least for the first year of measurements. For the period of measurements room temperature and humidity are tracked and a humidifier is installed to increase air humidity if it falls below 40 % relative humidity. Target values for room temperature and relative humidity during stay in the anechoic chamber for *PROD1-PROD6* are 20 °C / 40 %. Since the humidifier emits noise when in operation, it is switched off for the hours of measurements.
The temperature in the anechoic room is not directly controllable and is a result of incoming air flow from the ventilation system, incoming tempered

[147] `https://www.kistler.com/en/product/type-5134b/`, accessed in March 2019

air for periods where the door is opened regularly (between measurements), solid body transmission through the walls (two walls facing outside conditions, two facing temperature-controlled inside conditions), and heat emission by researchers during measurements.
Detailed data on climate conditions for every measurement period is given in appendix A.1. Detailed discussion about the assumed impact of changing climate conditions on the vibroacoustic behavior of the soundboard is given in Section 3.2.3. For the time period between *PROD7* and *PROD8* (being played in a European concert hall for one year) the climate conditions are not tracked by the author but are controlled by the concert hall to be 20 °C / 45 % to 70 %. Target values for room temperature and relative humidity during stay in the anechoic chamber for *PROD7* and *PROD8* are 20 °C / 40 %.

4.4. Data Structure

The extent of the project required a systematic data structure with redundant storage on two server systems. A single 25 s microphone recording with 48 kHz and 24 bit resolution takes 3.5 MB of storage space. The needed total space for the raw recording data of 346,680 files is 1.25 TB as a result of 2 instruments $\times$ 6 production stages $\times$ 15 input positions $\times$ 18 array recordings $\times$ (105 microphones + 2 sensors) $\times$ 3.5 MB. After deconvolution, the impulse responses are stored in binary format and take 354 MB per input position, which adds up to a total of 63 GB per post-processing step. In total, approx. 3 TB of storage space are used for the project data.

5. Methods

5.1. Exponential Sine Sweep Technique

To obtain impulse responses (IR) from the recorded data the so-called exponential sine sweep (ESS) technique is utilized.[148] The method has originally been proposed for measurements of weakly non-linear systems in room acoustics (e.g. loudspeaker excitation in a concert hall) but can also be adapted to structure-borne sound.[149] For the excitation an exponential sine sweep $f(t)$ is used:

$$f(t) = \sin\left[\frac{T\omega_1}{\ln(\frac{\omega_2}{\omega_1})}\left(\exp^{\frac{t}{T}\ln(\frac{\omega_2}{\omega_1})} - 1\right)\right], t \in [0, T] \tag{5.1}$$

with $\omega_1 = 2\pi * 1$ rad s^{-1}, $\omega_2 = \pi * 24{,}000$ rad s^{-1} and $T = 25$ s. The deconvolution is realized by a linear convolution of the measured output $y(t)$ with the temporal reverse of the excitation sweep signal $f(t)$ (5.1):

$$h(t) = y(t) * f^{-1}(t). \tag{5.2}$$

Additionally to reversing $f(t)$ along the time axis, an amplitude modulation is added to compensate the energy generated per frequency, reducing the level

[148] Angelo Farina (2000). "Simultaneous measurement of impulse response and distortion with a swept-sine technique." In: *Audio Engineering Society Convention 108*, pp. 1–24. DOI: 10.1109/ASPAA.1999.810884; Angelo Farina (2007). "Advancements in Impulse Response Measurements by Sine Sweeps." In: *Audio Engineering Society Convention 122*, pp. 4–9.

[149] Ege, "La table d'harmonie du piano-Études modales en basses et moyennes fréquences."

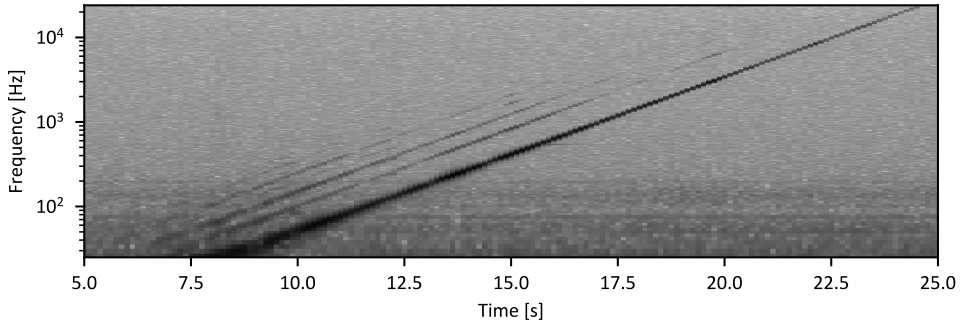

Figure 5.1.: Spectrogram of an exemplary output of one of the array microphones. Harmonic distortions of several orders are observable.

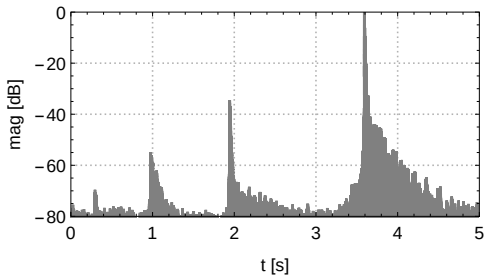

Figure 5.2.: Obtained impulse response of the signal in Figure 5.1 after deconvolution. The harmonic distortions are separated in time and precede the linear part at $t \approx 3.5$ s.

by 6 dB/octave, starting with 0 dB at $t = 0$ s and ending with -6$\log_2(\omega_2/\omega_1)$ dB at $t = T$.

Figure 5.1 shows a spectrogram of an exemplary output of one of the array microphones. Since the frequency axis has logarithmic scaling, the sweep appears as a straight line. Due to non-linearity in the shaker excitation the system shows harmonic distortions parallel to the sweep. Linear deconvolution with the inverse filter $f^{-1}(t)$ delays $y(t)$ of an amount of time varying with frequency. The delay is proportional to the logarithm of frequency. $f^{-1}(t)$ therefore stretches the signal with a constant slope, and compresses the linear part to a time delay corresponding to the filter length. The harmonic distortions have the same slope as the linear part and are, therefore, also packed to

very precise times. If T is large enough, the linear part of an impulse response is temporally clearly separated from the non-linear pseudo IR (see Figure 5.2). This is the reason why T is chosen with such a high value. As a consequence, it is possible not only to calculate the linear impulse response of a mildly non-linear system, but also to gain information about the systems level of non-linearity. Ege, Boutillon, and Rébillat[150] used the ESS for piano soundboard measurements and found the second order distortions excited comparable to *fortissimo* playing to be in the range of 40 dB below the linear part of the IR. Figure 5.2 shows an exemplary IR in time domain after deconvolution with the linear IR part preceded by three non-linear parts. Comparable to Ege, Boutillon, and Rébillat,[151] the second order pseudo IR is found to be 40 dB below the linear part.
The 3.46×10^5 raw output files are deconvolved with the ESS algorithm and resulting IR are stored in binary format on a server for further processing.

[150] Kerem Ege, Xavier Boutillon, and Marc Rébillat (2013). "Vibroacoustics of the piano soundboard: (Non)linearity and modal properties in the low- and mid-frequency ranges." In: *Journal of Sound and Vibration* 332.5, pp. 1288–1305. DOI: 10.1016/j.jsv.2012.10.012. arXiv: arXiv:1212.2323v1.

[151] Ibid.

5.2. Back-Propagation of Radiated Sound Pressure

A crucial part of the experimental design was to back-propagate the obtained sound pressure from the microphone array plane down to the soundboard surface. In the following, the required methodology is described. An exemplary use case for a single-array application is presented, showing the good performance of the method. Finally, the challenges to propagate radiation data from the implemented multiple-array measurements are described in detail. Even if this first-time application was not successful, a number of valuable conclusions can be drawn for future projects and are, therefore, discussed in detail.

5.2.1. Methodology

Microphone array techniques are well established methods for the evaluation of the radiation pattern of musical instruments.[152] The minimum energy method proposed by Bader[153] assumes the radiated complex pressure field to be a result of a finite number of virtual radiating source points p^i on the structure surface.[154] The multipole radiation is defined as

$$p^j = \sum_{i=1}^{N} R_{ij} p^i, \tag{5.3}$$

[152] Bader, "Radiation characteristics of multiple and single sound hole vihuelas and a classical guitar"; Christopher Waltham et al. (2013). "Acoustic imaging of string instrument soundboxes." In: 19, pp. 035004–035004. DOI: 10.1121/1.4799438; Rolf Bader (2012a). "Outside-instrument coupling of resonance chambers in the New-Ireland friction instrument lounuet." In: *Proceedings of Meetings on Acoustics*. Vol. 15, p. 035007. DOI: 10.1121/2.0000167; Sylvie Le Moyne et al. (2012). "Restoration of a 17th-century harpsichord to playable condition: A numerical and experimental study." In: *The Journal of the Acoustical Society of America* 131.1, p. 888. DOI: 10.1121/1.3651092.

[153] Rolf Bader (2010). "Reconstruction of radiating sound fields using minimum energy method." In: *The Journal of the Acoustical Society of America* 127.1, pp. 300–308. DOI: 10.1121/1.3271416.

[154] Mathematical formulations below follow the descriptions by ibid. and Rolf Bader (2014). "Microphone Array." In: *Springer Handbook of Acoustics*. Ed. by Thomas D. Rossing. New York, NY: Springer New York. Chap. Microphone, pp. 1179–1207. DOI: 10.1007/978-1-4939-0755-7_29.

with p^j the resulting pressure field as a sum of p^i and a radiation matrix R_{ij}. The radiation of p^i can be monopoles, but also can be narrowed normal to the surface. The radiation matrix R_{ij} is the Green's function for the free field:

$$R_{ij} = \frac{1}{\Gamma^{ij}} \exp^{\mathrm{i}kr^{ij}}, \tag{5.4}$$

with wave vector k and distances r_{ij} between p^i and p^j. $\Gamma^{ij}(\alpha)$ attenuates the amplitude dependent on the directivity parameter α as:

$$\Gamma^{ij}(\alpha) = r_{ij}(1 + \alpha(1 - \beta^{ij})), \tag{5.5}$$

and

$$\beta^{ij} = \left| \frac{r^{ij}}{|r^{ij}|} n^i \right|, \tag{5.6}$$

with the normal vector n^i and the normalized distance vector matrix $r^{ij} = x_g^i - x_m^j$ $(i, j = 1, 2, 3, ..., N)$.
With $\alpha = 0$, the source radiates as a perfect monopole and the amplitude attenuation in the Green's function is just $1/r^{ij}$. With $\alpha > 0$, the monopole is narrowed with the greatest amplitude in direction normal to the radiating surface.
Since after Bader,[155] the best representation for the source pressure field with a directivity parameter α is found when the reconstruction energy is minimum, as a first step the right directivity has to be found by trying. Therefore, the linear equation system

$$R(\alpha)p_g = p_m, \tag{5.7}$$

with p_g and p_m being the pressures as vectors and $R(\alpha)$ the radiation matrix, has to be solved iteratively for different α. Figure 5.3 a) shows the reconstruction energy for the radiation at a specific frequency. If α is chosen too low, the influence of adjacent sources is overemphasized leading to unreasonably large

[155] Bader, "Reconstruction of radiating sound fields using minimum energy method."

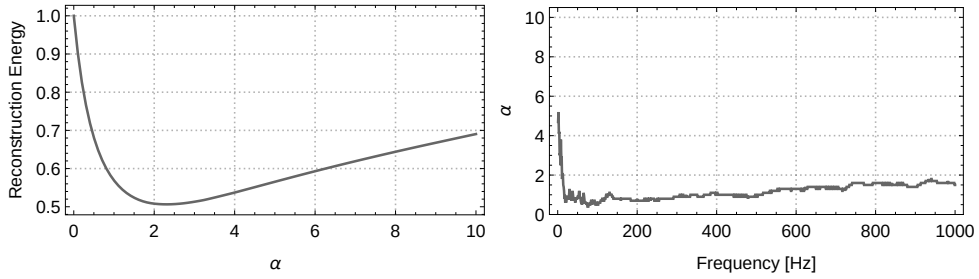

(a) **(b)**

Figure 5.3.: a) Exemplary reconstruction energy for different α values, minimum at α = 2.3. b) Progression of calculated α values for a broad frequency band.

reconstructed values. If α is too high, each source point is considered to radiate it's energy only in normal direction which, again, blows up the solution. For the search iteration, it has proven useful to test different α in integer steps and reverse and refine the search to 0.1 steps when a minimum is crossed. In the example in Figure 5.3 a) the minimum reconstruction energy is found with α = 2.3. Figure 5.3 b) shows a reasonable progression of calculated directivity parameters in a wider frequency band with a slight increase towards higher frequencies[156].

The method relies on the detection of evanescent waves (compare e.g. Cremer, Heckl, and Petersson[157] or Williams[158]), therefore, the microphone array is positioned in the near field of the radiating surface. The acoustic near field is frequency dependent and is defined as a distance of less than one wavelength λ from the source, but in practice distances of less than 1/8 λ are used.[159] Figure 5.4 a) shows 1/8 λ per frequency. Taking into account the average distance from the microphone array plane to the soundboard for *PROD1-PROD5* (see Figure 4.5), a (conservative) measure can be derived for the maximum frequency per production stage which can be considered as in near field (see Figure 5.4 b)).

[156] See Section 3.1.5 for the effect of the so-called *critical frequency*.

[157] Cremer, Heckl, and Petersson, *Structure-Borne Sound*.

[158] Earl G. Williams (1999). *Fourier Acoustics - Sound Radiation and Nearfield Acoustical Holography*. London: Academic Press Inc.

[159] Thomas R. Moore (2018). "Measurement Techniques." In: *Springer Handbook of Systematic Musicology*. Ed. by Rolf Bader. Springer H. Springer. Chap. 5, pp. 81–103. DOI: 10.1007/978-3-662-55004-5.

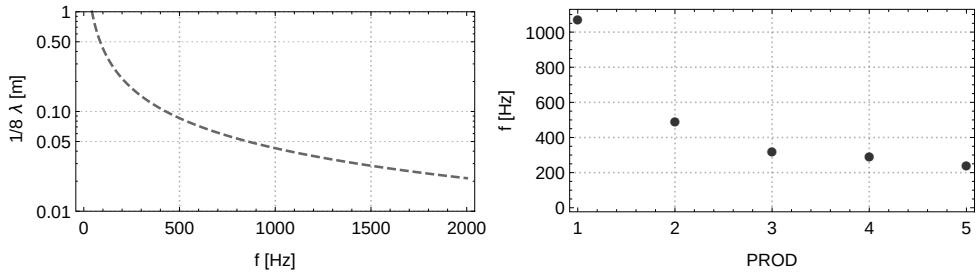

(a) (b)

Figure 5.4.: a) Maximum distance from microphone to surface per frequency for $c = 343\,\mathrm{m\,s^{-1}}$ to be considered as in *near-field* (1/8 λ).
b) Resulting maximum frequency in near-field for production stages of *D1* ($c = 343\,\mathrm{m\,s^{-1}}$).

Challenges and Possible Error Sources

Even small artificial gradients in the spatial amplitude or phase pattern can yield a failure in the linear equation system solution. In the following section, challenges are described for the method in general and with regard to the measurement conditions for the present work.

Room: The method relies on the fact that the defined virtual source points are the only sound emitting structures in the environment. Therefore, measurements have to be performed in reflection free conditions (anechoic chamber or free field). Reflective surfaces not taken into account can lead to reflections which are incorporated for the propagation, without having a geometry being a possible source for the radiation. The algorithm considers the virtual source points to be the only sources responsible for the resulting pressure field. Scattering effects near complex three dimensional structures are also not taken into account. In regard of the grand piano measurements, the self-built frame could have introduced unwanted reflections for the early production stages. Once the soundboard is glued to the frame (*PROD5*), the inner frame surfaces could have introduced reflections which were not taken into account for the propagation. Also the vertical surfaces of the bass and treble bridge are not factored in.

Setup:

- The microphone plane has to be placed as near to the radiating surface as possible. The smaller the distance from source plane to radiated plane, the greater are the differences between distances from adjacent radiating points to a microphone. This way, vectors in the radiation matrix differ more, which increases the condition of the radiation matrix. Due to the strong curvature of the piano soundboard and the application to the outer frame, the distance between microphone plane and radiating surface had to be insufficiently large for the last production stages (compare Figure 4.3 and Section A.2).

- The microphone distances in the x,y plane determine the spatial frequency limit. For wavelengths smaller than twice the microphone distance, aliasing will appear.

- Differences between suspected and real spatial microphone positions in regard to the radiating structure and in regard to the adjacent microphones, have to be minimized.

Converters and Recording:

- Measurement noise will occur in the signal path, low signal levels lead to an increasing influence of background noise (of e.g. ventilation systems), or amplification noise by the measuring equipment.

- The frequency dependent amplitude curves of the microphones have to be taken into account. For the microphones at hand, calibration data per 1/3 octave band is provided by the manufacturer and is used to normalize the different behavior between microphones.

- The degree of pre-amplification of the used converters turned out to slightly vary between channels and in dependence of the run time of the devices, possibly due to extreme heating up. Therefore, noise level measurements are performed before, during, and after measurements. A normalization with the noise level per channel has proven useful for the recording quality.

- MADI is a serial transmission method. Therefore, each device in a ring configuration introduces a latency. The converters at hand get out of sync by 3 samples per consecutive converter in the ring. The used converters have a function implemented to re-synchronize the MADI stream, but signals out of sync by a few samples have been detected in almost all measurements. The main purpose for the used equipment is recording for audio production in studio and live situations. In these scenarios, a latency of 3 samples between two adjacent converters, or even 21 samples between the first and last MADI ID, might not be crucial for music recording[160]. However, for the purpose of imaging wave propagation in solids with high velocities, an error of even one sample can be relevant: If a bending wave velocity of 6,000 m s^{-1} for spruce in grain direction is assumed, the wave front would travel 0.125 m between two samples (at a sample rate of 48 kHz) which corresponds to a spatial offset of three microphones. Provided that the latency between the signals in MADI stream 1 and 2 is constant over one measurement, it can be re-matched: The latency can be approximated by cross-correlations between the signals of the bordering microphones between stream 1 and 2. In the present work, for each *ARRAY1-ARRAY18* microphones *MIC62-MIC64* are compared to their neighbors *MIC65-MIC67*. For each microphone the latency with the highest cross-correlation is calculated for each orthogonal and diagonal neighbor. The average latency is taken for the corresponding array measurement to shift one of the MADI streams in time. However, since the soundboard is still sampled with an insufficient spatial resolution, a subsequent shift by one sample can still leave latencies between the streams. Since the MADI throughput allows only 64 channels per stream with 48 kHz, an increase of the sample rate would require more MADI channels for the given number of microphones which, again, could cause latency issues among one another.

Particular attention should be paid to the described possible error sources in the signal path, since they can easily lead to disadvantageous conditions for a subsequent propagation. An artificially high gradient in amplitude or phase between two adjacent microphones can be hard, or even impossible to explain

[160] With a sample rate of 48 kHz, 3 samples corresponds to a latency of 0.06 ms, which should not be perceivable. Even with 21 samples, the latency is in a scale of the transmission time through air between a violin body and the player's ears.

physically with a combination of monopoles radiating from a distant surface. Therefore, even small calibration errors will certainly inhibit a reasonable solution.

5.2.2. Single-Array Application

Figure 5.5 shows an exemplary application of the back-propagation method on a guitar (model *Sonora* built in 2018 by Michael Wichmann). The top plate surface allows a response acquisition with 40 mm spatial resolution in a single take. A plucked *E2* string is recorded with 128 microphones. The signals are transformed into the frequency domain and resonant frequencies are estimated by automated peak picking. Row a)-d) shows the real part of the pressure field of several resonance frequencies in the microphone array plane. Respective resonances are highlighted by red grid lines in the averaged spectrum. Figure 5.5 a) seems to be the Helmholtz mode at 83 Hz, but the lower top plate part could be in opposite phase motion. After back-propagation (Figure 5.5 e)) it is obvious that the top plate is not contributing to the resonance at all. The radiation pattern is much sharper and the alleged contribution of the lower plate part is gone. In Figure 5.5 d) an upper partial at 912 Hz is observable. The top areas near the soundhole vibrate in opposite phase, but it is not clear whether the soundhole does contribute to the radiation. After back-propagation (Figure 5.5 h)), it is obvious that the soundhole does not contribute to the radiation pattern at all. Thereby, the method gives insights into the structural vibrations of the musical instrument which would not be accessible with recorded pressure fields alone. The obtained vibration pattern on the structure surface could easily be forward propagated to any point in space for further analysis of the far-field radiation behavior of the instrument.

5.2.3. Multiple-Array Application

The existing microphone array has been successfully used for radiation measurements of numerous musical instruments. However, the studied structures were of a size which allowed the acquisition of radiation data with only one take without having to considerably cut the spatial resolution.
Measurements where the radiation of a vibrating structure is recorded with

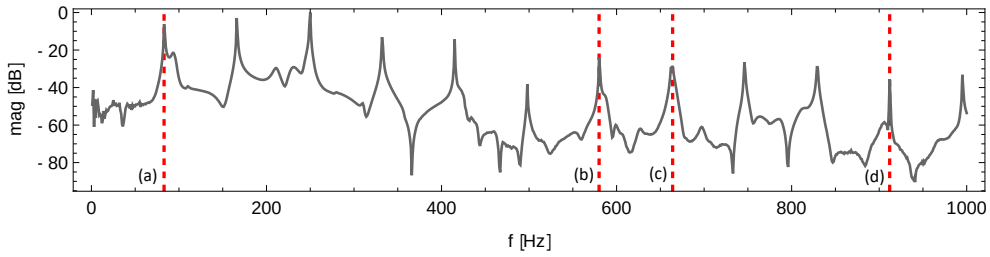

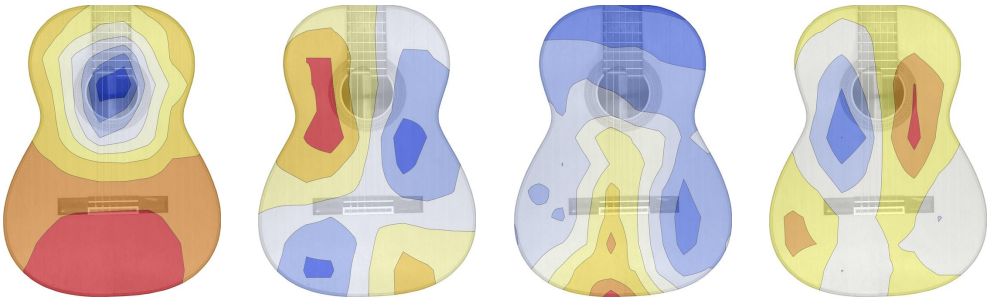

(a) 83 Hz **(b)** 580 Hz **(c)** 664 Hz **(d)** 912 Hz

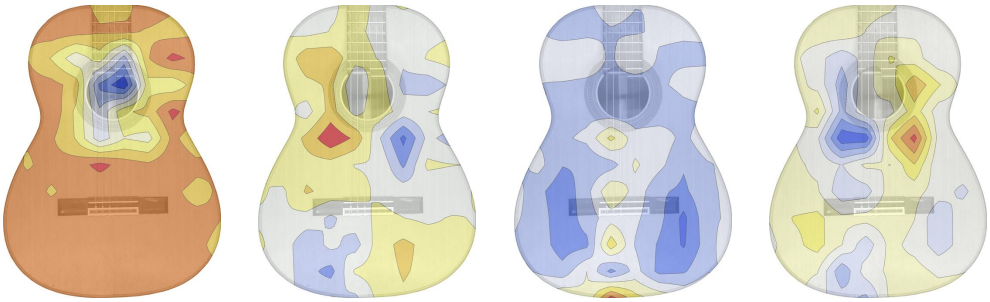

(e) 83 Hz, $\alpha = 2.1$ **(f)** 580 Hz, $\alpha = 2.4$ **(g)** 664 Hz, $\alpha = 2.0$ **(h)** 912 Hz, $\alpha = 2.0$

Figure 5.5.: a)-d) Real part of pressure field at resonance frequencies highlighted in the spectrum above. Obtained with a microphone array of 128 microphones in 40 mm distance to the soundboard. Plucked $E2$ string on a guitar (model *Sonora* built by Michael Wichmann.).
e)-h) Pressure field back-propagated to the soundboard surface utilizing the minimum energy method.

several takes are hereinafter referred to as *multiple-array measurements*. Reasons for such an approach can be to a) increase the spatial resolution above the given array resolution, or b) to be able to cover a structure surface which is greater than the area of the given microphone array. For the present work, it was decided to successively measure parts of the piano soundboard surface to retain a spatial resolution of 40 mm. This approach has been applied for the first time with the given measurement setup.

Challenges and Possible Error Sources

As described above, the algorithm is sensitive to noise. Even small artifacts in the signal composition can cause the solution to blow up. In the following, conditions specific for multiple-array measurements are described which can easily lead to massive artifacts and thereby inhibit a propagation.

- **Synchronization between Arrays:** The used DAW and all other components in the signal path have to provide sample precision to ensure a synchronization between the individual measurements. In the case of MADI signal transmission, this can be crucial not only between converters or MADI streams, but also between two consecutive measurements.
- **Changes in Excitation:** For a multiple-array application, the excitation has to be highly reproducible. In regard of the piano measurements, the excitation by a shaker in combination with bedding the soundboard on foam turned out to give insufficient results: A different input force amplitude or phase between measurements (See Figure 5.6) has to be a result of a positional change of the soundboard in the foam bed since the input signal and position of the shaker (attached to a very rigid steel tripod) can considered to be constant over the measurements. A positional change of the soundboard will lead to a different input position, input angle and/or a different pre-load and, therefore, must result in different IRs or, in case of a changed pre-load and different boundary conditions, even result in IRs describing a different vibrational system.

Given the described circumstances, the decision was taken not to back-propagate the recorded pressure fields.

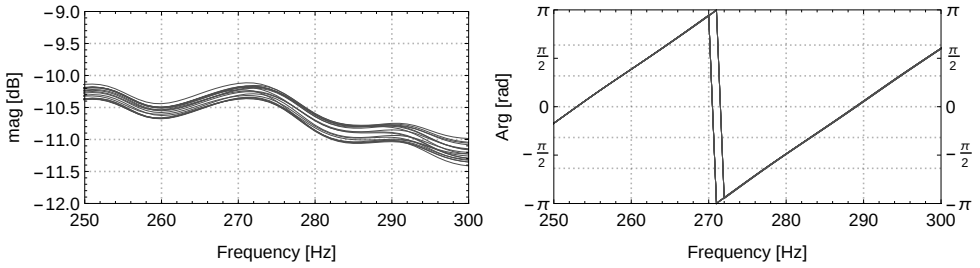

(a) **(b)**

Figure 5.6.: Exemplary differences in force excitation between measurements for *ARRAY1* to *ARRAY18*. a) Variation in magnitude, b) Phase variation, obtained by Fourier transforms of the time domain force excitation signal measured at the stinger.

6. Results

6.1. Structural Properties

Additionally to acoustical measurements, alteration of geometrical and material properties of the considered soundboards are monitored during the production process. While parameters like *grain angle*, *number of wooden stripes*, and *annual ring width* are considered to be constant, the *curvature* undergoes significant changes over the time period of production. The overall *weight* not only changes due to attachment of bridge, ribs, and varnish, but also with absorption and release of moisture in response to changing climatic conditions which in turn alters the *density*.

6.1.1. Number of Wood Stripes / Annual Ring Width

As decided shortly after starting the experiment, the amount of observed soundboards was reduced from four to two. On this occasion, the soundboards with the greatest deviation of the so far observable structural properties where chosen: With 1,462 to 972, *D4* has a higher number of annual rings than *D1* by 1.5 times (see Table 6.1). The corresponding average ring widths of 1 mm to 2 mm meet the range of prescribed quality standards for high grade soundboard spruce.

Table 6.1.: Annual ring width per piano.

	Number of annual rings	Average ring width
D1	972	1.52 mm
D4	1462	1.01 mm

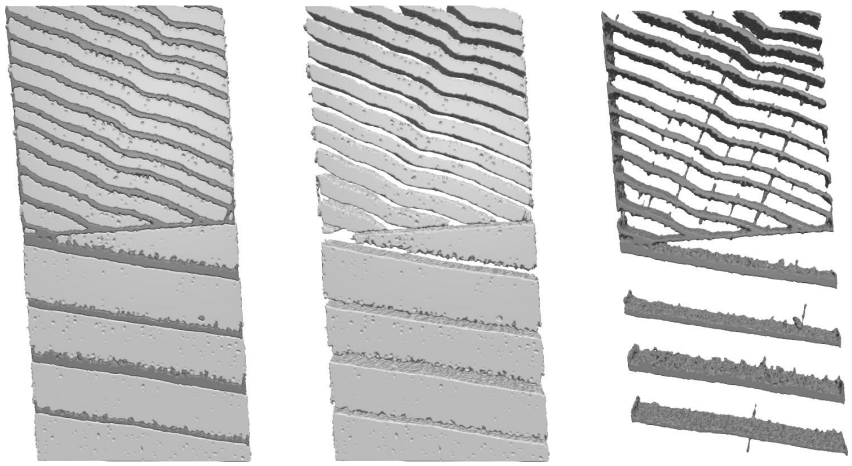

(a) Sitka spruce **(b)** Early wood **(c)** Late wood / glue

Figure 6.1.: X-ray micro computed tomography (CT) of a glued piece of soundboard spruce. Segmentation into early wood and late wood.

Additionally, the number of processed spruce stripes varies by a factor of 1.3 from *D1* to *D4*. Increasing the number of glued joints slightly increases the ratio of glue to wood. Nevertheless, X-ray based micro computed tomography (CT) measurements of glue joints show negligible penetration of the wood structure by the glue (see Figure 6.1). The cured glue has a density comparable to the spruce late wood and, therefore, should not have an exceptional influence on the soundboard behavior.

6.1.2. Mass and Density

Table 6.2 shows the development of the soundboard mass per production stage. Additionally, the bridge and the ribs are weighted prior to application in *PROD2* and *PROD3*. Note that the measured data in later production stages deviate from the simple summation of the individual masses. Reasons are a) the conduction of water due to changed climatic conditions, b) addition of varnish, c) removal of material by tapering the ribs and the bridge topside, and d) application of the bridge pins.
In consideration of these uncertainties the following statements can be made:

Table 6.2.: Soundboard mass per production stage in [kg].

PROD	1	2	3	4	5	6	7	Ribs	Bridge
D1	7.92	11.92	15.28	14.20	13.70	13.70	13.70	4.17	3.15
D4	8.22	12.22	15.64	14.59	14.09	14.09	14.09	4.15	3.15

***PROD1*:** Despite having the exact same geometry in the first production stage, *D4* is 3.8 % heavier than *D1*. This can be explained with the much higher annual ring width and thereby a higher proportion of late wood, which leads to a higher density (see Section 6.1.1).

***PROD2*:** The untreated ribs add 4 kg to the soundboard (no difference between *D1* and *D4*).

***PROD3*:** The untreated bridge adds another 3.25 kg to the structure (only slight difference between *D1* and *D4*).

***PROD4*:** Tapering the ribs removes 1 kg, which corresponds to a quarter of the ribs volume (no difference between *D1* and *D4*). Tapering reduces the total soundboard mass by approx. 7 %.

Therefore, the differences in soundboard mass between *D1* and *D4* through the production are solely a result of different wood density of the spruce stripes, which is a result of differing ring widths.

Since the volume of the soundboard is known from computer-aided design (CAD) technical drawings at least for the first production stage ($V_{PROD1} = 1.96 \times 10^{-2}\,\mathrm{m}^3$), the average spruce density for the blank soundboard can be derived for *D1* ($\rho_{D1} = 404.08\,\mathrm{kg/m}^3$) and *D4* ($\rho_{D4} = 419.39\,\mathrm{kg/m}^3$), in good agreement to data given by Conklin.[161]

[161] Conklin, "Design and tone in the mechanoacoustic piano. Part II. Piano structure."

6.1.3. Curvature

For each production stage the soundboard curvature is measured with a laser range finder (*Bosch PLR 15*) in a grid with a spatial resolution of 40 mm in x and y direction (approx. 1,300 measurement points) and an uncertainty of $\pm$ 1 mm in all three directions. Figure 6.3 illustrates the development of the curvature through the production process of *D1* (all axes have mm units). The ribs are milled in a convex shape and, therefore, cause a bending of the soundboard when glued to the bottom side (see Figure 6.3). The convex bending is mainly produced orthogonal to the grain direction (grain direction: 130°, rib angle: 40°) and most prominently on the outer ends of the soundboard (due to lower stiffness), yielding a concave shape in grain direction. The bridge is milled in a light convex shape (see Figure 3.1) and, therefore, bends down the upper and lower ends when glued to the soundboard (see Figure 6.3). Notching the ribs reduces the stiffness on the outer soundboard ends. The outer edges bend further down and thereby enhance the overall convex curvature (see Figure 6.3). The effect is additionally amplified by the fact that in this stage the soundboard is varnished only from the bottom side. In contrast to the upper side, the bottom side is thereby sealed and cannot expand due to water absorption.
Figure 6.2 shows the curvature in a cross-section at $y = 1.22$ m, which corresponds to the center of mass of the soundboard. The following statements can be made:

- The application of ribs causes a curvature of approx. 20 mm.
- The average crowning in the soundboard center stays constant until it is glued into the rim, which leads to a decrease to approx. 15 mm.
- Stringing and tuning does not result in an immediate reduction of the curvature.

Comparison of *D1* and *D4* (see Section A.2) leads to the following statements:

- Although the *D4* soundboard should have a greater stiffness due to the higher ratio of late wood, it bends distinctly more than *D1* when attaching the ribs and the bridge.

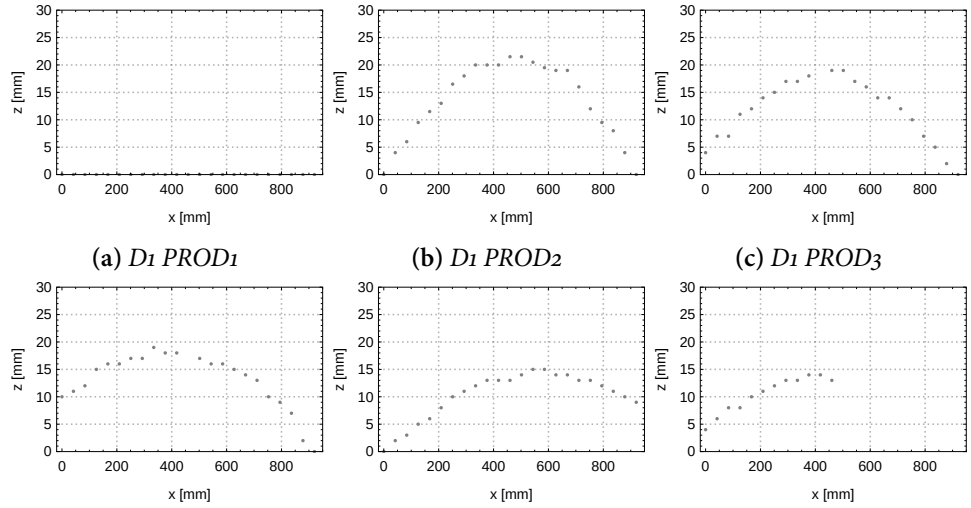

(a) *D1 PROD1* (b) *D1 PROD2* (c) *D1 PROD3*

(d) *D1 PROD4* (e) *D1 PROD5* (f) *D1 PROD6*

Figure 6.2.: Cross section through the curvature profile at $y = 1.22$ m per production stage for *D1*. Due to the applied cast iron frame, for *PROD6* only the left half could be measured.

- When glued into the rim (*PROD4* -> *PROD5*), the differences in shape between *D1* and *D4* vanish. There is thus reason to assume that *D4* should undergo a greater pre-stress when forced into the same rim profile (see Section 3.1.4).

6.2. Harmonic Responses

The vibrational behavior of a piano soundboard can be considered in two frequency regions (see Section 6.3 for exemplary spectra): For low frequencies, modal density and damping are low and, therefore, distinct resonances are observable and can be analyzed with classic methods of experimental modal analysis, as performed in numerous studies.[162] In this so-called *modal domain*, the

[162] Suzuki, "Vibration and sound radiation of a piano soundboard"; Giordano, "Simple model of a piano soundboard"; Corradi, Fazioli, and Marforio, "Modal analysis of a grand piano soundboard."

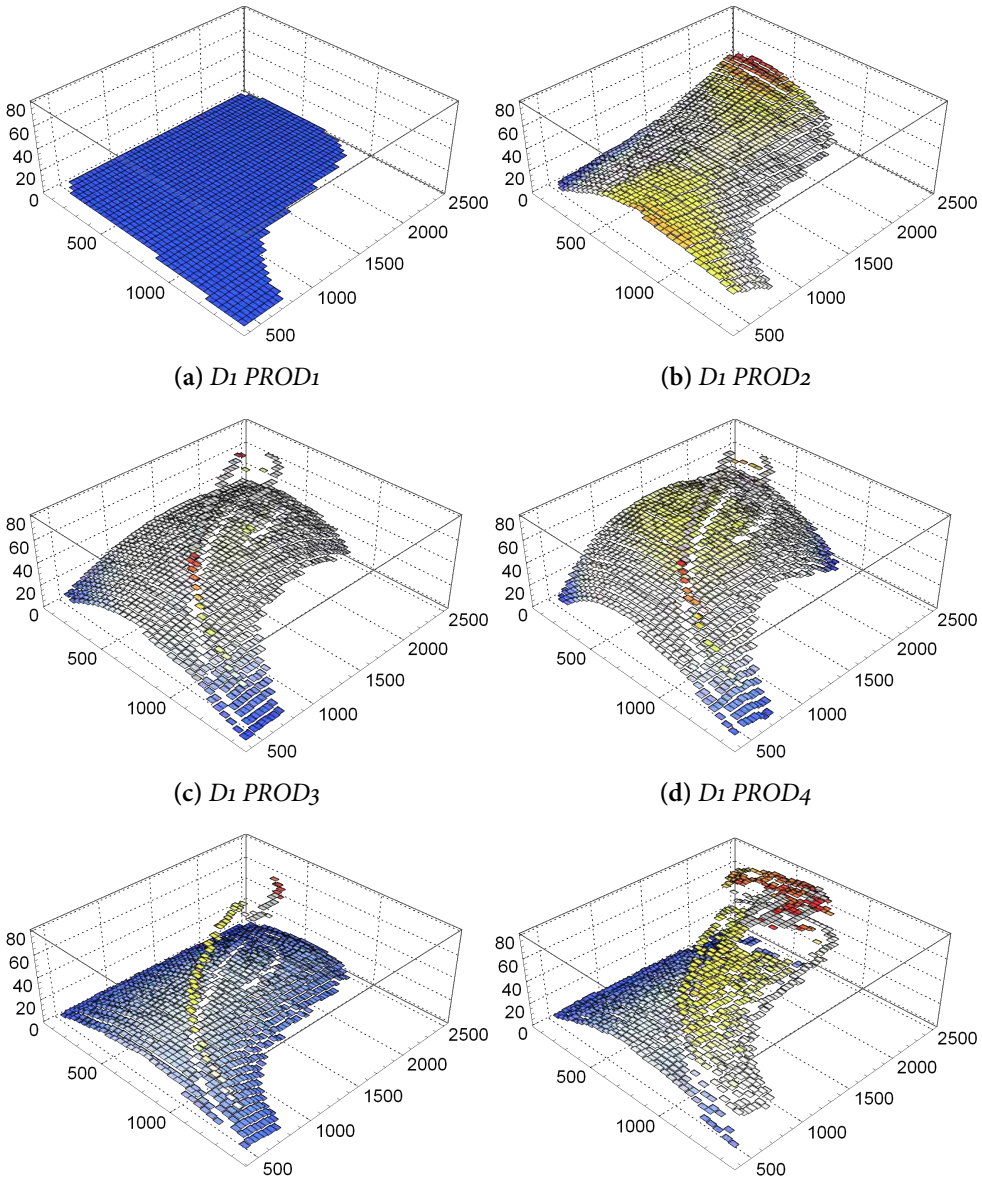

(a) *D1 PROD1*

(b) *D1 PROD2*

(c) *D1 PROD3*

(d) *D1 PROD4*

(e) *D1 PROD5*

(f) *D1 PROD6*

Figure 6.3.: Development of soundboard curvature over the production process for *D1*. All axes have mm units.

operating deflection shape[163] (ODS) at a resonance frequency is similar to the corresponding theoretical mode shape. Due to a high Q and low modal density, the adjacent modes are not activated at this frequency. Figure 6.4 shows ODS for the first three resonances of the soundboard in different production stages. The responses are composed solely of the mode at the corresponding frequency. The structure behaves like a homogeneous plate and a driving point dependency is given only for resulting amplitudes of vibration, but not for the generated shapes. Figure 6.5 illustrates this behavior: If the soundboard is excited close to, or right on a nodal line, the ODS at this frequency will be reduced in amplitude, or completely suppressed. As the ODS is composed only of one modal shape, the shape of the response does not change when changing the input position. As shown by Berthaut, Ichchou, and Jézéquel,[164] this regime ends for the grand piano soundboard with a frequency limit of approx. 200 Hz[165], when the modal overlap factor (the product of modal density, frequency, and loss factor) reaches 30 % to 50 %.

For higher frequencies, damping and modal density, and thereby the modal overlap increases and the harmonic response at a certain frequency is a composition of several contributing modes. Thereby, when changing the driving point position, the altered contribution of the involved modes can lead to a different ODS.[166] Here, a driving point dependency exists not only for the generated amplitudes, but also for the generated shape of deflection. Figure 6.6 illustrates this phenomenon with responses on different driving points at 2 kHz: Each driving point position generates a different ODS. Strong localization is apparent, in parts the greatest deflection starts to follow the driving point position.
For frequencies greater than approx. 1.1 kHz, the ribbed soundboard does not act like an equivalent homogenized plate without ribs anymore.[167] When wave-

[163] M. H. Richardson (1997). "Is it a mode shape, or an operating deflection shape?" In: *Sound and Vibration* 30th Anniversary Issue, pp. 1–8.

[164] Berthaut, Ichchou, and Jézéquel, "Piano soundboard: Structural behavior, numerical and experimental study in the modal range."

[165] The presented values are given for measurements on a soundboard in a production stage comparable to *PROD4* with free-free boundary conditions.

[166] Chaigne, Cotté, and Viggiano, "Dynamical properties of piano soundboards."

[167] Berthaut, Ichchou, and Jézéquel, "Piano soundboard: Structural behavior, numerical and experimental study in the modal range"; Kerem Ege and Xavier Boutillon (2010b). "Vibrational and acoustical characteristics of the piano soundboard." In: *Proceedings of 20th*

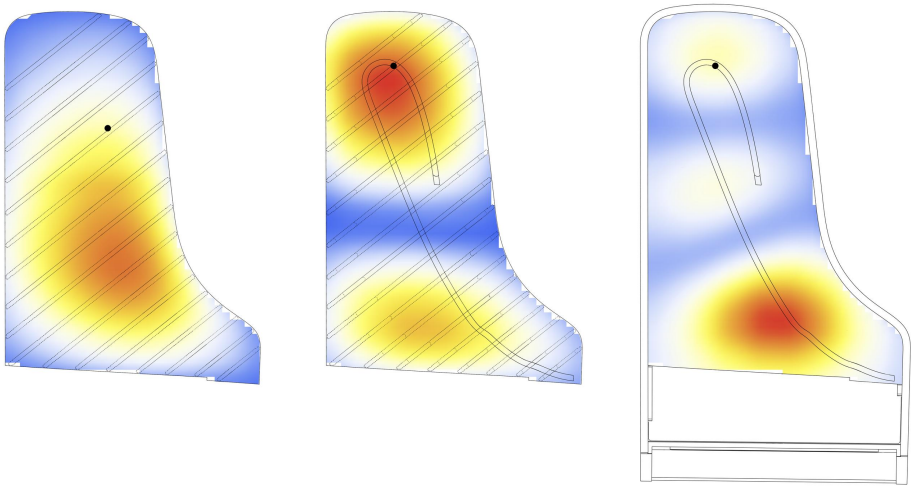

(**a**) *PROD2*, *POS3*, 15 Hz (**b**) *PROD4*, *POS1*, 27 Hz (**c**) *PROD5*, *POS1*, 113 Hz

Figure 6.4.: Modulus of operating deflection shapes for the first three soundboard resonances. Black dots depict driving point positions.

lengths are smaller than twice the rib spacing, ribs start to act as rigid obstacles for the propagating waves. Thereby, deviations from an exact equidistant rib spacing can contribute to localization effects for higher frequencies.[168] This effect is observable in Figure 6.6 for the bottom left examples (*POS10* and *POS11*): Most of the vibrational energy is trapped between the ribs adjacent to the driving point position.
As in this frequency region single modes can not be distinguished from their neighbors, traditional modal identification is not feasible. Possible ways to describe and predict the responses in this frequency range can be in terms of mean values of the frequency response functions[169] or admittance functions for discrete points (see Section 6.3). Another approach to increase the modal domain is based on algorithms which model the impulse responses as combina-

International Congress on Acoustics, pp. 1–7.

[168] Chaigne, Cotté, and Viggiano, "Dynamical properties of piano soundboards."

[169] Eugen Skudrzyk (1980). "The mean value method of predicting the dynamic response of complex vibrators." In: *The Journal of the Acoustical Society of America* 67.4, pp. 1105–1135. DOI: 10.1121/1.384169.

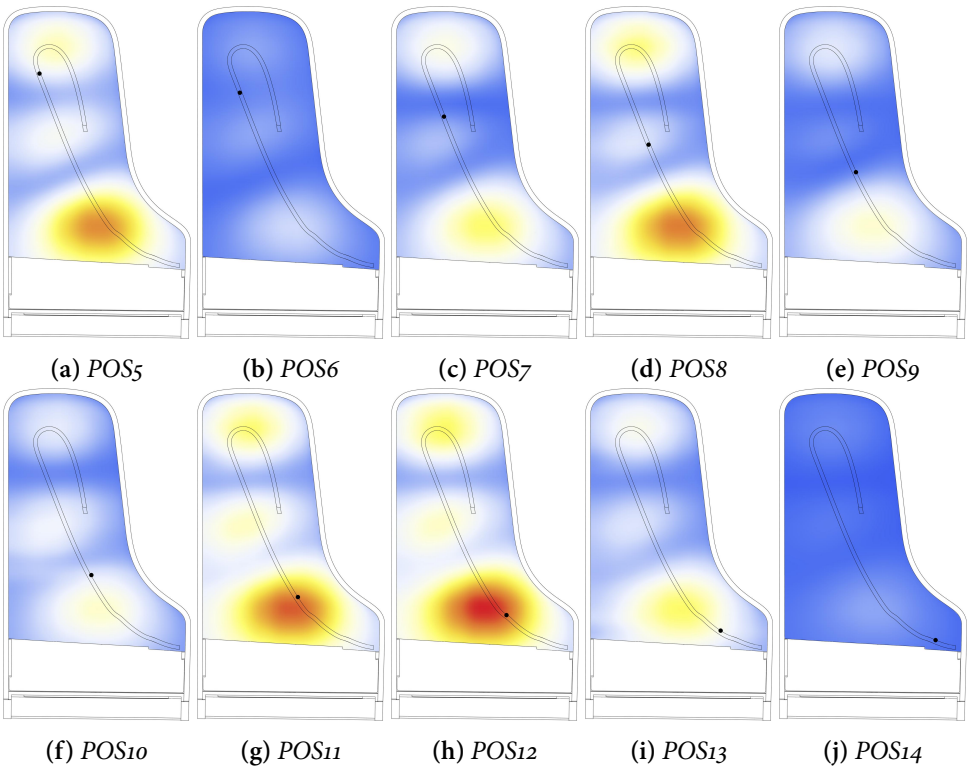

(a) *POS5* (b) *POS6* (c) *POS7* (d) *POS8* (e) *POS9*

(f) *POS10* (g) *POS11* (h) *POS12* (i) *POS13* (j) *POS14*

Figure 6.5.: Operating deflection shapes of third resonance (114 Hz) for *D1 PROD5 POS5-POS14*. Modulus, low (blue) to high (red) deflection, black dots depict driving point positions.

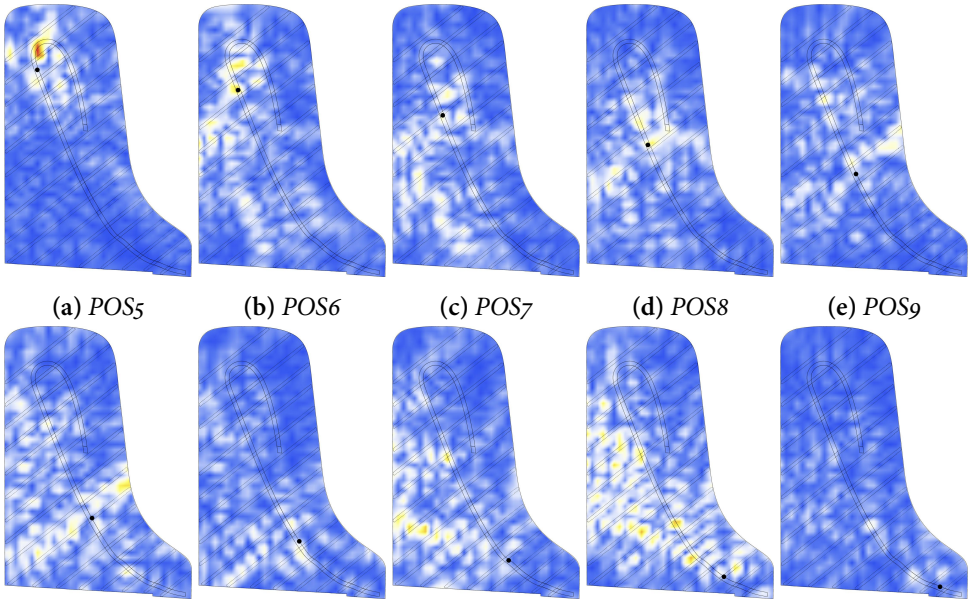

(a) *POS5* (b) *POS6* (c) *POS7* (d) *POS8* (e) *POS9*

(f) *POS10* (g) *POS11* (h) *POS12* (i) *POS13* (j) *POS14*

Figure 6.6.: Driving point dependency for operating deflection shapes at 2 kHz for *D1 PROD3 POS5-POS14*. Modulus, low (blue) to high (red) deflection, black dots depict driving point positions.

tions of complex exponentials.[170] By means of utilizing the ESPRIT algorithm, Ege and Boutillon[171] extended the region of possible modal identification for the piano soundboard to 2.5 kHz.

6.3. Driving Point Mobility

Measurements are taken on the soundboard of *D1* in six stages of production (*PROD1-PROD6*). The soundboard is excited at 15 positions associated with string termination points on the bass and treble bridges (*POS1-POS15*). An

[170] Laroche, "The use of the matrix pencil method for the spectrum analysis of musical signals"; Roy and Kailath, "ESPRIT - Estimation of Signal Parameters via Rotational Invariance Techniques."

[171] Ege and Boutillon, "Vibrational and acoustical characteristics of the piano soundboard."

impact hammer (*Kistler 9722A500*) with 0.1 kg head weight is used for excitation. For the sake of comparison, a miniature impact hammer (*Dytran 5800 SL*) with a mass of 0.01 kg is used for a series of measurements. Although above 4 kHz the induced energy is greater than for the heavier hammer, the mobility functions obtained do not differ below 5 kHz. The heavier hammer is chosen for the experiment due to the much greater amount of energy transmittable in the frequency band up to 2 kHz. The response is captured with a piezoelectric transducer (*PCB 352C23*) with a mass of 0.2 g, situated on the bridge with a distance of approx. 2 mm to 3 mm from the hammer impact position.

In Figure 6.7 a) mobility functions dependent on production stage vs. frequency are presented, where dark colors imply low, and bright colors imply high mobility values. Consequently, clear bright lines illustrate resonances. That way the general development of driving point mobilities through the production process can be illustrated: For the first production stage (*PROD1*), the blank soundboard has an overall high level of mobility. The first two resonances at 13 Hz and 25 Hz (see Figure 6.8) are the only remarkable ones. Attachment of the ribs (*PROD2*) decreases the overall level of mobility. A more distinct resonance behavior is observable up to 300 Hz. Attachment of the bridge (*PROD3*) further decreases the overall mobility level. Notching the ribs (*PROD4*) has no impact on the general mobility. Changing the boundary conditions by gluing the soundboard into the rim (*PROD5*) affects the vibrational behavior fundamentally in the low to mid frequency range: Up to 300 Hz distinct resonances appear.
Figure 6.7 b) focuses on mobilities for *PROD5* dependent on the driving point position. An upper frequency limit for distinct resonances between 250 Hz and 300 Hz is observable. Driving point positions near the ends of the bass bridge (*POS1* and *POS4*) and treble bridge (*POS5* and *POS15*) have generally higher mobility levels than the rest. The clamping particularly prevents low frequency resonances in the treble register. In the highest octave, the soundboard only shows some spurious resonances between 200 Hz and 300 Hz.
Figure 6.8 shows the development of the first three soundboard resonance frequencies through the production process.

Figure 6.10 shows modulus of mobility vs. frequency at exemplary driving point positions for the four most influential construction steps. Each function is the mean of five independent measurements. Without ribs, the soundboard exhibits no resonance characteristic except for the first two resonances at 13 Hz

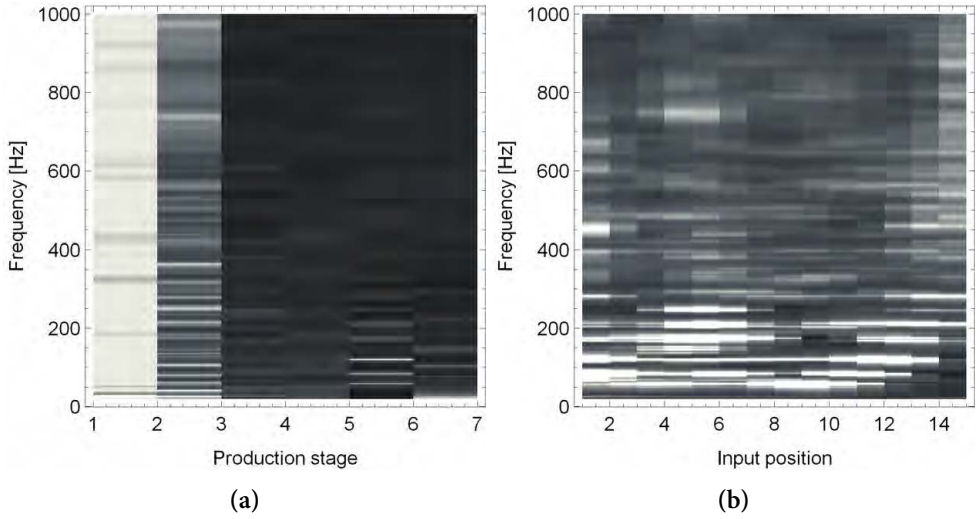

Figure 6.7.: Mobility maps for a) average mobility per production stage, and b) mobility per driving point position for *PROD5*. Dark colors imply low, and bright colors imply high mobility values.

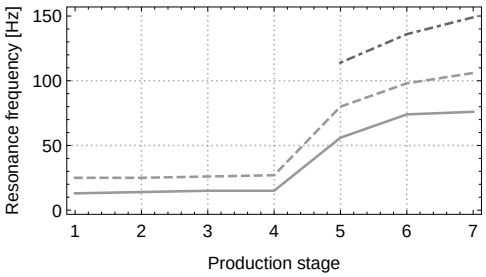

Figure 6.8.: Frequencies of the first three soundboard resonances per production stage. Corresponding to operating deflection shapes in Figure 6.4: a) line, b) dashed, c) dot-dashed. Deflection shape c) is not observable in production stages *PROD1-PROD4*.

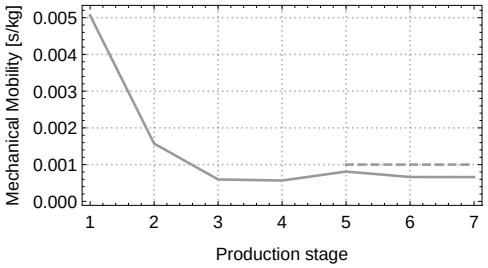

Figure 6.9.: Average mobility 50 Hz to 1000 Hz per production stage (solid). Measurements on upright pianos by Wogram[172] and Giordano[173] (dashed).

and 25 Hz. Above 50 Hz, the mean mobility remains constant. Attaching the ribs decreases the mobility level by 10 dB in the low and mid frequency range. In the range up to 500 Hz resonance characteristics arises (see Figure 6.10 a)). Application of the bridge further decreases overall mobility by 10 dB and 10 dB to 20 dB above 1 kHz (see Figure 6.10 b)). Besides a small increase of resonance frequencies in the low frequency range, notching the ribs causes no observable alteration of mobility functions. A major change in low frequency behavior evolves when the soundboard is glued into the rim, observable as a development of strong resonance peaks up to 300 Hz. From 500 Hz to 5000 Hz the mean mobility stays constant (see Figure 6.10 c)). Up to 350 Hz, the application of strings and frame causes an increase of resonance frequencies of approx. 20 Hz (see Figure 6.9) and a decrease of resonance amplitudes by approx. 10 dB (see Figure 6.10 d)).

The decrease of general mobility by application of ribs and bridge is assumed to result of stiffening the soundboard. Clamping the soundboard into the rim, and thereby changing the boundary conditions, has the most prominent effect on its vibrational behavior: Below 300 Hz sharp resonances appear. An upper frequency limit for distinct resonances between 250 Hz and 300 Hz is observable and confirms data presented by Suzuki[174] and Berthaut, Ichchou, and Jézéquel.[175] Up to 350 Hz, the application of strings and frame causes an increase of resonance frequencies of approx. 20 Hz and a decrease of resonance

[174] Suzuki, "Vibration and sound radiation of a piano soundboard."

[175] Berthaut, Ichchou, and Jézéquel, "Piano soundboard: Structural behavior, numerical and experimental study in the modal range."

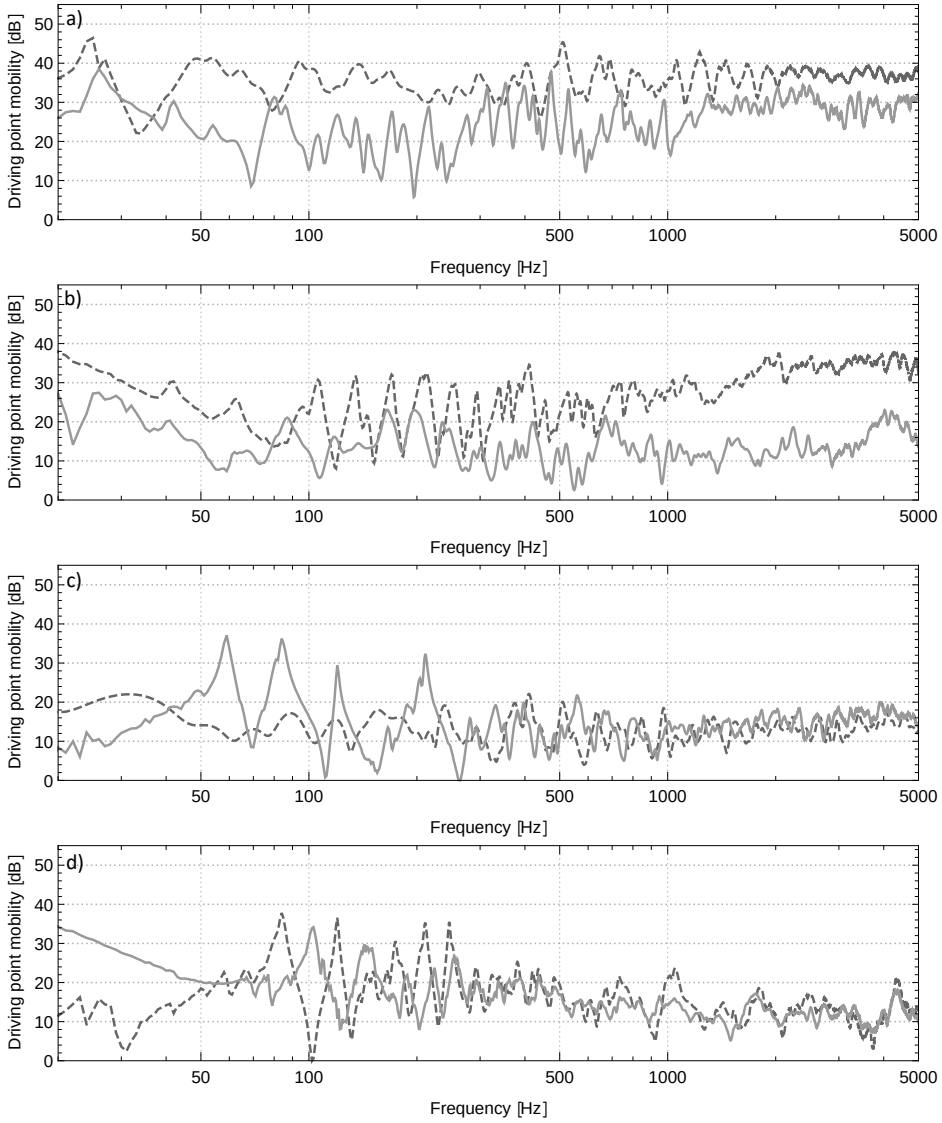

Figure 6.10.: Modulus of mobility for different stages of production before (dashed) and after (solid) the modification is applied. a) Attachment of ribs (*POS5*), b) Attachment of the bridge (*POS11*), c) Gluing the soundboard into the rim (*POS10*), d) Stringing (*POS5*).

amplitudes by approx. 10 dB. This is in good agreement with Conklin[176] and Mamou-Mani, Frelat, and Besnainou.[177] In contrast to Conklin, who observed an influence of stringing for a range up to 1 kHz, in the present case the effect is only observable up to 350 Hz. In the frequency range above 1 kHz the presented results can not confirm a sudden increase in mobility. The mean mobility stays more or less constant for the cases when the soundboard is clamped.

6.4. Bending Wave Propagation on the Soundboard

Due to the combination of the microphone array with the ESS method, it is possible to visualize the initial bending wave propagation on the soundboard when struck by a pulse at high spatial and temporal resolutions. In the following section, the general propagation behavior of the soundboard is described dependent on production stage and input position. Subsequently, particular attention is paid to the angle dependent bending wave velocity per production stage. An extensive series of propagation images and calculated velocity ratios per input position can be found in Section A.3.

***PROD1*:** The material anisotropy is clearly observable (see Figure 6.11): For any given t the propagation in grain direction is advanced compared to the direction normal to grain. Even if the soundboard is already tapered, this behavior does not differ between the input positions. Besides the influence of early reflections from the soundboard edges, the soundboard seems to have constant vibrational properties independent of the location. For the input positions *POS14-POS15* the bending waves are confronted very early with structural boundaries for the bigger part of the propagation directions, the initial wave field propagating to the soundboard center is already scattered due to early reflections from the boundaries (see Figure 6.12).

[176] Conklin, "Design and tone in the mechanoacoustic piano. Part II. Piano structure."
[177] Mamou-Mani, Frelat, and Besnainou, "Numerical simulation of a piano soundboard under downbearing."

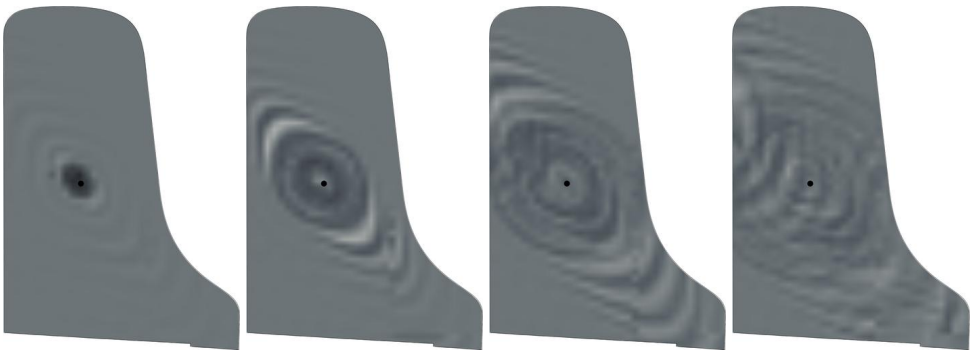

Figure 6.11.: Bending wave propagation for *PROD1*, *POS8*, 0.5 ms intervals.

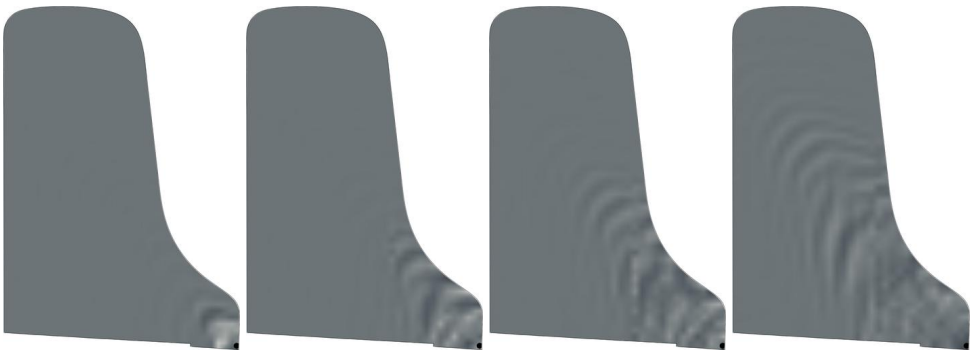

Figure 6.12.: Bending wave propagation for *PROD1*, *POS15*, 0.5 ms intervals.

***PROD2*:** The application of ribs has a crucial impact on the propagation behavior of the initial bending waves. As described in Section 3.1, besides the static strengthening to withstand the load of the strings, the main reason to apply ribs to the soundboard is to compensate the anisotropy given by the material properties of the spruce.[178] After Lieber,[179] instrument builders tend to overcompensate the anisotropy but this is not observable for the instruments at hand.[180] In general, the propagation is circular. However, on closer examination parts of the vibrational energy seem to be trapped between the ribs (see Figure 6.13). In direction normal to grain the propagation is not circular but rather a traveling plane wave front, as a result of superposition of reflections between the ribs. The longer the initial wave travels the more it looks like the planar wave deforms to a convex wave front with the outer edges being faster than the central part. A plausible explanation for the observed plane wave propagation is given by Ege and Boutillon.[181] In the lower frequency region the ribbed soundboard behaves like a homogeneous isotropic plate. However, above a critical frequency determined by the inter-rib distance (compare Section 3.1), the soundboard behaves like a set of wave guides confined by the ribs. Therefore, two sets of wave regimes travel on the soundboard: Parts with wave numbers which fit between the ribs get trapped and are reflected back and forth between the ribs. At the same time, as the wave velocity is dependent on the stiffness of the soundboard, these waves could travel faster near the ribs than between them (compare the increase of local propagation velocity when attaching the bridge in Figure 6.15). For wave numbers greater than twice the inter-rib distance, the soundboard acts as an isotropic plate, forming the observable circular propagation pattern.

***PROD3*:** The influence of the bridge is clearly observable in the initial bending wave pattern: Stiffening increases the wave velocity locally, the propagation seems to follow the bridge direction (see Figure 6.15). Note that when the

[178] Conklin, *U.S. Patent No. US3866506 A: Soundboard construction for stringed musical instruments*.

[179] Lieber, "The influence of the soundboard on piano sound."

[180] Wogram advised to avoid overcompensation for high quality pianos, see Klaus Wogram (1984). "Akustische Untersuchungen an Klavieren - Teil 1:Schwingungseigenschaften des Resonanzbodens." In: *Der Piano- und Flügelbau*, pp. 380–404

[181] Ege and Boutillon, "Vibrational and acoustical characteristics of the piano soundboard."

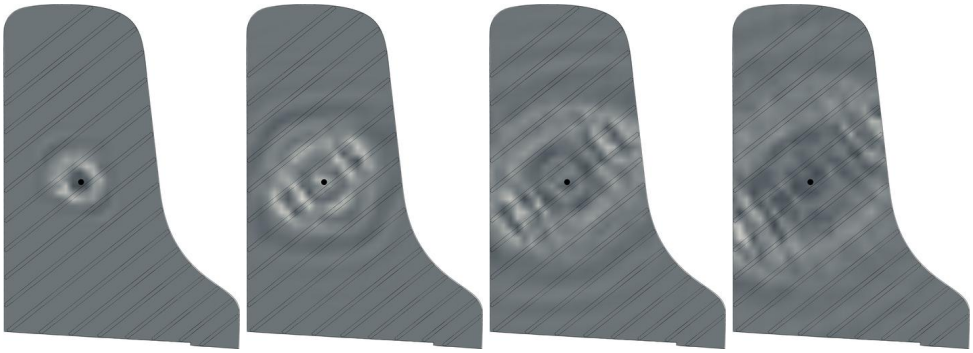

Figure 6.13.: Bending wave propagation for *PROD2*, *POS8*, 0.5 ms intervals.

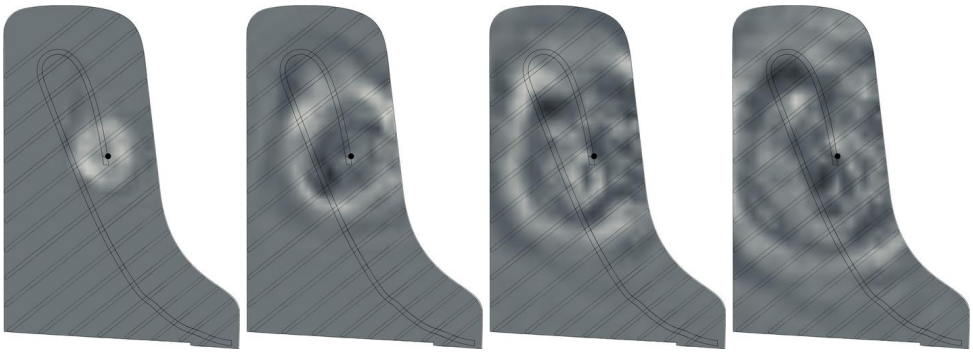

Figure 6.14.: Bending wave propagation for *PROD3*, *POS4*, 0.5 ms intervals.

bass bridge is activated at its end corresponding to key *E2* (see Figure 6.14) the initial wave front confronts two very different structures: Downwards in key direction the propagation is circular with shape and velocity similar to the state without a bridge. Upwards away from the keys the wave front follows the stiff bass bridge with greatly increased velocity.

***PROD4*:** Notching the ribs has no observable effect on the shape of the initial bending wave propagation (compare Figure 6.15 and 6.16).

***PROD5*:** When the soundboard is glued into the rim, boundary conditions are changed drastically, which is also observable in the initial propagation pattern. The combination of added ribs, bridge and fixation causes a quasi

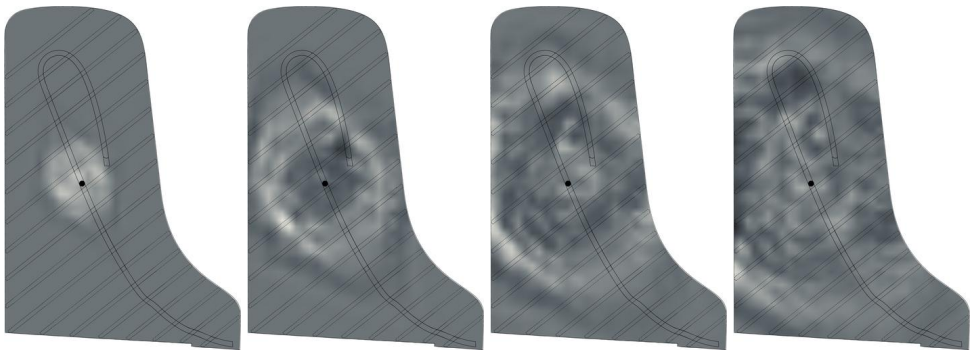

Figure 6.15.: Bending wave propagation for *PROD3*, *POS8*, 0.5 ms intervals.

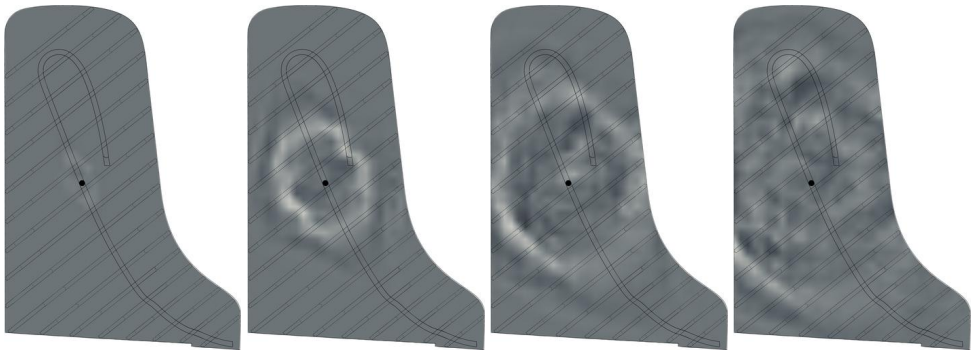

Figure 6.16.: Bending wave propagation for *PROD4*, *POS8*, 0.5 ms intervals.

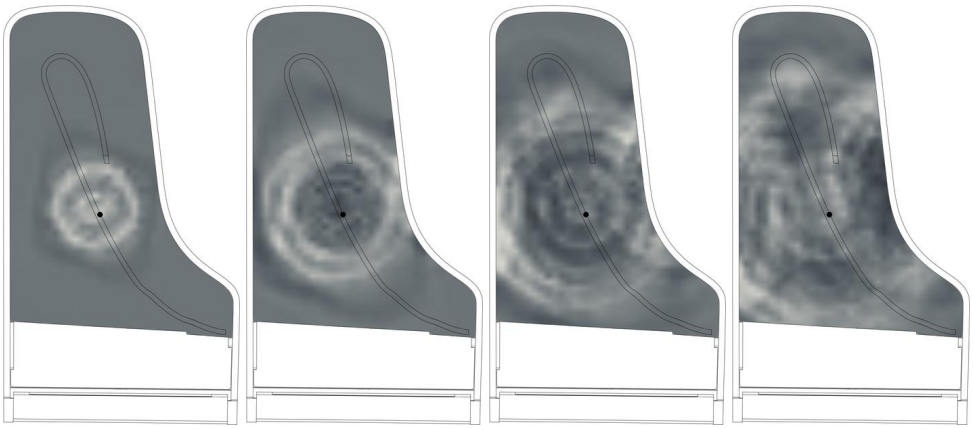

Figure 6.17.: Bending wave propagation for *PROD5*, *POS9*, 0.5 ms intervals.

isotropic behavior of the plate with the only directivity given by the locally added stiffness of the bridge (see Figure 6.17). The clamped boundary conditions lead to a greater part of the energy being reflected from the edges and the first reflection of the initial wave front is observable (see Figure 6.17).

6.5. Grain Angle dependent Bending Wave Velocity Ratio

The exact quantitative estimation of propagation velocities is difficult with the given experimental design. The recorded response signal does not represent the exact time and position of the bending wave on the structure, but the arrival in the array plane after traveling through the soundboard and then being radiated through air from the location under the microphone for the distance z. As described in Section 6.1, in the later production stages greater z distances were necessary due to the curvature of the soundboard and the piano frame in *PROD5*. Provided that the propagation velocity in the soundboard is higher than the speed of sound in air by a factor of 10-20, the increasing distances from array plane to instrument surface bias the result significantly. Assume e.g. a traveling distance in the soundboard of 2 m between input position and $\{x|y\}$ coordinate of a microphone and subsequently a z distance to the array

plane of 0.1 m. With the expected velocities, the propagation would need similar times for 2 m in wood as for 0.1 m through air. The resulting measured propagation velocity would halve due to the distance between surface and array plane.
Nevertheless, even if the exact quantities are not known, it is possible to estimate the velocity ratio between in grain (v_{LL}) and normal to grain direction (v_{RR}).

As described in Section 3.2.1, bending wave propagation is dispersive, meaning there is a non-linear dependence of phase velocity c_B and angular frequency. For the estimation of travel time Δt the bending wave group velocity is estimated. For that reason, the time delays between the microphone signal closest to the input position (IR_{ref}) and all other microphones (IR_n) are estimated by cross-correlations. The maximum of the cross-correlation function indicates the position in time with the best alignment between the two pulse shapes even when they are deformed due to the dispersion (see Figure 6.20).
The distances and angles between the 1,300 array microphones are known with an uncertainty of $\pm$ 1 mm. With the obtained Δt values, velocities can be calculated per microphone couple. Estimation of velocity values for 1,300 microphones covering the soundboard surface $\times$ 15 input positions gives velocity point clouds with 19,500 measurements per production stage as seen in Figure 6.18. The point cloud is reduced by calculation of a moving average over 360 deg (See Figure 6.19) and the ratio of v_{LL} and v_{RR} can be read out.

Figure 6.21 summarizes the evolution of the velocity ratio between in grain and normal to grain direction. For *PROD1* a velocity ratio of $v_{LL}/v_{RR} = 3.8$ is measured, which is in good agreement with factors for v_{LL} over v_{RR} of approx. 3.6, given by Haines[182] and Bucur[183] for spruce plates. This shows that even if the absolute velocity values can not be estimated, the method works well to give information about the ratio of velocities. Application of ribs nearly compensates the anisotropy to a ratio of 1.1. Overcompensation of the anisotropy is not observable. The bridge is attached on the soundboard in grain direction for most of its length. As seen in Section 6.4, the bridge causes a local stiffening which leads to higher velocities along its direction and, therefore, an increase of v_{LL}/v_{RR}. Tapering of the ribs (*PROD4*) partially reverses the

[182] Haines, "On musical instrument wood - part 2."
[183] Bucur, *Acoustics of Wood*.

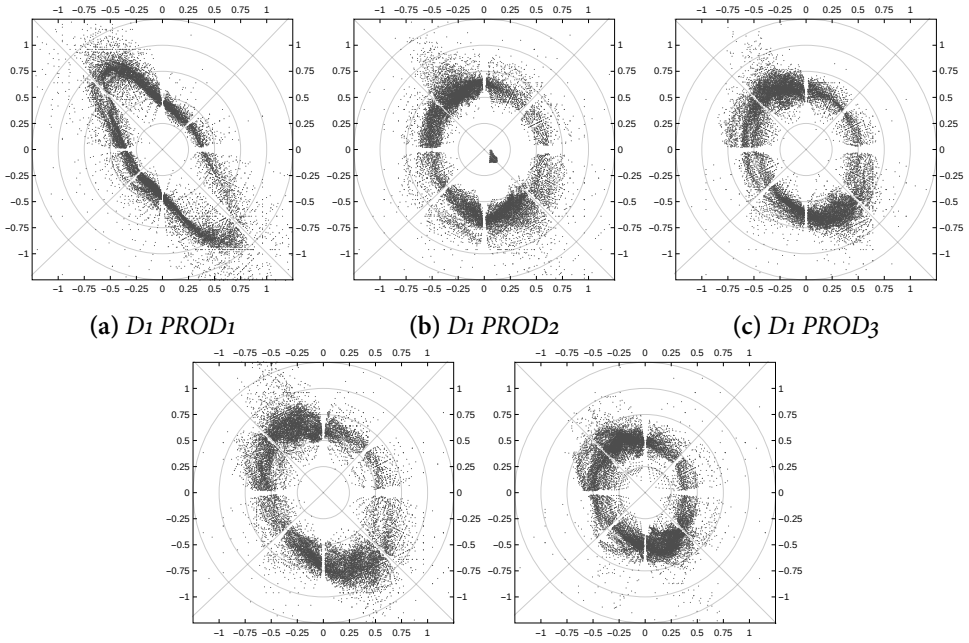

(a) *D1 PROD1* **(b)** *D1 PROD2* **(c)** *D1 PROD3*

(d) *D1 PROD4* **(e)** *D1 PROD5*

Figure 6.18.: Angle dependent wave velocity for *D1 PROD1-PROD5* as a combination of propagation through soundboard and air. 19,000 measurement points per production stage. Diagonal grid lines depict grain angle (v_{LL}: bottom right to top left).

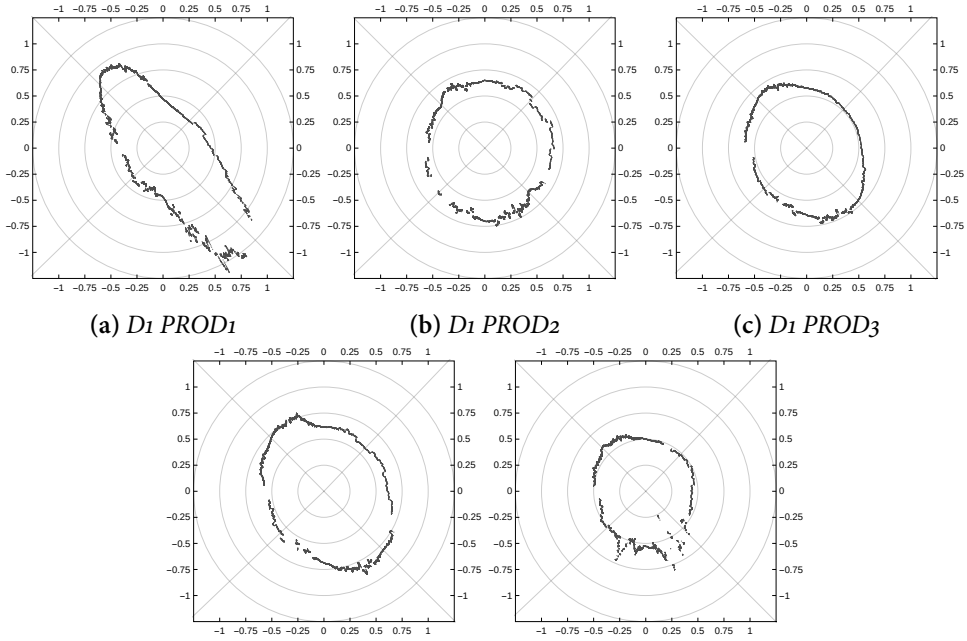

(a) *D1 PROD1* **(b)** *D1 PROD2* **(c)** *D1 PROD3*

(d) *D1 PROD4* **(e)** *D1 PROD5*

Figure 6.19.: Moving average of angle dependent bending wave velocity ratio for *D1 PROD1-PROD5*. Diagonal grid lines depict grain angle (v_{LL}: bottom right to top left).

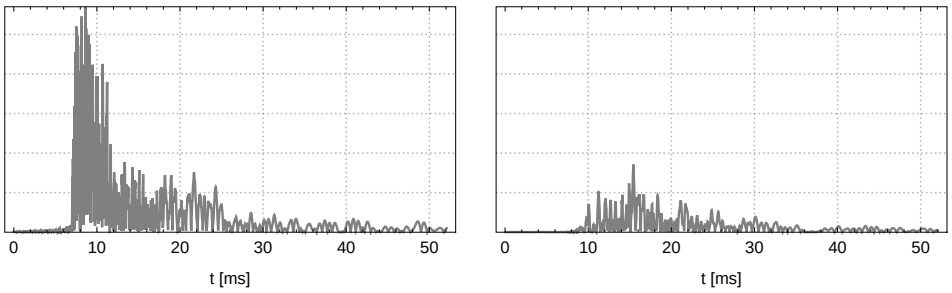

(a) IR_{ref} **(b)** IR_n

Figure 6.20.: Modulus of impulse response before (IR_{ref}) and after (IR_n) traveling approx. 2 m through the soundboard in L direction

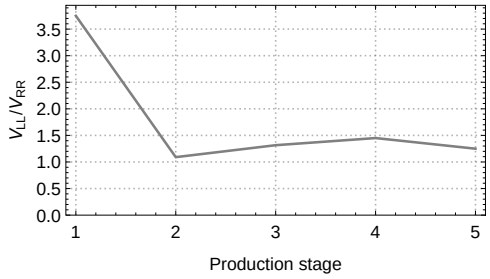

Figure 6.21.: Bending wave velocity ratio of v_{LL} over v_{RR} per production stage.

effect of the ribs on the outer edges of the soundboard and further increases v_{LL}/v_{RR}. Gluing the soundboard into the rim (*PROD5*) changes the system dramatically but, in total, leads back to nearly the general 'isotropic state' it had in *PROD2*. One contributing factor could be the stiffening of the outer edges due to the clamped boundary conditions, which increases v_{RR}. It would have been very interesting to learn about v_{LL}/v_{RR} for *PROD6* when the pre-load from the strings was applied. Since in that condition $2/3$ of the soundboard surface is covered with the cast iron frame, unfortunately a measurement was not possible. Measurements for *D4* show no significant differences.

6.6. Angle Dependent Dispersion

As described in Section 3.2.1, the bending wave velocity in wood is frequency dependent. Thereby, when a wave front travels across the soundboard, the initial zero-phase pulse is blurred to a sweep, since higher frequencies run ahead of lower frequencies. The attack time as the time range from beginning to the end of the initial signal part (see Section 12.1.3 for a description of the utilized algorithm) can be used as an indicator for the grade of dispersion of the structure: The longer the initial bending wave front travels in a homogeneous dispersive structure, the flatter the slope of signal envelope should be (and, thereby, the greater the measured attack time should be). Figure 6.22 shows the attack time, averaged over all impulse responses, per production stage. The application of the ribs, and gluing the soundboard into the rim have the greatest general impact on the average blurring of the wave front.

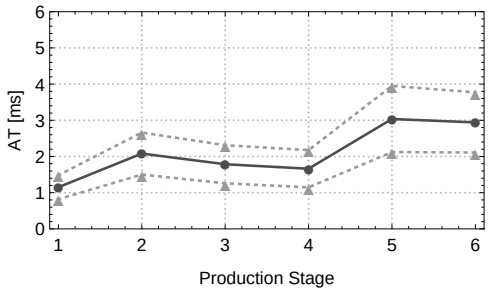

Figure 6.22.: Average attack time of impulse responses per production stage for *D1*. Dashed lines depict range of standard deviation.

Visualizing the attack time per microphone for the soundboard reveals a relation between dispersion and bending wave velocity (compare with Figure 6.15): Figure 6.23 shows how the slope of the pulse changes depending on direction and distance to the input position. Similar to the velocity, the greatest gradient for the attack time slope follows the bridge. Measurements of *D4* show no significant differences to *D1*.

6.7. Damping

As described in Section 3.2.5, measuring the individual contributions of the different damping types for a complex structure is non-trivial and often impossible. The measured decay of a deflection of a vibrating structure is always caused by a combination of energy dissipation through radiation, boundary conditions, and internal friction. For the work at hand, damping is observed as the decay of sound pressure in the near field of the soundboard. Therefore, no explicit information is obtained about the internal friction in the structure, or about energy drain through the boundary conditions. Nevertheless, since information about the transient wave propagation is available, the energy loss can be described not only as the general signal decay, but can also be given exclusively for the initial propagation on the soundboard before any reflections or drain at the boundaries.

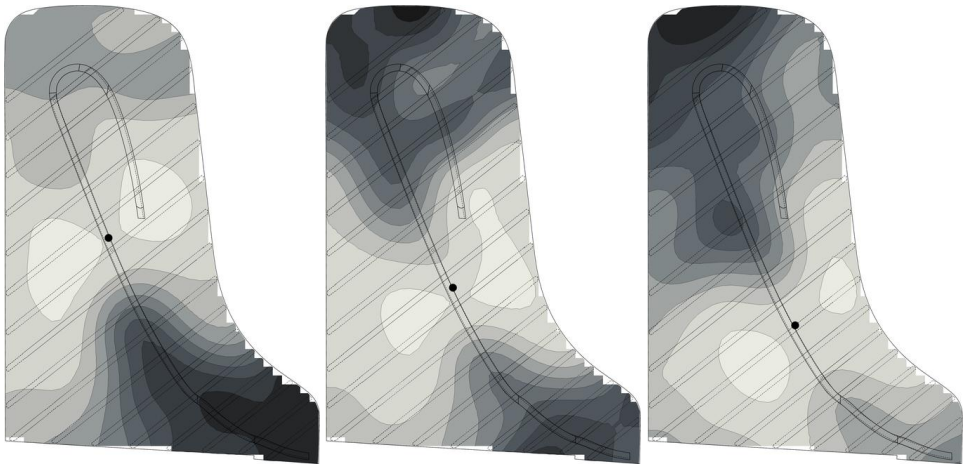

(a) *POS8* **(b)** *POS9* **(c)** *POS10*

Figure 6.23.: Spatial distribution of attack time for *D1 PROD3*. Bright for small values to dark for high values.

6.7.1. Damping as Reverberation Time T_{60}

Figure 6.24 shows the average decay of all impulse responses per input position as T_{60} values. The decay is calculated in time domain using the Schroeder backward integration method.[184] Gluing the soundboard into the rim causes a significant increase in decay time.

A detailed comparison reveals a relationship between damping and driving point position for *PROD5*: Figure 6.25 b) shows a significant decrease of decay time for the upper treble range while the rest of the soundboard shows a constant T_{60} value of approx. 0.5 s[185]. That is in accordance to previous observations of distinct differences between the highest treble range and the rest of the soundboard. As shown in Section 6.2, the treble range does not participate in the lowest modes, which also have the slowest decay. Due to the construction, the vibrating area is small and, for the highest notes, the bridge

[184] M. R. Schroeder (1965). "New Method of Measuring Reverberation Time." In: *Journal of the Acoustical Society of America* 37.3, p. 409. DOI: 10.1121/1.1909343.

[185] Which, in room acoustics, would correspond to the reverberation time of a well-furnished living room.

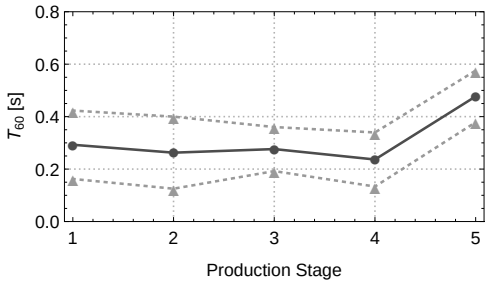

Figure 6.24.: Average impulse response decay as T_{60} per production stage for *D1*. Dashed lines depict the range of standard deviation.

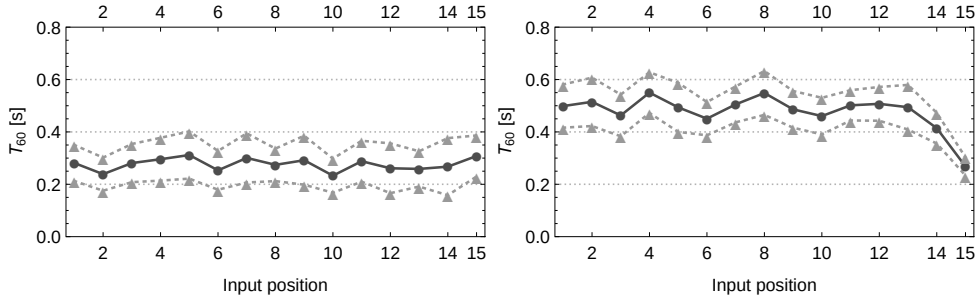

(a) *D1 PROD3* **(b)** *D1 PROD5*

Figure 6.25.: Average decay per input position a) before, and b) after gluing the soundboard into the rim. Bright lines depict range of standard deviation.

is positioned over the rim, forming a stiff connection to the frame. From an instrument builder's perspective, it is preferable to stiffen the soundboard in the treble range. A softer soundboard would decrease the impedance mismatch between strings and soundboard and, thereby, shorten the produced tones. Achieving sustained and rich high notes is a challenge that already existed with harpsichords[186] and one that is still crucial in modern piano manufacture.

6.7.2. Damping of Initial Wave Front Propagation

Observation of the first reflection-free wave propagation in time domain can provide a good estimation of damping on the soundboard structure. In the

[186] Good, *Giraffes, Black Dragons, and Other Pianos*.

following section, two cases are compared:
Firstly, the energy loss in the initial wave front is characterized by looking at the development of the maximum value per impulse response A_{max}. Note that in the given case the decrease of the maximum value of the wave front is a result of both, energy loss through damping, and due to dispersion. Even for a hypothetical undampened but dispersive structure, A_{max} would decrease because higher frequencies would travel ahead and, thereby, decrease the total energy in the main front. Nevertheless, with the obtained information about the angle dependent dispersion per production state in mind (see Section 6.6), A_{max} allows an assessment about energy loss in the initial propagation. Note that the presented figures of A_{max} (6.26-6.30) do not display a common point in time, but the maximum of the IR per microphone, whenever it occurs.
Secondly, A_{max} is compared to the root mean square (RMS) of the complete IR. For a homogeneous infinite, and thereby reflection free, plate the RMS per IR should decrease, dependent on the distance from input position, following an exponential decay.

***PROD1*:** A clear difference in damping is observable between L and R direction for the blank soundboard: The energy loss per traveled distance is twice as large in radial, than in longitudinal direction (see Figure 6.26). Since this direction dependence is not observable in the dispersion measurements, the directivity in A_{max} should be caused mainly by damping. Plotting the RMS per microphone shows a similar general shape, which is more blurred due to several reflections on the structure boundaries. Still, the greatest portion of the supplied energy is preserved in grain direction.

***PROD2*:** After application of the ribs, the directivity is inverted and the majority of the supplied energy is preserved in radial direction. This is directly related to the structural modifications: E.g. at *POS11*, the soundboard is excited between two ribs, which act as boundaries for a great part of the vibrational energy (see Figure 6.27). Large parts of the supplied energy are 'trapped' between two ribs. Again, when looking at the complete signal, the reflections at the boundaries, and now also 'leakage' from the section between ribs, cause a softer gradient. Note that at the input position a local minimum (with regard to the soundboard surface between the adjacent ribs) is observable for A_{max},

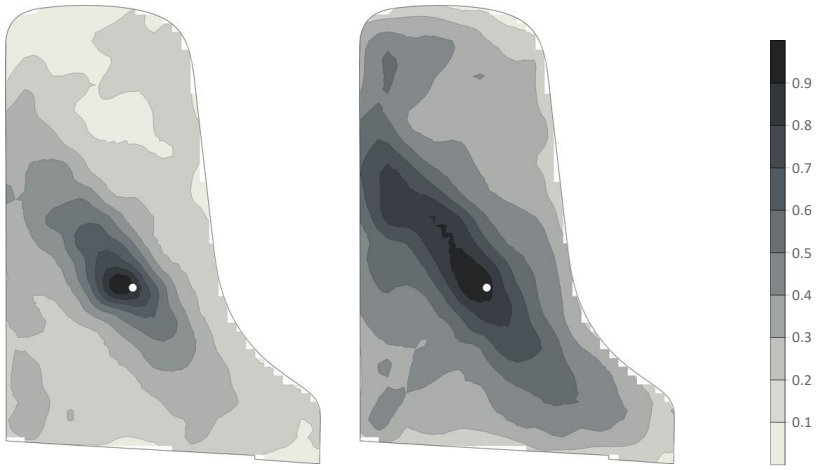

(a) (b)

Figure 6.26.: Energy loss on the soundboard for *PROD1 POS9*. a) Normalized A_{max}, b) Normalized RMS of complete IR. White dots depict the input position.

as well as for the RMS. A possible explanation could be based on the measurement setup: If the total energy between the ribs becomes greater than the input energy of the shaker, the stinger could dampen the vibrations at the input position. Based on the behavior of the soundboard, a possible explanation could be negative interference. Both cases would have to be closer examined.

***PROD3*:** After application of the bridge, the previous split in two distinct directions is diminished (see Figure 6.28). The loss in R direction is still smaller than in L, but the supplied energy seems to be able to distribute more uniformly due to the local stiffness increase by the bridge, acting as a waveguide in mainly L direction. A remarkable effect is observable regarding the applied bridge: The bass bridge and the connected lower treble bridge part form a loop in the upper half of the soundboard. This structure confines parts of the vibrational energy. Due to the form, vibrational energy is trapped in the loop, which leads to the effect that for an input position in the treble range, although the structure surrounding the input position initially has the highest amplitudes, throughout the duration of the decay the bridge loop seems to collect vibrational energy and has RMS values higher than near the input posi-

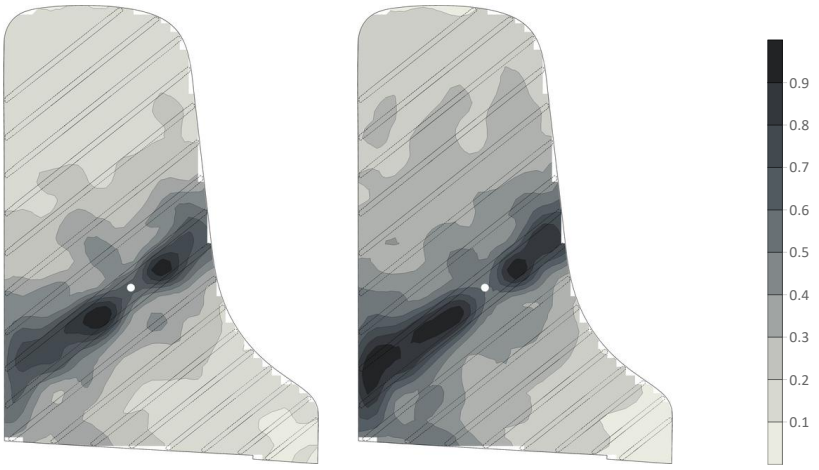

Figure 6.27.: Energy loss on the soundboard for *PROD2 POS11*. a) Normalized A_{max}, b) Normalized RMS of complete IR. White dots depict the input position.

tion (see Figure 6.28 b)). The bass- and treble bridge are connected by a part of approx. 20 cm which is not attached to the soundboard surface. As observable in Figure 6.28, this aperture allows energy exchange from and into the loop.

***PROD4*:** After tapering the ribs, the local stiffness on the outer edges is decreased and parts of the vibrational energy can cross the ribs (see Figure 6.29). For *POS8*, the propagation leftwards is wedge shaped with increasing distribution across ribs as it approaches lesser stiff regions near the edge. The part propagating rightwards gets trapped in the 'bridge loop'. Only a small proportion can pass through the bass bridge. Strong RMS values at the left soundboard edge give indication that the boundary conditions on the felt bed are not perfectly simply supported.

***PROD5*:** After gluing the soundboard into the rim, the boundary conditions seem to lower the gradient, the distribution of vibrational energy is more uniform than ever before. Still, great parts of energy are trapped between bridges.

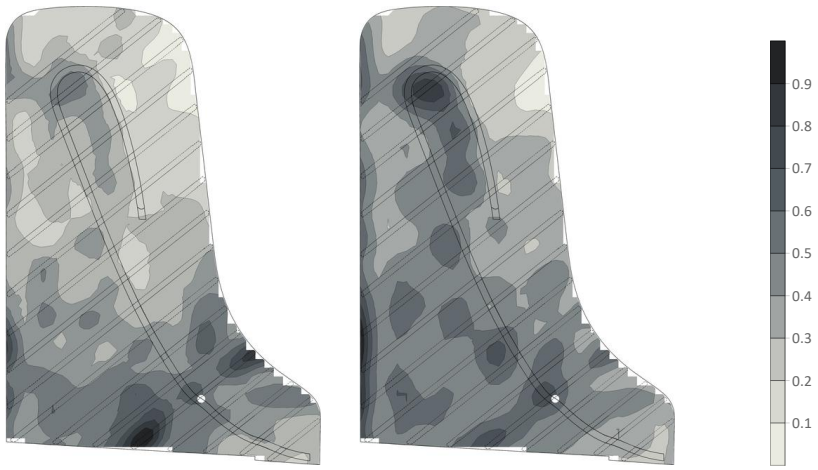

(a) (b)

Figure 6.28.: Energy loss on the soundboard for *PROD3 POS12*. a) Normalized A_{max}, b) Normalized RMS of complete IR. White dots depict the input position.

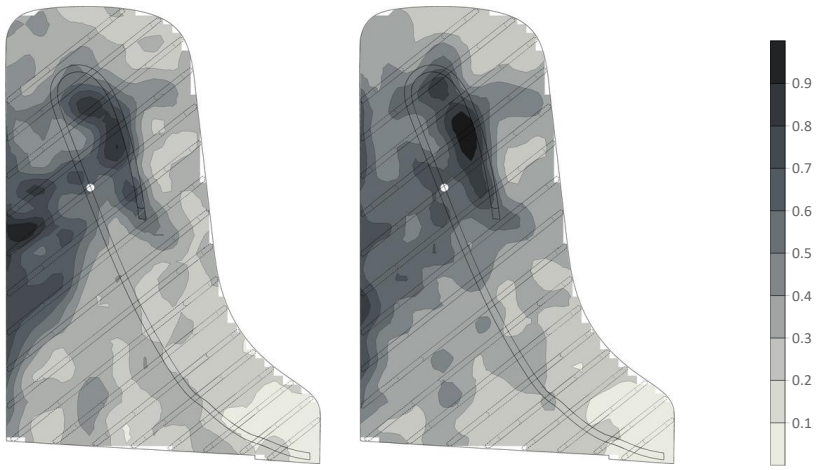

(a) (b)

Figure 6.29.: Energy loss on the soundboard for *PROD4 POS8*. a) Normalized A_{max}, b) Normalized RMS of complete IR. White dots depict the input position.

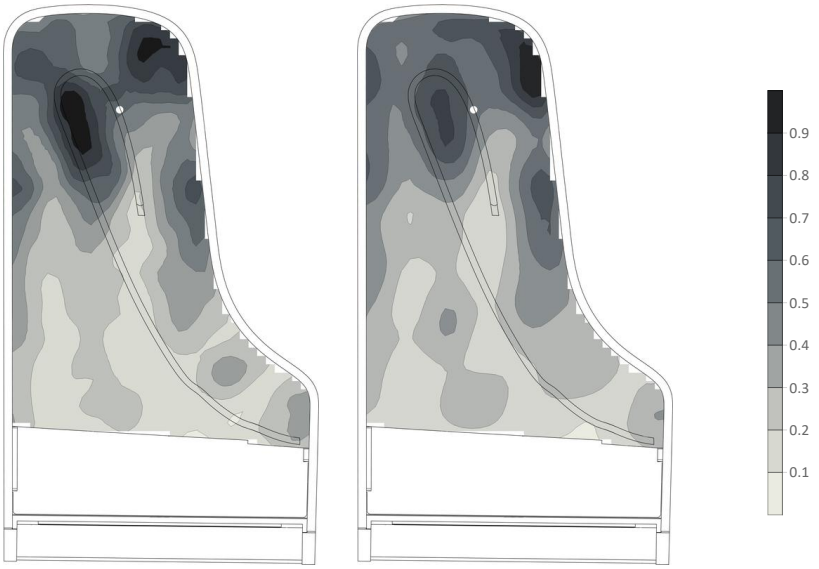

Figure 6.30.: Energy loss on the soundboard for *PROD5 POS2*. a) Normalized A_{max}, b) Normalized RMS of complete IR. White dots depict the input position.

6.8. Exponential Model for Spatial Attenuation per Frequency

As shown in the previous sections, several frequency regions can be distinguished which might be influential for the energy distribution on the soundboard: a) the *modal domain* up to 200 Hz, where the spatial energy distribution is not dependent on the driving point position due to low modal density and damping. b) a *transition domain* from 200 Hz to 1200 Hz where the soundboard shows modal behavior but individual modes can not be identified. Operating deflection shapes are composed of several modes due to increasing modal density and damping. c) For frequencies higher than approx. 1.2 kHz, the ribs form stiff boundaries. In combination with varying inter-rib distances, this leads to increased localization effects and the energy distribution is not independent of the driving point position anymore. d) For frequencies higher than 2 kHz the non-linearly increasing internal damping could further increase localization effects and in an extreme case, the damping could prevent the formation of standing waves at all.
To investigate this issue, an assumption is made based on the idea that for a highly damped plate, a bending wave traveling towards an edge would attenuate too much to reflect at all. Even if a small amount would get reflected, it would die out before being able to constitute a standing wave and produce modal behavior. In this extreme case, the finite plate would behave like an infinite plate, showing an $1/r$ exponential decay, dependent on the distance r from the input position. Thus, the energy distribution on the soundboard is modeled with an exponential function $A(r)$ for any frequency as

$$A(r) = a \exp(-\kappa r), \tag{6.1}$$

with a being the energy at the input position $r = 0$ m and κ being the exponential decay constant. Note that for the non-linear fitting κ can be any real number. $\kappa = 1$ would lead to an exponential decay expected for the distribution of vibrational energy in an infinite plate or the sound pressure of a spherical wave front radiating from a point source.[187] $\kappa = 0$ would describe

[187] Eduard Ventsel and Theodor Krauthammer (2001). *Thin Plates and Shells*. Boca Raton: CRC Press. DOI: 10.1201/9780203908723. arXiv: 1401.5045.

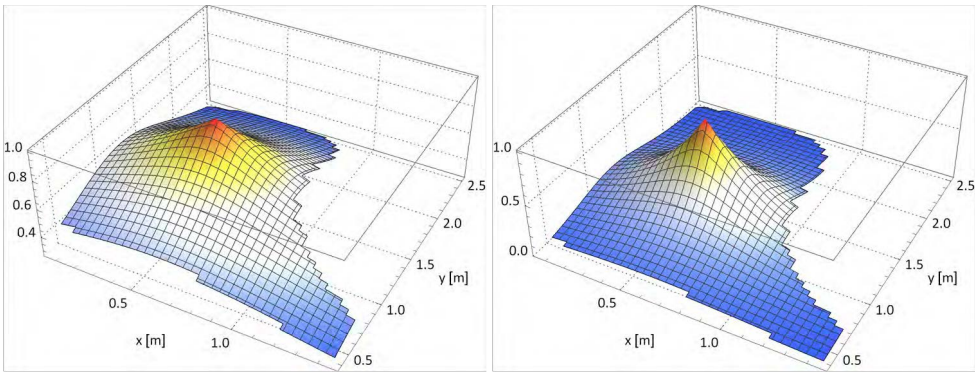

(a) $a = 1$, $\kappa = 1$ **(b)** $a = 1$, $\kappa = 3$

Figure 6.31.: Modeled spatial attenuation on the soundboard for exemplary cases a) $\kappa = 1$, and b) $\kappa = 3$.

a constant magnitude on the entire soundboard. Negative values for κ would lead to negative damping. Figure 6.31 shows two modeled exponential attenuation shapes on the piano soundboard for *POS9* with a) $\kappa = 1$, and b) $\kappa = 3$.

For the calculation the magnitudes per frequency at 1,300 microphone positions are included. Note that the utilized data represents the pressure field over the soundboard and not the deflection of the vibrating structure. This should blur the obtained data. However, the dimensions of the soundboard are greater than the microphone distance by a factor of 25 to 50 and the recorded pressure should reflect the magnitude of motion of the corresponding soundboard region in a good approximation. Another simplification is that for the exponential model only the distance to the input position is considered but not the angle. As shown in the previous section, even in the first production stage the damping on the plate is dependent on the direction of propagation. After attachment of ribs and bridge, the angle dependency gets even greater, or at least more complex. This angle dependency is excluded for the calculation.
For each frequency, a and κ are optimized resulting in the smallest squared error for the fitting function. Figure 6.32 illustrates the process: Discrete dots show the 1300 measured points on the soundboard with magnitude per angle-independent distance from the input position *POS9*. Figure 6.32 a) shows the 'monopole' mode shape at the first resonance frequency. Since *POS9* is sit-

uated in the center of the soundboard, the mode shape is recognizable as a magnitude decrease with increasing distance in all directions. The dark line shows the best fitted exponential attenuation with the parameter $\kappa = 1.77$. For this input position, the error for the least squared fit is relatively small, but for an input position like *POS1* at the highest end of the bass bridge, an exponential fitting would not give a reasonable result. Figure 6.32 b) illustrates this mismatch: For the 'dipole' mode shape at the second resonance frequency, *POS9* is situated on the nodal line. Therefore, two mode 'hills' are observable when plotting magnitude per distance. The best exponential fit gives $\kappa = 0.09$, which would assume a nearly constant magnitude over the entire soundboard. To summarize, it can be stated that as long as the soundboard behaves modal, in a way the generated shape is not, or only very little depending on the input position, the exponential fit will give unreasonable and highly fluctuating results. As soon as the energy distribution increasingly depends on the input position, the exponential fittings should become meaningful and fluctuations should decrease. Figure 6.32 c) shows an exemplary case at 400 Hz, which is in the transition domain where no individual mode shapes are recognizable anymore. However in the point cloud, patterns are still observable. The fitting gives $\kappa = 1.26$ but the fitting error still can be great for several input positions. Figure 6.32 d) shows an exemplary distribution at 2.5 kHz. No patterns are observable and the general distribution should be completely driving point dependent.

The parameters a and κ are optimized for each frequency in 1 Hz resolution up to 5 kHz. Figure 6.33 shows a) κ per frequency, and b) the standard deviation $\sigma(\kappa)$ per frequency (window size: 5 Hz, step size: 1 Hz) for *PROD3*, averaged over all 15 input positions. Several distinct domains are observable: The modal domain up to 200 Hz is clearly separated with by far the greatest standard deviation values. For frequencies higher than 200 Hz, there is a significant drop in fluctuation strength, still fluctuations are observable up to approx. 1.4 kHz. The parameter κ increases between 1.6 kHz and 2.4 kHz from approx. 0.5 to 1 and then varies between 1 and 1.5.

Figure 6.34 shows the influence of the manufacturing process on the parameter κ. Application of the ribs does not seem to have great influence on the modal domain, which is in agreement with previous findings, that the lowest resonance frequencies change significantly only after changing the boundary conditions (*PROD4*-*PROD5*). For frequencies higher than approx. 1 kHz, κ

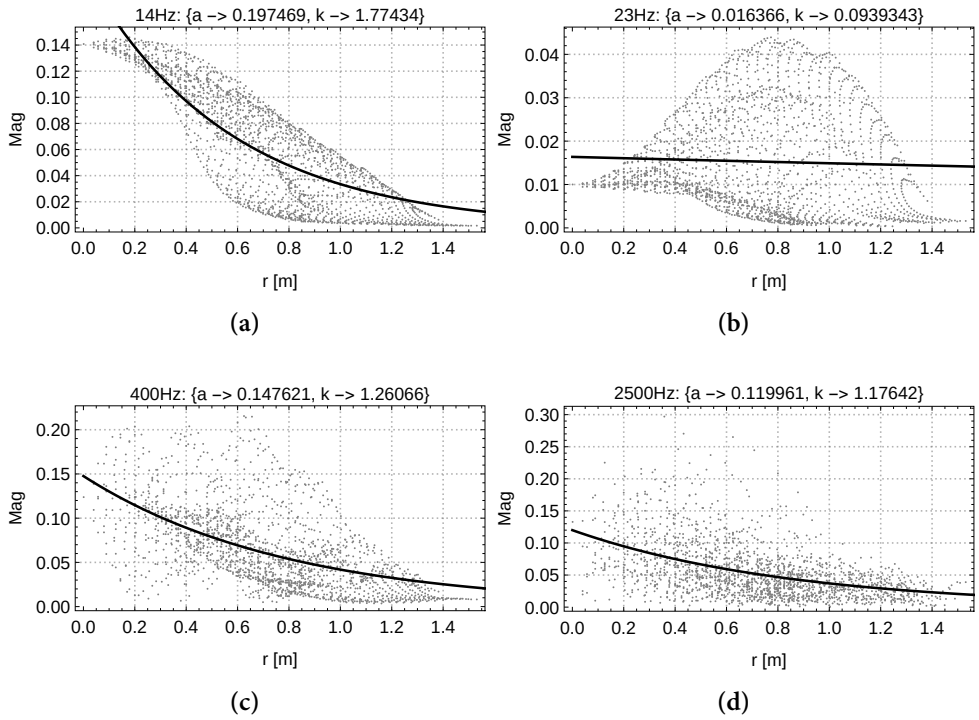

Figure 6.32.: Exponential fittings for magnitude per distance from the input position. Different exemplary frequencies at *POS9*.

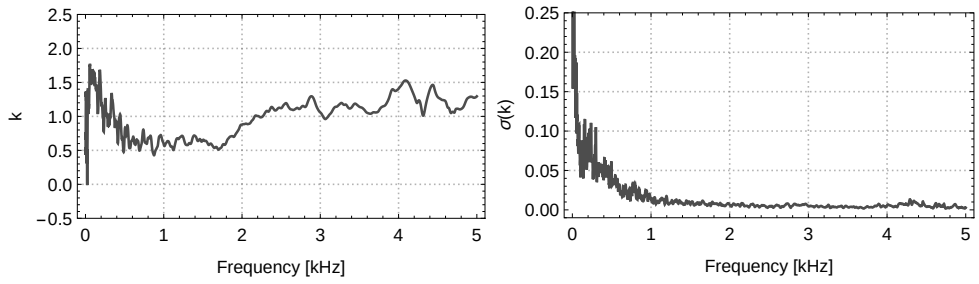

Figure 6.33.: κ per frequency for *PROD3*.

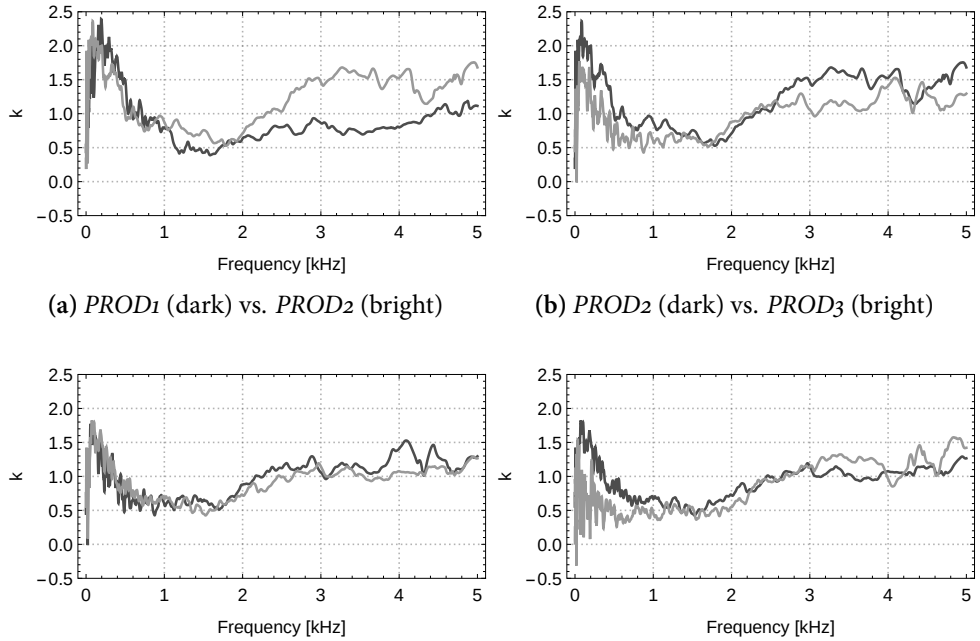

(a) *PROD1* (dark) vs. *PROD2* (bright)

(b) *PROD2* (dark) vs. *PROD3* (bright)

(c) *PROD3* (dark) vs. *PROD4* (bright)

(d) *PROD4* (dark) vs. *PROD5* (bright)

Figure 6.34.: Influence of production step on parameter κ.

is always greater than without ribs, with the greatest increase from approx. 2 kHz. This can be explained with the increasing influence of the ribs for the bending wave propagation, leading to localization. As shown in the previous section, for high frequencies great proportions of the vibrational energy do not propagate through the entire soundboard but are trapped between the ribs adjacent to the input position. This leads to higher κ values in L direction. The attached bridge facilitates propagation in L direction and κ decreases for high frequencies. In agreement to previous findings, tapering the ribs has no significant observable effect on the behavior of the soundboard. Clamping the soundboard into the rim, and thereby changing global stiffness and boundary conditions, drastically increases modal frequencies. This is observable as an expansion of the modal domain with high κ fluctuations. However, this drastic change has relatively small impact on higher frequencies.

The findings can be summarized as follows:

- The model is capable of distinguishing the different frequency domains

for a vibrating piano soundboard. It displays the transition from modal- to driving point dependent domain as a decrease of the standard deviation of κ.

- Although localization effects can produce deviating vibrational patterns in high frequencies, the averaged behavior can be approximated with an exponential decay. For frequencies greater than 3 kHz, κ has values between 1 and 2.

7. Discussion Part 1

7.1. Critique of Method

In order to be able to make statistically verified statements about the vibrational behavior and, to a limited extend, to generalize the statements to every piano of the given kind, it would have been required to examine a high number of instruments. Due to several constraints this was not possible: The measurement process for only two instruments took nearly two years. The organizational effort was enormous: The instruments had to be taken out of the production line after each production step and transported to the institute. Measurements of one piano in a certain production stage sometimes took several weeks. After measurements, the instruments had to be transported back to the factory and to be reintegrated into production. The company generously provided personnel for monitoring and organization at the factory. Due to the frequent measurements, manufacture of the considered instruments took twice as long as in normal operation, which resulted in significant additional costs for the company. Therefore, the consideration of more instruments was not possible for reasons of cost, availability and timing.
The necessary organizational effort also prevents regular use of the method in the workshop.

Since the instruments were to be sold after manufacture, a fundamental prerequisite for the measurements was to strictly avoid any visible modifications of the soundboard. Therefore, the utilized shaker could not be rigidly connected to the structure with the aid of glue or screws. To prevent contact-loss during excitation, the shaker had therefore to be pressed on the soundboard with a static pre-load of approx. 1 kg. The induced pre-stress is known to slightly alter the vibrational behavior of the plate.

The existing microphone array has been successfully used for radiation measurements of numerous musical instruments. However, the studied structures were of a size which allowed the acquisition of radiation data with only one take without having to considerably cut the spatial resolution. For the present work it was decided to successively measure parts of the piano soundboard surface to retain a spatial resolution of 40 mm. This approach has been applied at the institute for the first time with the given setup.
Due to the strong curvature of the piano soundboard and the application to the outer frame, the distance between microphone plane and radiating surface had to be insufficiently large for the last production stages. This alone would significantly reduce the observable frequency range for the last production stages.
The degree of pre-amplification of the used converters turned out to slightly vary between channels and in dependence of the run time of the devices.
Signals out of sync by a few samples have been detected in almost all measurements. This might not be crucial in music production but it turned out to be relevant when imaging wave propagation with high velocities. For future work it is recommended to deactivate the automatic re-sync functionality and compensate the shift of 3 samples per MADI ID in the post-processing. A doubling of the sample rate to 96 kHz would also help to overcome the spatial undersampling. However, for the same number of utilized microphones, 4 parallel MADI streams would be required, which is currently difficult to realize on one workstation. Systems based on network protocols like *Dante* or *AVB* could be considered to overcome the throughput limit.
To summarize: A back-propagation was not possible with the given setup as the excitation would have been needed to be highly reproducible. Nevertheless, as shown in the previous sections, a wide variety of measures can be obtained from the pressure field data, even if not been propagated. As a result of the multiple-array application, the soundboard behavior could be captured with a remarkable spatial resolution with 1,300 discrete points on the surface. Due to the combination of microphone array and the ESS method, it has been possible to visualize the initial reflection free bending wave propagation on the piano soundboard at high spatial and temporal resolutions.

The chosen placement of the soundboard on felt in the rim profile turned out to play an important role for the impossibility to exactly reproduce the measurements. Berthaut, Ichchou, and Jézéquel[188] performed measure-

[188] Berthaut, Ichchou, and Jézéquel, "Piano soundboard: Structural behavior, numerical and

ments on a grand piano soundboard, hanging vertically on flexible cables and achieved free-, and thereby reproducible, boundary conditions. However, it was planned to accompany the instrument through the complete production, which included the finished piano. Thus, a vertical suspension would not have been possible for a 500 kg instrument. Additionally, the soundboard just fitted into the anechoic chamber horizontally. The room height would not have allowed a vertical orientation.

7.2. Reflection on Results

7.2.1. Development of Structural Properties

The only observable structural difference between the soundboards is a 3.7 % higher average density for *D4* as a result of smaller annual ring widths. The average crowning in the soundboard center stays constant until it is glued into the rim, which leads to a decrease to approx. 15 mm. In contrast to consensus belief, stringing and tuning does not result in an immediate observable reduction of the curvature. Although the *D4* soundboard should have a greater stiffness due to the higher ratio of late wood, it bends distinctly more than *D1* when attaching the ribs and the bridge. When glued into the rim, the differences in shape between *D1* and *D4* vanish. There is thus reason to assume that *D4* should undergo a greater pre-stress when forced into the same rim profile. It is remarkable that the observable differences in wood material properties between the two examined soundboards are not reflected in the acoustic measurements. This leads to the assumption, that in this range of variation, the geometry plays a predominant role for the resulting behavior.

7.2.2. Development of Vibrational Behavior

The application of ribs has a crucial impact on the propagation behavior of the initial bending waves. In direction normal to grain, the propagation is not circular but rather a traveling plane wave front, as a result of superposition of

experimental study in the modal range."

reflections between the ribs. The ribs act as waveguides for higher frequencies with locally changed stiffness. The influence of the bridge is clearly observable in the initial bending wave pattern: Stiffening increases the wave velocity locally, and the propagation seems to follow the bridge direction, even when curved.

It is possible to estimate the flexural wave velocity ratio between longitudinal and radial direction on the soundboard: Application of ribs nearly compensates the anisotropy to a ratio of 0.9. Overcompensation is not observable. The attached bridge causes a local stiffening, mainly in grain direction, which leads to higher velocities along its direction and thereby a decrease of v_{RR}/v_{LL}. Gluing the soundboard into the rim changes the system dramatically but, in total, leads back to nearly the general 'isotropic state' it had with only the ribs.

The energy loss can be described exclusively for the initial propagation on the soundboard before any reflections or drain at the boundaries:
The energy loss per traveled distance is twice as large in radial, than in longitudinal direction for the blank soundboard. The greatest portion of the supplied energy is preserved in grain direction. After application of the ribs, the majority of the supplied energy is preserved in radial direction between adjacent ribs. After attaching the bridge, the supplied energy seems to be able to distribute more uniformly due to local stiffness increase by the bridge, acting as a waveguide in mainly longitudinal direction. The bass bridge and the connected lower treble bridge part form a loop in the upper half of the soundboard, which confines significant parts of the vibrational energy (*bridge loop effect*).

The spatial distribution of vibrational energy on the soundboard per frequency can be approximated with exponential decays. The model is capable of distinguishing the typical frequency domains for a vibrating piano soundboard: It displays the transition from modal- to driving point dependent domain as a decrease of the standard deviation of exponent κ. Although localization effects can produce deviating vibrational patterns in high frequencies, the directional averaged behavior can be approximated with an exponential decay. For frequencies greater than 2 kHz to 3 kHz, κ has values between 1 and 2. With $\kappa = 1$, the soundboard behaves like a reflection free plate; higher values of κ can be explained with local waveguide effects by ribs and bridge.

Part II.

Influence of Playing on the Tonal Characteristics of a Concert Grand Piano - an Observational Study

8. Theory

In the following section, possible factors for a long-term change in tonal characteristics are listed and discussed for musical instruments and, in particular, for pianos in concert business. The issue is approached with regard to three main influences:

- **Aging:** When addressing the long-term development of musical instruments, most published works focus on the time-conditioned degeneration of wood, eventually accelerated by periodic humidity alterations. For the piano, this might be relevant for material properties as well as geometry of the wooden soundboard with bridge and ribs. In connection with aging, the influence of climate conditions on wooden instrument parts has to be taken into account. In regard to other instrument parts, aging could show up as material fatigue of strings or mechanical parts in the action.
  Aging might be a crucial factor for the preservation of an instrument, particularly when dealing with historical instruments within the museum context. However, since this work attempts to address the possible changes in tonal quality for only the first year of a concert instrument under intensive supervision, other aspects gain in importance:

- **Playing:** The vibrational properties of wood change when it is subject to vibrations for extended periods of time. Thereby, regular playing could cause an audible change in vibrational characteristics of piano soundboards.[189] For other instrument parts, the influence of playing could show up as wear-out of mechanical connections in the action or as localized plastic deformations of the hammer felt.

[189] Weldert, "Sound Enhancement of Musical Instruments by 'Playing them in': Fact or Fiction?"

- **Maintenance:** A grand piano at a concert hall is intensively monitored by a technician. It is tuned several times a week and prior to each concert, substantial adjustments to keys, action, and hammers might be made in consultation with the player to achieve a certain requested playing feel and tonal character. Since the purpose of maintenance work is to adjust and thereby to refine the tonal characteristics, an impact in the context of this work can be expected.

This section follows the process of tone production through the piano and describes the respective factors which presumably contribute to a difference in tonal quality of a piano when being played for one year. The suspected proportion of impact by each factor is estimated. The extent and interrelation of identified influential factors leads to considerations regarding the type of study design, as discussed in the subsequent section.
Presented information about maintenance work on grand pianos is in part based on conversations and informal interviews with several piano technicians, including the technician responsible for the piano under observation at the concert hall, and the technician who tuned the piano prior to the measurements[190]. Furthermore, Junghanns[191] and Reblitz[192] give comprehensive overviews of service work on grand pianos.

8.1. Influential Factors

8.1.1. Keys and Action

An important part of maintenance work on the piano is adjusting the interrelation of keys, action, and pedals, so-called *regulating*. The keys are adjusted to have certain weights needed to descend when depressed, called *down weight* (ger. *Spielschwere / Niederdruckschwere*) and to rise back up, called *up weight* (ger. *Aufgewicht*). The average down weight is between 50 and 55 grams, but

[190] see Appendix A.6 for transcriptions of informal interviews with the technician after tuning the instrument and prior to the measurements.
[191] Herbert Junghanns (1984). *Der Piano- und Flügelbau*. Verlag Erwin Bochinsky.
[192] Arthur A. Reblitz (1993). *Piano Servicing, Tuning, and Rebuilding*. Vestal Press Inc.

professional players often have their own preference of a lighter or heavier playing feel. A possible way to change the touch weight of a key is to add or to remove lead weights from the key body. Due to a changed inertia, different touch weight leads to a different acceleration of the key per input force and thereby will produce a different spectral distribution. Since the recorded examples are compared according to a similar key bed force, the implemented maintenance work on the keys is expected to have an impact on a potentially perceivable difference of the tonal quality of the piano. For the piano under observation the touch weight has been decreased for several keys by counterboring lead weights behind the balance rail axis.
Comparable to the keys, maintenance work on the action mechanism could result in an altered acceleration behavior of the hammer per input force. Again, this would modify the resulting spectral composition as the string would be confronted with a harder or softer hammer (see Section 2.0.2). Thereby, maintenance on the action can be expected to be influential and to possibly have impact on the tonal quality within one year.

8.1.2. Hammers

During production of a hammer, the layers of felt are glued around the hammer molding with high pressure. Thereby the inner felt parts are compressed while the outer parts are stretched. If a hammer is too hard, the produced tone will be harsh and bright, if it is too soft, the tone will be too dull (see Section 2.0.2). Brand new hammers (but also old worn hammers) are often too hard.
The adjustments of hammers performed to gain a consistent tonal character is called *hammer voicing* (ger. *Intonation*). The technician can influence the hammer properties in several ways: One way is to needle the hammer felt in certain areas with a special tool. The needles separate felt fibers and thereby soften a hammer region. To harden the felt in a certain region, acetone or nitrocellulose lacquer can be applied to the felt. The lacquer soaks into the hammer and hardens a certain region.
The piano under observation has had several hammer voicings within the year. Since the only purpose of these adjustments is to change the tonal behavior of a note, it clearly can have impact on the perceived difference between *PROD7* and *PROD8*.

Since the instrument is revised several times a week during the year, an impact by material aging or mechanical wear-out is not expected for keys, action, and hammers.

8.1.3. Strings

Under beneficial conditions piano strings degenerate within a period of decades. Under heavy workload e.g. in a conservatory, the average lifespan decreases to 8-10 years with possible tears and breaks after approx. 5-6 years. Old strings are said to gain a clinking (ger. *klirrend*) sound which can originate from the string itself, but is often also associated with loose bridge pins.
A possible explanation for the degeneration of steel strings is strengthening by plastic deformation (*work-hardening*). The increase of string stiffness could have the unwanted effect of increasing the inharmonicity of the string. However at least for wound strings, Houtsma[193] shows that the long-term increase of string inharmonicity can be explained by changes in mass distribution due to repeated stretching. Within one year, effects by aging, playing, or maintenance of the strings on the tonal quality of the piano is expected to be negligible.

8.1.4. Soundboard

A possible change of wood properties could be caused by two, often interrelated, factors: a) the aging of wood under certain climate conditions, and b) changes of material properties due to regular playing.
The effects of aging of wooden instrument parts on the vibrational behavior are studied mainly for violins, an overview is given by Bucur.[194] In particular, the gradual loss of hemicellulose is found to decrease the density but not to affect the Young's modulus. This raises the sound radiation coefficient E/ρ. For instruments in static high relative humidity the greatest change of vibrational properties is found in radial direction, increasing the degree of anisotropy.[195]

[193] Adrian J. M. Houtsma (1982). "Inharmonicity of wound guitar strings." In: *The Journal of the Acoustical Society of America* 71.S1, S9. DOI: 10.1121/1.2019676.
[194] Bucur, *Acoustics of Wood*.
[195] Brémaud and Gril, "Effect of transitional moisture change on the vibrational properties of violin-making wood."

The time-dependent deformation under constant load (so-called *creep*) is enhanced by periodic humidity alterations and leads to changes in the radiated spectrum.[196] Furthermore, vibrations accelerate the creep.[197]

As known from conversations with the responsible technician, the piano soundboard curvature decreases and increases with a periodicity of one year. In autumn and winter the concert hall is artificially heated which decreases the relative humidity down to 20 % at the extreme. As a result, the moisture content in the soundboard wood decreases. The wood shrinks and the soundboard 'sinks in'. This has far-reaching consequences: With the soundboard also the bridge sinks in, which changes the angles between strings and bridge. With the angles also the static bridge pressure decreases with all implications on the pre-stressed vibrational behavior of the soundboard.[198] With the bridge also the strings sink in which changes the spatial alignment between strings and hammers. Thereby, as a compensation for changing climate conditions, the technician has to readjust the regulation.
When the heating is disabled in spring and summer, moisture content in the soundboard wood increases and the soundboard rises up again. The static bridge pressure and thereby the pre-stress conditions increase, the strings misalign with the hammers and the action has to be readjusted again. In that respect, technicians speak of 'artificial aging through air conditioning'.

Hunt and Balsan[199] find that playing at generally high humidities leads to increased stiffness and decreased loss coefficient. As a consequence, 'old fiddles (are said to) sound sweeter' than new ones. Hutchins[200] finds that long term playing (5-8 years) of violin family instruments leads to increased amplitudes of body cavity air modes. Bissinger[201] reports a general decrease of modal frequencies for a violin after approx. 250 hours of professional playing. Clemens

[196] Beavitt, "Humidity cycling."
[197] E. Segerman (2001). "Some aspects of wood structure and function." In: *Catgut Acoustical Society Journal* 4.3, pp. 5–9.
[198] Mamou-Mani et al., "Prestress effects on the eigenfrequencies of the soundboards: Experimental results on a simplified string instrument."
[199] Hunt and Balsan, "Why old fiddles sound sweeter."
[200] Hutchins, "A Measurable Effect of Long-term Playing on Violin Family Instruments."
[201] George Bissinger (1995). "Modal Analysis Comparison of New Violin Before and After 250 Hours of Playing." In: *Proc.13th Intern. Modal Analysis Conf.- Soc. Exp. Mechanics* July, pp. 822–827.

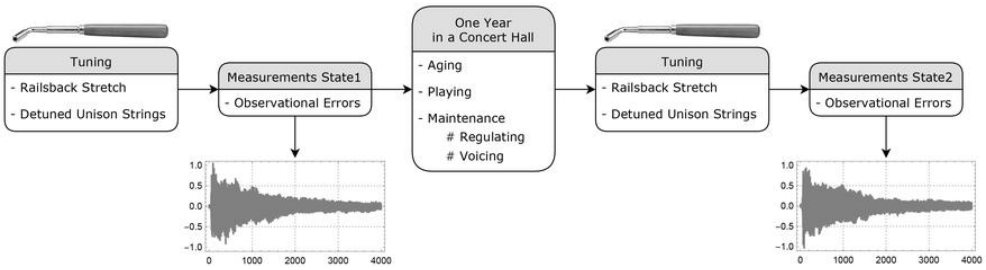

Figure 8.1.: Influential factors and disturbances for the experimental design.

et al.[202] find no evidence for changes of the vibrational behavior of guitars due to artificial vibration treatment. Structural modifications on the soundboard are not part of regular maintenance work. In very rare cases, the static bridge pressure might be modified as a one-time adjustment by changing the angle between strings and bridge but this is by no means part of the daily work in a concert hall.

Figure 8.1 summarizes the identified influential factors for the given experimental design as discussed in the previous section.

8.2. Disturbances Determined by the Experimental Design

8.2.1. Tuning the Instrument

Prior to recording the instrument, a technician (the same person in both states) has been asked to tune the instrument with the only instruction to give the piano a regular concert tuning. The technician could have influenced the tonal quality of the piano in two ways:

1. Pianos are tuned with stretched octaves to compensate for the inharmonic overtone spectrum (*Railsback stretch*).[203] The degree of tuned oc-

[202] B M Clemens et al. (2014). "Effect of Vibration Treatment on Guitar Tone: A Comparative Study." In: *Savart Journal*, pp. 1–9.
[203] Railsback, "Scale Temperament as Applied to Piano Tuning."

tave stretch relies on the judgment of the technician. Following Martin and Ward,[204] deviations from the Railsback curve could be the tuners handling of soundboard resonances. In this regard, different octave stretches could be the technicians response to a change in the vibrational behavior of the piano. In the same course, different octave stretches could lead to perceivable pitch differences between *PROD7* and *PROD8* for the bass and treble range.

2. Technicians usually detune the unison strings by 1-2 cents to give the decay of the tone a complex varying structure.[205] A different degree of detuning of the unison strings for *PROD7* and *PROD8* could lead to a perceivable difference in the temporal development of the tones' overtone structure.

Thus, the technician who tuned the piano prior to the measurements could have strongly influenced the resulting sound. Both aspects of tuning could have crucial impact on the test, because if the piano tones could be discriminated based on effects of a different tuning, in the worst case listeners would only discriminate the impact of tuning the instrument and not impact of time, playing, and maintenance on the instrument.

8.2.2. Measurement Errors

Unsystematic measurement errors could have been introduced by placing the dummy head differently or adjusting the recording equipment wrongly, but these disturbances are considered to be small compared to the other factors mentioned.

8.3. Study Design Considerations

The decision for a study design depends on the research question under consideration, and is always a trade-off between two contrastive approaches with

[204] Martin and Ward, "Subjective Evaluation of Musical Scale Temperament in Pianos."

[205] Roger E. Kirk (1959). "Tuning Preferences for Piano Unison Groups." In: *The Journal of the Acoustical Society of America* 31.12, pp. 1644–1648. DOI: 10.1121/1.1907673.

their respective advantages and drawbacks: On one side an artificial but highly controlled investigation in the laboratory where in an ideal case one independent variable is manipulated and its effect on one or more dependent variable(s) is measured. If well realized, an *experiment* can provide definitive evidence by causal relationships between individual independent- and dependent factors. Nevertheless, these abstracted studies often simplify the problem and thereby lack real relevance to the actual environment.
On the opposite side is the observation of an instrument 'in the field'. The investigation is much closer to real use and practice but control of the influential factors is limited or, in extreme cases, impossible. Randomized assignment to a control group by the researcher is not possible or a control group does not even exist. Although *observational studies* cannot provide definitive evidence by causal relationships due to the possible presence of confounding, they can show correlations between factors. Interpreted with care, these can provide valuable information about real-life use and practice.[206]

Maintenance work by the piano technician is an inseparable part of 'playing' in concert business. It is unlikely that an instrument would be chosen for concert if it wasn't finely adjusted. Furthermore, many professional players demand substantial adjustments on the instrument they choose for concert.[207] As described in the previous section, there are numerous influential factors for the tonal characteristics which potentially are highly correlated. Moreover, most certainly there are confounding factors: E.g. the periodic curvature change of the soundboard as an independent variable affects dependent variables (psychoacoustic parameters derived from the recordings), but also affects other influential factors like the timing in the action mechanism. Furthermore, for financial as well as logistical reasons it is not possible to have a control group in form of a brand new grand piano with a value of more than 100,000 € placed into the same concert hall and not be touched or played. And it is not possible to externally control the independent variables (e.g. the author could not instruct the technician to adjust parts with a certain frequency or not to adjust

[206] Paul R. Rosenbaum (2010). *Design of Observational Studies*. Vol. 27. Springer Series in Statistics 2. New York, NY: Springer New York, pp. 83–85. DOI: 10.1007/978-1-4419-1213-8.

[207] Extensively documented in the awarded documentary film *Pianomania* from 2009, which covers the work of tuner and technician Stefan Knüpfer from Vienna preparing pianos for concerts: http://www.wildartfilm.com/new/index.php?lang=en&Itemid=136, accessed in June 2019.

them at all).
The influence of playing a piano in concert business on its tonal characteristics can therefore not be reduced to an artificial experiment where it is 'just played'. An examination can only be done with all its disturbances in the field as an observational study.

9. Experimental Arrangement

9.1. Instrument

A concert grand piano is used for the present work (denoted as *D1* in the first part). Measurements are performed on the instrument after manufacture finished and after regulation, intonation and tuning (further denoted as *PROD7*). Subsequently, the instrument is employed by the manufacturer as a rental piano (ger. *Gestellungsflügel*), lent to a concert hall in Munich, Germany. After having been played for one year at approx. 40 concerts, the instrument is brought back to Hamburg. The previous measurements are rerun with the exact same conditions (denoted as *PROD8*). Ahead of both measurements, a piano technician tunes the instrument. The piano is tuned by the same technician for *PROD7* and *PROD8*. Instructions to the technician are similar and include to give the piano a regular concert tuning with the chamber tone at 442 Hz. For the recordings the piano is carried into an anechoic room and the lid is dismounted.

Table 9.1.: Denotation of production stages

PROD	
7	after regulation, voicing and tuning - concert tuned state
8	after being played in a concert hall for one year

Figure 9.1.: Experimental arrangement: The piano is located in an an-echoic room, an artificial head is situated in player position.

9.2. Utilized Hardware

9.2.1. Excitation

For each production stage a set of 440 forte played single notes is recorded (88 keys $\times$ 5 takes). Since the spectral content of a piano tone is highly dependent on the hammer/string contact time and thereby is a function of the key velocity, the usage of a mechanical finger would have been preferable to ensure similar key-pressings in all measurements. Unfortunately, such a device could not be used for the study at hand. The sensor head of an impact hammer (Kistler 9722 A 500) is used instead to press the keys[208]. Thereby, the force F_{key} can be measured taking effect when the key hits the key bed (*key-bottom impact*). Figure 9.2 shows F_{key} as a function of time for the key-key bed contact of an exemplary keystroke. For subsequent calculations, the point in time of key-key bed contact t_{key} is defined to be the sample with the maximum absolute force value. The maximum absolute force value is set to be F_{key}. Figure 9.4 shows the distribution of F_{key} for *PROD8* of *D1*. As a pre-processing step for the analysis the 5 $\times$ 5 takes are filtered regarding a maximum F_{key} difference. If multiple combinations of takes fulfill the condition for one key, the two takes with the smallest nominal force difference are used for comparison. Figure 9.3 shows the number of matched pairs per defined maximum F_{key} difference. Up to a

[208] The keys are pressed and not struck. Therefore, the sound of finger-key contact could not be used a an identification cue in the listening test.

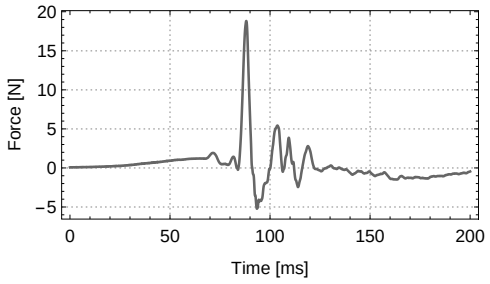

Figure 9.2.: Time series of measured force for the key / key bed contact of an exemplary keystroke.

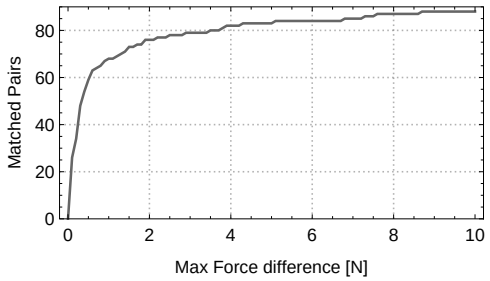

Figure 9.3.: Number of matched recording pairs between *PROD7* and *PROD8* per defined maximum F_{key} difference.

threshold of 0.6 N, the number of matched pairs grows rapidly with increased threshold. For higher thresholds the growth decreases. Based on a pre-test, a maximum difference of 0.6 N is chosen for the analysis and is later verified by the listening test. This procedure reduces the data base to 1×1 for 74 keys but ensures a highly standardized input.

9.2.2. Response

A calibrated artificial head (*Head HSU 3.2*, sensitivity left channel: 46 mV Pa^{-1}, sensitivity right channel: 45.2 mV Pa^{-1}) is placed in player position (ear channel distance to keyboard $y = 0.37$ m, ear channel distance to ground $z = 1.31$ m. A piezoelectric ICP accelerometer (*PCB 352C23*, sensitivity: 0.5 $mV/m/s^2$, mass: 0.2 g) is attached to the bridge at the corresponding string termination point in direction normal to the soundboard. Due to the overstringing of the

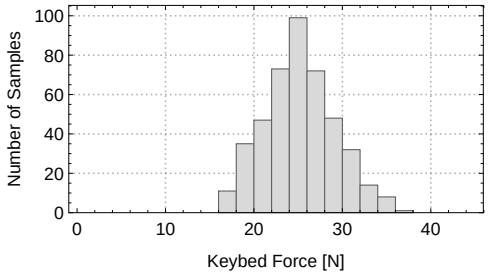

Figure 9.4.: Distribution of F_{key} values for *PROD8* of *D1* (arithmetic mean = 25.16 N, standard deviation $\sigma = 3.9$).

Table 9.2.: Acceleration sensor position on the bridge per played key.

played key	01-27	28-30	31-34	35-88
position of acceleration sensor	01-27	27	35	35-88

bass strings, some bridge positions are not accessible for an attachment. If so, the nearest bridge position is used (see Table 9.2). A four channel preamplifier and analog-to-digital converter (ADC) is used to record the sensor signals (*Tasler LTT24-4*) with 50 kHz sample rate, 32 bit resolution and 5 seconds recording length. Additionally to the artificial head, a set of four condenser microphones (*AKG C 4000*) record the sound radiation from fixed positions (See Figure 9.1). However, the obtained data is not used for the subsequent analysis.

10. Methods

10.1. Listening Test

10.1.1. Aim

The aim of the listening test is to answer the following questions:

1. Is a tonal difference audible for a played grand piano before (*PROD7*) and after (*PROD8*) a year of concert business?

2. What sound properties lead to a perceivable difference? How do listeners verbalize these differences?

The first part of the experiment only tests if a difference of tonal quality is perceivable after a year of monitored playing and maintenance. Therefore, the following hypothesis is stated:

- **Null hypothesis** H_0**:** No difference is noticeable for played tones of a concert grand piano before and after the first year of concert business. Results of the listening test are due to chance alone.

- **Alternative hypothesis** H_1**:** Results are due to a factor other than chance.

The second question is approached by analyzing the free text input with text analysis methods.

10.1.2. Design

The design of the listening test follows the recommendations of the *International Telecommunication Union*[209] and the *Deutsche Gesellschaft für Akustik*.[210] Participants are asked to use headphones during the experiment to standardize the experimental arrangement as much as possible and to allow the inclusion of inter-aural measures.
Each participant receives a randomized sample of 25 trials out of 74 possible comparisons. These 25 trials are presented in randomized order to avoid sequence effects. Trials could be skipped by the participant and would then be excluded from the evaluation (in contrast to the original ABX methodology where a skipped trial counts as 'failed to discriminate'). The ABX double-blind comparison scheme after Clark[211] is an established method to identify differences between stimuli, often used for the evaluation of audio codecs or loudspeaker quality, but it has also been used frequently to evaluate research questions in piano acoustics.[212] The participant is presented with two known samples (A and B) followed by an unknown sample X that randomly matches either A or B. As it is a forced choice methodology, the participant has to choose if X is more similar to A or to B, even if they do not perceive a difference between the samples. Therefore, matching X to the right input could occur because the participant is able to perceive a difference between A and B, or they are guessing randomly and getting lucky. Resulting data from the ABX test is of boolean type (*succeeded* or *failed*).

With the original ABX methodology every participant is confronted with 25 repetitions of the same example. Thus, the analysis takes account of the prob-

[209] International Telecommunication Union (2003). *ITU-R Recommendation BS.1284-1 General methods for the subjective assessment of sound quality*. Tech. rep., pp. 1–13.

[210] Wolfgang Ellermeier et al. (2008). *Kompendium zur Durchführung von Hörversuchen in Wissenschaft und industrieller Praxis*. Tech. rep. Berlin: Deutsche Gesellschaft für Akustik e.V., pp. 1–56.

[211] David Clark (1982). "High-Resolution Subjective Testing Using a Double-Blind Comparator." In: *Journal of the Audio Engineering Society* 30.5, pp. 330–336.

[212] Alexander Galembo et al. (2001). "Effects of relative phases on pitch and timbre in the piano bass range." In: *The Journal of the Acoustical Society of America* 110.3, pp. 1649–1666. DOI: 10.1121/1.1391246; Bank and Lehtonen, "Perception of longitudinal components in piano string vibrations."; Fredrik Öberg and Anders Askenfelt (2012). "Acoustical and perceptual influence of duplex stringing in grand pianos." In: *The Journal of the Acoustical Society of America* 131.1, pp. 856–871. DOI: 10.1121/1.3664049.

ability of one attribute (here: key) per participant. This approach might be useful when comparing only a few attributes (e.g. several compression rates for .mp3 audio files), but is not feasible with a greater number of attributes like in the given case of 74 played tone pairs even with a high number of participants. For the work at hand, every participant is confronted with a sub-set of 25 unique key pairs without repetition of trials. Therefore, the subsequent analysis can not give statistics about an explicit combination of participant and key, but rather gives either statistics for a specific participant (and various keys) or a specific key (and various participants).

After each discrimination task, the participant is asked to describe the 'property which led to a possible discrimination'. The single term *property* is used intentionally instead of *sound property*, which would reduce possible answers to the sound domain. The corresponding answer for each trial can be typed into a free form data entry field limited to 50 characters (See Figure A.48).

10.1.3. Instructions

During the listening test, the following instructions are given to the participants (see Section A.7 for screen shots of the front end in the German and English versions):

Front Page

```
Thanks for your interest in participating in the
listening test.
Procedure:
1. You will hear played piano tones labelled A, B and X.
   The playback can be repeated at will.
2. Please decide whether the tone X corresponds more to A
   or to B.
3. Please name one or more properties by which you where
   able to recognize a difference between A and B.

- The listening test consists of 25 comparisons and takes
  approx. 10 minutes.
- Finally, please answer a few questions about your experience
  with piano tones.
- Attention: Please wear headphones.
```

Trial Pages

```
1. Click the boxes to start / stop playback.
2. Please choose the sound that is most similar to X.
3. Please specify one or more properties that could help you
   identify a difference between A and B.
```

Participant Page

```
Thank you!
- Finally, please answer a few questions about your experience
  with piano tones.
- Then transfer the results by clicking on the "Submit" button.
  In addition to your entries, no personal data will be stored.
- You are also welcome to leave a comment. If you have any
  questions, please contact me: niko.plath[ät]uni-hamburg.de.
Thank you for your participation!

- How many years of experience do you have as a piano builder?
- How many years of experience do you have as a
  piano technician?
- How many years of experience do you have as a piano player?
- For how many years have you been playing a different
  instrument?
- In which country do you live?
- Your comment: _____________________________________________
```

10.1.4. Implementation

The listening test is implemented using *BeaqleJS*, a HTML5/JavaScript framework developed by Kraft and Zölzer.[213] The provided ABX template is utilized for the first research question and extended to address the second research question (see Section A.7 for screenshots). The stimuli are presented as *.wav* file recordings of 5 seconds length with a 100 ms pre-trigger. An automatic 50 ms fade in and fade out is applied to avoid clicks at start and end of the signal. The listening test is hosted on a private website and can be reached worldwide over the internet.[214] The test result of each repetition is stored on the server as a *.json* file and is downloaded for analysis.

[213] Sebastian Kraft and Udo Zölzer (2014). "BeaqleJS : HTML5 and JavaScript based Framework for the Subjective Evaluation of Audio Quality." In: *Linux Audio Conference (LAC-2014)* May.

[214] `http://culturalheritage.digital/listeningtest/`, accessed in December 2018.

10.1.5. Participants

Subsequent to the 25 trials, participant variables are sampled by the following questions:

1. How many years of experience do you have as a piano builder?
2. How many years of experience do you have as a piano technician?
3. How many years of experience do you have as a piano player?
4. For how many years have you been playing a different instrument?
5. In which country do you live?

Since the listening test is accessible worldwide and implemented in English and German language, acquisition of participants has been done mainly over the internet through international discussion boards and *Facebook* groups. Most of the participants related to the *players* group are recruited from *Clavio*[215], the biggest German-speaking piano forum. Most of the participants related to the *builders* and *tuners* groups were found in a *Facebook* group with approx. 1600 members called *Piano Technicians International*.[216]

10.1.6. Statistical Analysis

For the statistical analysis cumulative binomial probabilities are used after Boley and Lester[217] with the two following preconditions: a) correct answers have to be randomly distributed throughout the test, and b) when a participant is unable to discriminate the two cases, the response has to be random and not correlated to the test.
For a number of trials n, and a number of correct responses c, the proportion of events in population if chance alone is operating p_{chance} can be calculated. p_{chance} represents the probability of randomly getting more correct discriminations under the same conditions.

[215] `https://www.clavio.de/forums/`, accessed in December 2018.
[216] `https://www.facebook.com/groups/653450328080194/`, accessed in December 2018.
[217] Jon Boley and Michael Lester (2009). "Statistical Analysis of ABX Results Using Signal Detection Theory." In: *Audio Engineering Society Convention 127*.

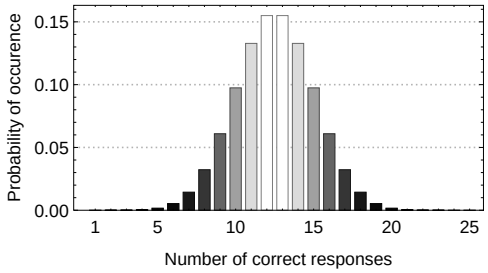

Figure 10.1.: Binomial distribution for 25 trials of a Bernoulli experiment.

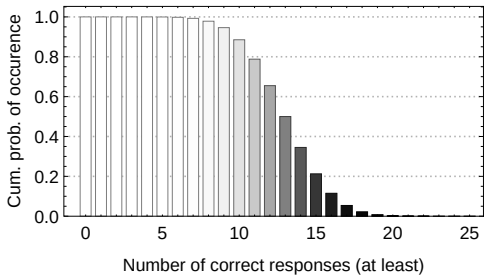

Figure 10.2.: Inverse cumulative binomial distribution for 25 trials of a Bernoulli experiment. Note that the probabilities are given for getting **at least** the number of correct answers, e.g. the probability of giving **0 or more** correct answers by chance is 1.

Following the binomial distribution (see Figure 10.1 for an exemplary case of 25 trials), the probability of getting c correct answers is

$$B(c, n, p_1) = \binom{n}{c} p_1^c (1 - p_1)^{n-c} \tag{10.1}$$

with $p_1 = 0.5$ in the case of the ABX testing scheme (denotation after Burstein[218][219]).

For significance at a given confidence level (CL), the inverse cumulative probability of getting c or more correct answers in a given random trial (see Figure

[218] Herman Burstein (1988). "Approximation Formulas for Error Risk and Sample Size in ABX Testing." In: *Journal of the Audio Engineering Society* 36.11, pp. 879–883.

[219] Herman Burstein (1989). "Transformed Binomial Confidence Limits for Listening Tests." In: *Journal of the Audio Engineering Society* 37.5, pp. 363–367.

10.2) has to be smaller or equal CL:

$$\sum_{N=c}^{n} B(N, n, 0.5) \leq CL. \tag{10.2}$$

Or in a simplified form:

$$\sum_{N=c}^{n} \binom{n}{N} * 0.5^n \leq CL. \tag{10.3}$$

Take, for example, 18 correct responses out of 25 trials. The probability p_{chance} for giving 18 correct responses only by chance is 0.0216426 or 2.16 %. Conversely this means, that one of 46 experiments will produce 18 correct responses just by chance.
Since participants can skip tasks and since the keys are assigned to participants in a completely randomized way, sample size n can vary per participant and key.

11. Listening Test Results

11.1. Participant Variables

Participants from 12 different countries completed the listening test with the majority coming from Germany (see Table 11.1 for an enumeration). Figure 11.1 shows the total number of test completions per key. Since the selection of keys presented to the participant is randomized, the number of completions varies from 25 to 50.

Figure 11.2 shows histograms for the professional background of the participants which can be summarized as follows:

- 10% of the participants have more than one year experience as piano builders.
- 25% of the participants have more than one year experience as piano tuners.
- 80% of the participants have more than one year experience as piano players.

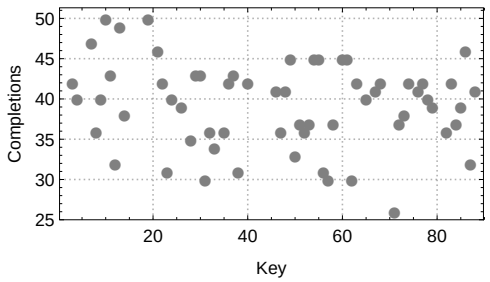

Figure 11.1.: Listening test total number of completions per key.

Table 11.1.: Number of participants per country.

Country	Participants
Germany	74
U.S.A.	10
United Kingdom	4
Greece	3
Switzerland	3
Australia	1
Austria	1
Belgium	1
Canada	1
France	1
Norway	1
Portugal	1

- 50% of the participants have more than one year experience playing other musical instruments.
- 8% of the participants have one or less years experience accumulated in building, tuning and playing.

For the following analysis, three sub-groups (disjoint sets) are defined regarding their experience as non-experts, players and builders/tuners (see Table 11.2). With a hit ratio of 96.3% the builders/tuners sub-group has the highest result, followed by the players group with a hit ratio of 93.3%. The non-experts still have a high hit ratio of 90.3%.

11.2. ABX Test

Trials are chosen with a maximum F_{key} difference of 0 N to 0.6 N. When calculating the average hit probability for sub sets with F_{key} differences from 0 N to 0.6 N in 0.01 N steps, in the given range no positive dependency is observable (see Figure 11.3). On the contrary, the smallest sub sets 0 N to 0.1 N give the best hit ratio. In other words, when choosing a greater maximum F_{key} difference the results do not get better. This finding confirms the pre-test and

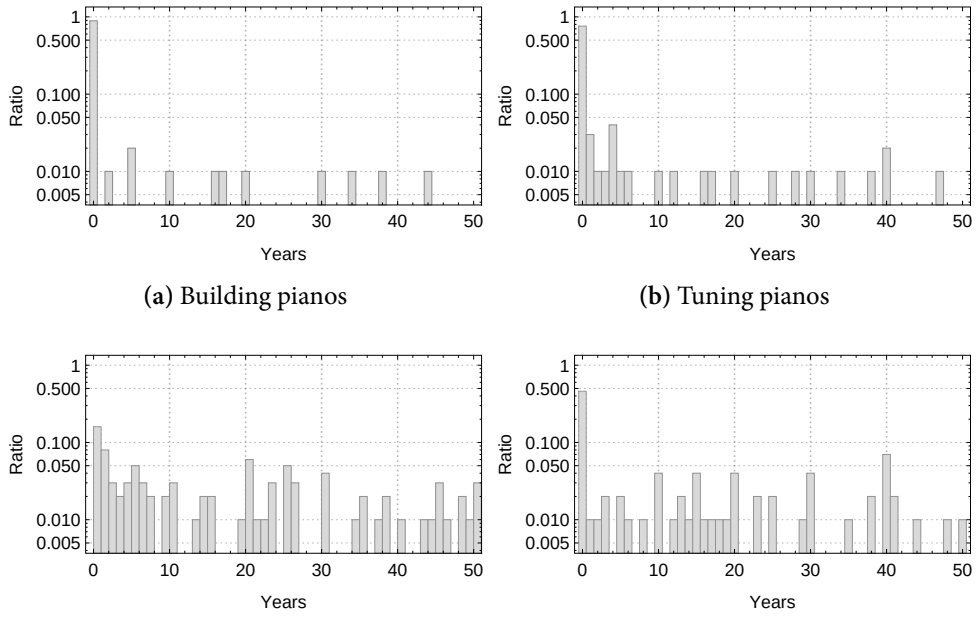

(a) Building pianos

(b) Tuning pianos

(c) Playing piano

(d) Playing other instruments

Figure 11.2.: Histograms for professional background of participants.

Table 11.2.: Definition and hit ratio for sub-groups (disjoint sets).

Sub-Group	Qualification	Σi	n	c	$c/n*100$
Non-Experts	one or less years experience accumulated in building, tuning and playing.	8	185	167	90.3
Builders/Tuners	more than one year experience in building or tuning pianos.	22	544	524	96.3
Players	more than one year experience in playing piano or other instruments and not member of Builders/Tuners sub-group.	70	1708	1593	93.3

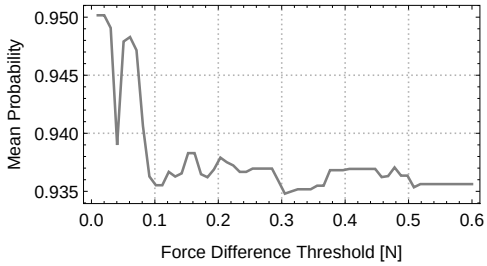

Figure 11.3.: Average hit probability per F_{key} difference.

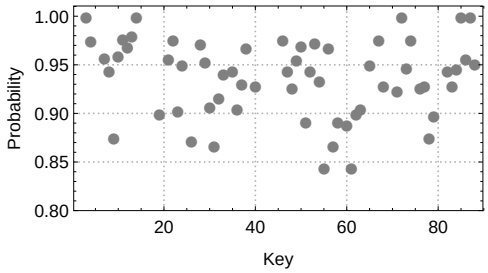

Figure 11.4.: Hit probability per key at 0.6 N maximum F_{key} difference.

implies that in this range a difference in key bed force does not lead to perceivable tonal difference and can therefore not be used as a cue for discrimination. Figure 11.4 shows the hit ratio per key with a maximum F_{key} difference of 0.6 N.

As discussed in Section 10.1, statistics for the listening test are calculated according to keys as well as to participants. Table A.1 to A.2 shows the results per key (notes given as key number 1-88). With an average probability p_{chance} that chance alone is operating of approx 1e-9, H_0 has to be rejected for both confidence levels 95% ($CL_{95\%}$) and 99% ($CL_{99\%}$) for all measured keys. In other words, participants can distinguish between the two piano tones for all keys due to one or more factor(s) other than chance.
With an average probability p_{chance} that chance alone is operating of approx 1e-7, H_0 has to be rejected for $CL_{95\%}$ for all but one out of 100 participants. When utilizing the stricter $CL_{99\%}$, H_0 has to be rejected for all but 5 out of 100 participants. In other words, 99% (or 95% for $CL_{99\%}$) of the participants can distinguish between the two piano tones due to one or more factor(s) other than chance. The five participants 'failing' the listening test under $CL_{99\%}$ con-

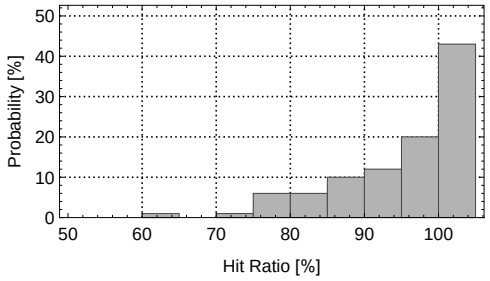

Figure 11.5.: Histogram for probability per hit ratio.

ditions are further denoted as H_0-group. As an intermediate result, a strong ceiling effect is observable (see Figure 11.5).

Regarding the sub-groups the following statements can be made:

- The builders/tuners group has the highest hit ratio (96.3%), followed by the players (93.3%) and the non-experts (90.3%).
- H_0 has to be rejected for all participants in the builders/tuners group. In other words, no builder/tuner fails in the listening test.
- Two out of five members of the H_0-group are non-experts (participant id 9 and 71) with 0.5 and 1 year experience in piano playing.
- Three out of five members of the H_0-group are players (participant id 48, 85 and 97) with 54, 40 and 16 years of experience in instrument playing.
- The participant failing the test even under $CL_{95\%}$ conditions is a non-expert.

11.3. Verbalizations

The verbalization data is pre-processed using the following text-mining methods:[220]

[220] Anne Kao and Stephen R. Poteet, eds. (2007). *Natural Language Processing and Text Mining*. London: Springer London. DOI: 10.1007/978-1-84628-754-1.

- **Tokenization**: As the participants are free to formulate full sentences of up to 50 characters per trial, as a first step, each text paragraph is broken down into single words. E.g., {*'Slight difference in brightness of attack'*} is divided into {*'Slight', 'difference', 'in', 'brightness', 'of', 'attack'*}
- **Stop Word Removal:** Word relationships within a sentence do not play a role in the subsequent analysis, as the data is analyzed only regarding single words. The data set contains text in German and English language. Based on a *stop word data set* [221], the most common English and German words are filtered out of the data set. E.g., filtering of {*'Slight', 'difference', 'in', 'brightness', 'of', 'attack'*} leads to {*'brightness', 'attack'*}.
- **Stemming:** To allow quantitative analysis of word frequencies, all words are reduced to a common word root. In the present case, if possible, words are transformed to its comparative adjective form. E.g., *'brightness'*, *'bright'*, *'brightest'* are transformed to *'brighter'*. At the same time, orthographic mistakes are corrected and capitalized characters are transformed to lower-case form.

After the described pre-processing steps, the data set contains 2267 total words and 776 unique word forms. Figure 11.6 shows the 100 most commonly used words, font size and font gray value represent word frequency (darker meaning more often). The 15 most frequently used words and their number of occurrence are summarized in Table 11.3. The most commonly used words are *brighter*, *partials*, *higher*, *pitch*, *beating*, *dumpfer*, *tuning*, *longer*, *anschlag*, *lower*, *attack*. A classification of the given word forms is performed, and each word is assigned to one of the domains *Timbre*, *Temporal*, *Pitch*, *Loudness*, and *Spatial*. Most dominant are timbre, pitch, and temporal key words. Note that the first spatial key word comes only in 15th place.

Examining the data set, a second possible approach of classification becomes apparent: A similar phenomenon can be described in terms of three levels of foreknowledge, hereafter denoted as *descriptive*, *technical*, and *causal*. On the descriptive level, one would verbalize a sensation in terms of descriptive, often metaphoric adjectives, e.g. as *'rough'* or *'dirty'*. On the *technical* level, the terms used would presume a certain educational background. E.g. one would write about *'temporal development of higher partials'*, where the term *'Partial'*

[221] `https://code.google.com/archive/p/stop-words/`, accessed in February 2019.

Figure 11.6.: Word cloud for the 100 most commonly used words to describe the sound property which led to a discrimination of two given examples (font size and gray value depict word frequency).

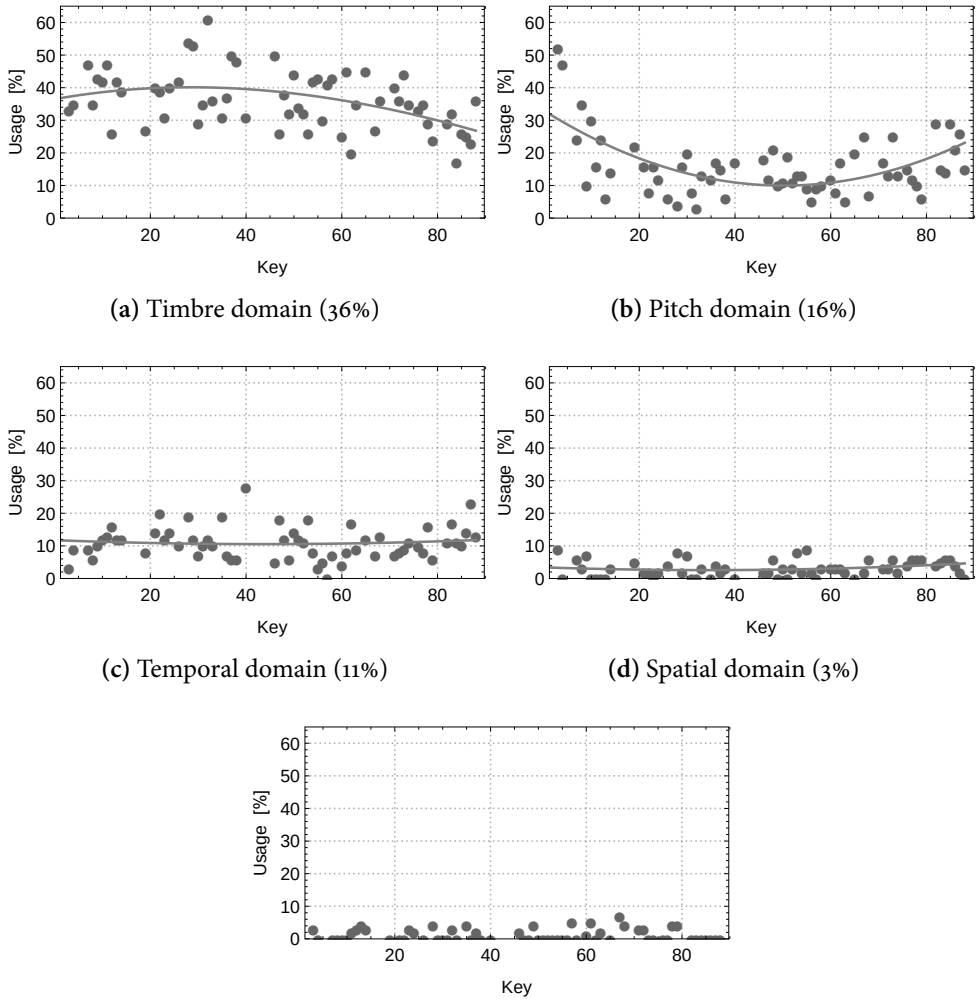

(a) Timbre domain (36%)

(b) Pitch domain (16%)

(c) Temporal domain (11%)

(d) Spatial domain (3%)

(e) Loudness domain (1%)

Figure 11.7.: Percentile of words used from each defined perceptual domain per key (average values in brackets).

Table 11.3.: The 15 most frequently used words and their frequency of occurrence.

Frequency	Word	Frequency	Word	Frequency	Word
127	*partials*	75	*beating*	39	*attack*
124	*higher*	60	*dumpfer*	36	*unisons*
120	*brighter*	57	*tuning*	33	*cleaner*
106	*pitch*	56	*anschlag*	32	*brillanter*
78	*lower*	39	*longer*	30	*nachhall*

would imply a certain musical or scientific education. On the *causal* level, participants would not describe the acoustical sensation but the instrument component they hold accountable for the sensation. E.g. they would write *'unison strings'*. The described levels of foreknowledge moreover can be understood as representations of different concepts of knowledge: The *technical* vocabulary requires a form of education where technical terms are taught, often related to science and engineering. In contrast, the *causal* vocabulary does not require any theoretical knowledge but a high degree of empirical knowledge, which can be informal and hardly verbalizable, but needs years (or sometimes generations) to establish.[222]

[222] Petersen, *Vom "Schwachstarktastenkasten" und seinen Fabrikanten - Wissensräume im Klavierbau 1830 bis 1930*.

Table 11.4.: Classification of the 50 most frequent words into perceptual domains (average usage percentage in brackets) and levels of foreknowledge.

	Timbre (36%)	Pitch (16%)	Temporal (11%)	Spatial (3%)	Loudness (1%)
causal	*strings, unisons, hammer, needling*				
technical	*partials, beating harmonics, intonation, obertonreicher, resonanz, chorrein*	*pitch, tuning frequency detuned*	*attack, onset sustain, puls decay, nachhall*	*panning stereo, envelope*	*volume loudness*
descriptive	*cleaner, brillanter harder, rounder clearer, metallischer stronger, darker sharper, brighter dumpfer, softer*	*higher lower*	*longer, shorter faster, duration shifting*	*direkter farther*	*louder leiser*

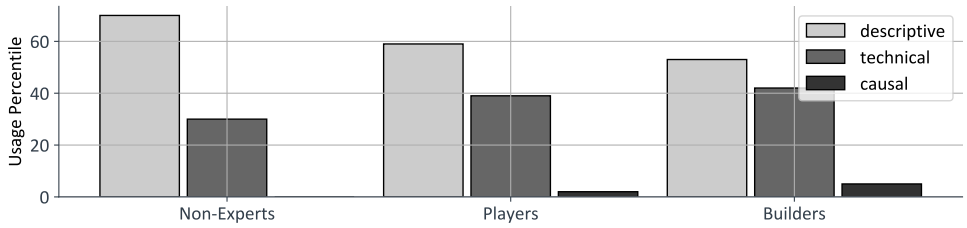

Figure 11.8.: Percentage of terms used per sub-group and category.

Figure 11.8 shows the proportional usage of defined vocabularies for non-experts, players and builders, which can be summarized as follows:

- *Descriptive* vocabulary is most frequently used by non-experts, but even builders and technicians use *descriptive* vocabulary to a high degree (53%).
- The proportion of *technical* vocabulary increases from non-experts over players to builders and tuners.
- Non-experts do not use *causal* vocabulary at all. Builders have the highest, yet only a 5% proportion of used *causal* vocabulary.

12. Comparison with Psychoacoustic and Structural Metrics

12.1. Psychoacoustic Features

12.1.1. Timbre Domain

According to the given statements by the participants, timbre is the most important factor for the discrimination of individual piano tones of the same pitch. The average proportion of used timbre-related words per key is 35%, with lowest values in bass and treble ranges (compare Figure 11.7). In the following section, findings from the listening test are compared to the following psychoacoustic features: Spectral Centroid (SC), Fractal Correlation Dimension (FCD), and Roughness (R).

Spectral Centroid

The Spectral Centroid (SC) as a well established indicator for the perception of brightness of complex tones is calculated after Beauchamp[223] as the weighted mean of frequencies in the spectrum $A(f)$:

$$SC = \frac{\sum_{i=1}^{N} A_i f_i}{\sum_{i=1}^{N} A_i}. \tag{12.1}$$

[223] James W Beauchamp (1982). "Synthesis by Spectral Amplitude and Brightness Matching of Analyzed Musical Instrument Tones." In: *J. Audio Eng. Soc.* 30.6.

Only spectral components higher than −60 dB are incorporated in the calculation. The window length for the FFT is defined per key based on the calculated decay time RT_{60} (see Section 12.1.3) to avoid overemphasis of the noise floor. All SC values are averaged over the left and right dummy head microphone channels and 5 recorded takes per key. Figure 12.1 shows the SC per key for a) *PROD7* and b) *PROD8*:

- In general, SC values follow, but are higher than f_1 due to energy content in higher partials.
- For the bass to mid range, variation decreases from *PROD7* to *PROD8* which is an indication for maintenance work towards a more homogeneous tonal quality between keys.
- For the highest octave, SC values decrease from *PROD7* to *PROD8* which is in accordance with statements by the responsible technician that the treble was too harsh when the piano was delivered and hence had to be adjusted within the following months by needling the hammer felts.

Figure 12.2 shows the SC difference between *PROD7* and *PROD8* vs. the percentage of used timbre domain verbalizations. For the highest octaves, SC values decrease from *PROD7* to *PROD8*. Nevertheless, a comparison with the proportion of timbre related verbalizations does not reflect this development: The treble range with the highest SC difference has the lowest proportion of used timbre related words.

Fractal Correlation Dimension

As shown by Bader,[224] the fractal correlation dimension (FCD) is an appropriate tool to characterize the chaoticity of an initial transient. The calculated FCD value has good agreement with the number of harmonic overtone structures in a complex sound: A single harmonic overtone spectrum would yield a FCD value of 1, independent of the number of involved partials. Each additional harmonic structure increases the FCD by 1. For piano tones, the transient signal part consists among others of a) the transversal string spectrum which is

[224] Rolf Bader (2002). "Fraktale Dimensionen, Informationsstrukturen und Mikrorhythmik der Einschwingvorgänge von Musikinstrumenten." PhD thesis; Rolf Bader (2013). *Nonlinearities and Synchronization in Musical Acoustics and Music Psychology*. Springer.

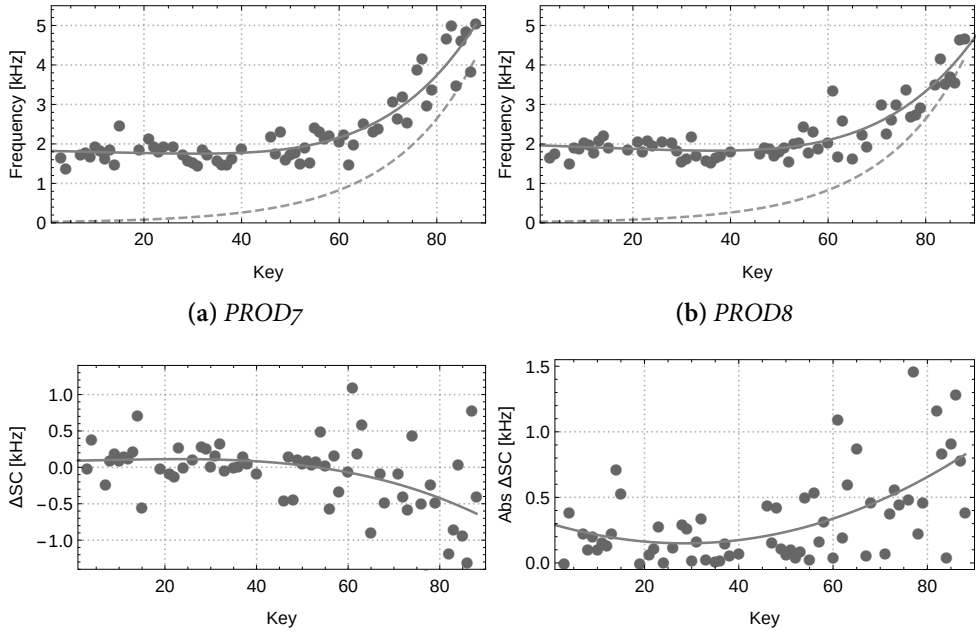

(a) *PROD7*

(b) *PROD8*

(c) Difference of spectral centroid per key between *PROD7* and *PROD8*.

(d) Modulus difference of spectral centroid per key between *PROD7* and *PROD8*.

Figure 12.1.: Spectral centroid of radiated sound (at player position) for *PROD7* and *PROD8*. f_1 per key is represented by the dashed line. Straight lines illustrate quadratic fittings.

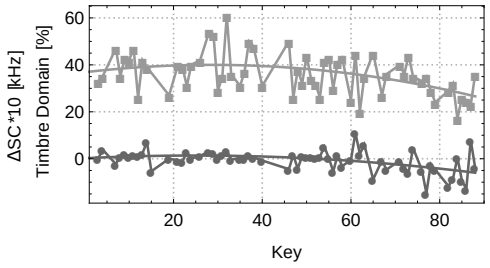

Figure 12.2.: SC difference between *PROD7* and *PROD8* vs. proportion of used timbre domain related words per key. Straight lines illustrate quadratic fittings.

more or less harmonic, b) possibly a longitudinal string spectrum which is inharmonic, c) possibly one ore more duplex string spectra which are more or less harmonic, and d) the key bed impact noise. Hence, FCD values ≥ 2 can be expected for a radiated piano tone.
Firstly, to express the noisiness/complexity of the transient attack part of the recorded tones, the FCD is calculated for the first 100 ms in 50 ms windows and a step size of 1 ms. Secondly, the FCD is calculated for the first 2000 ms in 50 ms windows and a step size of 50 ms. Given values are averaged over 50 calculated values per recording $\times$ left and right dummy head channel $\times$ 5 takes per key.

Figure 12.3 shows the average fractal correlation dimension for a) the first 100 ms, and b) for the first 2 s per key. A general decrease from low to high notes is observable. In the bass range several more harmonic systems are present than in the treble range, e.g. partials due to longitudinal string vibration, phantom partials, and up to 85 audible transversal partials. Since the increase of vibration frequency for each partial is proportional to the square of the partial number for a real stiff string (see Section 2.0.3), a much greater amount of inharmonic partial intervals is present for the bass notes. This increases the FCD in the bass range compared to the treble range where on one side the inharmonicity coefficient increases again due to the string scale but on the other hand the number of audible partials decreases heavily to a minimum of approx. 4 for the highest keys.[225] The knocking noise by the key bed contact should have an impact on the FCD but is not expected to change significantly within the year.
A comparison of *PROD7* and *PROD8* shows:

- An increase of noise in the transient part for the bass range up to *C4*.
- In the treble range a decrease of noisiness is observable for keys 70-88.

[225] For the highest note *C8* with f_1 = 4186 Hz, only the harmonic partials f_1 = 8372 Hz, f_2 = 12 558 Hz, and f_3 = 16 744 Hz fit into the human audible range with f_3 being barely audible for adults.

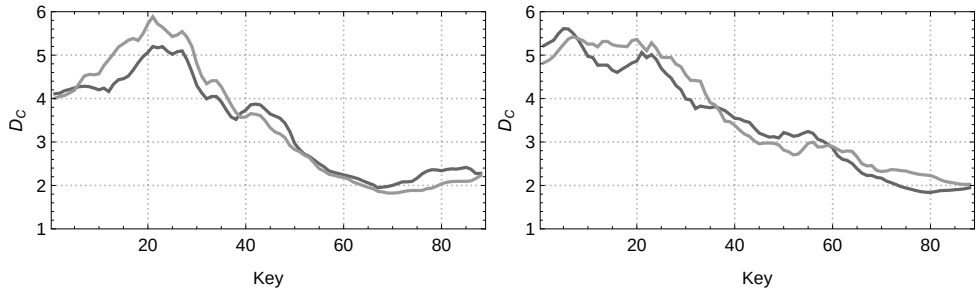

Figure 12.3.: a) Average fractal correlation dimension for the transient part (first 100 ms) of the piano tone per key for *PROD7* (dark) and *PROD8* (light).
b) Average fractal correlation dimension for the first 2 s per key for *PROD7* (dark) and *PROD8* (light).

Roughness

Amplitude modulation of higher partials of a piano tone is mainly a result of coupling of slightly detuned unison strings. Technicians usually detune the unison strings by 1-2 cents to give the decay of the tone a complex varying structure.[226] Detuning f_1 of the three unison strings results in a quasi-harmonic spectrum with up to three peaks per partial. Following Helmholtz's ideas of roughness based on the perception of dissonance and consonance, the three peaks per partial have frequency differences, which should contribute to the perception of roughness.[227] However, compared to the peaks of the next partial triplet the differences should be too great to considerably add to the sensation of roughness. The perceived roughness of a piano tone should therefore be heavily dependent on the degree of detuning of the unison strings (apart from the impact noise of key and key bed contact).

Figure 12.4 shows a suggested 1 cent minimum detuning of f_1 in Hz per key. The frequency resolution of 0.25 Hz allows to display a 1 cent detuning for *D4* and higher notes. A peak picking is performed around f_1 for the recordings of keys 42-88. Three frequency differences (string 1 vs. 2, 1 vs. 3, and 2 vs. 3) are

[226] Kirk, "Tuning Preferences for Piano Unison Groups."
[227] Hermann von Helmholtz (1863). *Die Lehre von den Tonempfindungen als physiologische Grundlage für die Theorie der Musik*. Braunschweig: Vieweg.

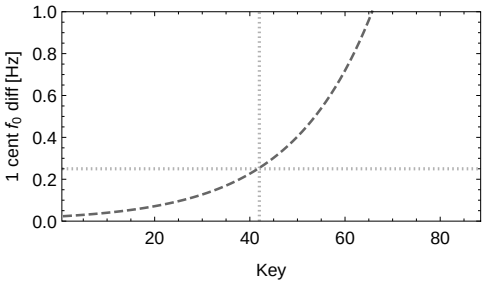

Figure 12.4.: One cent f_1 difference in Hz per key. Grid lines depict the key from which on the expected unison string detuning of ≥ 1 cent is greater than the Shannon-Nyquist sampling uncertainty of 0.25 Hz.

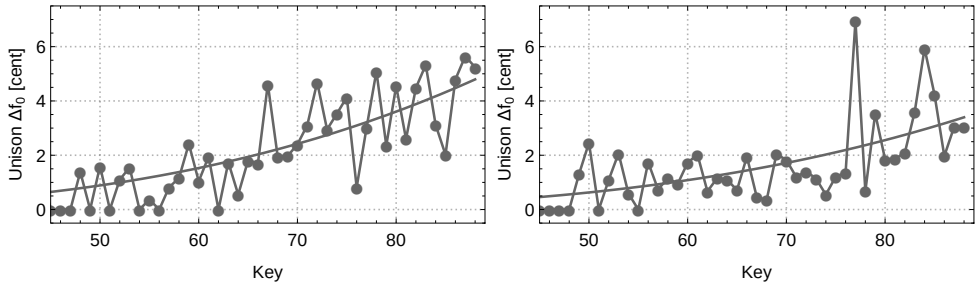

(a) *PROD7* **(b)** *PROD8*

Figure 12.5.: Average f_1 detuning of unison strings for *PROD7* and *PROD8*. Straight lines illustrate quadratic fittings.

measured per recording and are averaged over 5 takes and left/right channel. Figure 12.5 shows the detuning of unison strings per key in cent. Up to *F6* the average detuning is in the range proposed by Kirk with differences between strings of approx. 1-2 cent. In the high treble range differences of up to 5 cent appear.

The roughness R for a combination n of two partials is calculated following the algorithm proposed by Schneider, Ruschkowski, and Bader[228] as

[228] Albrecht Schneider, Arne von Ruschkowski, and Rolf Bader (2009). "Klangliche Rauhigkeit, ihre Wahrnehmung und Messung [Timbre roughness, its perception and measurement]." In: *Musical Acoustics, Neurocognition and Psychology of Music*. Ed. by Rolf Bader. Hamburger. Frankfurt am Main: Peter Lang, pp. 101–144.

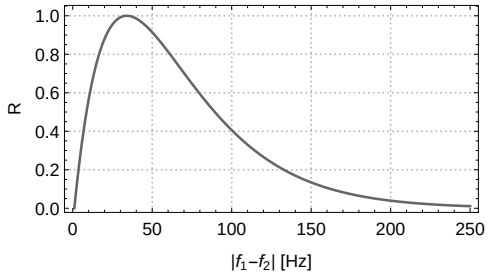

Figure 12.6.: Perceived roughness per frequency difference $|f_1 - f_2|$ and $A_1 = A_2 = 1$ after Schneider, Ruschkowski, and Bader.[233]

$$R(n) = A_1 A_2 \frac{|f_1 - f_2|}{f_r e^{-1}} e^{-|f_1 - f_2|/f_r}, \tag{12.2}$$

with A_1, A_2 being the amplitudes and f_1, f_2 being the frequencies of the corresponding partials. The method is based on Sethares,[229] who fitted a model on experimental data by Plomp and Levelt.[230] In contrast to Sethares, the method by Schneider, Ruschkowski, and Bader[231] does not incorporate an adjustment of the interval Δf_r with the greatest perceived roughness for each critical band. Since deviations introduced by the critical band adjustments are found to be negligible, Δf_r is set to 33 Hz for all intervals, as proposed by Helmholtz[232] (See Figure 12.6).

For each note a peak picking is performed for spectral components greater than -60 dB. Subsequently, for each combination of n $\times$ m spectral components the roughness is calculated. Since the number of audible partials varies strongly between bass range (up to approx. 85 partials for the lowest notes, which leads to 3,570 individual pairs) and treble range (approx. 4 partials for the highest notes, which leads to 6 individual pairs), the total roughness per

[229] William A. Sethares (1993). "Local consonance and the relationship between timbre and scale." In: *The Journal of the Acoustical Society of America* 94.3, pp. 1218–1228. DOI: 10.1121/1.408175.

[230] R. Plomp and W. J. M. Levelt (1965). "Tonal Consonance and Critical Bandwidth." In: *The Journal of the Acoustical Society of America* 38.4, pp. 548–560. DOI: 10.1121/1.1909741.

[231] Schneider, Ruschkowski, and Bader, "Klangliche Rauhigkeit, ihre Wahrnehmung und Messung [Timbre roughness, its perception and measurement]."

[232] Helmholtz, *Die Lehre von den Tonempfindungen als physiologische Grundlage für die Theorie der Musik*.

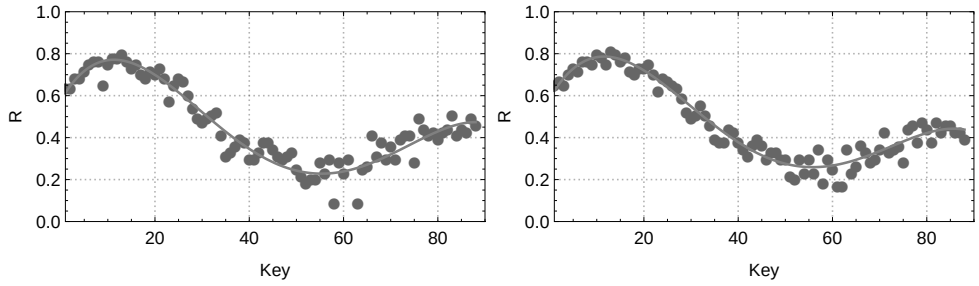

(a) *PROD7* **(b)** *PROD8*

Figure 12.7.: Perceived roughness per key for *PROD7* and *PROD8*. Straight lines illustrate cubic fittings.

note is not given as the sum of roughness values of all pairs but as the average. This way, the total roughness has values $0 \leq R \leq 1$, independent of the number of contained partials.
Figure 12.7 shows the calculated roughness per key for *PROD7* and *PROD8*. Greatest R values are in the bass range with a peak on the bass bridge and decreasing values towards the mid range. This is in good agreement with the general perception of strongest dissonance for the lowest notes due to the number of transversal partials, string inharmonicity, and the audible presence of longitudinal string partials. The roughness increase in the treble range is in good agreement with the measured unison string detuning (compare Figure 12.5).

12.1.2. Pitch Domain

As described in Section 2.0.3, the piano is tuned with stretched octaves to compensate for the inharmonic overtone spectrum (*Railsback stretch*). Note that the lowest measurable partial does not always have to coincide with the perceived pitch[234]. Although pitch can not always be sufficiently described with just the fundamental frequency, f_1 is utilized for the work at hand since it is known for which keys f_1 should not be present. The degree of tuned octave

[234] For the lowest notes the soundboard is not capable to project f_1 and the lowest measurable frequency component is the octave. Nevertheless, due to the periodicity implied by the overtone structure the pitch of the tone is perceived at the *missing fundamental* frequency.

stretch relies on the judgment of the technician. Following Martin and Ward,[235] deviations from the Railsback curve could be the tuners handling of soundboard resonances. In this regard, different octave stretches between *PROD7* and *PROD8* could be the technicians response to a change in the vibrational behavior of the piano. In the same course, different octave stretches can lead to perceivable pitch differences between *PROD7* and *PROD8* for the bass and treble range (see Section 8.2).
Fundamental frequencies are estimated from FFT based spectra for all keys by automated peak picking. 2 s windows yield a frequency resolution of 0.5 Hz. If multiple f_1 frequencies are observable due to de-tuned unison strings, the mean value is used.
Figure 12.8 shows the tuned deviation from equal tempered tuning for *PROD7* and *PROD8* in cent. In accordance to Young,[236] the greatest deviation is observable in the bass and treble range. Figure 12.8 c) shows the f_1 difference between *PROD7* and *PROD8* in cent. The differences can be summarized as follows:

- Apart from three strong outliers, the keys on the bass bridge (key 1-20) are tuned without measurable differences.
- In the mid range deviations of approx 2.5 cent are observable.
- In the highest octave deviations of up to 10 cent are observable. These notes are also the hardest to tune properly.

A quadratic curve fitting shows greatest average detuning in the bass and treble range with the minimum in the midrange. The curve can be explained with a differently tuned octave stretch since this would be most noticeable in bass and treble range. Professional musicians can differentiate pitch differences of a few cent,[237] therefore pitch could be a cue in the listening test at least for some keys.

A comparison of the measured f_1 differences and the pitch related verbalizations shows some remarkable results (compare Figure 12.9): For the general

[235] Martin and Ward, "Subjective Evaluation of Musical Scale Temperament in Pianos."
[236] Young, "Inharmonicity of Plain Wire Piano Strings."
[237] Mari Tervaniemi et al. (2005). "Pitch discrimination accuracy in musicians vs nonmusicians: an event-related potential and behavioral study." In: *Experimental Brain Research* 161.1, pp. 1–10. DOI: 10.1007/s00221-004-2044-5.

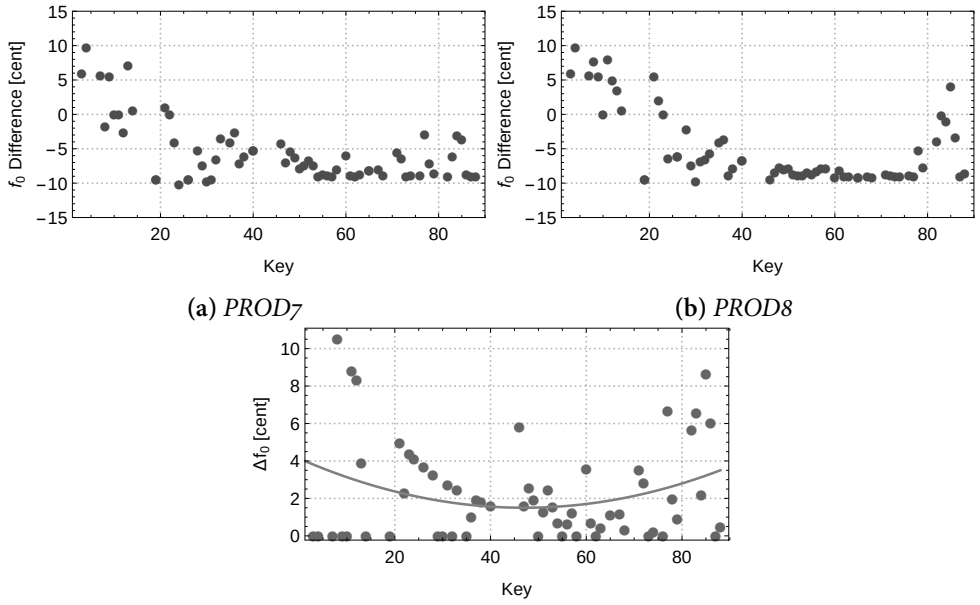

(a) *PROD7* **(b)** *PROD8*

(c) *PROD7-PROD8*

Figure 12.8.: a)-b) f_1 deviation from equal tempered tuning for *PROD7* and *PROD8*. **c)** f_1 difference between *PROD7* and *PROD8*. Straight lines illustrate quadratic fittings.

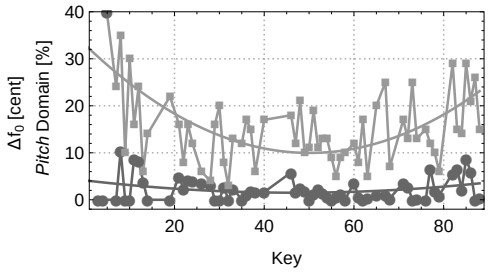

Figure 12.9.: f_1 differences between *PROD7* and *PROD8* in cent (dark) vs. usage percentile of pitch related verbalizations (bright). Straight lines illustrate quadratic fittings.

trend there is good agreement between measurements and verbalizations with higher values in bass and treble range. However, when looking at the relations in detail, the highest proportion of pitch related verbalizations are given for keys with no measurable difference in f_1 values. For the lowest bass notes, this could be explained with the general difficulty to determine a pitch due to the quantity of audible transversal partials, a high degree of inharmonicity, and audible longitudinal partials. But also for some higher notes, 20%-30% of the verbalizations are pitch-related with corresponding measured f_1 differences of 0-1 cent. In other words, participants hear a pitch difference, where there is at least no f_1 difference. This can be explained by the fact that for complex tones participants have difficulties to ignore alterations in brightness (due to changes in the spectral distribution) when making pitch judgments (due to changes of the fundamental frequency).[238]

The results can be summarized as follows:

- According to the percentile of related verbalizations, pitch was the second most important factor for the discrimination of piano tones with the greatest relevance in bass and treble range.
- f_1 difference measurements show a similar general trend with greatest

[238] A. J. Oxenham (2012). "Pitch Perception." In: *Journal of Neuroscience* 32.39. DOI: 10.1523/JNEUROSCI.3815-12.2012; Brian C. J. Moore and Brian R. Glasberg (1990). "Frequency discrimination of complex tones with overlapping and non overlapping harmonics." In: *The Journal of the Acoustical Society of America* 87.5, pp. 2163–2177. DOI: 10.1121/1.399184.

deviations in bass and treble range with several values that should be greater than the just noticeable difference. The general curve can be explained by differently tuned octave stretches.

- For several keys, high proportions of pitch related verbalizations are given with no measurable difference in f_1 values.

12.1.3. Temporal Domain

Attack Time

The attack time (AT) gives a good estimation of the initial buildup of a musical tone. For a piano tone, AT is determined by the dynamic play range, regulation of the action, hammer mass and voicing - or in general, all factors that have an impact on the hammer-string contact time (see Section 2.0.2).
The AT is calculated with a fixed-threshold as the time frame Δt [ms] in the squared envelope of the signal determining the start and the end of the attack phase. The noise floor is taken into account by setting the start threshold to 10% of the maximum amplitude. Since for complex signals the maximum amplitude could occur not at the end of the first gradient but later, the end threshold for the attack phase is set to 90% of the maximum amplitude.[239] Given values are averaged over 5 takes per key and left and right dummy head channel.
Figure 12.10 shows the attack times of the radiated sound at player position as an average of left and right ear signals for *PROD7* and *PROD8*. A general trend is observable with the highest AT values in the bass range (Δt = 10 ms to 15 ms) and decreasing values for higher notes with average AT of Δt = 3 ms in the treble range. This finding is in correspondence with the fact that the hammer mass in a modern piano varies by a factor of 2-3 from bass range (approx. 10 g) to treble range (approx. 3.8 g).[240] In the same course, the hammer-string contact time decreases from bass to treble which leads to a higher gradient of

[239] G. Peeters (2004). *A large set of audio features for sound description (similarity and classification) in the CUIDADO project*. Tech. rep. 0. IRCAM, pp. 1–25.
[240] Fletcher and Rossing, *The Physics of Musical Instruments*.

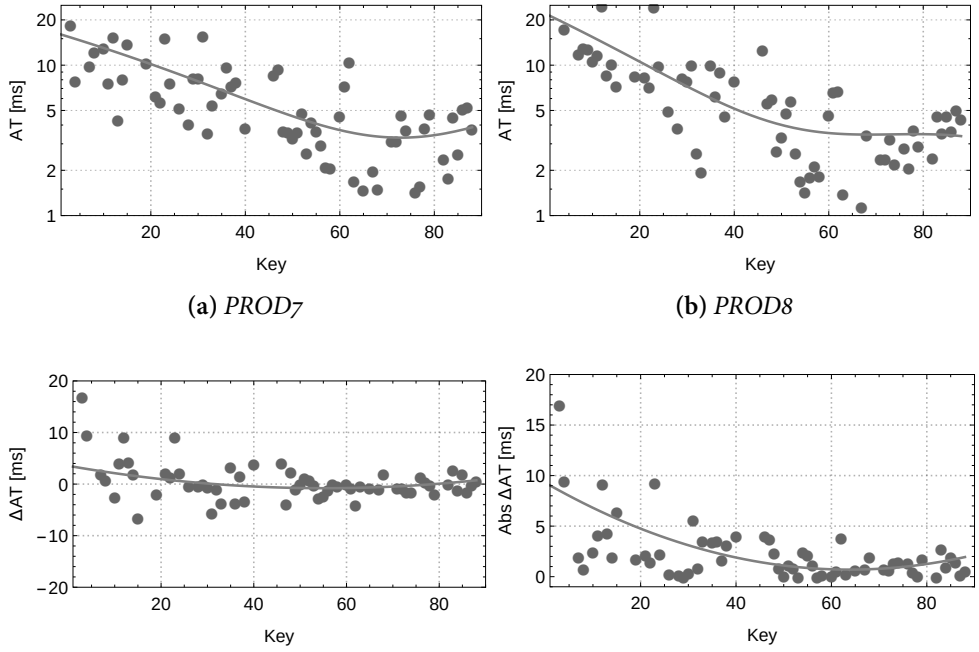

(a) *PROD7* **(b)** *PROD8*

(c) Difference *PROD8-PROD7* **(d)** Modulus of difference

Figure 12.10.: a-b) Attack time of radiated sound (at player position) for *PROD7* and *PROD8*.
c) Difference in attack time between *PROD7* and *PROD8*. Positive values indicate higher times for *PROD7*, negative for *PROD8*.
d) Modulus of Difference. Straight lines illustrate quadratic fittings.

the transient signal part for higher notes.[241]
The AT development between *PROD7* and *PROD8* (see Figure 12.10 b)) can be summarized as follows:

- A general trend to smaller or higher attack times is not observable.
- The total variation decreases following the general decrease of AT values to higher notes with a maximum difference of approx. 50%.
- No change in attack time values is observable for keys 58-78.

[241] Donald E. Hall and Anders Askenfelt (1988). "Piano string excitation V: Spectra for real hammers and strings." In: *The Journal of the Acoustical Society of America* 83.4, pp. 1627–1638. DOI: 10.1121/1.395917.

Decay time

The decay of a piano tone often does not follow a purely exponential decrease due to interaction of the slightly detuned unison strings and change of transversal string polarizations (see Section 2.0.3).[242] Although algorithms for modeling the a potential double decay exist,[243] for the work at hand the decay time is estimated utilizing the Schroeder backward-integration algorithm,[244] which assumes a single exponential decay (as it is originally developed for decay estimation in room acoustics).
Figure 12.11 shows the decay per key for *PROD7* and *PROD8* as a) damping with [dB s^{-1}] units, and b) as T_{60} values with [s] units. T_{60} values decrease from approx. 8 s to 10 s in the bass range to approx. 0.5 s in the treble range. In general, decay times do not differ between *PROD7* and *PROD8*, but great variation is observable for individual notes. For the treble range, no decay time difference is observable at all.

Notwithstanding the frequent use of words from the temporal domain (11% average per key), e.g. *attack, onset, faster, shorter,* and *decay*, no general difference is observable, neither for attack time nor the decay as reverberation time T_{60}.

12.1.4. Spatial Domain

Interaural Level Difference

The inter-aural level difference (ILD) is a measure for the perceived direction of the sound source in the horizontal plane. For sound wave lengths smaller

[242] Gabriel Weinreich (1977). "Coupled piano strings." In: *The Journal of the Acoustical Society of America* 62.6, p. 1474. DOI: 10.1121/1.381677; T. Chase Hundley, Hugo Benioff, and Daniel W. Martin (Nov. 1978). "Factors contributing to the multiple rate of piano tone decay." In: *The Journal of the Acoustical Society of America* 64.5, pp. 1303–1309. DOI: 10.1121/1.382116.

[243] Tian Cheng, Simon Dixon, and Matthias Mauch (2015). "Modelling the decay of piano sounds." In: *2015 IEEE International Conference on Acoustics, Speech and Signal Processing (ICASSP)*. IEEE, pp. 594–598. DOI: 10.1109/ICASSP.2015.7178038; M. Aramaki et al. (2001). "Resynthesis of Coupled Piano String Vibrations Based on Physical Modeling." In: *Journal of New Music Research* 30.3, pp. 213–226. DOI: 10.1076/jnmr.30.3.213.7472.

[244] Schroeder, "New Method of Measuring Reverberation Time."

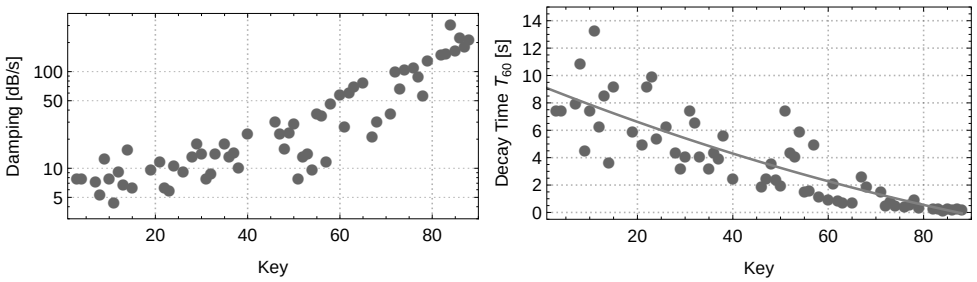

(a) *PROD7*

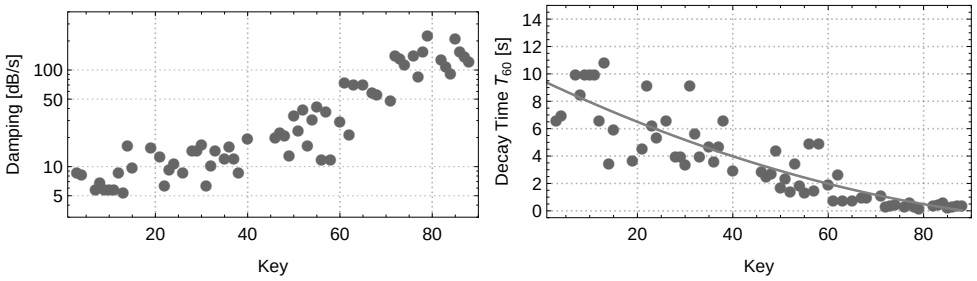

(b) *PROD8*

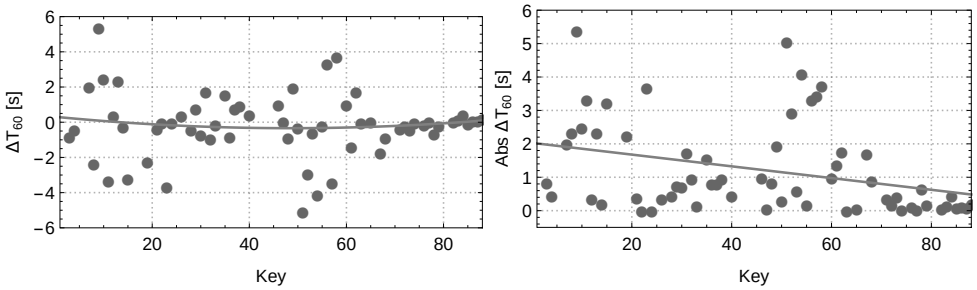

(c) T_{60} difference *PROD8-PROD7*

Figure 12.11.: a)-b) Damping of radiated sound at player position for *PROD7* and *PROD8* as damping in [dB/s] and T_{60} [s].
c) T_{60} difference *PROD8-PROD7*. Straight lines illustrate quadratic fittings.

than the dimension of the human head, unambiguous directivity determination by the inter-aural phase difference is not possible. For these frequencies ($\geq$ 1600 Hz), the inter-aural level difference gains importance for the auditory system to determine sound source directions. The ILD is calculated as the difference between left and right ear SPL values (in the given case frequency independent). Positive values indicate higher SPL for the left ear, negative values indicate higher SPL for the right ear. Figure 12.12 shows the development for the ILD per key for *PROD7* and *PROD8*:

- For the bass range and the lower mid range the average SPL is higher at the left ear by approx. 1 dB to 2 dB.
- For the higher mid range to treble range the average SPL is higher at the right ear by 4 dB with greater variance than in the bass range.
- As opposed to *PROD7*, for *PROD8* some keys in the mid and treble range are louder at the left ear by up to 5 dB.
- A comparison between *PROD7* and *PROD8* shows no difference in ILD values for notes up to *A4*. For notes higher than *A4*, the general trend stays unchanged with greatly increased variation for individual keys.

12.1.5. Loudness Domain

Sound Pressure Level

The sound pressure level (SPL) is calculated for the radiated sound at player position as the mean value of recorded sound pressure on left and right dummy head channel (p_{lr}) as

$$L_p = 20 \log_{10} \frac{p_{lr}}{p_0}, \tag{12.3}$$

with reference pressure p_0 = 20 µPa. According to Fastl and Zwicker,[245] the just noticeable difference for broad-band noise signals around 60 dB is approx. 0.5 dB.

[245] Hugo Fastl and Eberhard Zwicker (2007). *Psychoacoustics: Facts and models*. Springer, pp. 1–463. DOI: 10.1007/978-3-540-68888-4.

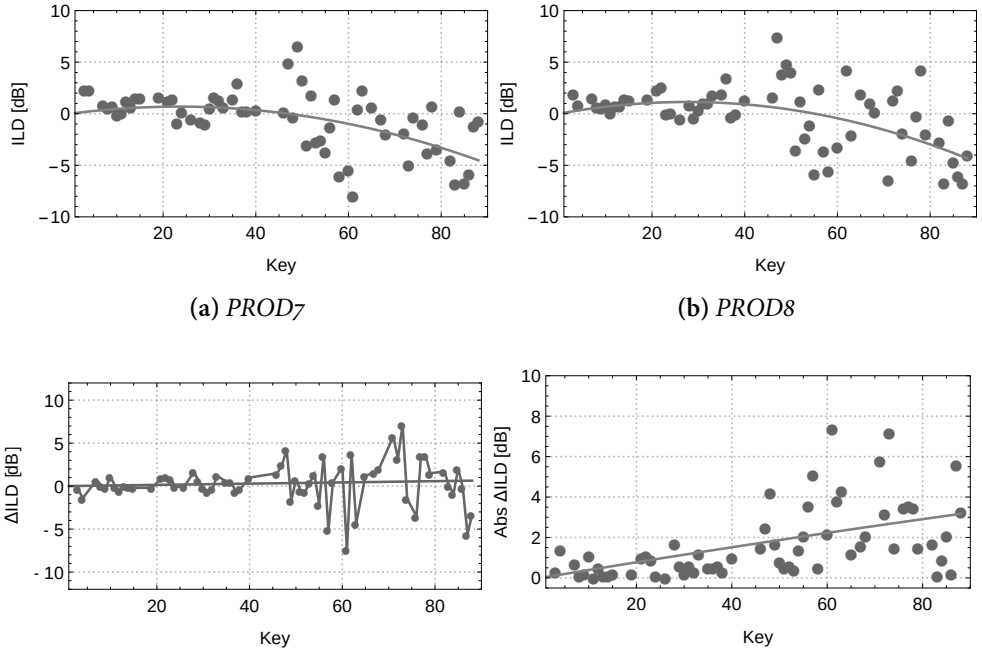

(a) *PROD7*

(b) *PROD8*

(c) ILD difference *PROD8-PROD7*

Figure 12.12.: a)-b) Inter-aural level difference at player position for played keys in *PROD7* and *PROD8*. Positive values indicate higher SPL for the left ear, negative values indicate higher SPL for the right ear.
c) ILD difference *PROD8-PROD7*. Straight lines illustrate quadratic fittings.

Figure 12.13 a) shows SPL values at player position per key for *PROD7* and *PROD8*. The average SPL values for the bass bridge notes decrease from 75 dB for *A0* to approx. 70 dB for *E2*. On the treble bridge the average SPL values increase from approx. 70 dB for *F2* to approx. 80 dB for *E7*. The development from *PROD7* to *PROD8* can be summarized as follows:

- In the bass- and low mid range, SPL values for the piano increase by up to 2 dB within the year.
- For notes higher than *C4*, SPL values tend to decrease by 1 dB to 5 dB but show a greater degree of variance. For the mid- to treble range, SPL values decrease within the year which can be explained with softer hammers due to several voicings.
- For single keys in the treble range, SPL values vary up to 10 dB, which should be perceivable. In the same course, with 3% average proportion of words used (compare Figure 11.7), loudness attributes may not play an important role for discrimination when differences in more dominant domains like timbre or pitch can be used for the evaluation.

12.2. Structural Metrics

12.2.1. Driving Point Mobility / Soundboard Crowning

Driving point mobility measurements are performed at the bridge in direction normal to the soundboard plane for both states. The same impact hammer and accelerometer as mentioned in Section 9.2 are utilized. The soundboard is excited at 10 string termination points on the bridge, all strings are damped, 10 takes per input are recorded. Figure 12.14 shows an exemplary comparison between *PROD7* and *PROD8* for key *F4*. The mean mobility for *PROD8* lies within the standard deviation of the *PROD7* measurement. Therefore, no significant difference can be observed.
The soundboard crowning height is measured at several points on the bridge for both states with a laser rangefinder. The maximum crowning difference between measurements is 1 ± 0.5 mm. As described in Section 8.1.4, the crowning is expected to vary within a year with amplitudes of up to several millimeters.

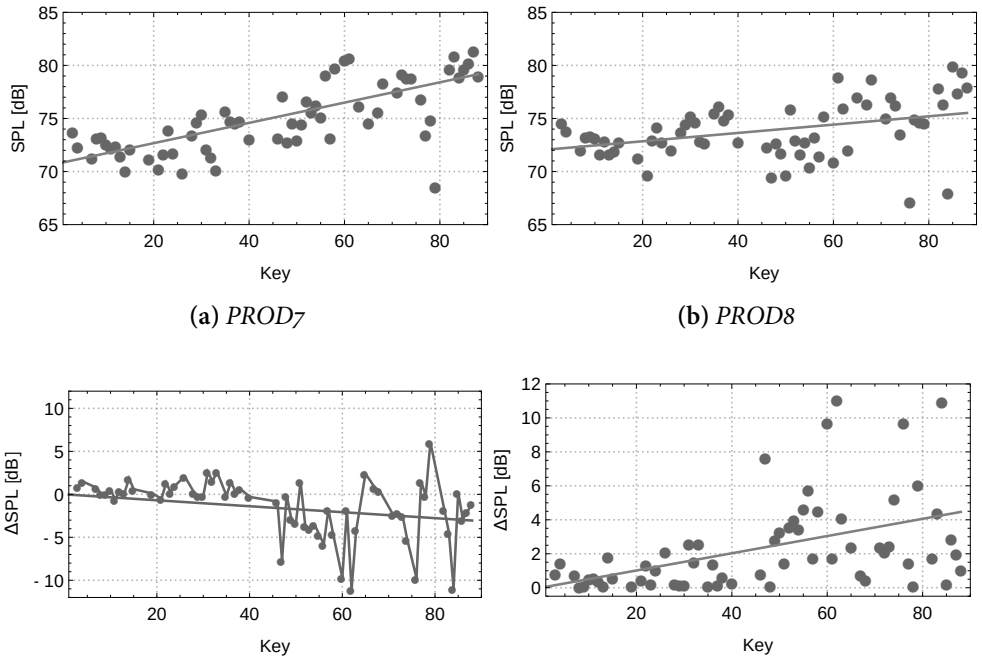

(a) *PROD7*

(b) *PROD8*

(c) SPL difference *PROD8-PROD7*

Figure 12.13.: a):-b) Sound pressure level at player position for played keys in *PROD7* and *PROD8*. Average of left and right ear. Mean *PROD7*: 75 dB, mean *PROD8*: 74,5 dB. Reference sound pressure $p_0 = 2 \times 10^{-5}$ Pa.
c) Difference of sound pressure level between *PROD7* and *PROD8*. Straight lines illustrate quadratic fittings.

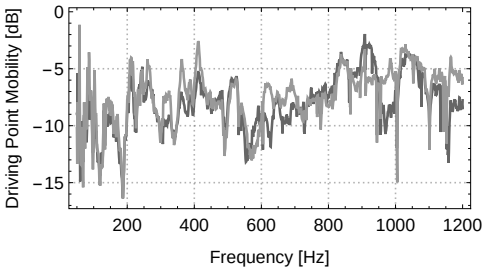

Figure 12.14.: Driving point mobility for *PROD7* (dark) and *PROD8* (bright) at *POS11*.

However, both measurements have been performed in the same season (winter) and therefore the soundboard should have a similar equilibrium moisture content.

12.2.2. Action Timing

The time delay Δt between key bed contact and vibrational activation of the piano is crucial for the sensation of how responsive the piano feels for the player.[246] Although this feature should not have audible impact for the listening test, it is a good example that shows empirical evidence for the work of the technician.
The time delay depends on the dynamical level of the tone played (compare Section 2.0.2). Figure 12.15 shows the time delay between key bed contact and activation at the bridge for *forte* played notes of *PROD7* and *PROD8*. For key 1-30 the bridge is activated after the key bed contact with decreasing tendency. Around *D3* the delay is 0 ms. From *C4* upwards the average delay is -2.5 ms. A general trend is observable with positive delays in the bass range decreasing to the mid range and a constant negative delay in the treble range. Comparison of *PROD7* and *PROD8* shows that the outliers in the bass range are leveled and the general variation decreases. This can be explained with maintenance work by the technician, who diminished the outliers by regulating, to yield a more consistent playing feel.

[246] Askenfelt and Jansson, "From touch to string vibrations. I: Timing in the grand piano action."

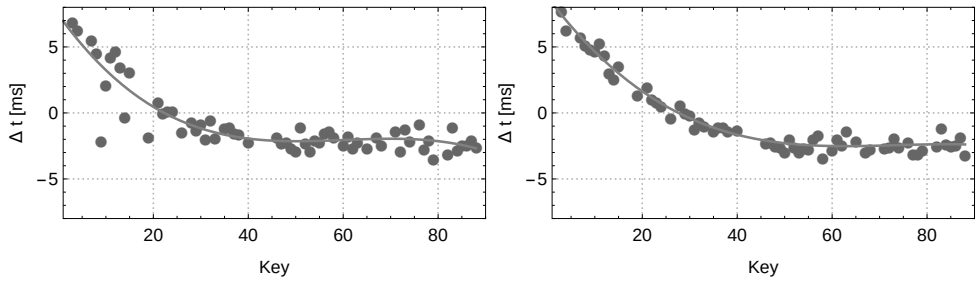

(a) *PROD7* **(b)** *PROD8*

Figure 12.15.: Time delay (Δt) between key bed contact and vibrational activation at the bridge for a) *PROD7* and b) *PROD8*. Positive values indicate that the bridge is activated after the key hits the key bed, for negative values the bridge is activated before the key hits the bed. Continuous lines illustrate cubic least-squares fittings.

12.3. Dimensional Reduction by Principal Component Analysis

As outlined above, individual well established psychoacoustic parameters do not seem to be capable to reflect the clear perceptibility of tonal differences. An indication can also be given by comparing histograms of the respective features: Figure 12.16 shows how the chosen parameters affect the target classes (here: Production stages). If the histograms of a feature would be clearly separated, the corresponding feature would most likely be capable to discern the classes *PROD7* and *PROD8*. This is not the case for any of the chosen features, thus they do not represent the audible difference in an ideal way. Nevertheless, this does not imply, that a certain projection into the feature space can not hold distinctness: in theory, two feature vectors could have the same value distribution while having a reversed value order. Therefore, an underlying difference could be revealed by a projection, even for a combination of features with similar distributions.

In an approach to reduce the number of dimensions, necessary to describe the current state of the piano, and to eventually find embedded distinctness between production states, a *principal component analysis* (PCA) is performed on the present feature space. PCA is a linear technique that transforms a data set

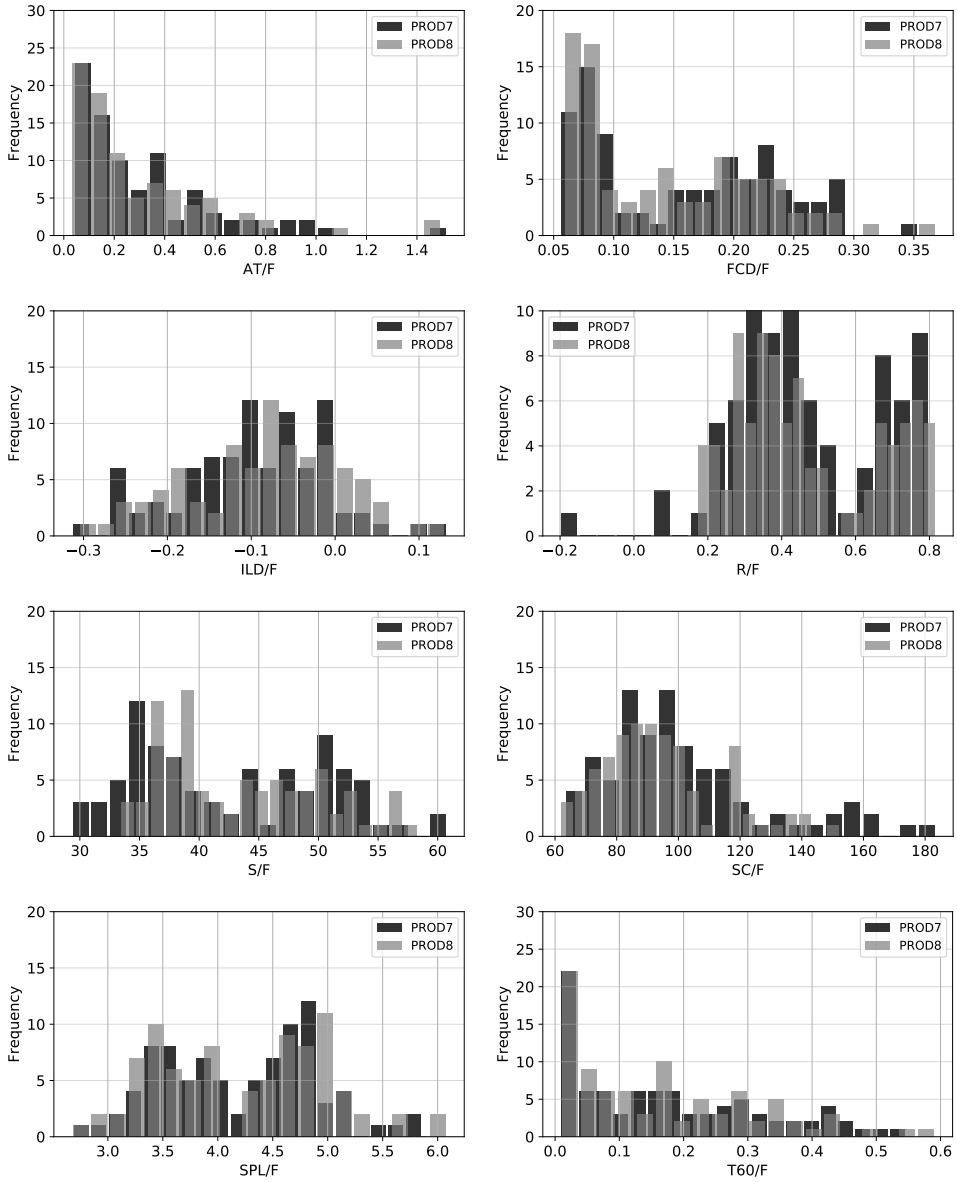

Figure 12.16.: Histograms of feature distributions for *PROD7* (dark) and *PROD8* (bright).

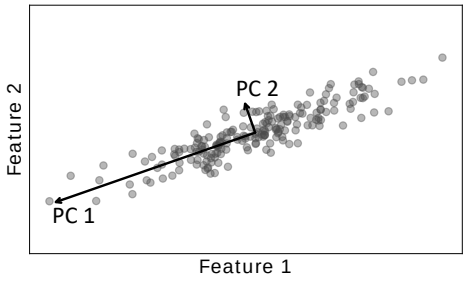

Figure 12.17.: Exemplary projection of a two dimensional dataset (Feature 1 and 2) onto two orthogonal principal components (PC 1 and 2).

into a lower-dimensional sub-space. It allows to preserve the most important information in the data set and to remove the non-essential parts with fewest variance. Since it is an unsupervised method, no information about the target class(es) is considered in the calculation. The resulting new vectors, also called *principal components* (PC), are complex mixtures of the original features and, therefore, must be interpreted by the researcher. The PCs are eigenpairs composed of eigenvectors coupled with eigenvalues, describing the directions in the original space with the greatest variance in the data set. Figure 12.17 shows an exemplary artificial two-dimensional data set. In this simple case, the linear relationship between feature 1 and 2 becomes apparent just from plotting them against one another. For high dimensional data however, relationships can be difficult to determine. Although, there are methods for estimating the number of principal components to retain,[247] the final choice is up to the researcher and depends on the research question and the interpretability of the components. As a rule of thumb, often a sharp bend (so-called *knee*) in the scree plot is chosen and all components within the steep descent are retained. Another approach is to ask, how much information loss can be allowed and how much information has to be preserved.

The PCA is implemented using the machine learning library *scikit-learn*[248]. Table 12.1 shows the included features (see Section A.10 for a complete specifi-

[247] William R. Zwick and Wayne F. Velicer (1986). "Comparison of five rules for determining the number of components to retain." In: *Psychological Bulletin* 99.3, pp. 432–442. DOI: 10.1037/0033-2909.99.3.432.

[248] `https://github.com/scikit-learn/scikit-learn`, accessed in July 2019.

Table 12.1.: Feature set for the principal component analysis.

AT	Attack Time
f_1	Fundamental Frequency
FCD	Fractal Correlation Dimension
ILD	Interaural Level Difference
R	Roughness
S	Sharpness
SC	Spectral Centroid
SPL	Sound Pressure Level
T60	Decay Time

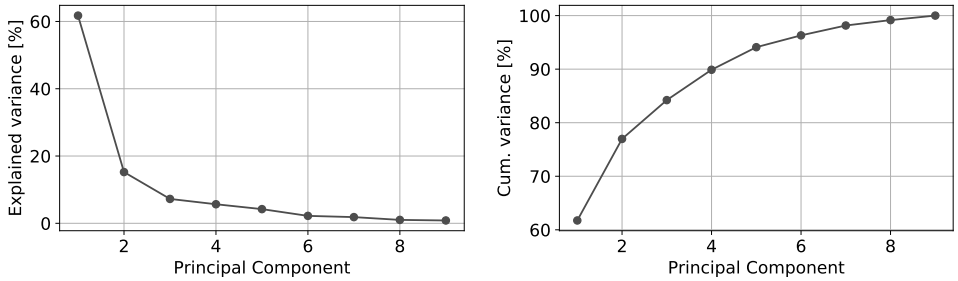

(a) Explained variance per principal component.

(b) Cumulative explained variance per principal component.

Figure 12.18.: Scree plots of explained variance per principal components.

cation of the feature space). Apart from f_1, all features are normalized by the key bed force F_{key}, since they could be depending on F_{key}. The production stage is chosen as the target variable, since the features with their states per key establish the piano in the given production stage.

Figure 12.18 illustrates, how much information (variance) each additional dimension contains. The *knee* appears between PC 2 and 3 with a respective total explained variance of 78% / 85%. In other words, 85% of the information in the feature space can be 'explained' with the first three components.

PC1 holds 62% of the systems information and is composed equally of the original features (see Figure 12.19 a)). When plotted against the keys, a linear relationship between PC1 and key number can be observed. PC1 could, thus,

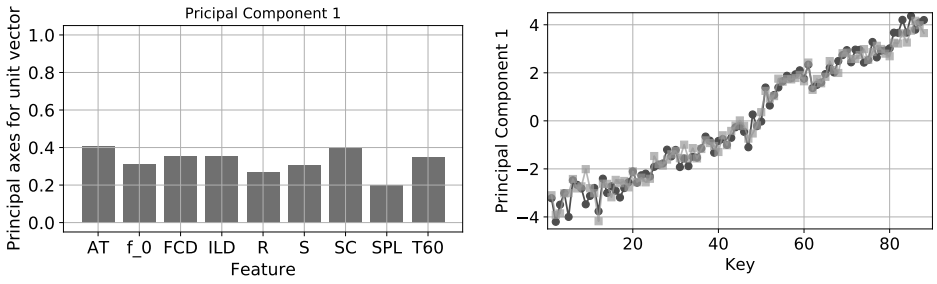

(a) Modulus of principal axis for unit vector of PC1 in original feature space.

(b) PC1 vs. keys for *PROD7* (dark) and *PROD8* (bright).

Figure 12.19.: Principal Component 1

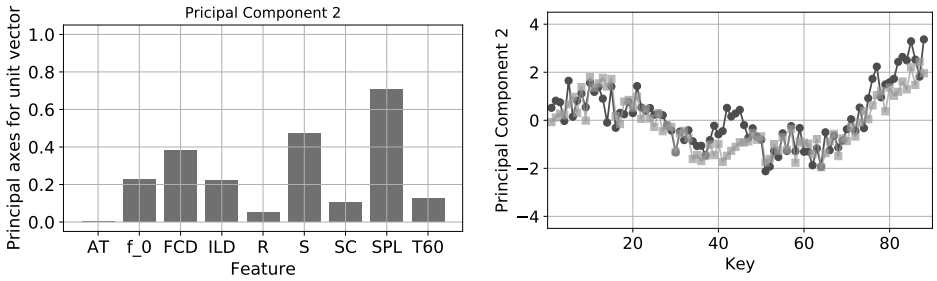

(a) Modulus of principal axis for unit vector of PC2 in original feature space.

(b) PC2 vs. keys for *PROD7* (dark) and *PROD8* (bright).

Figure 12.20.: Principal Component 2

be interpreted as the pitch dependency in each original feature. Comparison between *PROD7* and *PROD8* does not show distinct differences.

PC2 explains 18% of the existing variance and is mainly composed of spectral centroid and roughness, but also to smaller extent by the fundamental frequency (see Figure 12.20). The third principal component PC3 explains 8 % of information in the feature set and is almost completely composed of the roughness dimension.

The findings can be summarized as follows:

- Histograms of the selected features do not significantly differ between *PROD7* and *PROD8*, which gives indication, that they do not represent

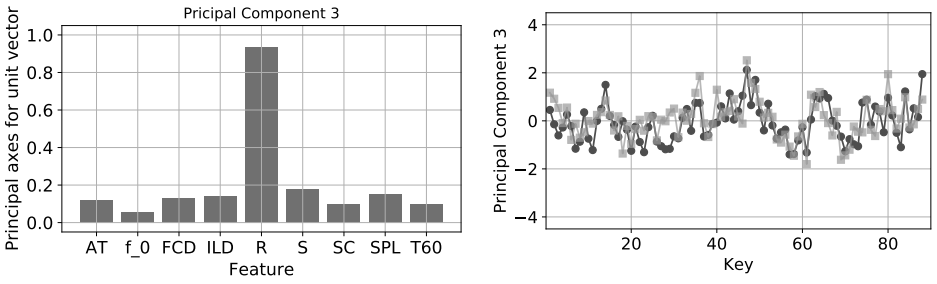

(a) Modulus of principal axis for unit vector of PC3 in original feature space.

(b) PC3 vs. keys for *PROD7* (dark) and *PROD8* (bright).

Figure 12.21.: Principal Component 3

the audible difference in an ideal way. However, in theory, a certain projection into the feature space could hold distinctness.

- 85% of the information in the original feature space can be 'explained' with three principal components.
- For none of the three obtained components, a significant difference is observable between target classes *PROD7* and *PROD8*. Hence, the PCA is not capable of revealing an underlying difference between target classes with regard to the feature space.

13. Discussion Part 2

13.1. Critique of Method

It cannot be ruled out that the process of tuning the instrument prior to the measurements may have influenced the tonal quality of the piano to an audible extent. The only instruction to the technician prior to tuning had been to tune to an identical chamber tone. An alternative approach would have been to play back the recorded tones from the first measurement during the second tuning of the piano, and instruct the technician to reproduce the exact same tuning. On one hand, this could have eliminated uncertainties due to tuning. On the other hand, it would have prevented any natural reaction of the technician on certain, eventually altered, characteristics of the piano. From a practical point of view, the reproduction of the exact same temporal development of the tones' spectral distribution for all keys would have been very difficult and hence, too time/cost intensive.

As exemplified in Section 8.3, due to the study design no causal relationships can be revealed. A more controlled design could have been implemented with the disadvantage of not capturing real-world conditions.

With substantial financial effort, a second instrument could have been stored in the concert hall without being modified or played over the course of the year. In doing so, the influence of aging under certain climate conditions could have been identified and isolated from the set of dependent variables with sufficient certainty.

The statistical results reveal a ceiling effect for the listening test. Within the scope of a controlled experiment, the discrimination task would have been

considered to be 'too easy' and could be adjusted to be more unlikely to accomplish. However, during the given study, none of the identified influential factors could be controlled.

As specified in Section 11.3, the semantic relationships within a sentence are not taken into account for the analysis of verbalizations. After pre-processing, the exemplary sentence *'Slight difference in brightness of attack'* leads to two keywords *'brightness'* and *'attack'*. These words are consequently assigned to the categories *Timbre* and *Temporal*. However, these two keywords also could have originated from an entry like *'Overall brighter. Shorter attack phase.'* which would have had a different meaning. *Part-of-speech tagging* would have allowed to specify the relationship of words in a sentence by assigning each word to its part of speech function (such as verbs, nouns, adjectives, etc.). Thereby, a context of meaning as in the example mentioned could have been detected, which would have led to a more precise verbalization analysis.

13.2. Reflection on Results

With regard to the listening test, it can be noted that a difference in tonal quality is perceivable for a piano after one year in concert usage, even for non-experts. Despite an observable ceiling effect in the test, builders and tuners have the highest competence to make a distinction between piano tones of the same pitch, which is a conclusive result, since this is one of their main professional skills. The builders/tuners group has the highest hit ratio (96.3%), followed by the players (93.3%) and the non-experts (90.3%).

The most stated properties used to distinguish between piano tones of the same pitch are *Timbre* related (36%), followed by *Pitch* (16%) and *Temporal* (11%) attributes. *Spatial* (3%) and *Loudness* (1%) related sensations do not seem to play an important role in discrimination, even when stimuli should exceed the just noticeable difference. Even experts in piano playing or building use descriptive and metaphoric vocabulary to a high degree in describing their sensations. The vocabularies of non-experts, players, and builders differ far less than assumed.

For the highest octave, Spectral Centroid values decrease from *PROD7* to *PROD8*, which is in accordance with statements by the technician responsible: That the treble range was too 'harsh' when the piano was delivered. This had to be adjusted during the following months by needling the hammer felts. Nevertheless, a comparison with the proportion of timbre-related verbalizations does not reflect this development: The treble range with the highest SC difference shows the lowest proportion of used timbre related words.
For the Fractal Correlation Dimension, a general decrease from low to high notes is observable. In the bass range, several more harmonic systems are present than in the treble range, e.g. partials due to longitudinal string vibration, phantom partials, and up to 85 audible transversal partials. Since the increase of vibration frequency for each partial is proportional to the square of the partial number for a real stiff string, a much greater amount of inharmonic partial intervals is present for the bass notes. This increases the FCD in the bass range compared to the treble range where, on the one hand, the inharmonicity coefficient increases again due to the string scale but, on the other hand, the number of audible partials decreases strongly to a minimum of approx. 4 for the highest keys. A general difference between states is not observable.
Positive correlation is found between the degree of detuning of the unison strings and perceived Roughness. Up to *F6*, the average degree of detuning is in the range proposed by Kirk, with differences between strings of approx. 1-2 cent. In the high treble range differences of up to 5 cent appear. This degree of detuning could have happened deliberately, but also could have been caused by general difficulties in tuning the instrument due to the unfamiliar room acoustics. Greatest Roughness values in the bass range with a peak on the bass bridge are in good agreement with the general perception of strongest dissonance for the lowest notes due to the number of transversal partials, string inharmonicity, and the audible presence of longitudinal string partials. A significant difference between states is not observable.

According to the percentage of related verbalizations, pitch was the second most important factor for the discrimination of piano tones with the greatest relevance in bass and treble range. f_1 difference measurements show a similar general trend with greatest deviations in the bass and treble range, with several values that should be greater than the just noticeable difference: In the mid range, f_1 differences of approx 2.5 cent are observable. In the highest octave, deviations of up to 10 cent are observable. Pitch, therefore, could be a

cue in the listening test at least for some keys. The general curve with highest differences in the bass and treble ranges can be explained by differently tuned octave stretches. Again, a contrasting picture between verbalized perception and corresponding psychoacoustic representation emerges: For several keys, high proportions of pitch-related verbalizations are given with no measurable difference in f_1 values. This could be explained by the fact that for complex tones, participants have difficulties in ignoring alterations in brightness (due to changes in the spectral distribution) when making pitch judgments (due to changes of the fundamental frequency).

Notwithstanding the frequent use of words from the temporal domain (11% average per key), e.g. *attack, onset, faster, shorter,* and *decay*, no general difference is observable, neither for attack time, nor the decay time T_{60}.

A comparison between states shows no difference in inter-aural level difference values for notes up to *A4*. For notes higher than *A4*, the general trend stays unchanged with greatly increased variation for individual keys.
For the mid- to treble range, sound pressure level values decreased within the year by 1 dB to 5 dB, which can be explained with softer hammers due to several voicings. For single keys in the treble range, SPL values vary up to 10 dB, which should be perceivable. In the same course, with 3% average proportion of used words, loudness attributes may not play an important role for discrimination when differences in domains like *Timbre* or *Pitch* can be used for the evaluation.

By comparison, a contrast becomes apparent between clear perceptibility of tonal differences on the one hand, and insufficient representability with well established psychoacoustic metrics on the other. Although even non-experts seem to perceive small differences in tonal quality of similar piano tones, individual well established psychoacoustic parameters do not seem to be capable of reflecting these differences.

Dimensional reduction by a principal component analysis does not reveal an underlying difference between target classes with regard to the feature space.

With regard to a change in physical properties, no significant differences (greater than standard deviation) in driving point mobility of the soundboard can be observed between states. The maximum crowning difference between

measurements is 1 ± 0.5 mm. The crowning is expected to vary with amplitudes of up to several millimeters within a year. However, both measurements have been performed during the same season (winter) and, therefore, the soundboard should have had a similar equilibrium moisture content.
Comparison of the time delay between key bed contact and vibrational activation at the bridge for *PROD7* and *PROD8* shows that outliers in the bass range are leveled and general variation decreases. This can be explained with maintenance work by the technician, who diminished the outliers by regulating to yield a more consistent playing feel.

Within the bounds, and given the described uncertainties of the study design, it can be stated with confidence that within the time frame of one year, the technician can be expected to have much more impact on the tonal development of the piano than the effects of wood aging or playing.

14. Conclusion and Outlook

In this thesis, the development of a grand piano's sound has been traced through its production, as well as its first year in concert business. In the following, the central achievements are presented:

14.1. Part 1

Two concert grand pianos have been accompanied with acoustic measurements through their manufacture to investigate the influence of successive production steps on the development of the pianos' final sound. The utilization of a microphone array led to insights about the vibrational behavior of the soundboard with remarkable temporal and spatial resolution, and allowed novel observations in time domain. The most important findings are:

- The application of ribs has a crucial impact on the propagation behavior of the initial bending waves. In direction normal to grain, the propagation is not circular but rather a traveling plane wave front, as a result of superposition of reflections between the ribs. The ribs act as waveguides for higher frequencies with locally changed stiffness. The influence of the bridge is clearly observable in the initial bending wave pattern: Stiffening increases the wave velocity locally, and the propagation seems to follow the bridge direction, even when curved.
- It has been possible to estimate the flexural wave velocity ratio between longitudinal and radial direction on the soundboard: Application of ribs nearly compensates the anisotropy to a ratio of 0.9. Overcompensation is not observable. The attached bridge causes a local stiffening, mainly in grain direction, which leads to higher velocities along its direction and thereby a decrease of v_{RR}/v_{LL}. Gluing the soundboard into the rim

changes the system dramatically but, in total, leads back to nearly the general 'isotropic state' it had with only the ribs.

- The energy loss could be described not only as a general signal decay, but could also be given exclusively for the initial propagation on the soundboard before any reflections or drain at the boundaries:
  The energy loss per traveled distance is twice as large in radial, than in longitudinal direction for the blank soundboard. The greatest portion of the supplied energy is preserved in grain direction. After application of the ribs, the majority of the supplied energy is preserved in radial direction between adjacent ribs. After attaching the bridge, the supplied energy seems to be able to distribute more uniformly due to local stiffness increase by the bridge, acting as a waveguide in mainly longitudinal direction. The bass bridge and the connected lower treble bridge part form a loop in the upper half of the soundboard, which confines significant parts of the vibrational energy (*bridge loop effect*).

- The spatial distribution of vibrational energy on the soundboard per frequency has been approximated with exponential decays. The model is capable of distinguishing the typical frequency domains for a vibrating piano soundboard: It displays the transition from modal- to driving point dependent domain as a decrease of the standard deviation of exponent κ. Although localization effects can produce deviating vibrational patterns in high frequencies, the directional averaged behavior can be approximated with an exponential decay. For frequencies greater than 2 kHz to 3 kHz, κ has values between 1 and 2. With $\kappa = 1$, the soundboard behaves like a reflection free plate; higher values of κ can be explained with local waveguide effects by ribs and bridge.
  The method should be applicable to other structures for the discrimination between modal- and driving point dependent domain.

- The observable differences in wood material properties between the two examined soundboards are not reflected in the acoustic measurements. This leads to the assumption, that in this range of variation, the geometry plays a predominant role for the resulting behavior.

An alternative approach to classic modal analysis has been presented for the description of the vibro-acoustical behavior of piano soundboards. Even if the presented physical descriptions might not be relevant for the instrument

builder in daily practice, visualizations of the time dependent spatial distribution of vibrational energy on the soundboard should be comprehensible, and hopefully help piano builders to understand the effects of individual production steps for the final behavior of the instrument.

14.2. Part 2

In a second experiment, measurements on a concert grand piano have been performed before and after one year in concert business to identify influential factors for a presumed change in tonal quality. The most important findings are:

- A listening test engaging 100 players, tuners, and builders showed, that a difference in tonal quality is perceivable for a piano after one year in concert usage, even for non-experts.
- The most stated properties used to distinguish between similar piano tones were *Timbre* related, followed by *Pitch* and *Temporal* attributes. *Spatial* and *Loudness* related sensations do not seem to have played an important role in discrimination, even when stimuli should have exceeded the just noticeable difference.
- Semantic sub-grouping allowed for indication on the vocabulary listeners of varying expertise used to verbalize their sensation. Even experts in piano playing or building used descriptive and metaphoric vocabulary to a high degree when describing their sensations. The vocabularies of non-experts, players, and builders differed far less than presumed.
- A disparity has been found between clear perceptibility of tonal differences on the one hand, and insufficient representability with well established psychoacoustic metrics on the other. Although even non-experts seem to perceive small differences in tonal quality of similar piano tones, individual well established psychoacoustic parameters do not seem to be capable of reflecting these differences.
- With regard to a change in physical properties, no significant differences could be observed between states.

Within the bounds and given the described uncertainties of the study design, it can be stated with confidence, that within the time frame of one year the technician can be expected to have much more impact on the tonal development of the piano than the effects of wood aging or playing. The presented findings give the technician to the same extent the responsibility, but also the opportunity to turn a good concert instrument into an excellent one.

14.3. Outlook

- The back-propagation of a multiple-array measurement turned out to be unworkable under the given circumstances. However, the present thesis helped to identify crucial error sources and it is planned to implement the method considering the described challenges in the near future.
- As described, the angle dependency is ignored for the approximation of exponential attenuation. It is envisaged to include the directivity into the calculation, which should considerably decrease the fitting error. When calculated for *PROD1*, it should enable to estimate the grain angle dependent loss factor for a spruce plate.
- The presented results give a good impression about the energy distribution on a vibrating piano soundboard. It is planned to accompany the measurements with a statistical energy analysis (SEA), to model the flow and storage of vibrational energy among structural components.[249] The method is particularly suitable for the analysis of high frequency vibrations in complex structures and could give insight about the coupling between ribs, bridge and plate.
- A recent approach to efficiently dampen vibrating structures is to utilize the so-called *acoustic black hole effect*: If the thickness of a plate varies in height in a sufficiently smooth manner, a bending wave traveling through the plate does not 'see' any structural change and is, thereby, not reflected. Since the bending wave number depends on the plate height, it will tend to infinity as the height tends to zero. Thereby, "a

[249] Richard H. Lyon and Richard G. DeJong (1995). *Theory and Application of Statistical Energy Analysis*. Elsevier. DOI: 10.1016/C2009-0-26747-X.

wave originating in the thick part of the plate does not reach the tapered edge in any finite time and is therefore not reflected from it".[250] A plate or bar ideally tapered following a power law will totally absorb a flexural wave, hence the name *black hole*. In practice, it is not possible to manufacture a tapering which perfectly reduces to zero. The end of the edge will always have a truncation where the wave could reflect. Thereby, the theoretical reflection coefficient of zero is not feasible in practice. Nevertheless, damping systems with high efficiency for flexural waves can be realized.[251]

Therefore, it is an interesting question whether acoustic black hole effects could occur in a piano, even if not deliberately implemented. Since Bilhuber,[252] the plate is manufactured to a height profile with thinned edges. However, the height reduction from approx. 10 mm to 6 mm is rather smooth but goes nowhere near zero. Mironov[253] describes constrains for the desired effect as "even if the thickness of the plate varies by three orders of magnitude and the plate material has a very low Q, a substantial part of the wave energy is reflected". Thereby, no observable black hole effect can be expected due to thinning of the edges alone.

Another component worth considering are the notched ribs, since their tapered height profile perfectly follows a power law. However, the rib height is not lowered to zero and the ribs are rigidly connected to the soundboard. It is, therefore, questionable whether a damping effect could occur initiated by the height profile. Still, as a connected structure of plate and ribs, the height is reduced to a third, which has observable

[250] M. A. Mironov (1988). "Propagation of a flexural wave in a plate whose thickness decreases smoothly to zero in a finite interval." In: *Sov. Phys. Acoust.* 34.3, pp. 318–319.

[251] Stephen C. Conlon, John B. Fahnline, and Fabio Semperlotti (2015). "Numerical analysis of the vibroacoustic properties of plates with embedded grids of acoustic black holes." In: *The Journal of the Acoustical Society of America* 137.1, pp. 447–457. DOI: 10.1121/1.4904501; V. V. Krylov and F. J. B. S. Tilman (July 2004). "Acoustic 'black holes' for flexural waves as effective vibration dampers." In: *Journal of Sound and Vibration* 274.3-5, pp. 605–619. DOI: 10.1016/j.jsv.2003.05.010; Jacques Cuenca et al. (2012). "Improving the acoustic black hole effect for vibration damping in one-dimensional structures." In: *Proceedings of Acoustics 2012*, pp. 2189–2191.

[252] Bilhuber, *U.S. Patent No. 2,051,633: Soundboard for pianos and other instruments or devices using soundboards*.

[253] Mironov, "Propagation of a flexural wave in a plate whose thickness decreases smoothly to zero in a finite interval."

influence on the energy distribution. The question remains, why the ribs are historically notched with this particular profile. A trivial reason could lay in the way the corresponding plane irons used for notching the ribs are utilized. If the tapered profile is not only applied for practical reasons or visual appearance, it would be worth to investigate further.

- It is questionable whether the observed *bridge loop effect* is beneficial for vibration and radiation of a grand piano. If the bridge loop 'collects' vibrational energy, the resulting radiation should be narrower, more point-like, and more locally limited for high frequencies than without. A comparison of inter-aural cross correlation coefficients (IACC) from binaural recordings could provide clues for the apparent source width of pianos with and without implemented cross-stringing. Two main reasons were given in the patent[254] from 1859 for the cross-stringing being advantageous: a) The possibility of implementing longer bass strings and, thereby, reducing inharmonicity in the bass range. b) The possibility to position more of the string termination points closer to the soundboard center and, thereby, achieve greater amplitudes. The first argument has been refuted by Poletti,[255] who measured the respective parameters before and after implementation and found the cross-stringed version not to be significantly longer. High volume might have been a quality criterion for a musical instrument in the 19th century due to changing performance practice. However, with modern audio engineering methods, a concert instrument could be unnoticeable amplified. It could, therefore, be worth considering to exchange loudness for less point-like radiation.

[254] H. Jr. Steinway (1859). *U.S. Patent No. 26,300: Stringing Pianos*.

[255] P. Poletti (2000). "Steinway and the invention of the overstrung grand piano frame." In: *Matière et musique: The Cluny Encounter, Proc. European Encounter on Instrument Making and Restoration*. Labo19, pp. 241–263.

A. Appendix

A.1. Climate Conditions during Measurements

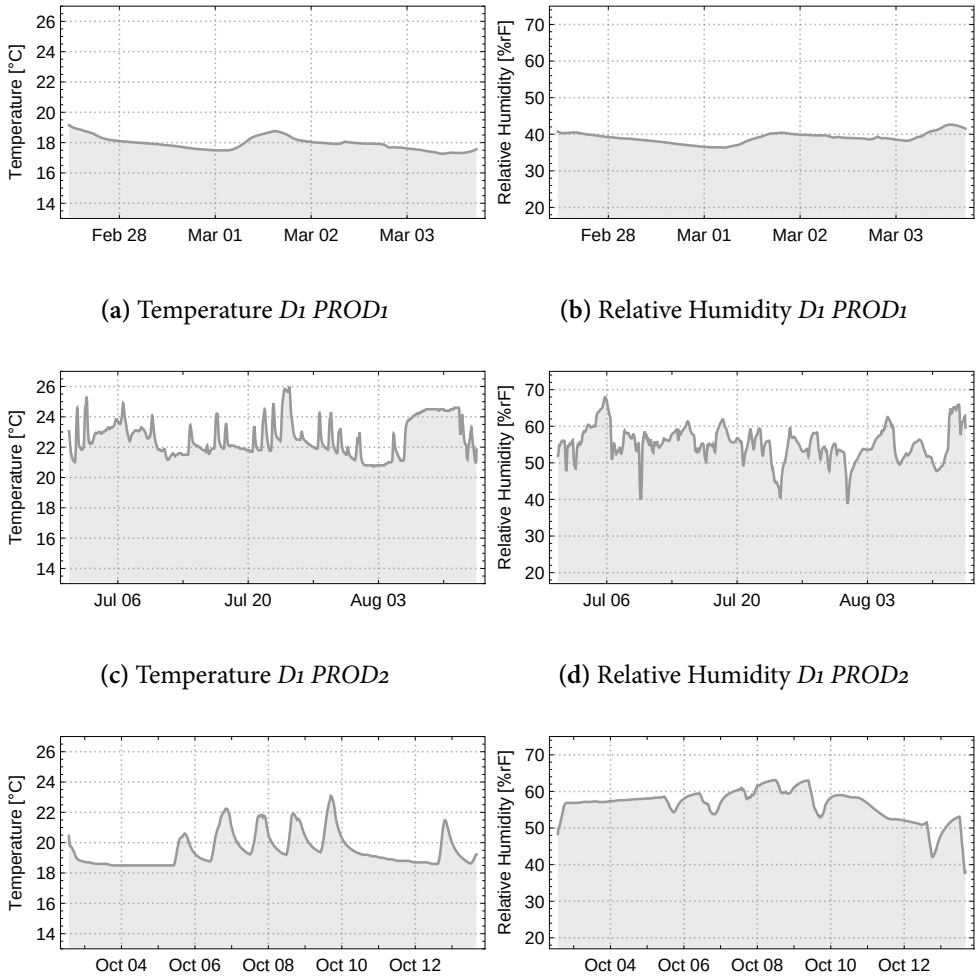

(a) Temperature *D1 PROD1*

(b) Relative Humidity *D1 PROD1*

(c) Temperature *D1 PROD2*

(d) Relative Humidity *D1 PROD2*

(e) Temperature *D1 PROD3*

(f) Relative Humidity *D1 PROD3*

Figure A.1.: Climate conditions during measurements of *D1 PROD1-PROD3*.

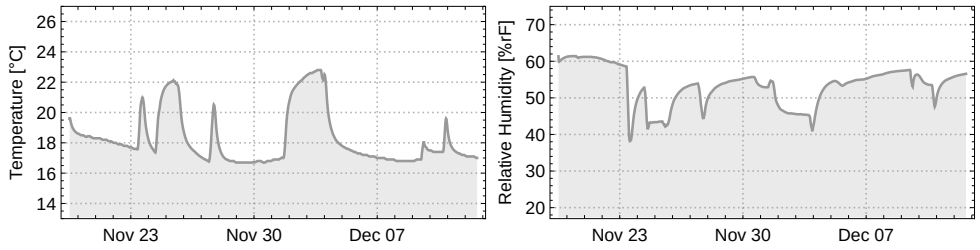

(a) Temperature *D1 PROD4*

(b) Relative Humidity *D1 PROD4*

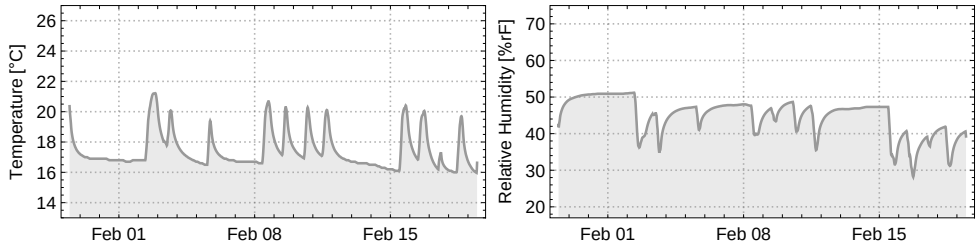

(c) Temperature *D1 PROD5*

(d) Relative Humidity *D1 PROD5*

Figure A.2.: Climate conditions during measurements of *D1 PROD4-PROD5*.

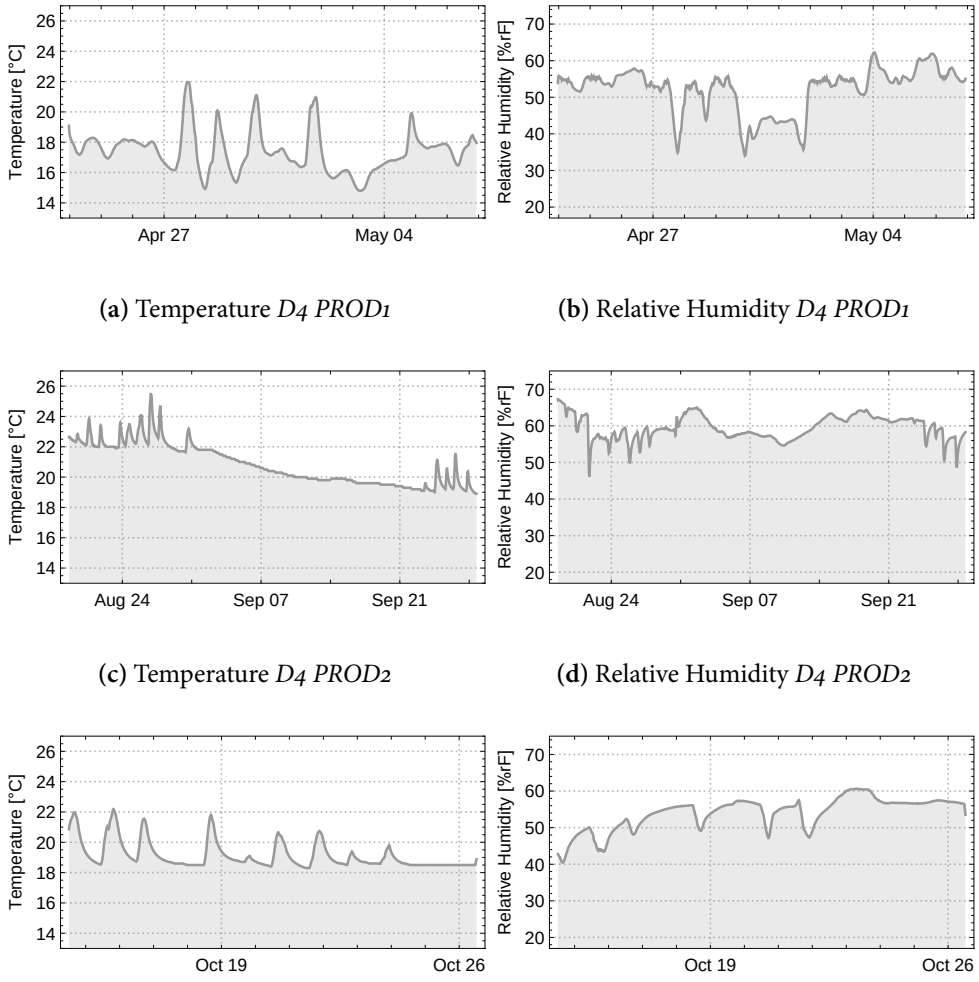

(**a**) Temperature *D4 PROD1*

(**b**) Relative Humidity *D4 PROD1*

(**c**) Temperature *D4 PROD2*

(**d**) Relative Humidity *D4 PROD2*

(**e**) Temperature *D4 PROD3*

(**f**) Relative Humidity *D4 PROD3*

Figure A.3.: Climate conditions during measurements of *D4 PROD1-PROD3*.

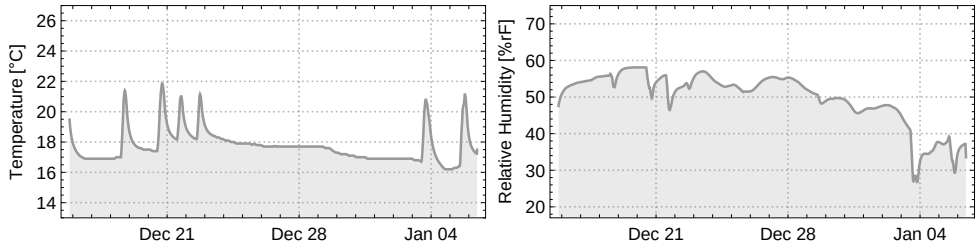

(a) Temperature *D4 PROD4*

(b) Relative Humidity *D4 PROD4*

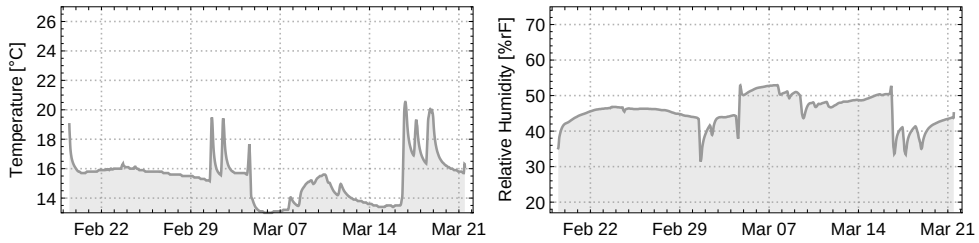

(c) Temperature *D4 PROD5*

(d) Relative Humidity *D4 PROD5*

Figure A.4.: Climate conditions during measurements of *D4 PROD4-PROD5*.

A.2. Crowning per Production Stage

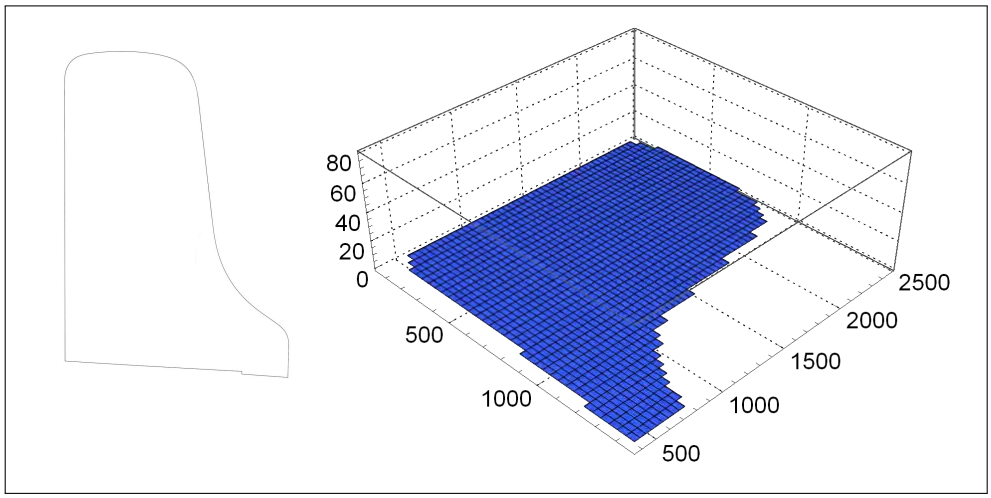

Figure A.5.: Crowning *D1 PROD1*.

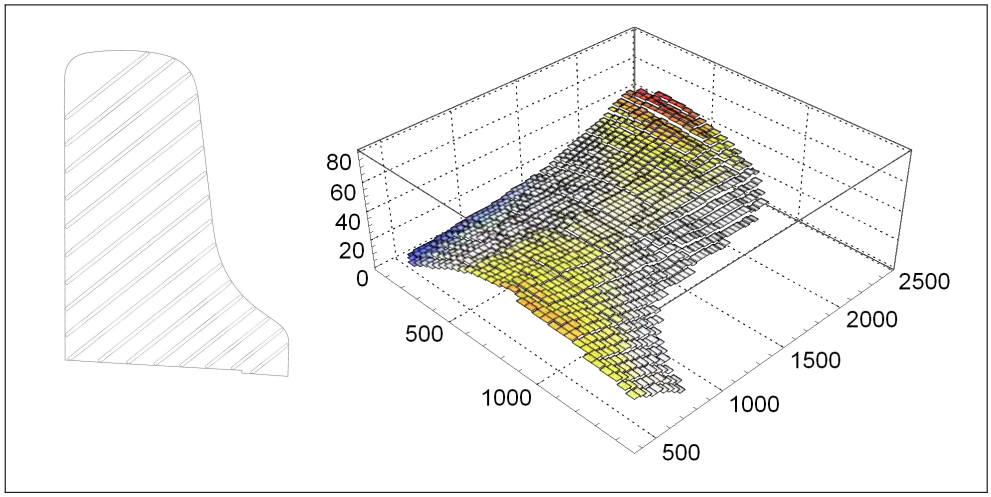

Figure A.6.: Crowning *D1 PROD2*.

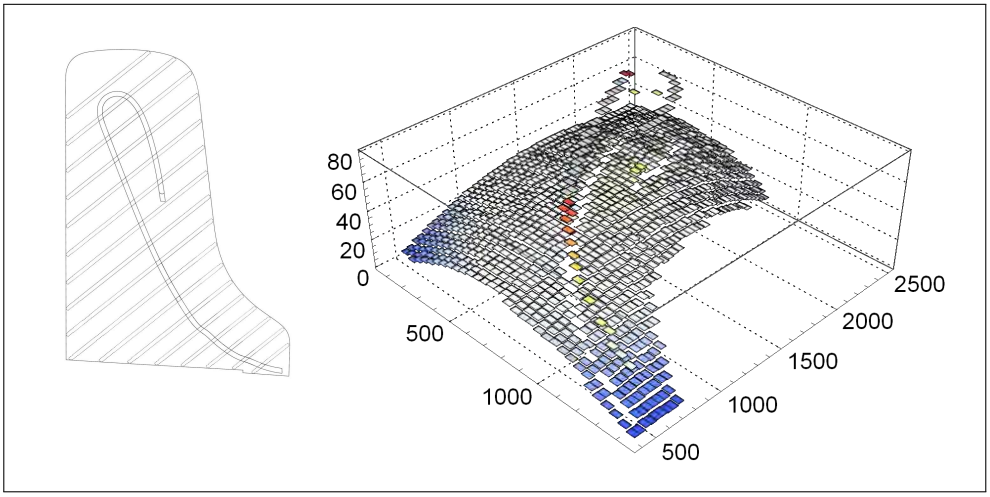

Figure A.7.: Crowning *D1 PROD3*.

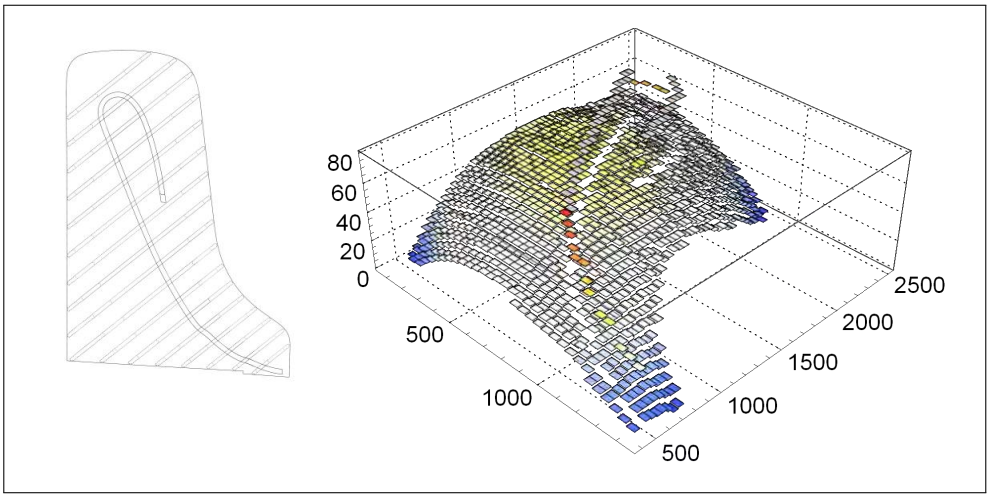

Figure A.8.: Crowning *D1 PROD4*.

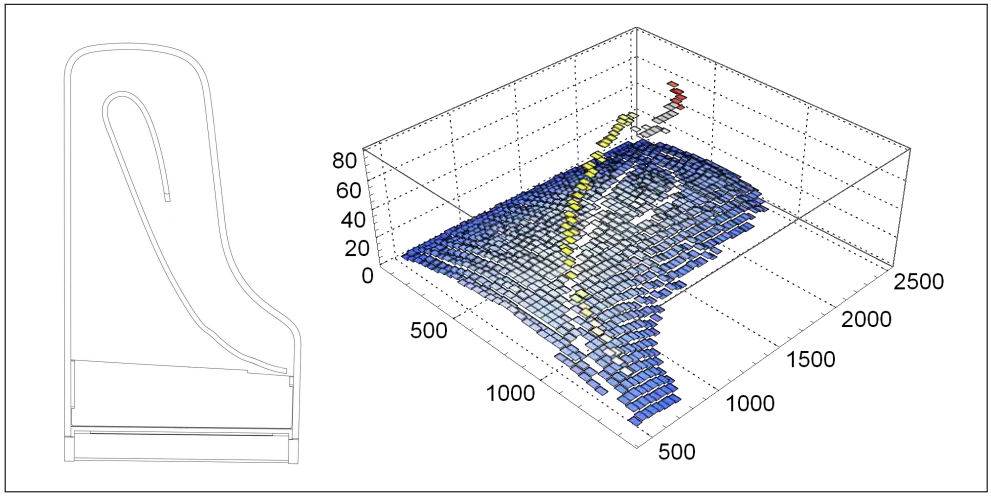

Figure A.9.: Crowning *D1 PROD5*.

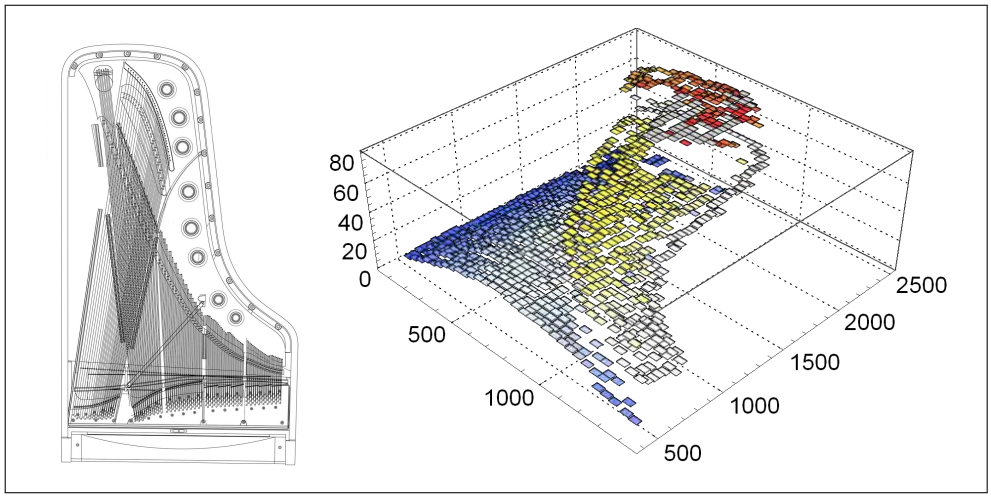

Figure A.10.: Crowning *D1 PROD6*.

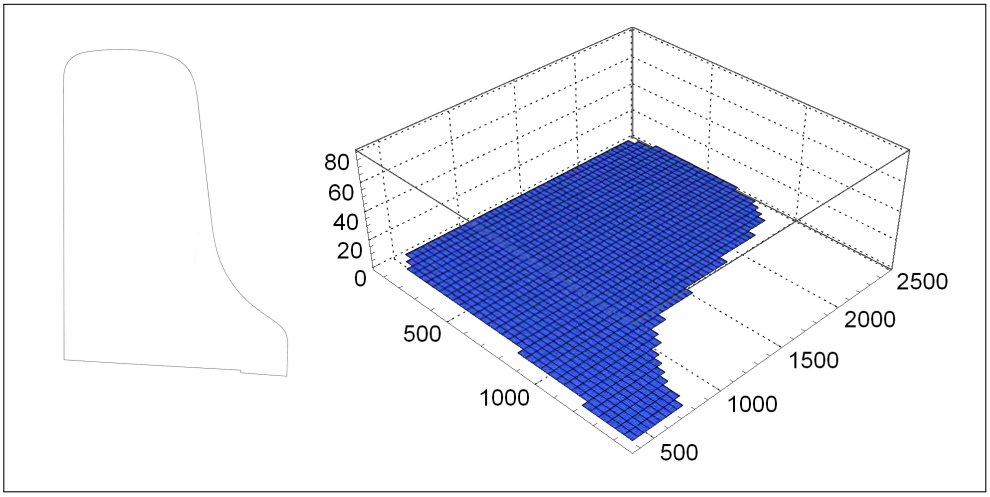

Figure A.11.: Crowning *D4 PROD1*.

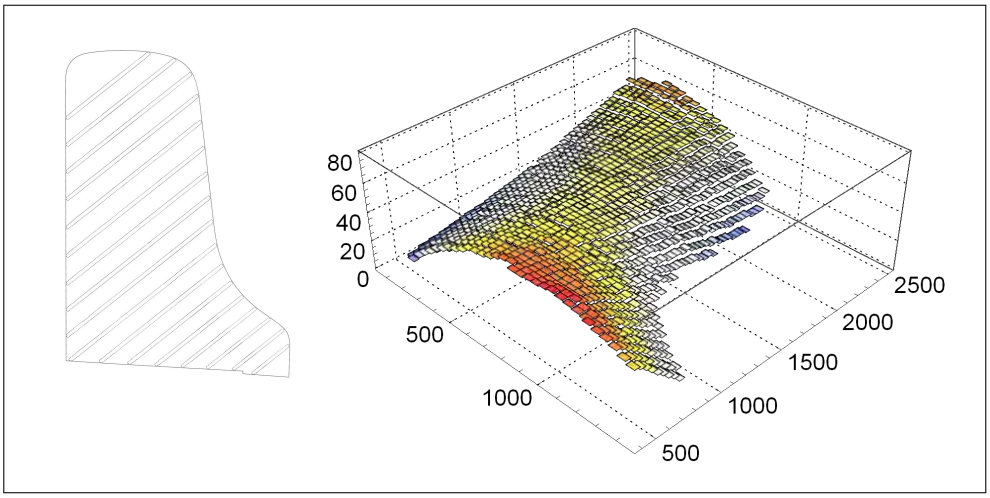

Figure A.12.: Crowning *D4 PROD2*.

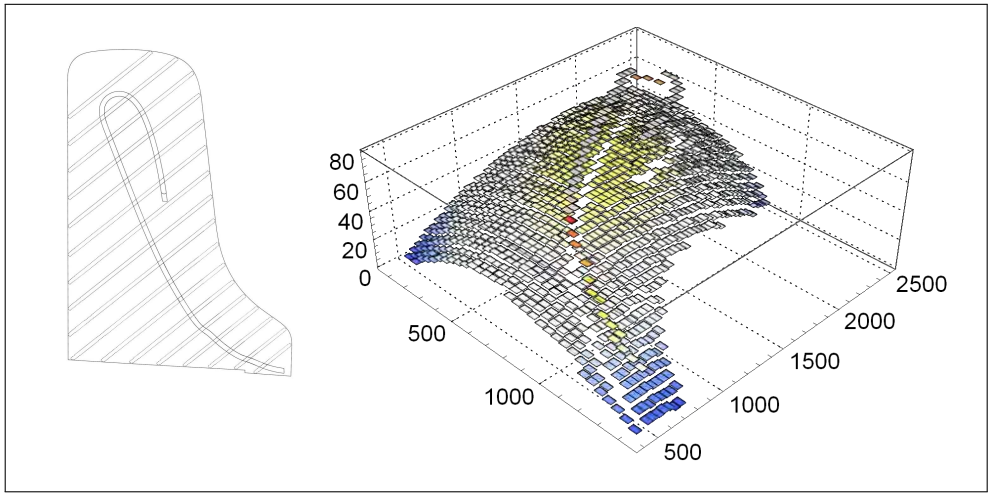

Figure A.13.: Crowning *D4 PROD3*.

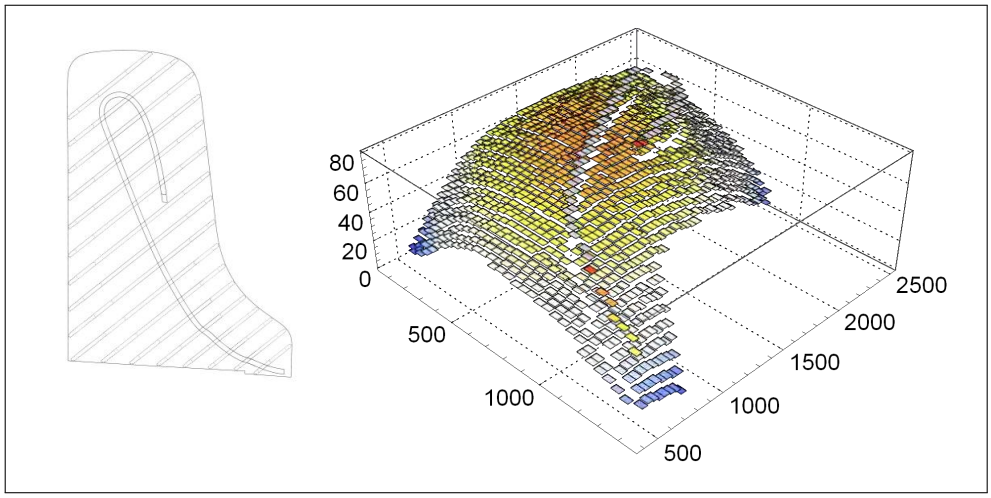

Figure A.14.: Crowning *D4 PROD4*.

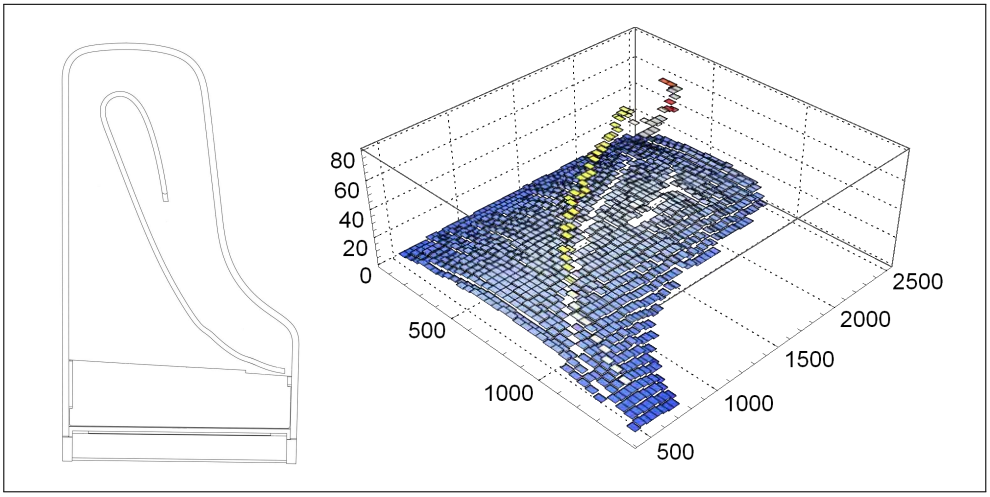

Figure A.15.: Crowning *D4 PROD5*.

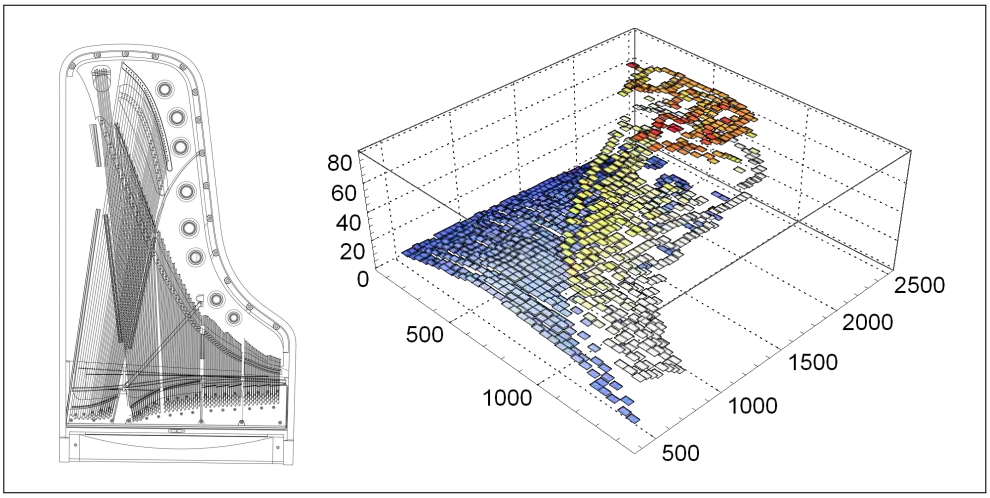

Figure A.16.: Crowning *D4 PROD6*.

A.3. Bending Wave Shapes

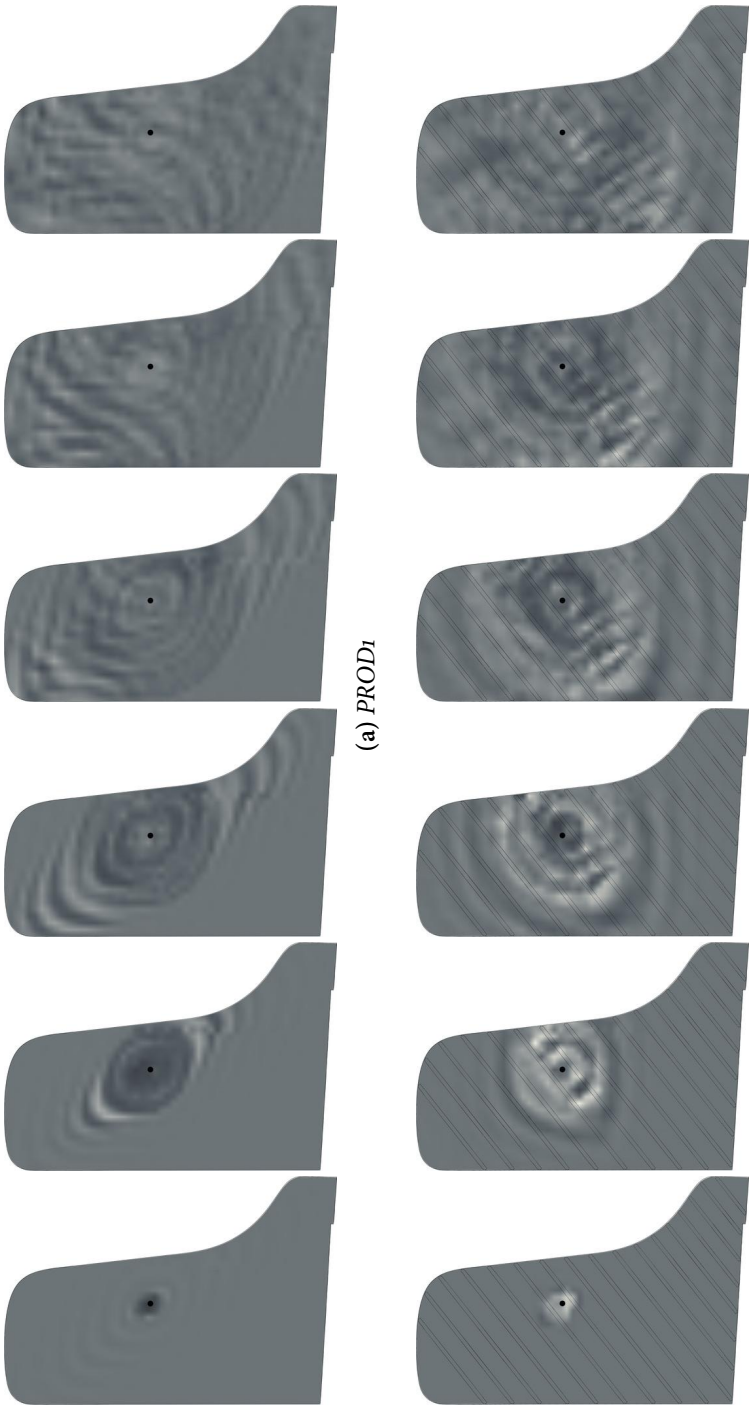

(a) *PROD1* (b) *PROD2*

Figure A.17: Bending wave distribution for *D1*, *PROD1* vs. *PROD2*, *POS04*, 0.5 ms intervals.

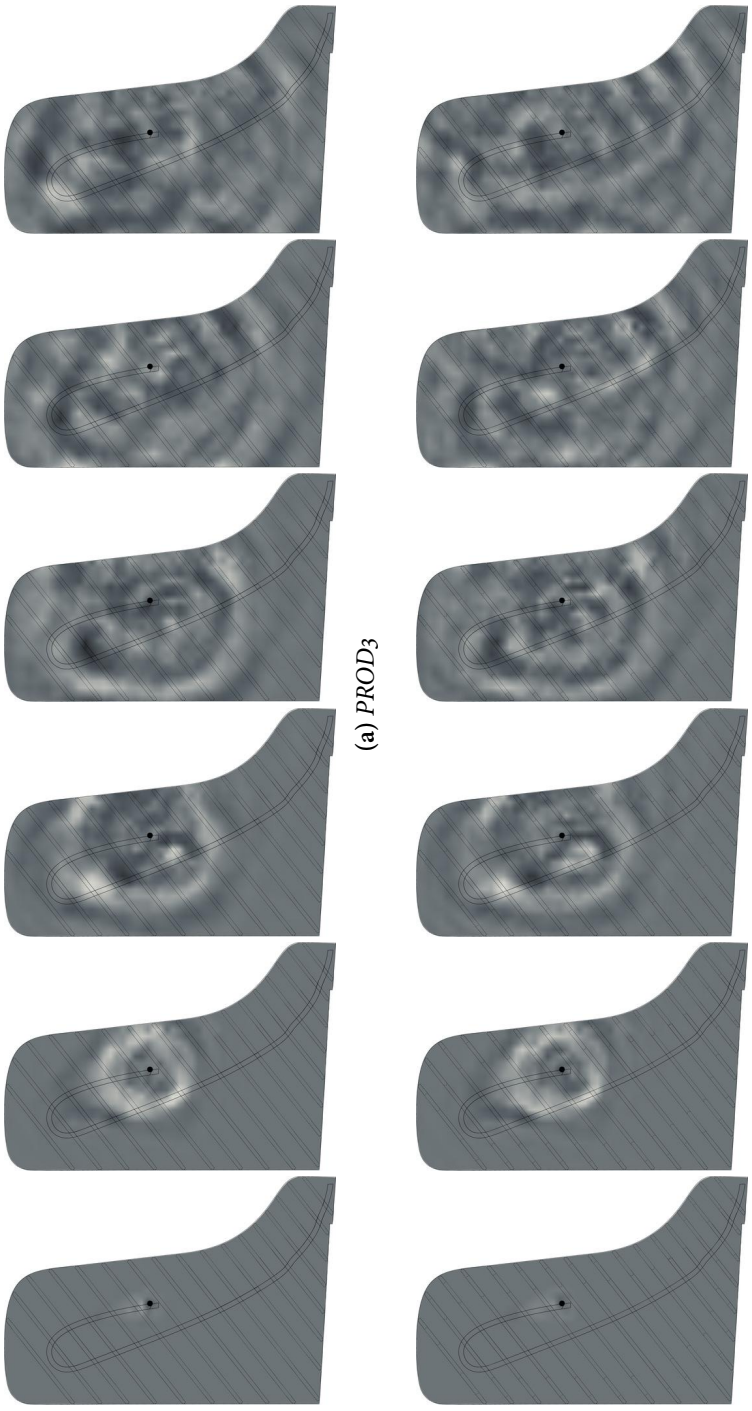

(a) *PROD3* (b) *PROD4*

Figure A.18.: Bending wave distribution for *D1*, *PROD3* vs. *PROD4*, *POS04*, 0.5 ms intervals.

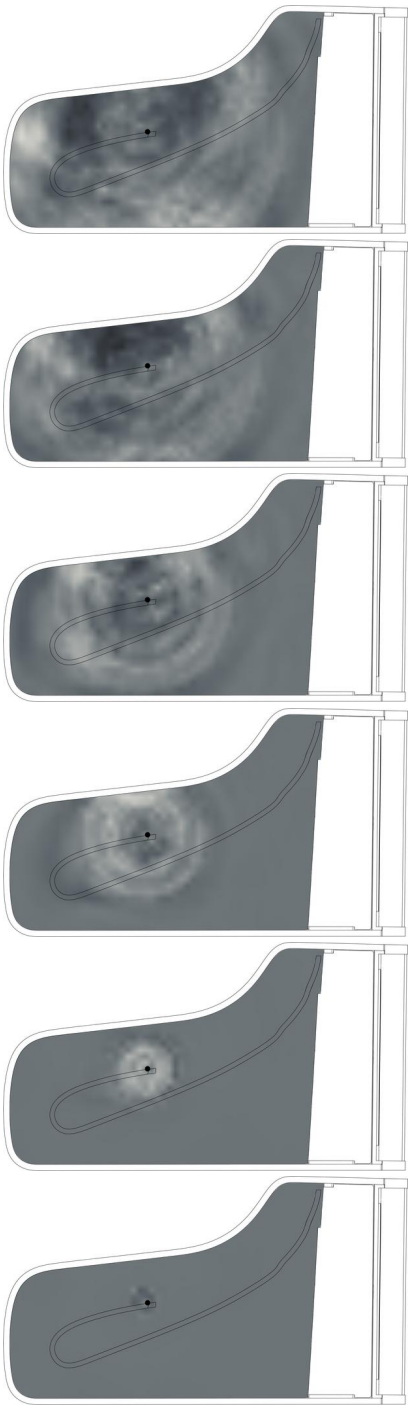

(a) *PROD5*

Figure A.19.: Bending wave distribution for *D1*, *PROD5*, *POS04*, 0.5 ms intervals.

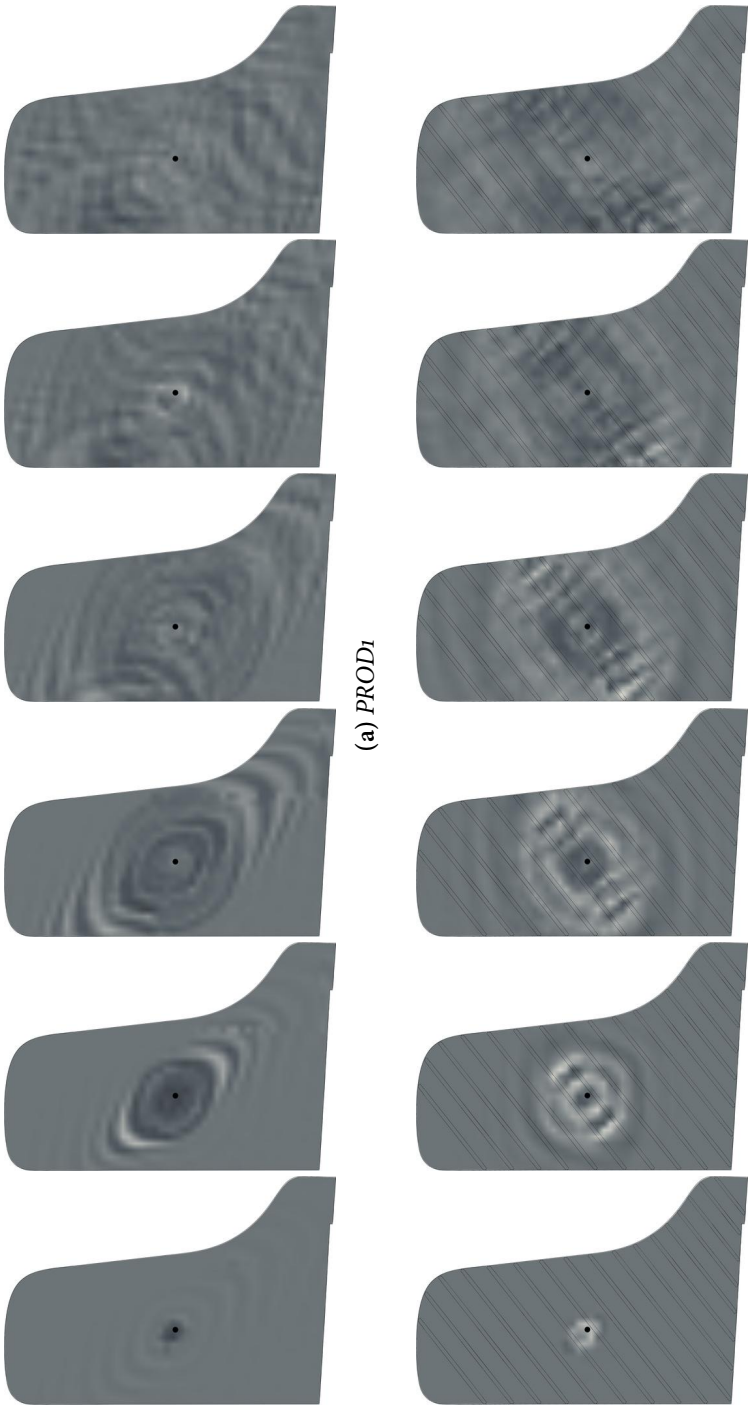

(a) *PROD1* (b) *PROD2*

Figure A.20.: Bending wave distribution for D_1, *PROD1* vs. *PROD2*, *POS08*, 0.5 ms intervals.

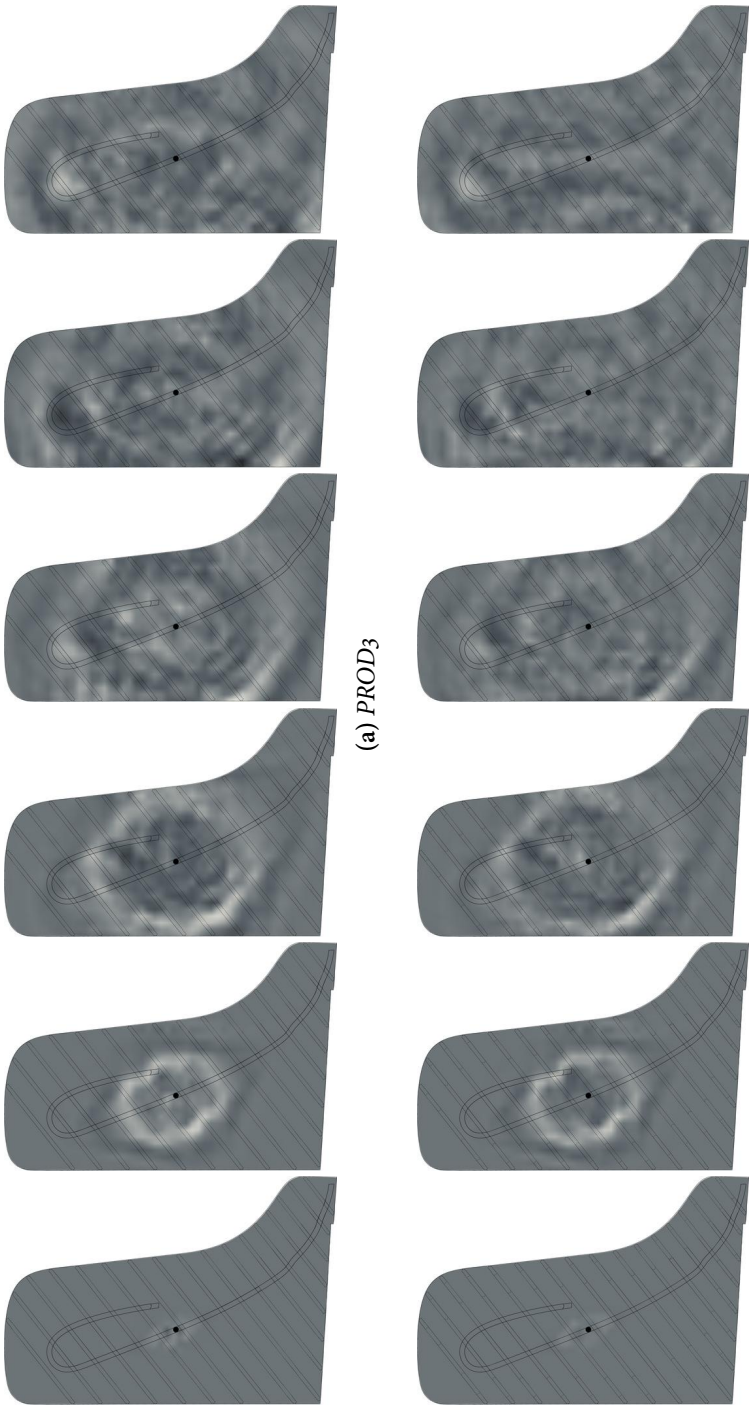

(a) *PROD3* (b) *PROD4*

Figure A.21.: Bending wave distribution for *D1*, *PROD3* vs. *PROD4*, *POS08*, 0.5 ms intervals.

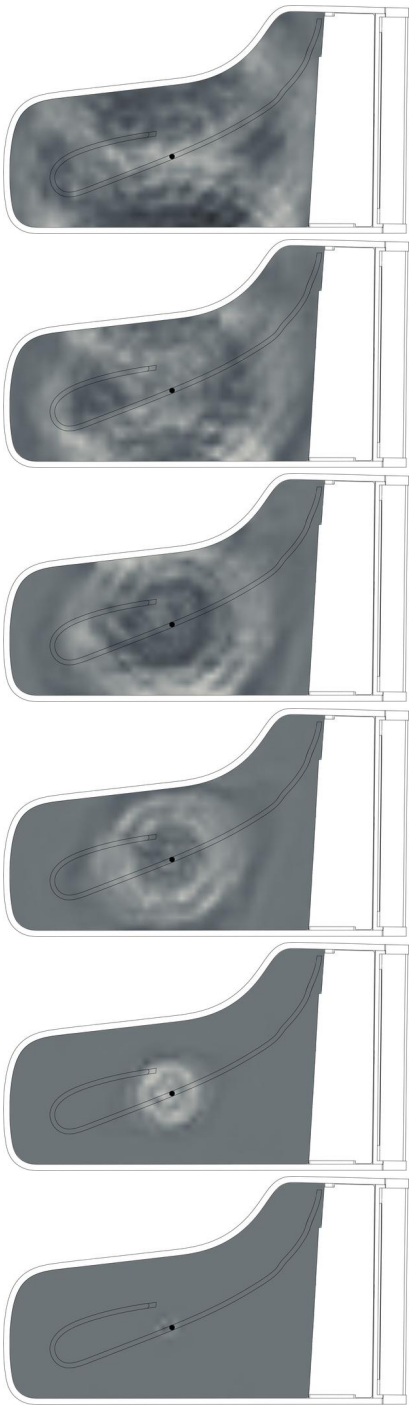

(a) $PROD_5$

Figure A.22.: Bending wave distribution for D_1, $PROD_5$, POS_{08}, 0.5 ms intervals.

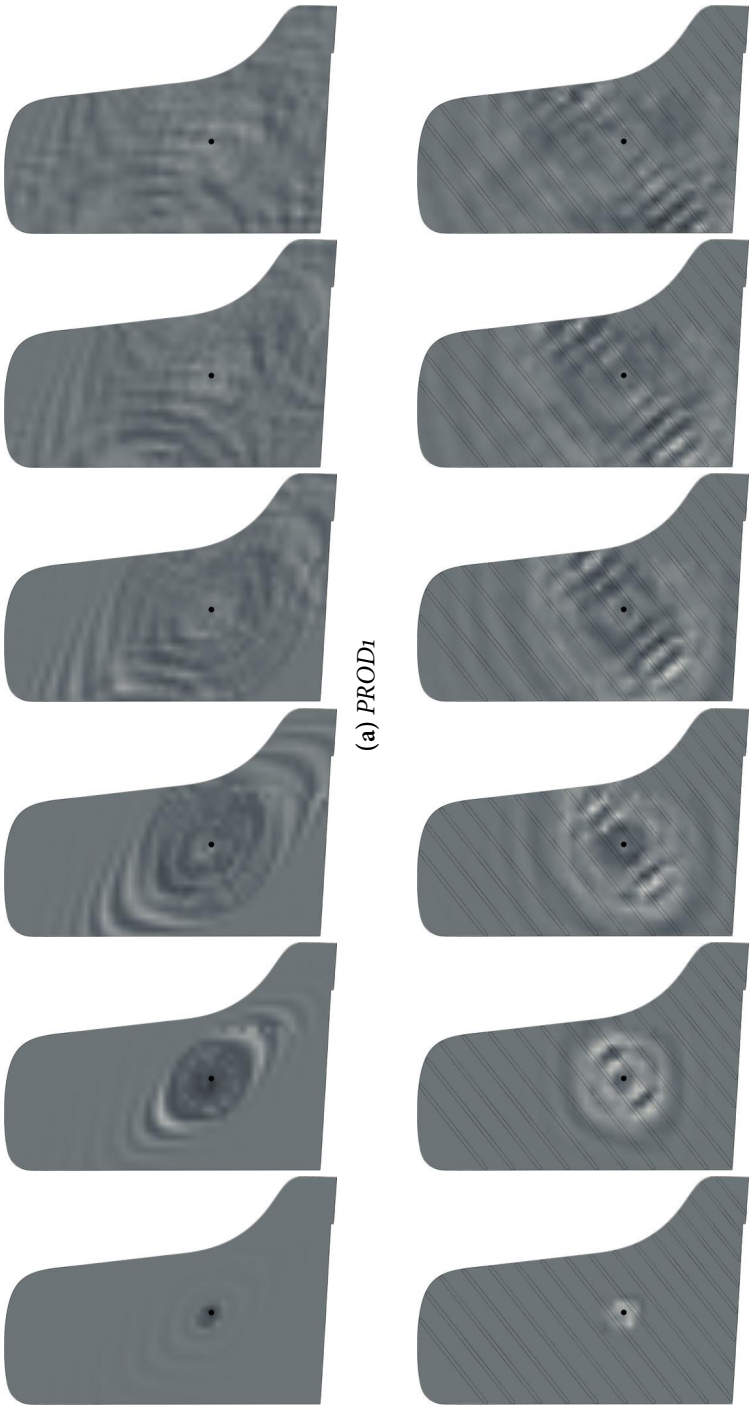

(a) *PROD1* (b) *PROD2*

Figure A.23.: Bending wave distribution for *D1*, *PROD1* vs. *PROD2*, *POS09*, 0.5 ms intervals.

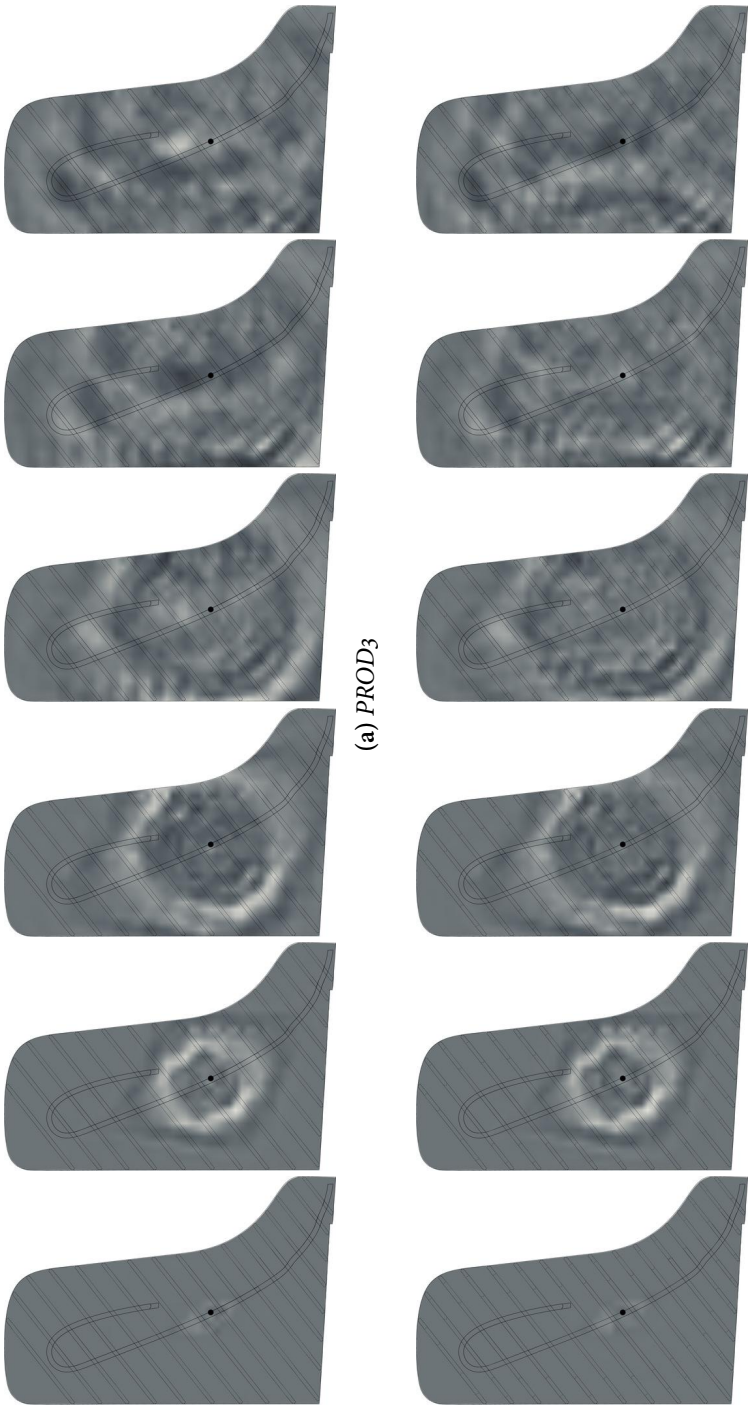

(a) *PROD3* (b) *PROD4*

Figure A.24: Bending wave distribution for *D1*, *PROD3* vs. *PROD4*, *POS09*, 0.5 ms intervals.

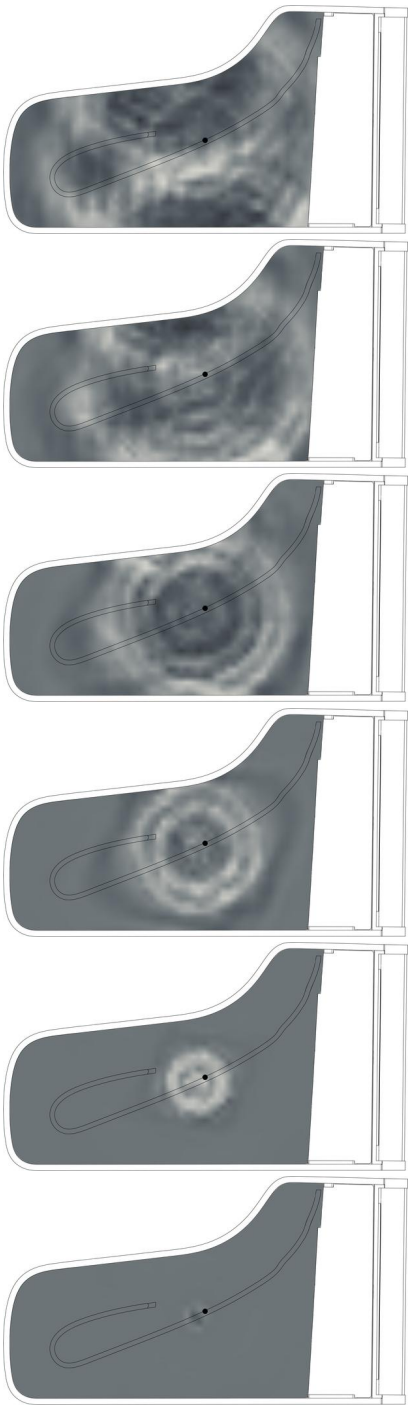

(a) *PROD5*

Figure A.25.: Bending wave distribution for *D1*, *PROD5*, *POS09*, 0.5 ms intervals.

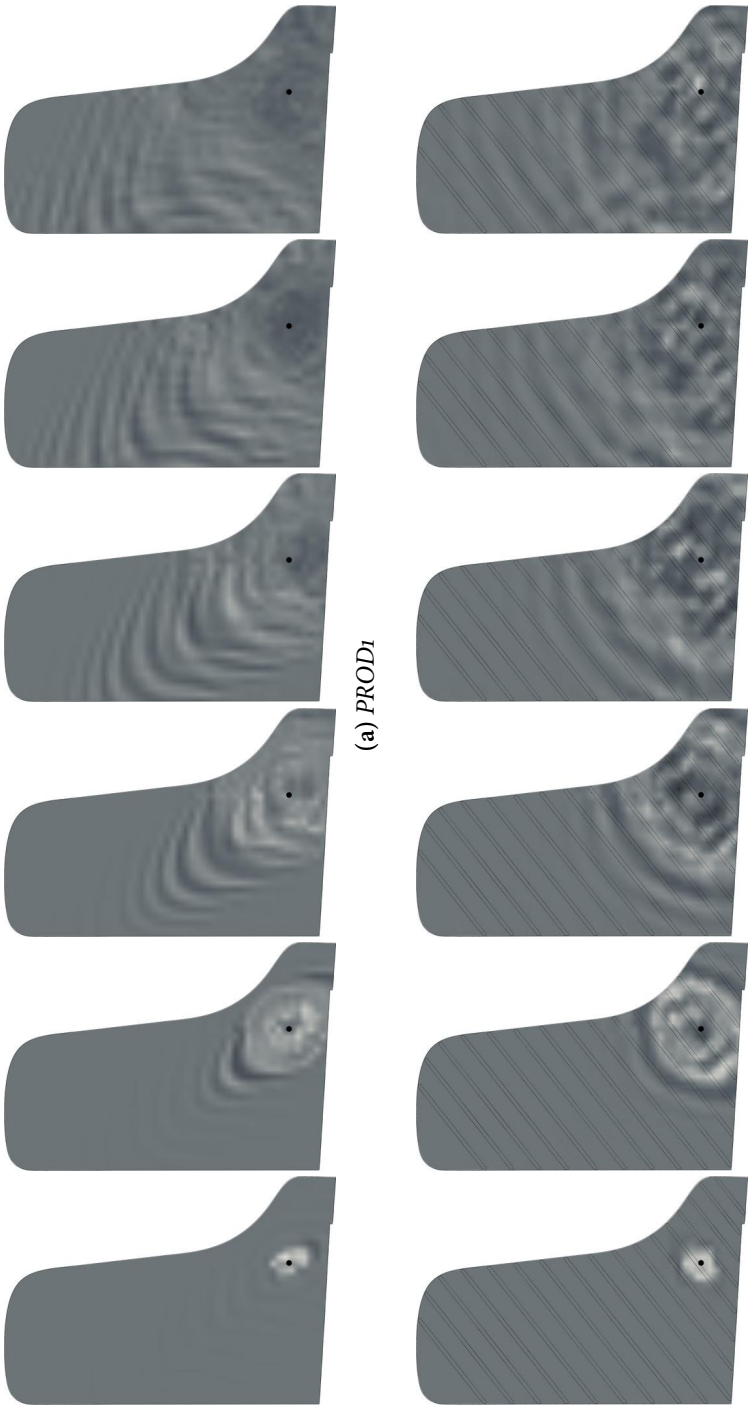

(a) *PROD1* (b) *PROD2*

Figure A.26.: Bending wave distribution for *D1*, *PROD1* vs. *PROD2*, *POS12*, 0.5 ms intervals.

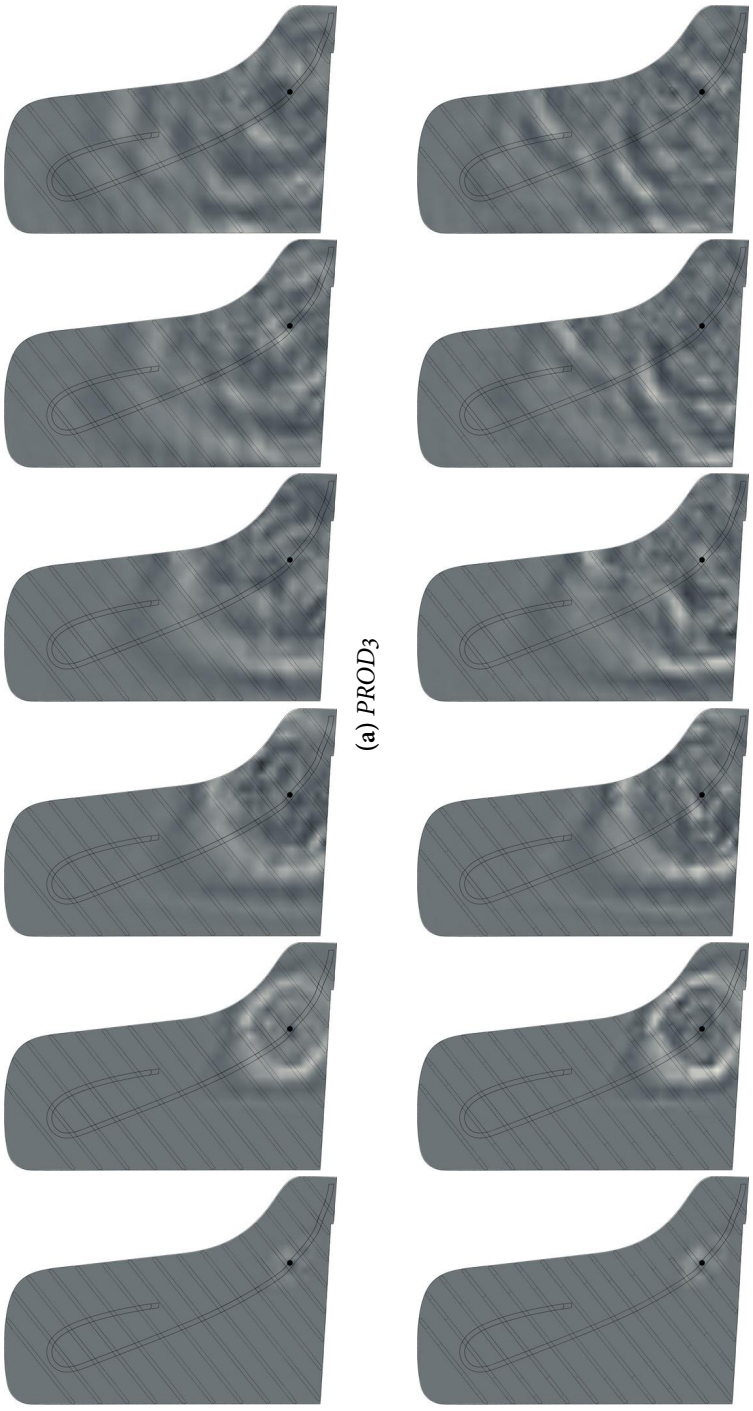

(a) *PROD3* (b) *PROD4*

Figure A.27: Bending wave distribution for *D1*, *PROD3* vs. *PROD4*, *POS12*, 0.5 ms intervals.

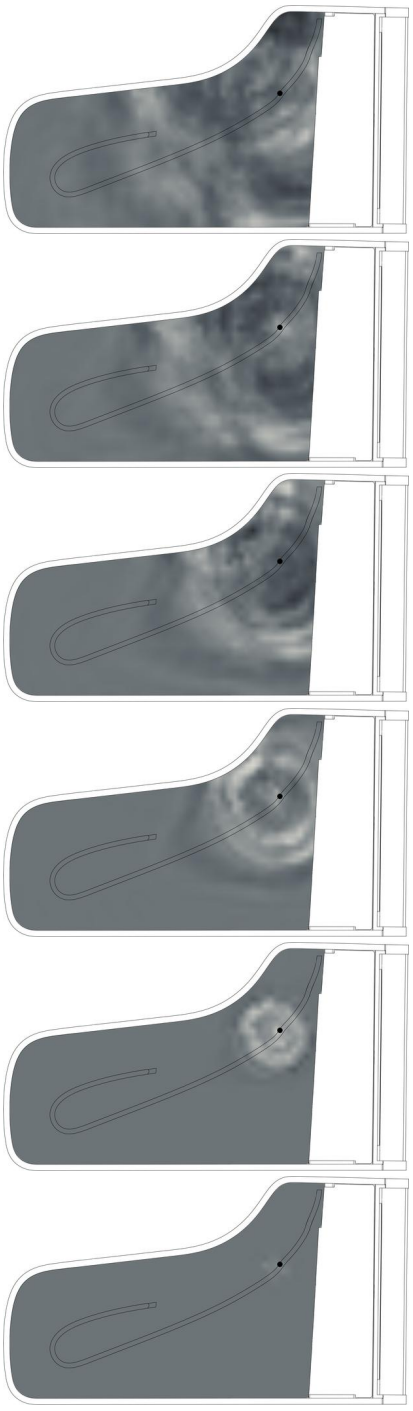

(a) $PROD_5$

Figure A.28.: Bending wave distribution for D_1, $PROD_5$, POS_{12}, 0.5 ms intervals.

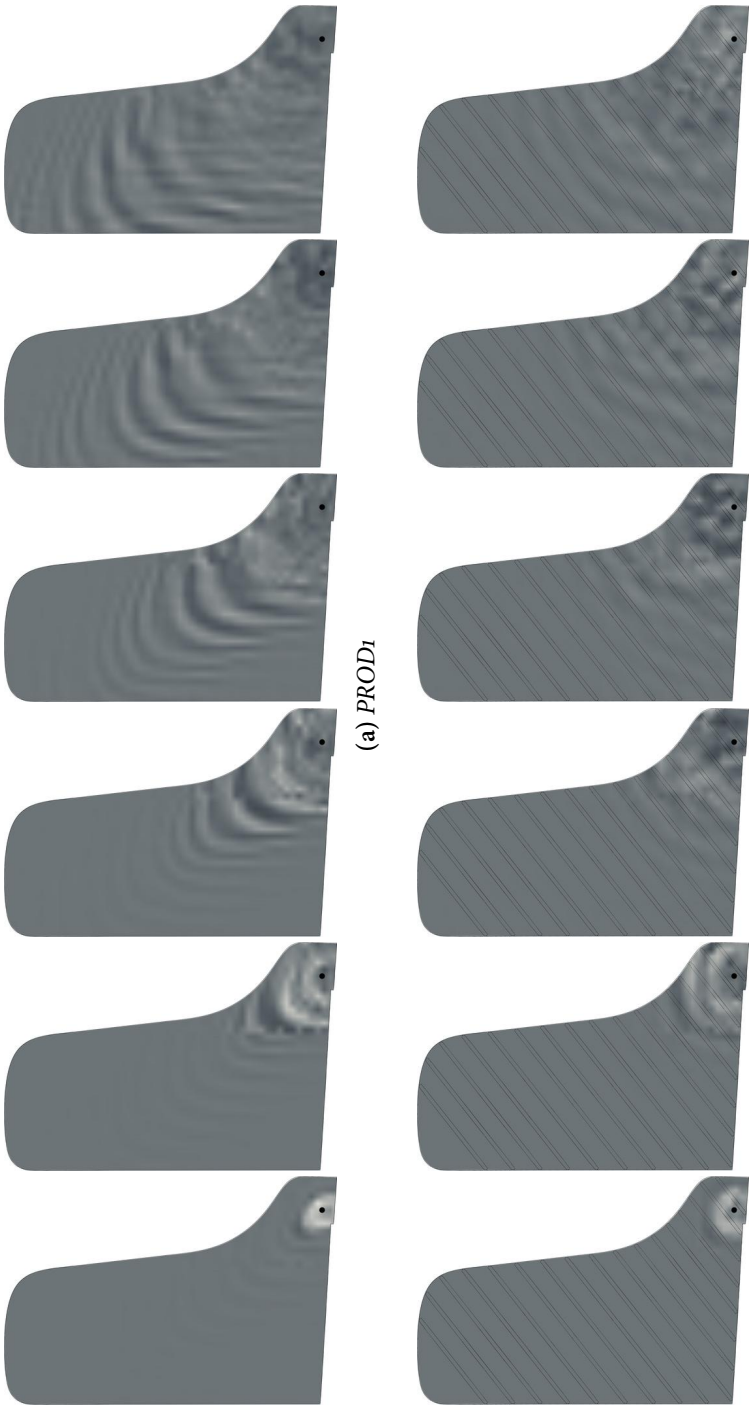

(a) *PROD1* (b) *PROD2*

Figure A.29.: Bending wave distribution for *D1*, *PROD1* vs. *PROD2*, *POS14*, 0.5 ms intervals.

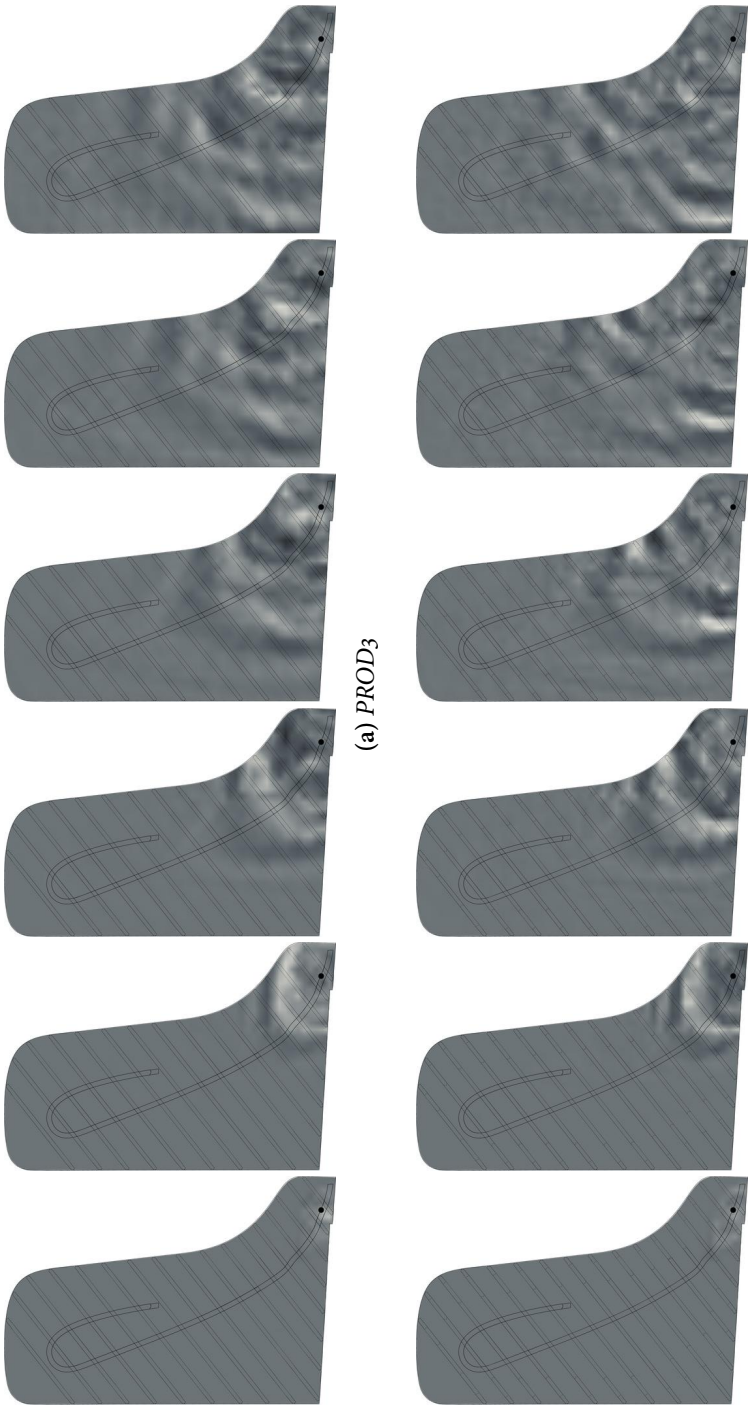

(a) *PROD3* (b) *PROD4*

Figure A.30.: Bending wave distribution for *D1*, *PROD3* vs. *PROD4*, *POS14*, 0.5 ms intervals.

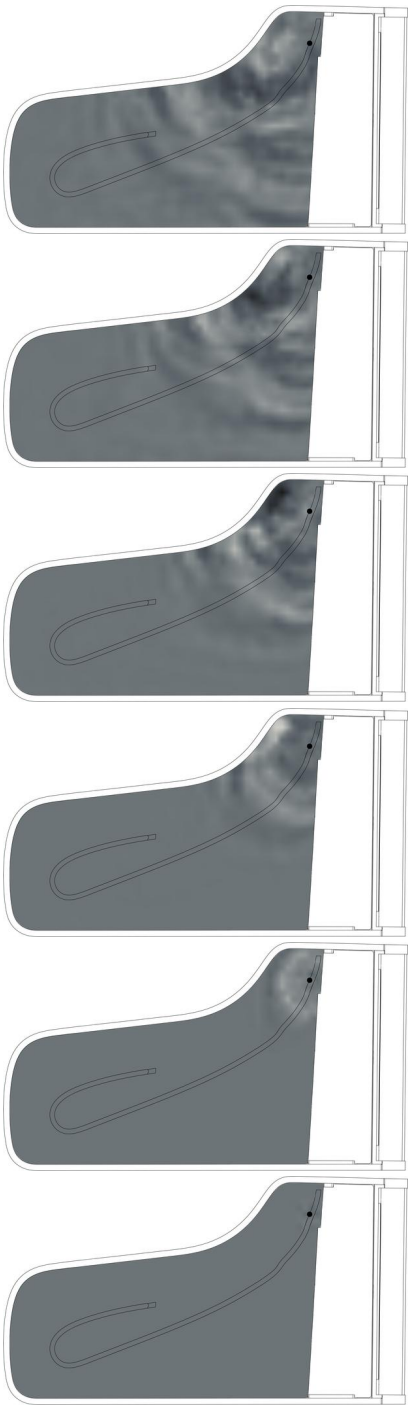

(a) *PROD5*

Figure A.31.: Bending wave distribution for *D1*, *PROD5*, *POS14*, 0.5 ms intervals.

A.4. Bending Wave Velocity Ratios

(a) *POS1* (b) *POS2* (c) *POS3* (d) *POS4* (e) *POS5*

(f) *POS6* (g) *POS7* (h) *POS8* (i) *POS9* (j) *POS10*

(k) *POS11* (l) *POS12* (m) *POS13* (n) *POS14* (o) *POS15*

Figure A.32.: Angle dependent bending wave velocity ratio for *D1 PROD1*.

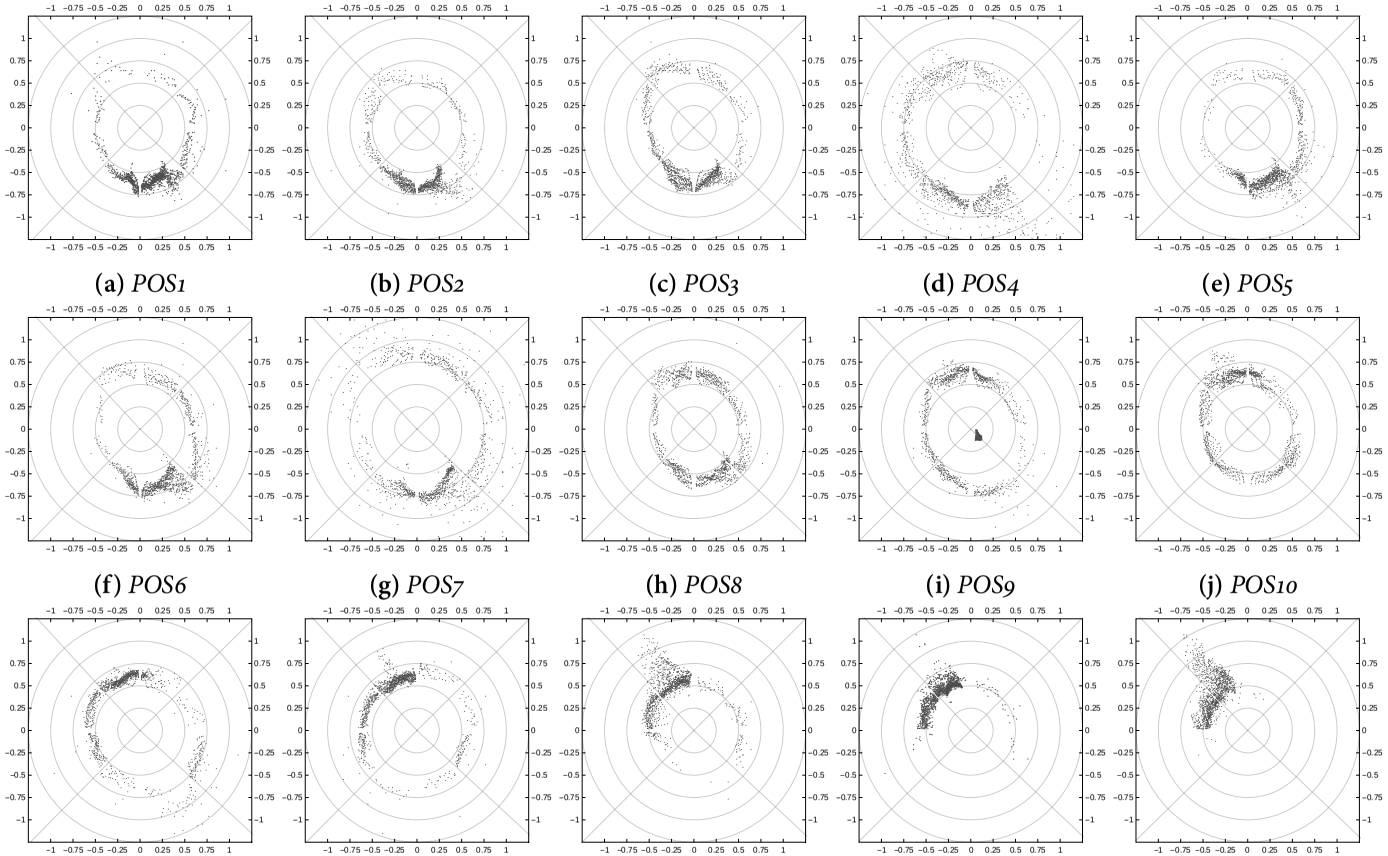

(a) *POS1* (b) *POS2* (c) *POS3* (d) *POS4* (e) *POS5*

(f) *POS6* (g) *POS7* (h) *POS8* (i) *POS9* (j) *POS10*

(k) *POS11* (l) *POS12* (m) *POS13* (n) *POS14* (o) *POS15*

Figure A.33.: Angle dependent bending wave velocity ratio for *D1 PROD2*.

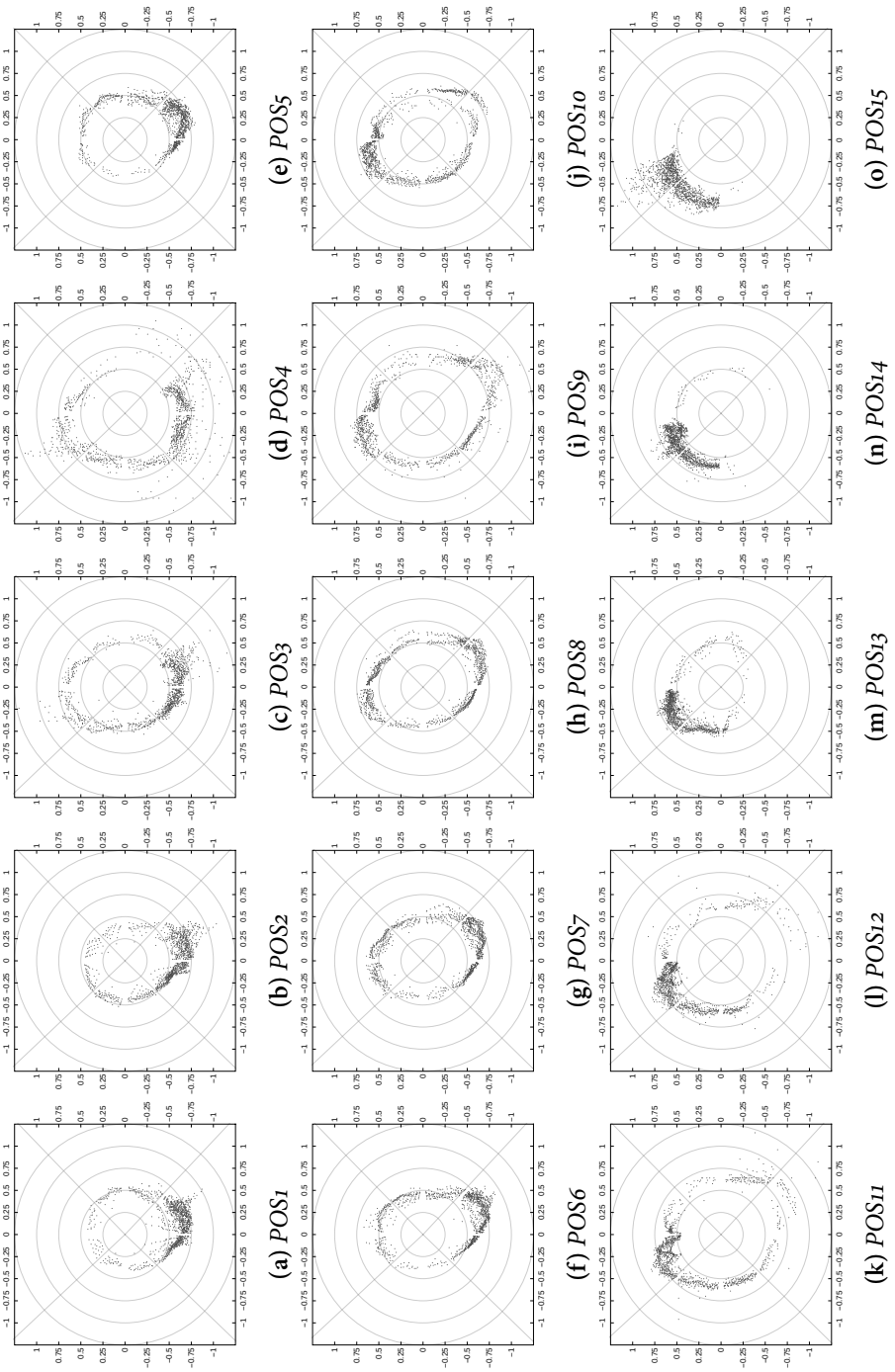

Figure A.34: Angle dependent bending wave velocity ratio for *D1 PROD3*.

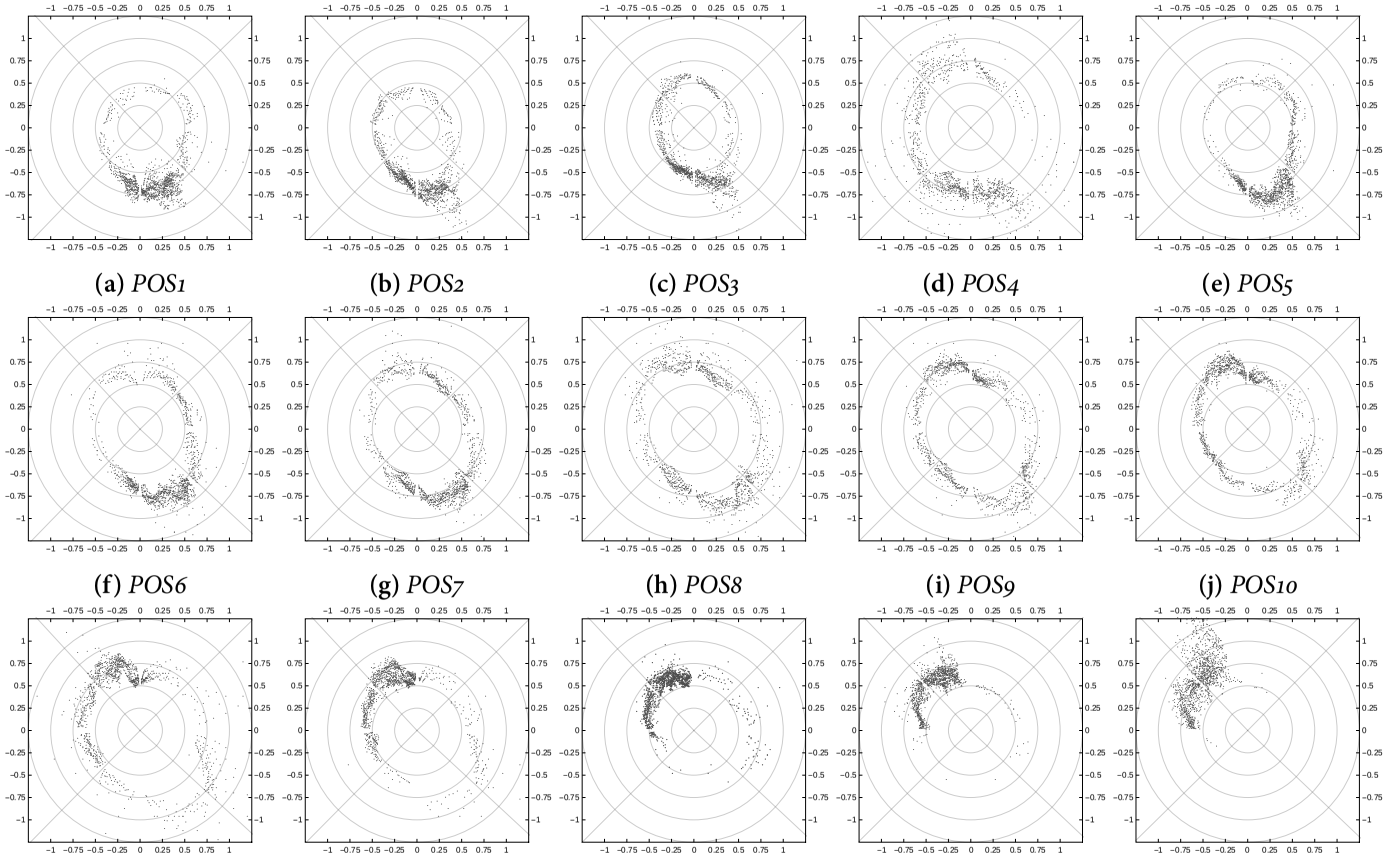

(a) *POS1* (b) *POS2* (c) *POS3* (d) *POS4* (e) *POS5*

(f) *POS6* (g) *POS7* (h) *POS8* (i) *POS9* (j) *POS10*

(k) *POS11* (l) *POS12* (m) *POS13* (n) *POS14* (o) *POS15*

Figure A.35.: Angle dependent bending wave velocity ratio for *D1 PROD4*.

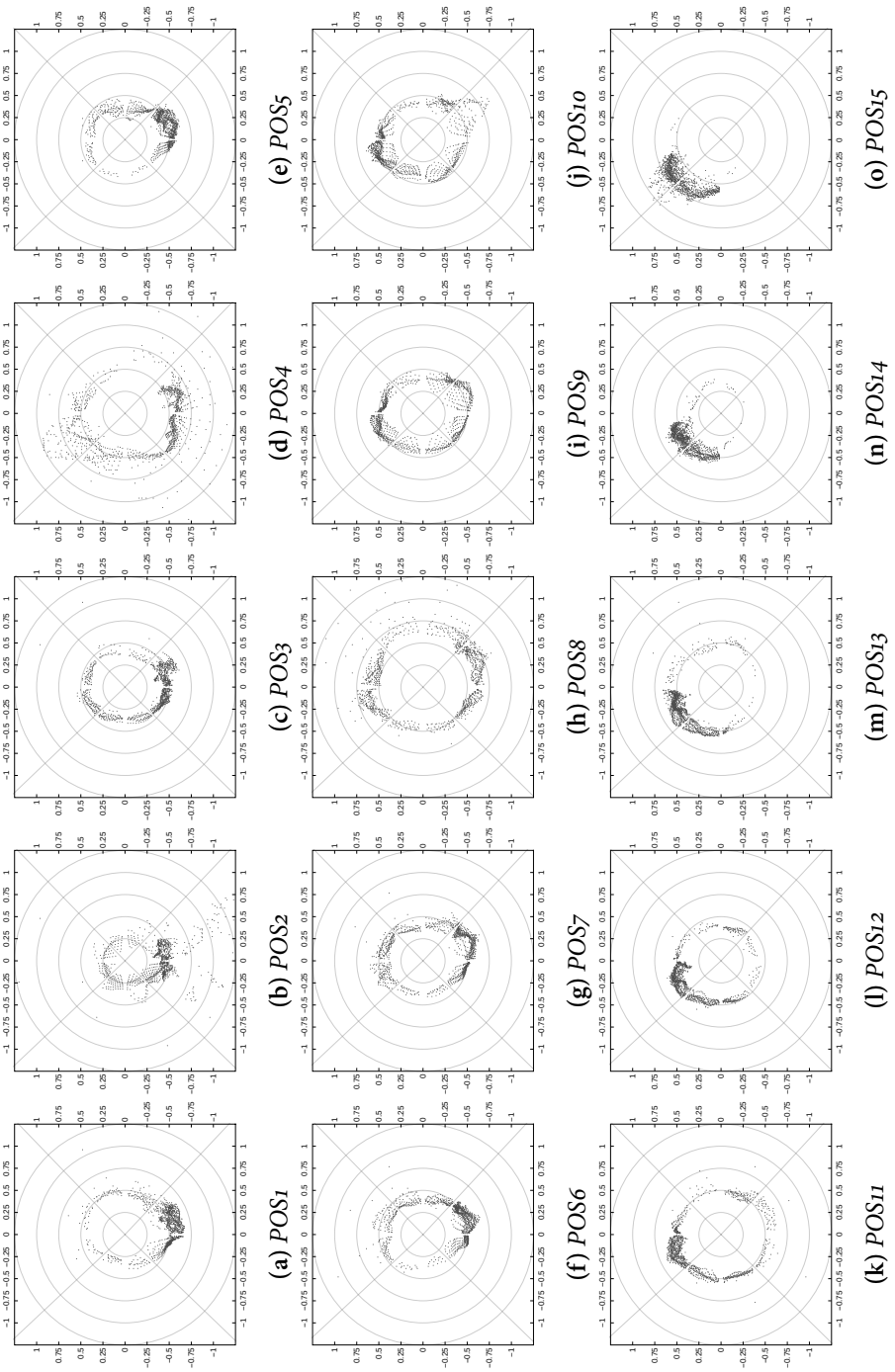

Figure A.36.: Angle dependent bending wave velocity ratio for *D1 PROD5*.

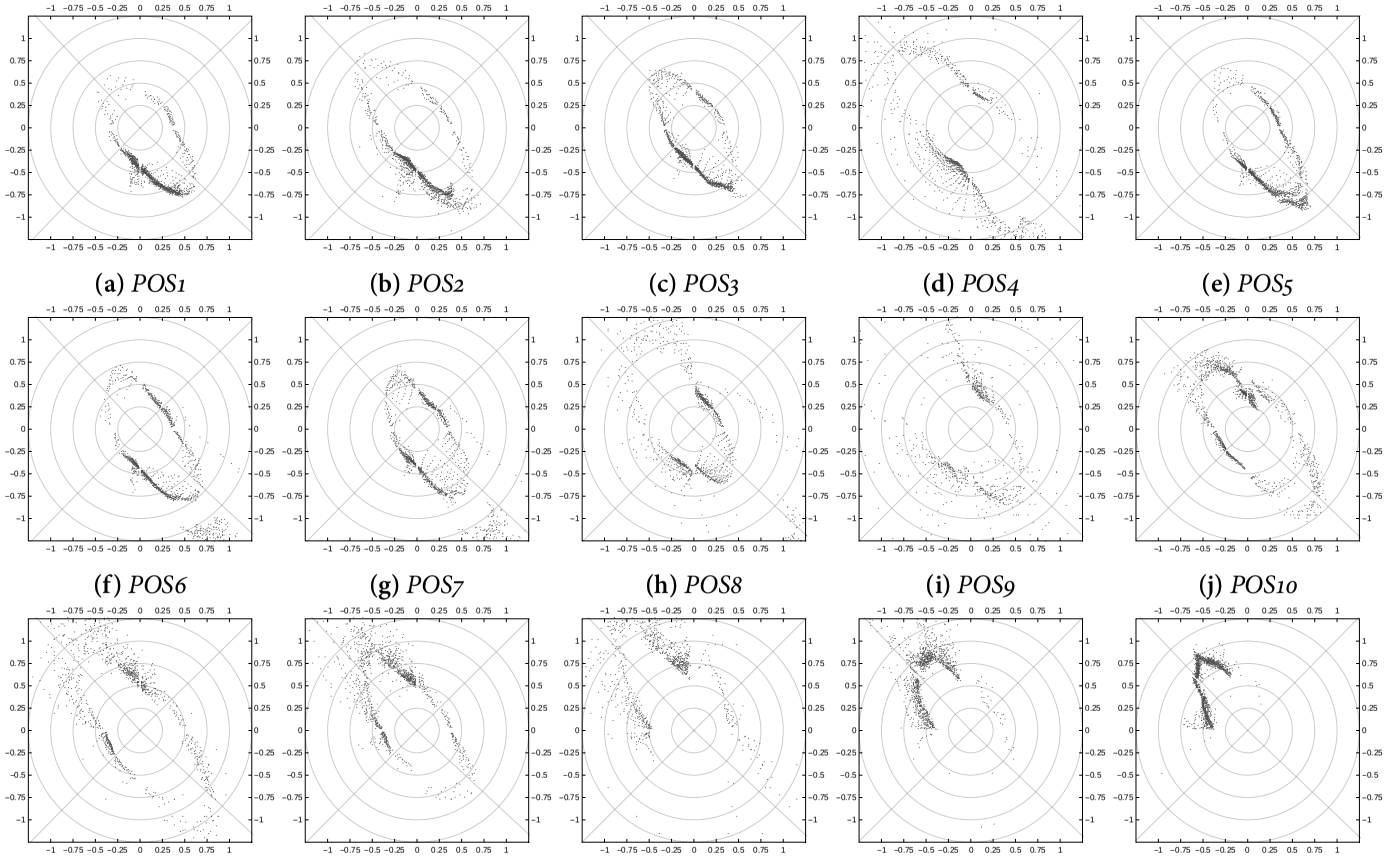

(a) *POS1* (b) *POS2* (c) *POS3* (d) *POS4* (e) *POS5*

(f) *POS6* (g) *POS7* (h) *POS8* (i) *POS9* (j) *POS10*

(k) *POS11* (l) *POS12* (m) *POS13* (n) *POS14* (o) *POS15*

Figure A.37.: Angle dependent bending wave velocity ratio for *D4 PROD1*.

Figure A.38.: Angle dependent bending wave velocity ratio for *D4 PROD2*.

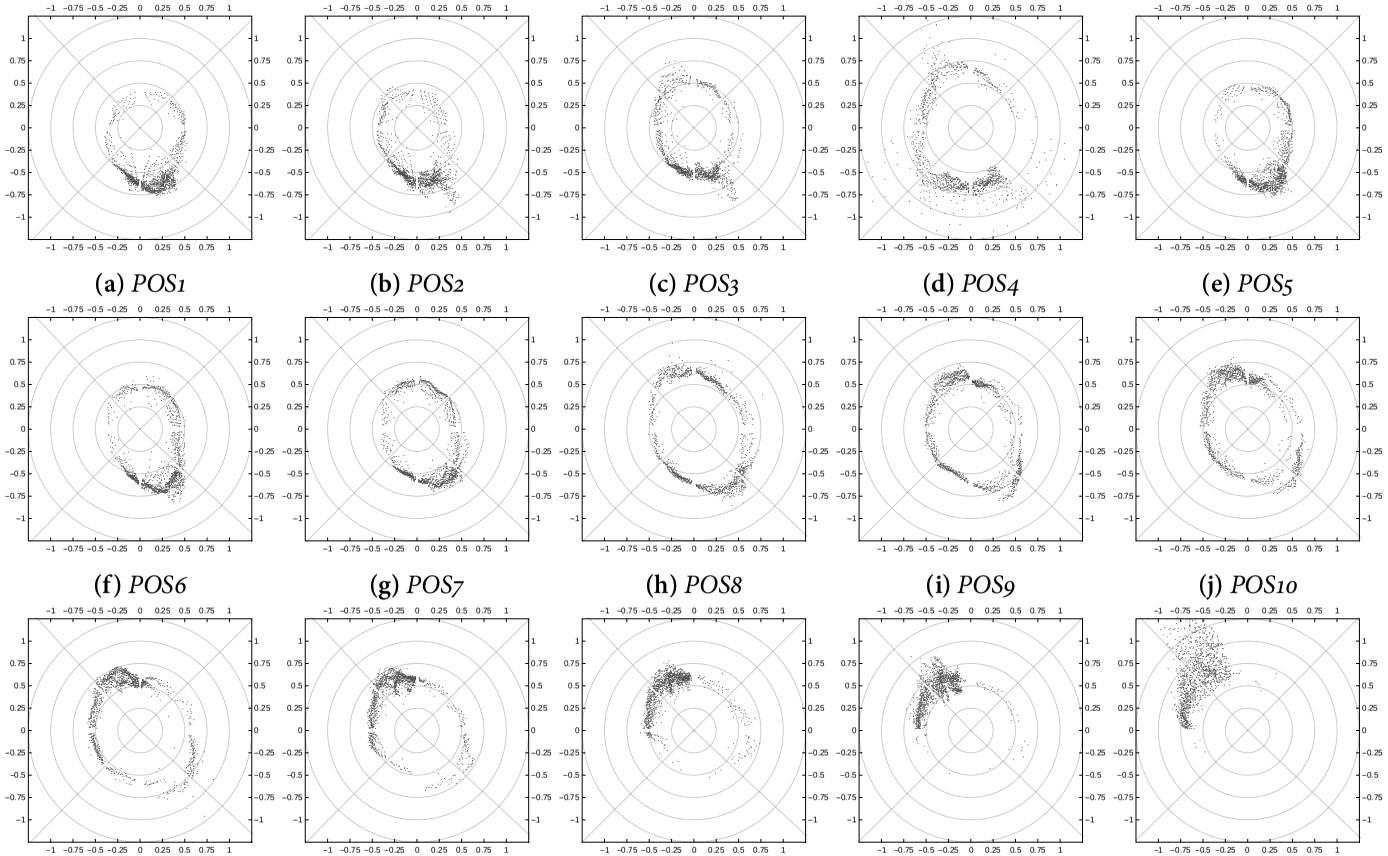

(a) *POS1* (b) *POS2* (c) *POS3* (d) *POS4* (e) *POS5*

(f) *POS6* (g) *POS7* (h) *POS8* (i) *POS9* (j) *POS10*

(k) *POS11* (l) *POS12* (m) *POS13* (n) *POS14* (o) *POS15*

Figure A.39.: Angle dependent bending wave velocity ratio for *D4 PROD3*.

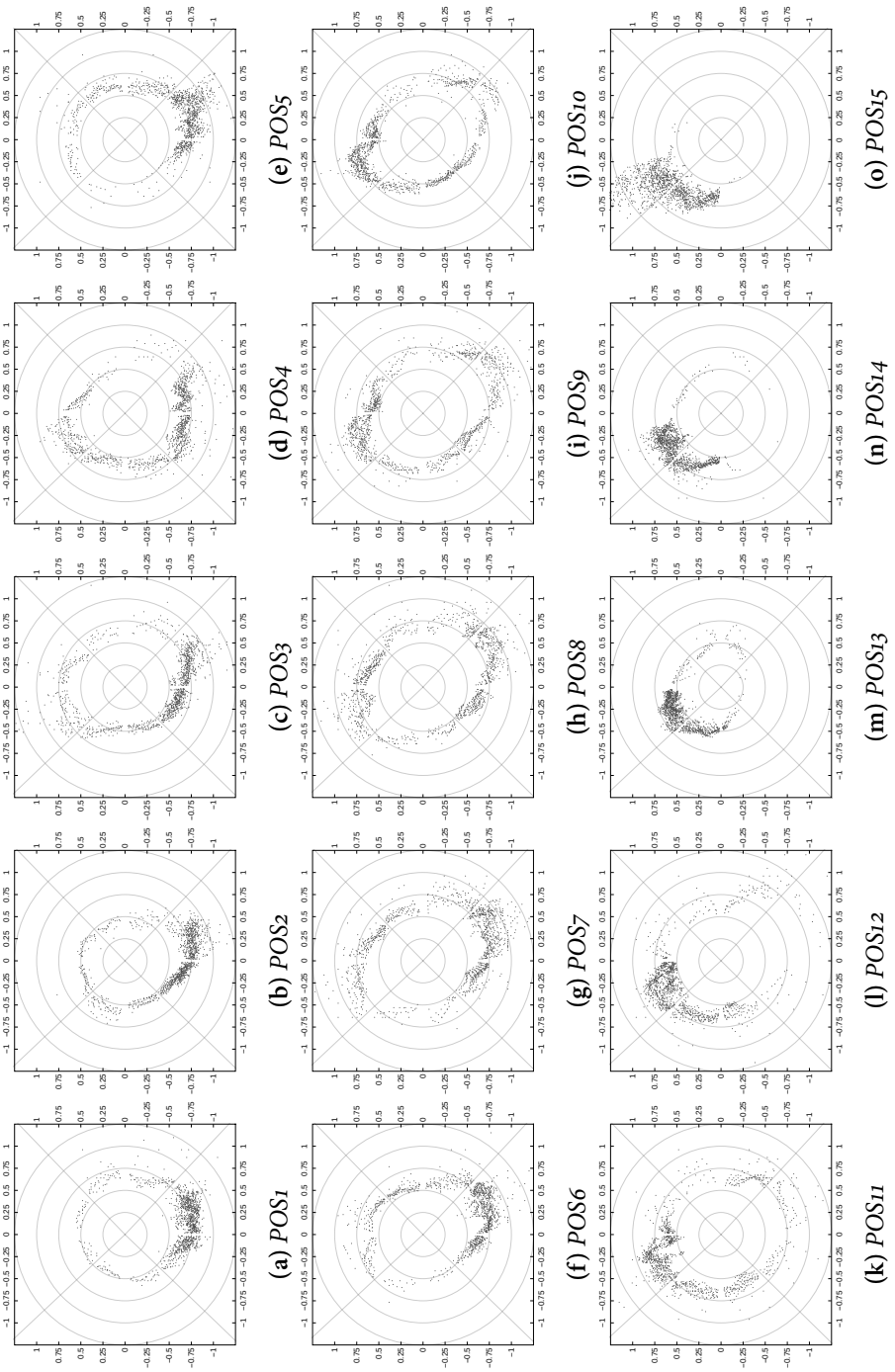

Figure A.40.: Angle dependent bending wave velocity ratio for *D4 PROD4*.

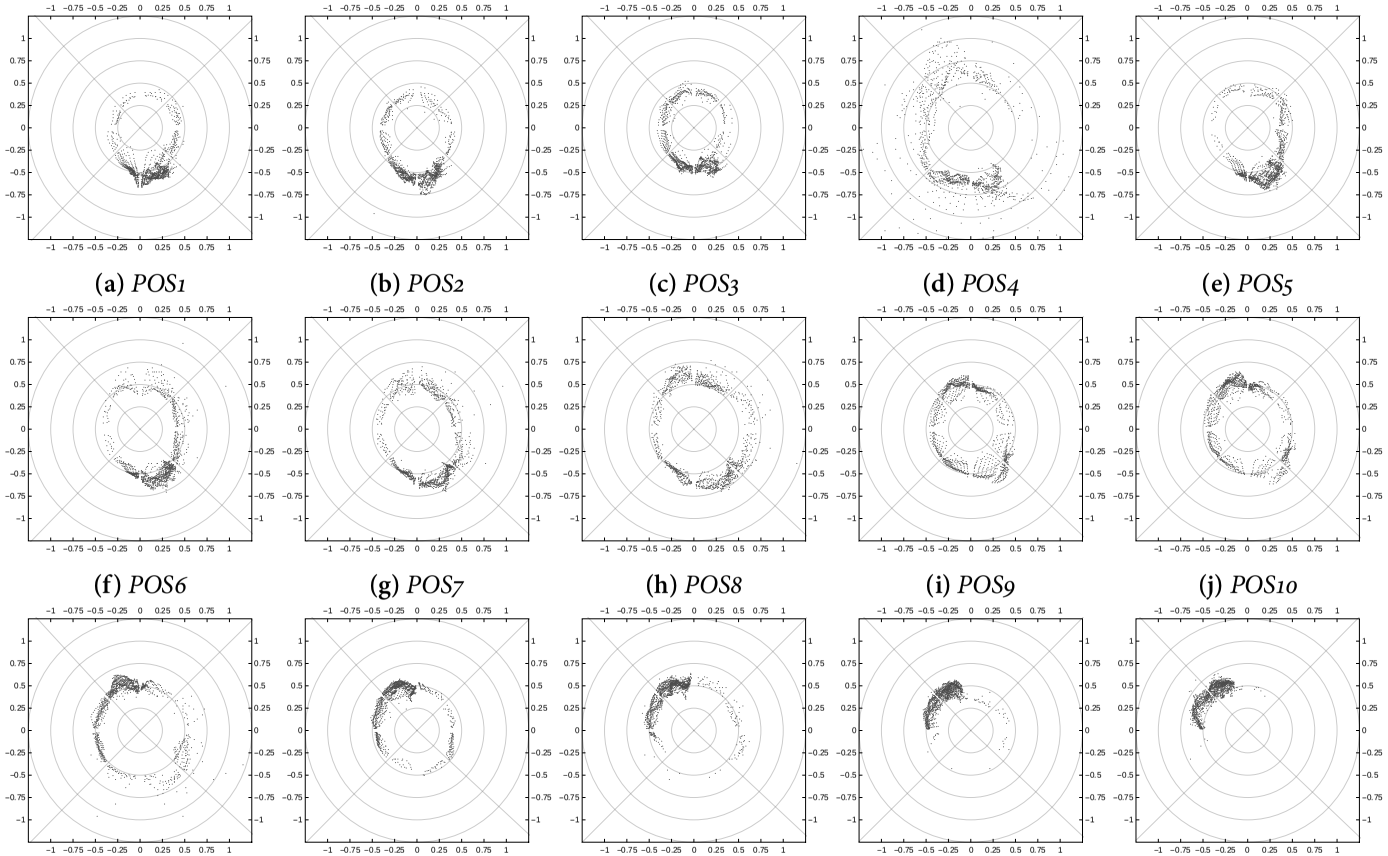

(a) *POS1* (b) *POS2* (c) *POS3* (d) *POS4* (e) *POS5*

(f) *POS6* (g) *POS7* (h) *POS8* (i) *POS9* (j) *POS10*

(k) *POS11* (l) *POS12* (m) *POS13* (n) *POS14* (o) *POS15*

Figure A.41.: Angle dependent bending wave velocity ratio for *D4 PROD5*.

A.5. Exponential Fitting for Attenuation per Frequency

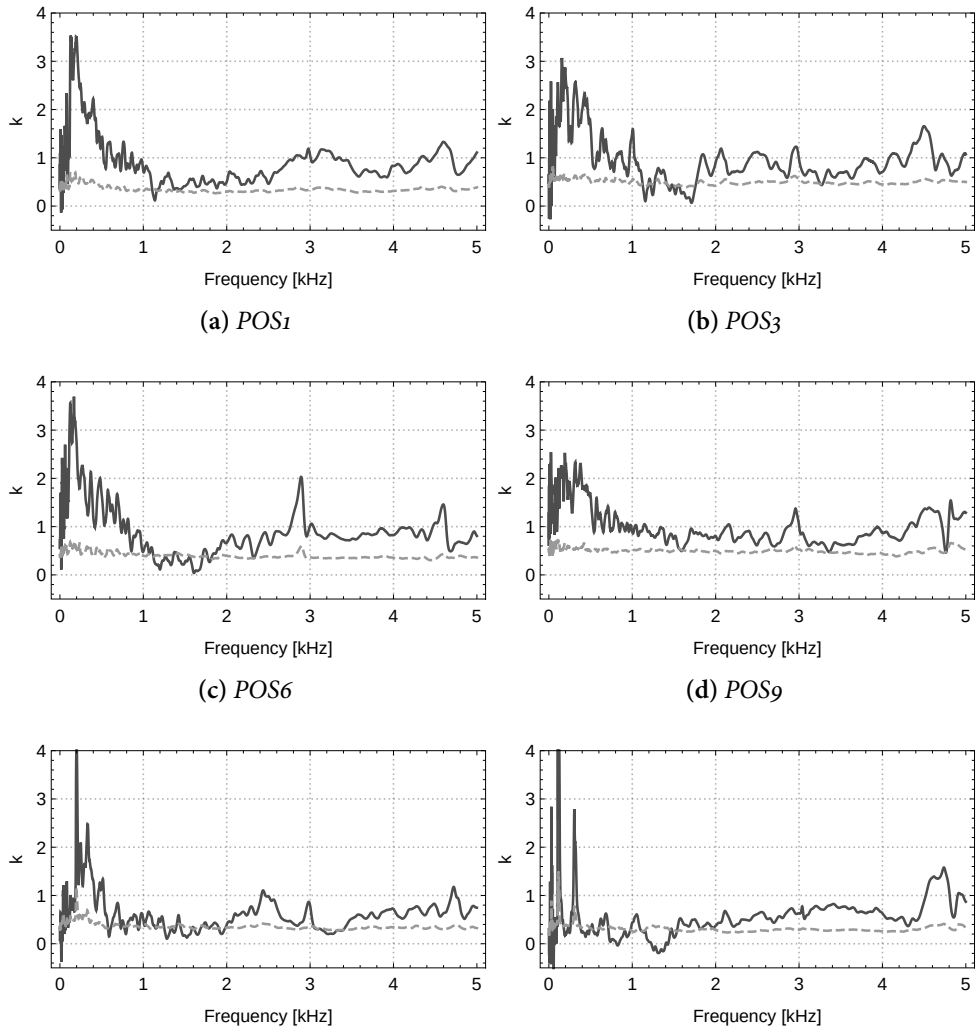

(a) *POS1* (b) *POS3*

(c) *POS6* (d) *POS9*

(e) *POS12* (f) *POS15*

Figure A.42.: Exponential fitting per frequency for *D1 PROD1*. Dashed lines depict the fitting error.

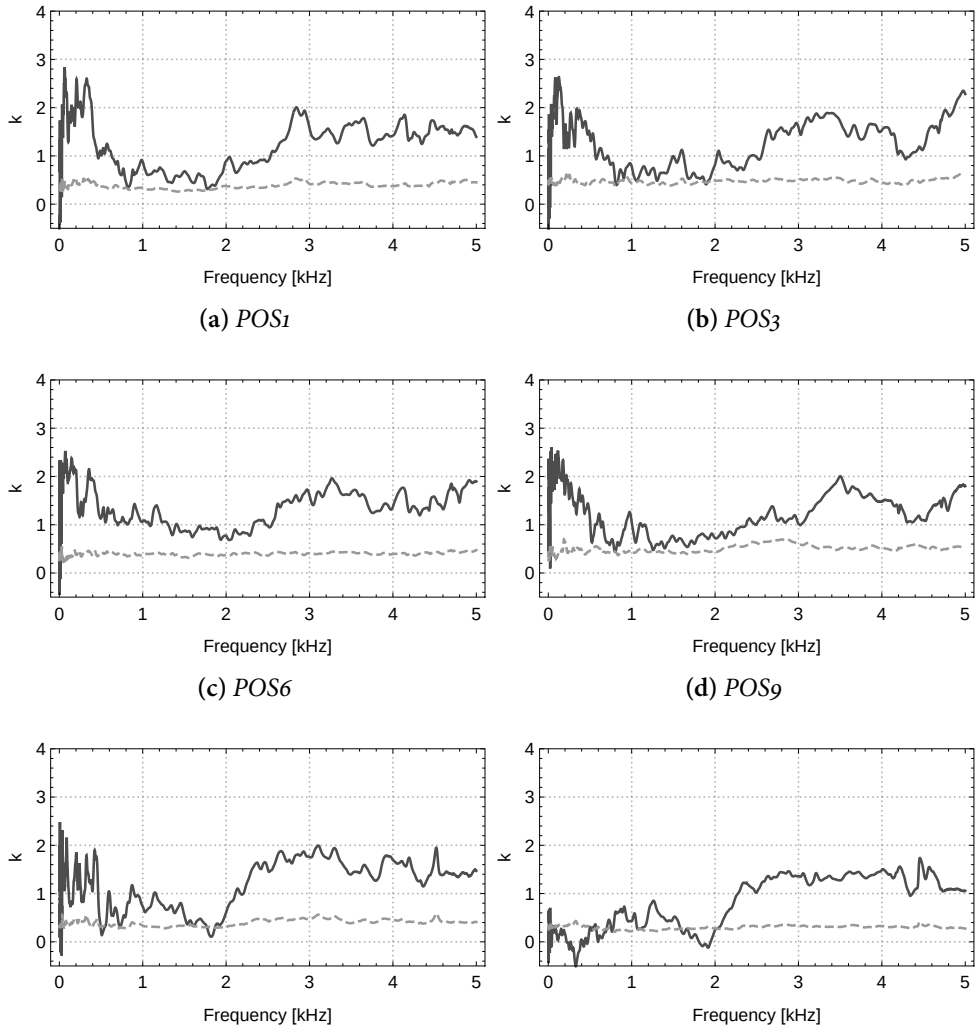

(a) *POS1*

(b) *POS3*

(c) *POS6*

(d) *POS9*

(e) *POS12*

(f) *POS15*

Figure A.43.: Exponential fitting per frequency for *D1 PROD2*. Dashed lines depict the fitting error.

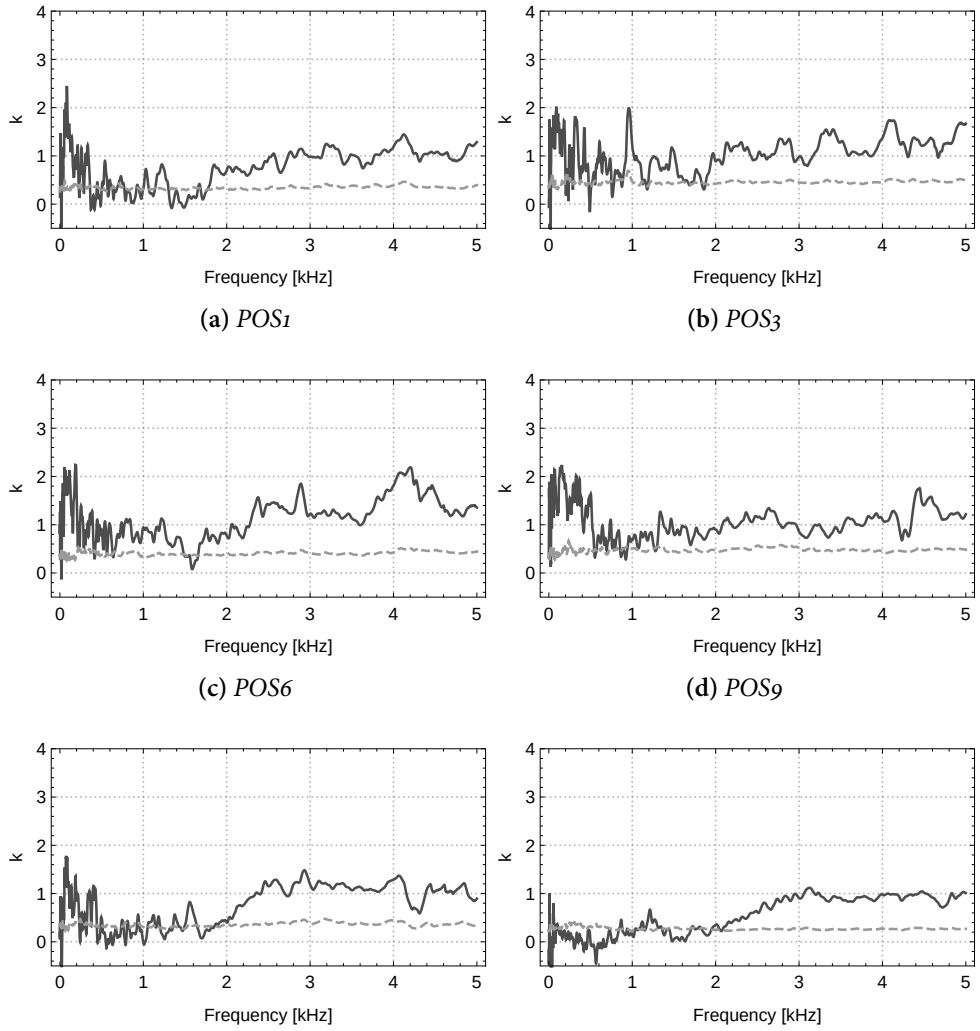

(a) *POS1* (b) *POS3*

(c) *POS6* (d) *POS9*

(e) *POS12* (f) *POS15*

Figure A.44.: Exponential fitting per frequency for *D1 PROD3*. Dashed lines depict the fitting error.

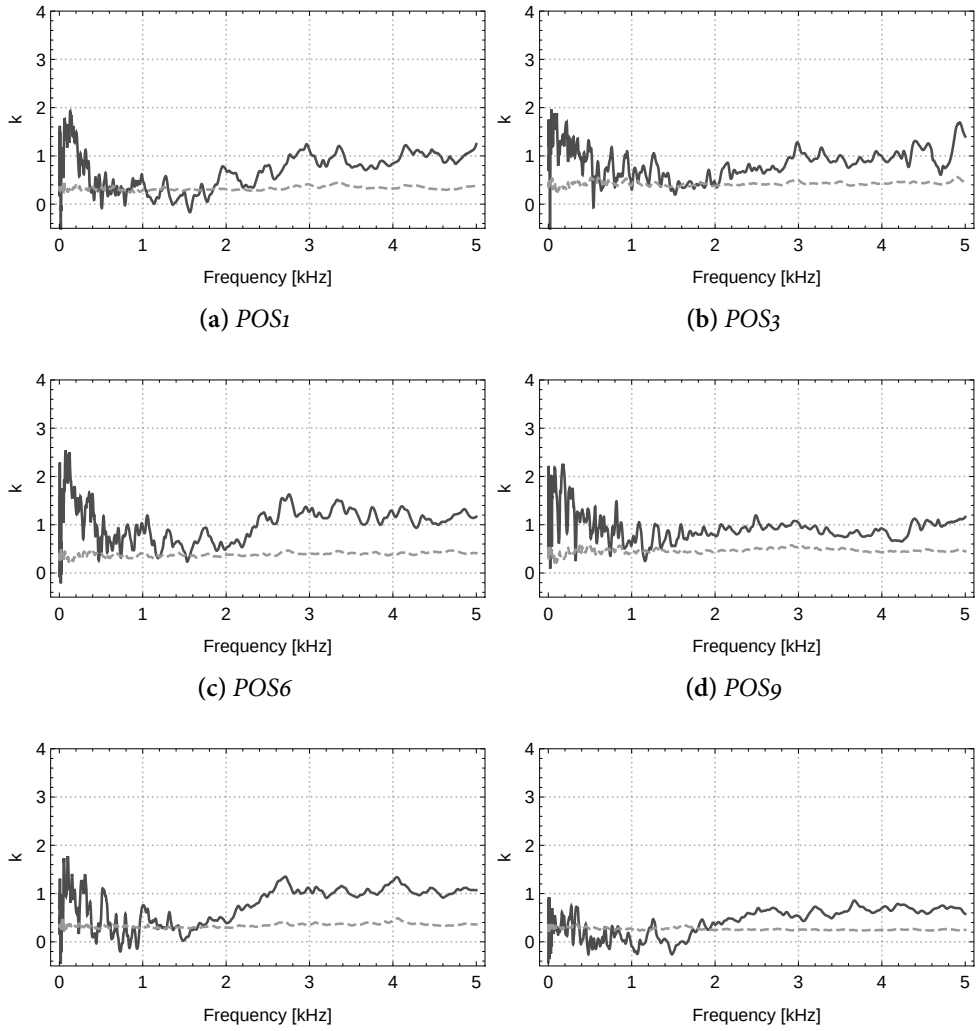

(a) *POS1* (b) *POS3*

(c) *POS6* (d) *POS9*

(e) *POS12* (f) *POS15*

Figure A.45.: Exponential fitting per frequency for *D1 PROD4*. Dashed lines depict the fitting error.

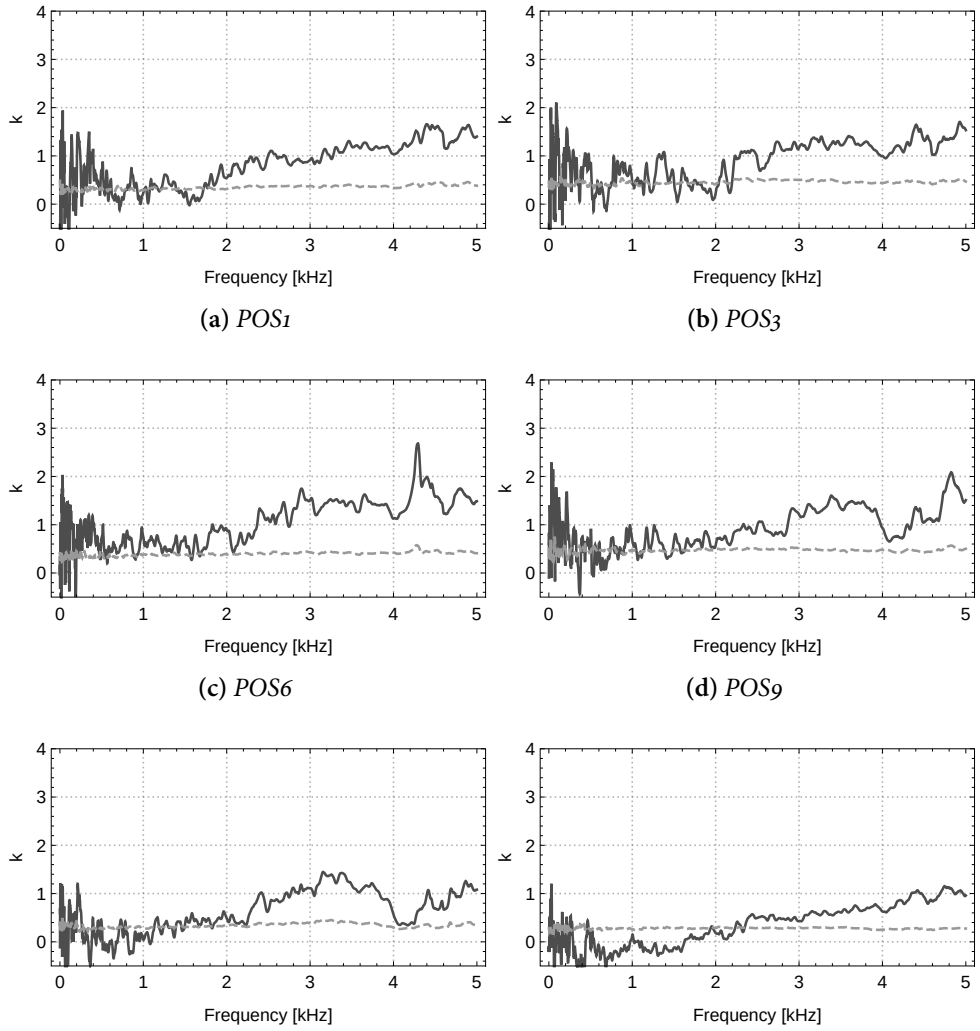

(a) *POS1* (b) *POS3*

(c) *POS6* (d) *POS9*

(e) *POS12* (f) *POS15*

Figure A.46.: Exponential fitting per frequency for *D1 PROD5*. Dashed lines depict the fitting error.

A.6. Interview Transcriptions

A.6.1. Interview with the Technician after Tuning *D1 PROD7*

Q: Wie war das Stimmen? Wie klingt der Flügel?

A: *Es war schwierig, die Situation ist sehr ungewohnt für mich durch den schalltoten Raum. Ich finde ihn aber vom Klang her gut, er hat einen schönen Bass, ich finde ihn eigentlich auch klar und brillant genug. Er wird zum Diskant hin ein bisschen schwächer. Da sind, wenn wir vom Konzertbetrieb reden, vielleicht noch ein paar Spitzchen drin, aber das muss man dann auch immer in dem jeweiligen Raum betrachten. Ich finde ihn so erstmal gut. Halbwegs gute Dynamik. Nach oben hin fällt es ein bisschen ab.*

Q: Was heißt, „es fällt ab"? Wie äußert sich das?

A: *Er wird von der Kraft her nach oben ein bisschen weniger. Da würde ich ihm mehr verpassen.*

Q: Könnte man das noch rausintonieren?

A: *Ja.*

Q: Wie ist der Übergang vom Bass auf den Hauptsteg?

A: *Ich finde, sehr gleichmäßig.* (spielt) *Man hat immer eine ganz leichte Änderung in der Farbe, einfach durch die umsponnenen Saiten. Und man hat sowieso immer einen minimalen Bruch zwischen den Spreizen.*

Q: Wie ist die *Ansprache*?

A: *Er reagiert sehr schnell. Ist jetzt ein bisschen schwierig hier im Raum. Manchmal ist es leichter für mich, wenn der Pianist spielt und ich im Saal hören kann. Wenn die Ansprache zu direkt, zu plötzlich oder offensiv ist, kann es auch unangenehm werden.*

Q: Was macht für Sie einen guten Flügel aus?

A: *Es ist schon das Gesamtpaket. Ich muss gestehen, wenn ich einen einzelnen, isolierten Flügel habe, ist eine Einschätzung immer sehr schwer. Es fällt natürlich wesentlich leichter, wenn man eine Palette an Instrumenten hat. Die Regulation muss sowieso perfekt sein. Und klanglich - ich brauche auf jeden Fall Dynamik. Dass ich eine große Bandbreite habe, dass ich wirklich einen gutes, leises piano spielen kann und mit dem gleichen Flügel ein richtig kräftiges forte. Und dass der Ton sich dabei entwickelt. Ich mag keine Töne, die, wenn man vom piano zum forte hin langsam lauter wird, einfach wie ein Radio lauter werden. Sondern, dass sie von einem schmalen Ton nach oben richtig aufgehen. Der Bass ist selten ein Problem, die sind meist alle kräftig. Problematisch wird es immer nach oben, gerade im ersten Diskantfeld - dass ich da auch Dynamik habe, dass ich eine Klarheit habe im Ton. Etwas Singendes. Lange Töne. Das hört man wahrscheinlich von jedem, aber ...* (lacht) *... ein langer Ton!*

Q: Welche Rolle spielt das Verhältnis zwischen der Energie, die sie hineingeben und dem was vom Flügel zurückkommt für Sie?

A: *Wenn ich das Gefühl habe, der spielt anders, der fühlt sich schwerer in den Fingern an, kann es sein, dass er physikalisch gesehen gar nicht schwerer ist. Sondern einfach viel Energie in der Mechanik verloren geht und entsprechend nicht das zurück kommt, was ich mit einer bestimmten Energie von meinem Finger erwarte.*

Q: Sind *Räumlichkeit* oder *Panorama* für Sie Begriffe, mit denen Sie arbeiten?

A: *Wie ist das gemeint?*

Q: Zum Beispiel, dass die Quelle sehr breit klingt oder nur von einem kleinen Punkt kommt? Klingt das Instrument sehr klein oder kommt der Klang von einer großen Fläche? Aber das scheinen für Sie keine wichtige Begriffe zu sein?

A: *Nein, also ich muss jetzt erstmal darüber nachdenken. Raum spielt für mich eine Rolle als der Raum in dem das Instrument steht. Weil das wirklich schon extrem beeinflussen kann, so wie z.B. heute. Aber auf das Instrument bezogen - weiß ich jetzt nicht, ob das ein Begriff ist, mit dem ich arbeite.*

Q: Mit welchen weiteren Begriffen beschreiben und bewerten Sie einen Flügel?

A: *Eigentlich sind das die Kriterien, glaube ich. Es steht und fällt immer mit dem Klang. Klang ist eben nicht nur intonieren, es ist das Komplettpaket. Dass er offen klingt. Dass er frei klingt. Vielleicht hat das dann doch etwas mit dem Begriff der Räumlichkeit zu tun. Dass er nicht eingezwängt klingt.*

Q: Sie sagen, „offen und frei" soll er klingen. Wie können Sie in die Richtung arbeiten? Was müssen Sie tun, damit das Instrument offener und freier klingt?

A: *Das ist im konkreten Fall oft ein Herumprobieren. Oft kann ich es durch das Stimmen beeinflussen.*

A.6.2. Interview with the Technician after Tuning *D1 PROD8*

Q: Wie klingt er?

A: *Der Flügel klingt angenehm. Für mich war es vom Arbeiten her wesentlich angenehmer, weil ich einen Deckel hatte. Ich habe jetzt das dritte Mal in diesem Raum gestimmt und gefühlt war es heute am einfachsten, wegen des Deckels. Ich habe den Unterschied gemerkt, dass ich eine glatte Fläche hatte. Ich habe, so wie sonst auch, von der Richtung* (links) *mehr gekriegt. Das war jetzt anders. Generell ist er klanglich gut, gleichmäßig. Es gibt Sachen, die mir nicht ganz so gefallen. Aber er ist insgesamt ein gleichmäßiger, guter Flügel.*

Q: Vor einem Jahr haben Sie gesagt, dass er zum Diskant her ein bisschen abfällt. Ist das immer noch so?

A: *Hätte ich jetzt wieder gesagt, aber nicht mehr so extrem. So wie ich bei der Stimmung gerne ein bisschen nach außen spreize, mag ich es lieber, wenn er nach oben ein bisschen spitzer wird. Nach oben hin kann er gerne so ein bisschen kantiger werden vom Klang. Aber wenn man das so einzeln durchhört, ist es eigentlich ziemlich linear wie es nach oben geht. Der Ton ist im Diskant sehr kurz, das heißt, wenn ich davor sitze ist es noch etwas*

anderes, als wenn ich zwei Meter Richtung Publikum oder noch weiter stehe - ich würde behaupten, dass spätestens dann jemand das Gefühl hätte, dass er oben abfällt. Weil er einfach nicht weit genug trägt.

Q: Dann gab es bei der Spreize einen Übergang, der Ihnen immer auffällt?

A: *Wenn es ums Intonieren geht, oder ums Klangliche, ist es immer der. Bei jedem D-Flügel höre ich da ein Zinseln in dem Ton.*

Q: Wie ist der Übergang vom Bass- zum Hauptsteg?

A: *Ich empfinde ihn als relativ gleichmäßig. Man hat immer einen leichten Bruch, die Saite klingt leicht anders. Aber der hat jetzt keinen wirklichen Bruch, den ich beanstanden würde.*

Q: Wir haben letztes Jahr unter anderem über *Ansprache* gesprochen. Wie verhält es sich damit bei diesem Flügel?

A: *Das ist für mich sprachlich etwas so in Richtung Dynamik, also wie schnell er anspricht. Meinen Sie den ersten Moment?*

Q: Das ist für mich erstmal offen. Wenn Sie den Begriff nutzen, wüsste ich gerne, was Sie darunter verstehen.

A: *Ich nutze ihn vielleicht gar nicht ganz so oft, wie andere. Wenn ich mit Pianisten zusammenarbeite, weiß ich, was darunter verstanden wird. Das ist im Prinzip in dem Raum entscheidend, vielleicht kann man das vergleichen mit einem Auto, wenn ich Gas gebe. Es geht nicht darum, wie er los rollt, sondern wenn ich mal richtig hineintrete und der Punkt, wann das Auto anfängt, loszuschießen.*

Q: Ist es etwas Zeitliches?

A: *Ja. Wie schnell bekomme ich die Reaktion: Ich drücke und ich bekomme einen Ton. Wie schnell ist das, wie direkt ist das, wie gering ist die Verzögerung. Da ist ein sehr großes Spiel zwischen Mechanik und Ton.*

Q: Und wie ist das bei diesem Flügel? Ist da irgendetwas auffällig? Wie verhält er sich?

A: *Das ist wieder sehr subjektiv. Für den Spieler ist die Regulation entscheidend. Das heißt, wie „knackig" ist die eingestellt, dass ich ein gutes Feedback in den Fingern habe. Die Regulation hat natürlich Einfluss darauf, wie der empfundene Klang ist. Man könnte jetzt zum Beispiel einen Flügel nehmen, den gleichen Flügel, man hätte jetzt zwei Mechaniken und, wenn man das könnte (das geht natürlich nicht), zwei Hammerköpfe oder man würde die umschrauben, also hätte den gleichen Hammerkopf, der die gleiche Saite trifft bei gleichen Flügel, nur eine perfekte und eine nicht so perfekte Regulation. Und der, der daneben steht, kann es wahrscheinlich sogar schon hören. Aber für den, der davor sitzt, wird es klanglich einen gigantischen Unterschied machen. Weil, wenn er so direkt kommt, wird er den Flügel als lauter empfinden. Weil er natürlich bei gleichem Kraftaufwand viel mehr hat. Gefühlt können Instrumente sehr leicht spielen und andere sehr schwer. Obwohl sie gewichtsmäßig exakt das Gleiche haben. Das ist im Prinzip das Ansprechen. Wie der einzelne Ton in der frühen Entwicklung anspricht.*

Q: Was erwarten Sie nach einem Jahr Konzertbetrieb an Änderungen bei einem Flügel?

A: *Das ist immer ganz schwer. Ich weiß, dass sich ein Flügel immer entwickelt - es kann positiv oder negativ sein, aber er entwickelt sich. Und man hofft natürlich immer zum Positiven. Wenn man sich einen aussucht und eine bestimmte Vorstellung hat und hofft, dass er in die Richtung geht - das funktioniert manchmal, aber manchmal eben auch nicht. Was schwierig ist, ist zu sagen, woran das jetzt genau liegt, weil man natürlich permanent daran arbeitet und irgendwie eine Idee im Kopf hat und die verfolgt. Das heißt, es wird zum Großteil wirklich der Flügel sein, der sich entwickelt und ein Teil ist dem Techniker geschuldet, der an dem Instrument arbeitet.*

Q: Was ist der Teil, den der Flügel beiträgt?

A: *Ich weiß es nicht. Wenn ich das wüsste, könnte ich es ja bei jedem hinkriegen. Ein klassisches Beispiel: Wir haben zwei Flügel bekommen, die wir selber ausgesucht haben. Einer für die Fabrik, einer für die Laeiszhalle. Wir haben mit den Kollegen zusammen „blind verkostet" und waren alle bei demselben Flügel. Der kam in die Laeiszhalle und wir waren am Anfang ganz glücklich, wurden aber, vielleicht auch, weil er selten ausgesucht wurde, immer unglücklicher und hatten das Gefühl, dass er sich*

nicht zum Positiven entwickelt. Und jetzt, nach einem Jahr, ist er wieder gut. Das ist leider das Problem, dass so viel Subjektives dabei ist. Wie gesagt, ich erwarte eine Entwicklung und sie ist eigentlich auch meist positiv. Ein Konzertflügel hat mit zwei Jahren, wenn er so richtig eingespielt ist, und eingegroovt an dem Ort an dem er steht, seinen Höhepunkt. Danach geht es bergab. Der braucht einfach am Anfang. Und ich denke schon, dass es damit zu tun hat, dass sich das einfach alles einspielen muss. Vieles, was ich gehört habe, geht leicht in den Esoterikbereich. Damit kann ich manchmal nicht viel anfangen, aber ich finde die Ansätze trotzdem nicht falsch. Wenn es um Dinge wie Bodenfreischwingen geht, ist aber manchmal schon ein bisschen viel Esoterik dabei.

Q: Dann haben Sie letztes Mal Begriffe genutzt wie „offen" und „frei". Können Sie dazu noch etwas sagen bezüglich des Flügels? Ist der offen und frei?

A: *In diesem Raum schwer zu sagen. Gerade das Offene ist natürlich abhängig davon, wie groß der Raum ist. Frei klingt er für mich, wenn ich das Gefühl habe, dass der Ton kein Limit hat. Hier im Diskant habe ich ein bisschen das Gefühl, als ob er festgehalten wird. Frei, das ist für mich ein Begriff, den man mit Umarmung beschreiben könnte. So von richtig quetschen bis einfach loslassen. Hier habe ich das Gefühl, da ist noch Potential. Der Ton kann bei zwei Flügeln eigentlich fast gleich klingen und bei dem einen hat man trotzdem das Gefühl, irgendwie ist der nicht frei. Irgendwie ist da noch etwas drin.*

Q: Letztes Jahr haben wir über „Räumlichkeit" und „Panorama" gesprochen. Darunter verstehe ich, wie „Stereo" der Flügel klingt oder wie groß Ihnen der abstrahlende Flügel im Vergleich zur Geometrie des Flügels vorkommt. Das ist heute in Bezug auf den Deckel interessant, dass Ihnen das Stimmen mit Deckel viel leichter fällt als ohne.

A: *Ja, zumindest hier in diesem Raum, in der Fabrik haben wir nie einen Deckel. In diesem Raum hat es mir geholfen, weil irgendetwas da war, das mal nicht geschluckt hat und ich etwas zurück bekommen habe. Diese zeitliche Verzögerung, die durch einen Rückwurf kommt, vielleicht brauche ich die fürs Stimmen. Ein ähnliches Phänomen haben wir auch mit Pianisten in der Elbphilharmonie. Wir nutzen im großen Saal wesentlich längere Stützen, einfach weil der Raum so hoch ist. Dadurch steht der Deckel steiler.*

Für die Pianisten ist das so ungewohnt, da waren auch welche dabei, die gesagt haben: „Super, ganz toll - aber für das Konzert: Nein, danke.". Das geht nicht, weil auf einmal das, was sie von links kriegen, etwas ganz anderes ist. Auf einmal haben sie auch nach links diese Weite, die man einfach nicht kennt. Das heißt, das Ding ist einfach für einen klassischen Konzertsaal ideal, dass es nach rechts abstrahlt. Aber natürlich limitiert ihn das eigentlich wiederum in dem Offensein oder in der Größe. Was meinen Sie, was es für einen klanglichen Unterschied macht, wenn ich die Tastenklappe raus nehme. Wenn ich arbeite, habe ich sie immer draußen, ich empfinde das immer gar nicht mehr so extrem. Aber ich habe das schon von Kunden gehört und Pianisten, wenn die nicht da ist. Natürlich ist es auch immer ein optisches Ding, denen fehlt dann diese Begrenzung. Die sind dann dadurch irritiert und dann ist auch schon wieder alles anders.

Q: Das letzte Mal habe ich *Panorama* und *Räumlichkeit* als Parameter genannt und das war Ihnen nicht so wichtig. Aber es fällt ja trotzdem sofort auf, ob ein Deckel drauf ist, oder nicht. Also scheint es schon wichtig zu sein?

A: *Ja, das stimmt, vielleicht nicht so offensichtlich. Deswegen machen solche Experimente ja auch mal Spaß. Und wir haben halt ganz viel mit Subjektivem zu tun, dessen man muss sich bewusst sein.*

A.7. Screenshots Listening Test

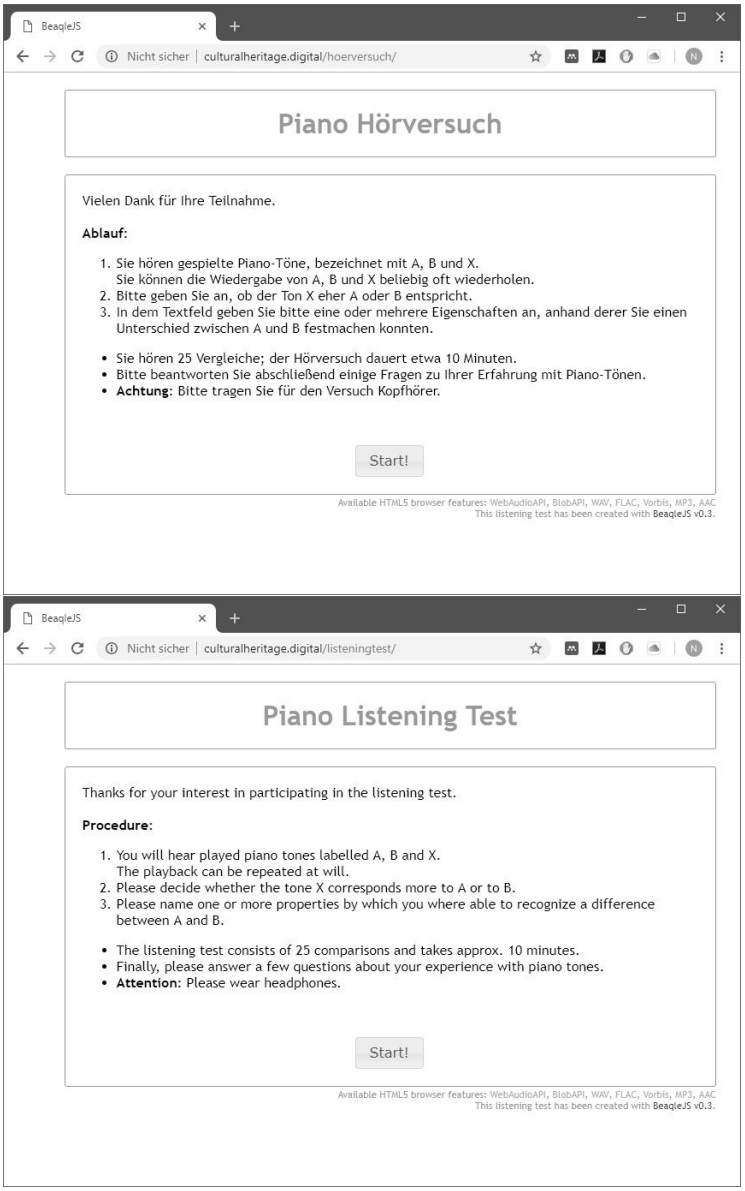

Figure A.47.: Front page for the listening test (English and German version).

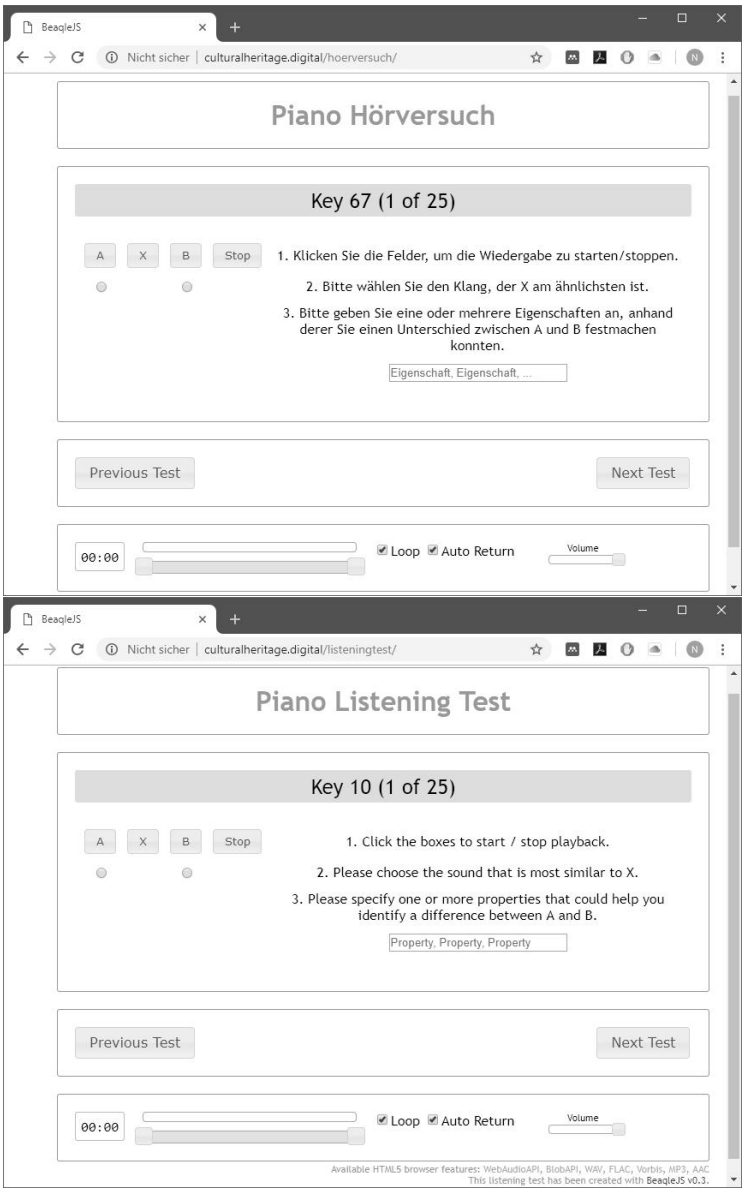

Figure A.48.: Exemplary trial page (English and German version).

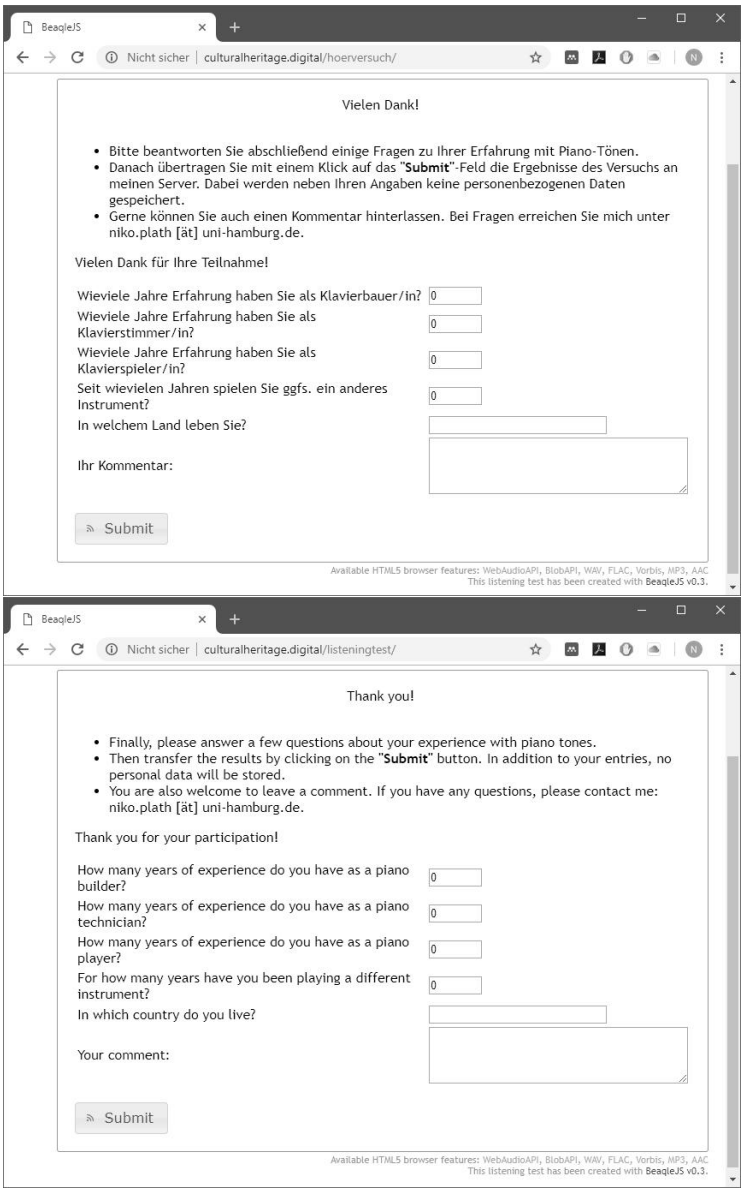

Figure A.49.: Conclusive survey page (English and German version).

A.8. Listening Test Results per Key

Table A.1.: Individual results per key.

Key	n	c	$c/n*100$	p_{chance}	$CL_{95\%}$: H_0 rejected?	$CL_{99\%}$: H_0 rejected?
3	42	42	100.00	2×10^{-13}	True	True
4	40	39	97.50	3.73×10^{-11}	True	True
7	47	45	95.74	8×10^{-12}	True	True
8	36	34	94.44	9.70×10^{-9}	True	True
9	40	35	87.50	6.91×10^{-7}	True	True
10	50	48	96.00	1.1×10^{-12}	True	True
11	43	42	97.67	5×10^{-12}	True	True
12	32	31	96.88	7.68×10^{-9}	True	True
13	49	48	97.96	1×10^{-13}	True	True
14	38	38	100.00	3.6×10^{-12}	True	True
19	50	45	90.00	2.10×10^{-9}	True	True
21	46	44	95.65	1.54×10^{-11}	True	True
22	42	41	97.62	9.8×10^{-12}	True	True
23	31	28	90.32	2.32×10^{-6}	True	True
24	40	38	95.00	7.46×10^{-10}	True	True
26	39	34	87.18	1.21×10^{-6}	True	True
28	35	34	97.14	1.04×10^{-9}	True	True
29	43	41	95.35	1.07×10^{-10}	True	True
30	43	39	90.70	1.55×10^{-8}	True	True
31	30	26	86.67	2.9×10^{-5}	True	True
32	36	33	91.67	1.13×10^{-7}	True	True
33	34	32	94.12	3.46×10^{-8}	True	True
35	36	34	94.44	9.70×10^{-9}	True	True
36	42	38	90.48	2.82×10^{-8}	True	True
37	43	40	93.02	1.51×10^{-9}	True	True
38	31	30	96.77	1.49×10^{-8}	True	True
40	42	39	92.86	2.81×10^{-9}	True	True
46	41	40	97.56	1.91×10^{-11}	True	True
47	36	34	94.44	9.70×10^{-9}	True	True
48	41	38	92.68	5.23×10^{-9}	True	True
49	45	43	95.56	2.94×10^{-11}	True	True
50	33	32	96.97	3.95×10^{-9}	True	True

Table A.2.: Individual results per key (continued from previous page).

Key	n	c	$c/n*100$	p_{chance}	$CL_{95\%}$: H_0 rejected?	$CL_{99\%}$: H_0 rejected?
51	37	33	89.19	5.42×10^{-7}	True	True
52	36	34	94.44	9.70×10^{-9}	True	True
53	37	36	97.30	2.76×10^{-10}	True	True
54	45	42	93.33	4.32×10^{-10}	True	True
55	45	38	84.44	1.56×10^{-6}	True	True
56	31	30	96.77	1.49×10^{-8}	True	True
57	30	26	86.67	2.9×10^{-5}	True	True
58	37	33	89.19	5.42×10^{-7}	True	True
60	45	40	88.89	3.93×10^{-8}	True	True
61	45	38	84.44	1.56×10^{-6}	True	True
62	30	27	90.00	4.21×10^{-6}	True	True
63	42	38	90.48	2.82×10^{-8}	True	True
65	40	38	95.00	7.46×10^{-10}	True	True
67	41	40	97.56	1.91×10^{-11}	True	True
68	42	39	92.86	2.81×10^{-9}	True	True
71	26	24	92.31	5.24×10^{-6}	True	True
72	37	37	100.00	7.3×10^{-12}	True	True
73	38	36	94.74	2.69×10^{-9}	True	True
74	42	41	97.62	9.8×10^{-12}	True	True
76	41	38	92.68	5.23×10^{-9}	True	True
77	42	39	92.86	2.81×10^{-9}	True	True
78	40	35	87.50	6.91×10^{-7}	True	True
79	39	35	89.74	1.67×10^{-7}	True	True
82	36	34	94.44	9.70×10^{-9}	True	True
83	42	39	92.86	2.81×10^{-9}	True	True
84	37	35	94.59	5.12×10^{-9}	True	True
85	39	39	100.00	1.8×10^{-12}	True	True
86	46	44	95.65	1.54×10^{-11}	True	True
87	32	32	100.00	2.32×10^{-10}	True	True
88	41	39	95.12	3.92×10^{-10}	True	True

A.9. Listening Test Results per Participant

Table A.3.: Individual results per participant.

i	y_B	y_T	y_P	y_I	n	c	$c/n*100$	p_{chance}	$CL_{95\%}$: H_0 rejected?	$CL_{99\%}$: H_0 rejected?
1	0	0	0	20	24	23	95.83	1.49×10^{-6}	True	True
2	0	0	37	38	24	21	87.50	1.3×10^{-4}	True	True
3	0	0	1	3	25	25	100.00	2.98×10^{-8}	True	True
4	0	2	23	16	25	25	100.00	2.98×10^{-8}	True	True
5	0	0	0	15	25	22	88.00	7.8×10^{-5}	True	True
6	0	0	38	0	24	24	100.00	5.96×10^{-8}	True	True
7	34	34	44	44	24	23	95.83	1.49×10^{-6}	True	True
8	1	0	30	15	25	22	88.00	7.8×10^{-5}	True	True
9	0	0	1	0	25	16	64.00	0.1147	False	False
10	4	0	20	0	25	25	100.00	2.98×10^{-8}	True	True
11	47	44	56	53	25	25	100.00	2.98×10^{-8}	True	True
12	20	20	45	40	25	25	100.00	2.98×10^{-8}	True	True
13	40	0	50	0	25	22	88.00	7.8×10^{-5}	True	True
14	6	0	25	0	25	25	100.00	2.98×10^{-8}	True	True
15	4	0	34	0	25	25	100.00	2.98×10^{-8}	True	True
16	4	0	19	0	25	25	100.00	2.98×10^{-8}	True	True
17	28	0	43	41	24	22	91.67	1.7×10^{-5}	True	True
18	1	0	3	13	25	25	100.00	2.98×10^{-8}	True	True
19	4	0	25	0	25	24	96.00	7.74×10^{-7}	True	True
20	0	0	0	0	25	25	100.00	2.98×10^{-8}	True	True
21	0	0	25	30	23	21	91.30	3.3×10^{-5}	True	True
22	0	0	0	0	25	24	96.00	7.74×10^{-7}	True	True
23	0	0	0	0	25	25	100.00	2.98×10^{-8}	True	True
24	0	0	20	0	25	22	88.00	7.8×10^{-5}	True	True
25	0	0	35	40	25	25	100.00	2.98×10^{-8}	True	True

Table A.4.: Individual results per participant (continued from previous page).

i	y_B	y_T	y_P	y_I	n	c	$c/n*100$	p_{chance}	$CL_{95\%}$: H_0 rejected?	$CL_{99\%}$: H_0 rejected?
26	25	5	30	18	25	24	96.00	7.74×10^{-7}	True	True
27	3	0	25	25	23	22	95.65	2.86×10^{-6}	True	True
28	10	0	30	30	25	25	100.00	2.98×10^{-8}	True	True
29	17	17	21	17	24	24	100.00	5.96×10^{-8}	True	True
30	12	10	14	20	25	25	100.00	2.98×10^{-8}	True	True
31	0	0	10	0	25	25	100.00	2.98×10^{-8}	True	True
32	0	0	9	0	25	25	100.00	2.98×10^{-8}	True	True
33	0	0	30	25	25	25	100.00	2.98×10^{-8}	True	True
34	0	0	45	0	24	24	100.00	5.96×10^{-8}	True	True
35	0	0	26	10	25	25	100.00	2.98×10^{-8}	True	True
36	0	0	13	3	25	25	100.00	2.98×10^{-8}	True	True
37	0	0	22	12	25	25	100.00	2.98×10^{-8}	True	True
38	0	0	9	5	25	21	84.00	4.5×10^{-4}	True	True
39	0	0	50	40	25	23	92.00	9.71×10^{-6}	True	True
40	0	0	45	40	25	24	96.00	7.74×10^{-7}	True	True
41	0	0	2	0	25	25	100.00	2.98×10^{-8}	True	True
42	0	0	1	40	25	25	100.00	2.98×10^{-8}	True	True
43	0	0	6	0	25	23	92.00	9.71×10^{-6}	True	True
44	0	0	4	0	25	25	100.00	2.98×10^{-8}	True	True
45	30	30	38	0	25	22	88.00	7.8×10^{-5}	True	True
46	0	0	3	0	25	22	88.00	7.8×10^{-5}	True	True
47	0	0	26	0	25	22	88.00	7.8×10^{-5}	True	True
48	0	0	54	0	24	18	75.00	0.011	True	False
49	0	0	2	0	25	25	100.00	2.98×10^{-8}	True	True
50	0	0	23	23	24	24	100.00	5.96×10^{-8}	True	True

Table A.5.: Individual results per participant (continued from previous page).

i	y_B	y_T	y_P	y_I	n	c	$c/n*100$	p_{chance}	$CL_{95\%}$: H_0 rejected?	$CL_{99\%}$: H_0 rejected?
51	40	0	40	0	25	20	80.00	2.0×10^{-3}	True	True
52	0	0	55	0	25	24	96.00	7.74×10^{-7}	True	True
53	0	0	1	0	10	10	100.00	9.7×10^{-4}	True	True
54	0	0	1	6	25	22	88.00	7.8×10^{-5}	True	True
55	0	0	5	0	25	25	100.00	2.98×10^{-8}	True	True
56	1	0	4	23	25	24	96.00	7.74×10^{-7}	True	True
57	0	0	48	48	25	25	100.00	2.98×10^{-8}	True	True
58	0	0	50	50	24	19	79.17	3.3×10^{-3}	True	True
59	0	0	49	41	25	24	96.00	7.74×10^{-7}	True	True
60	0	0	1	1	25	24	96.00	7.74×10^{-7}	True	True
61	0	0	25	10	24	24	100.00	5.96×10^{-8}	True	True
62	0	0	2	0	25	21	84.00	4.5×10^{-4}	True	True
63	0	0	7	0	22	21	95.45	5.48×10^{-6}	True	True
64	0	0	6	38	25	22	88.00	7.8×10^{-5}	True	True
65	0	0	57	0	25	24	96.00	7.74×10^{-7}	True	True
66	0	0	20	0	25	24	96.00	7.74×10^{-7}	True	True
67	5	0	35	35	24	24	100.00	5.96×10^{-8}	True	True
68	38	38	48	0	25	23	92.00	9.71×10^{-6}	True	True
69	0	0	15	0	25	25	100.00	2.98×10^{-8}	True	True
70	0	0	5	20	25	23	92.00	9.71×10^{-6}	True	True
71	0	0	0.5	0	25	18	72.00	0.021	True	False
72	16	16	26	10	25	25	100.00	2.98×10^{-8}	True	True
73	0	0	10	0	25	23	92.00	9.715×10^{-6}	True	True
74	0	0	0	8	25	23	92.00	9.715×10^{-6}	True	True
75	0	0	7	30	25	22	88.00	7.8×10^{-5}	True	True

Table A.6.: Individual results per participant (continued from previous page).

i	y_B	y_T	y_P	y_I	n	c	$c/n*100$	p_{chance}	$CL_{95\%}$: H_0 rejected?	$CL_{99\%}$: H_0 rejected?
76	0	0	46	0	25	19	76.00	7.3×10^{-3}	True	True
77	0	0	20	2	22	20	90.91	6.0×10^{-5}	True	True
78	0	0	15	5	25	24	96.00	7.74×10^{-7}	True	True
79	0	0	23	0	25	25	100.00	2.98×10^{-8}	True	True
80	0	0	1	0	25	25	100.00	2.98×10^{-8}	True	True
81	0	0	5	0	25	23	92.00	9.71×10^{-6}	True	True
82	0	0	0	19	25	19	76.00	7.3×10^{-3}	True	True
83	0	0	0	0	25	24	96.00	7.74×10^{-7}	True	True
84	0	0	5	0	25	24	96.00	7.74×10^{-7}	True	True
85	0	0	0	40	17	13	76.47	0.024	True	False
86	0	0	6	0	25	24	96.00	7.74×10^{-7}	True	True
87	0	0	10	0	25	20	80.00	2.0×10^{-3}	True	True
88	0	0	0	29	24	22	91.67	1.7×10^{-5}	True	True
89	0	0	0	13	24	24	100.00	5.96×10^{-8}	True	True
90	2	5	0	0	25	24	96.00	7.74×10^{-7}	True	True
91	0	0	0	30	19	19	100.00	1.90×10^{-6}	True	True
92	0	0	0	10	25	24	96.00	7.74×10^{-7}	True	True
93	0	0	0	40	25	21	84.00	4.5×10^{-4}	True	True
94	0	0	5	0	25	20	80.00	2.0×10^{-3}	True	True
95	0	0	60	64	16	16	100.00	1.5×10^{-5}	True	True
96	0	0	20	15	25	25	100.00	2.98×10^{-8}	True	True
97	0	0	1	15	24	18	75.00	0.011	True	False
98	0	0	4	14	25	25	100.00	2.98×10^{-8}	True	True
99	0	0	14	0	25	25	100.00	2.98×10^{-8}	True	True
100	0	0	20	20	25	23	92.00	9.71×10^{-6}	True	True

A.10. Feature Set for Principal Component Analysis

Table A.7.: Feature set for principal component analysis.

	PROD	Key	AT/F	f_1	FCD/F	ILD/F	R/F	S/F	SC/F	SPL/F	T60/F
0	7	1	0.6001	27.5000	0.2222	-0.0169	0.6548	29.988	105.7961	5.1087	0.1558
1	7	2	0.9741	29.2500	0.2512	-0.0445	0.6710	29.268	94.1072	5.8574	0.3291
2	7	3	0.9029	31.2000	0.2200	-0.0665	0.6548	29.838	94.8466	5.1498	0.4526
3	7	4	0.5315	32.7500	0.1964	-0.0346	0.7032	31.614	79.8651	4.8494	0.3739
4	7	5	1.0716	34.7500	0.2487	-0.0037	0.7355	33.292	111.7292	5.6300	0.3950
5	7	6	0.5842	36.7500	0.1817	-0.0110	0.7194	33.674	85.3295	3.9530	0.4292
6	7	7	0.5288	39.0000	0.2313	-0.1174	0.7677	35.172	92.9088	4.8446	0.4246
7	7	8	0.7694	41.5000	0.2054	-0.0759	0.7677	34.454	98.5195	4.6315	0.5187
8	7	9	1.5191	43.7500	0.1698	0.0418	0.7516	38.600	76.4577	4.0249	0.3264
9	7	10	0.6717	46.5000	0.2735	-0.0592	0.8000	34.570	106.2049	4.8580	0.5465
10	7	11	0.6555	49.2500	0.2341	-0.1252	0.7839	35.288	98.5734	5.0415	0.4441
11	7	12	0.9243	52.2500	0.2815	-0.0195	0.7516	35.500	101.1830	5.5139	0.3862
12	7	13	0.2641	55.0000	0.2085	0.0346	0.8161	36.314	105.3545	4.5890	0.4230
13	7	14	0.3670	58.5000	0.2011	0.1334	0.8000	33.394	82.9612	4.3880	0.2730
14	7	15	0.4935	61.8500	0.2294	0.0012	0.7677	35.132	114.9609	4.9966	0.4740
15	7	16	0.7199	65.5000	0.2016	-0.0520	0.7839	32.410	71.3552	4.3461	0.0126
16	7	17	0.9356	69.5000	0.2102	-0.0681	0.7194	34.112	75.7090	4.9751	0.3654
17	7	18	0.4895	74.5000	0.2022	-0.0324	0.7032	31.256	90.8111	5.0911	0.2998
18	7	19	0.5052	78.5000	0.2405	-0.0708	0.7355	34.566	100.0862	4.8898	0.2655
19	7	20	0.3982	83.0000	0.2209	-0.1466	0.7355	35.736	85.4987	4.7863	0.2786
20	7	21	0.3355	87.5000	0.3531	-0.0625	0.7516	37.652	115.0075	4.8101	0.2299
21	7	22	0.2384	92.7500	0.2786	-0.0911	0.7032	34.928	92.2629	4.7877	0.4253
22	7	23	0.8062	98.5500	0.2096	-0.1454	0.6226	35.688	87.0008	4.6333	0.3539
23	7	24	0.3386	104.7500	0.2885	-0.0519	0.6871	37.742	93.3471	4.7841	0.3008
24	7	25	0.2501	110.7500	0.2890	-0.0161	0.6710	39.108	93.9839	4.1793	0.1812
25	7	26	0.2338	117.5000	0.2930	-0.1063	0.6548	38.274	88.8459	4.4831	0.2913

Table A.8.: Feature set for principal component analysis (continued from previous page).

	PROD	Key	AT/F	f_1	FCD/F	ILD/F	R/F	S/F	SC/F	SPL/F	T60/F
25	7	26	0.2338	117.5000	0.2930	-0.1063	0.6548	38.274	88.8459	4.4831	0.2913
26	7	27	0.2589	124.2500	0.2596	-0.1391	0.6387	35.876	91.2547	4.7078	0.2530
27	7	28	0.1803	131.5000	0.2441	-0.1629	0.5903	39.364	84.3448	4.4653	0.1831
28	7	29	0.3786	139.5000	0.2021	-0.1705	0.5258	34.744	83.0467	4.7549	0.1692
29	7	30	0.3364	148.0000	0.1914	-0.0956	0.4935	35.898	63.1987	3.8445	0.1563
30	7	31	0.5949	156.7500	0.2237	-0.0835	0.5097	33.976	75.1971	4.3161	0.3471
31	7	32	0.2433	165.7500	0.2237	-0.0016	0.5581	34.934	74.1106	3.8383	0.2820
32	7	33	0.3095	175.2500	0.2795	-0.0073	0.5097	37.824	85.1405	4.5720	0.1417
33	7	34	0.4660	185.5000	0.1786	-0.0939	0.4613	35.374	74.6227	4.6631	0.1982
34	7	35	0.3120	196.7500	0.1589	0.0005	0.3968	33.146	82.6617	4.8460	0.1859
35	7	36	0.4809	208.2500	0.1177	-0.0117	0.3806	37.134	82.5444	4.6805	0.1485
36	7	37	0.3740	221.2500	0.1372	-0.1215	0.3806	38.118	65.9715	4.2643	0.1851
37	7	38	0.2679	234.2500	0.1716	-0.1023	0.4452	38.458	77.1041	4.4677	0.3052
38	7	39	0.2326	247.7500	0.2673	-0.0786	0.4290	37.108	94.7126	4.7753	0.2045
39	7	40	0.1996	262.7500	0.2043	-0.0961	0.3806	36.966	94.3869	4.7464	0.1317
40	7	41	0.2861	278.5000	0.1532	-0.0509	0.3484	38.916	101.8216	5.1016	0.1502
41	7	42	0.3940	295.0000	0.1956	-0.1066	0.3161	39.314	121.0084	5.8405	0.2746
42	7	43	0.2715	312.4167	0.2212	-0.0016	0.3645	42.314	116.7936	4.7434	0.1220
43	7	44	0.1031	331.1167	0.2561	-0.1013	0.3968	42.588	117.2723	4.4872	0.1001
44	7	45	0.3480	351.0000	0.1878	-0.0644	0.3645	44.314	119.6255	4.6446	0.2350
45	7	46	0.3702	371.2500	0.1833	-0.0155	0.3000	40.666	112.3734	4.5457	0.0936
46	7	47	0.4868	393.9500	0.1531	0.1038	0.3323	40.452	94.3667	4.7370	0.1310
47	7	48	0.1788	416.8333	0.1526	-0.0517	0.3323	43.808	109.0032	4.2980	0.1157
48	7	49	0.2239	442.0000	0.1643	0.0523	0.3000	44.408	100.3484	4.5056	0.1196
49	7	50	0.1641	468.4333	0.1641	-0.0789	0.3000	40.862	94.9590	4.6319	0.0936
50	7	51	0.1030	496.5000	0.0758	-0.1024	0.2194	44.614	64.8057	3.0442	0.2298

Table A.9.: Feature set for principal component analysis (continued from previous page).

	PROD	Key	AT/F	f_1	FCD/F	ILD/F	R/F	S/F	SC/F	SPL/F	T60/F
51	7	52	0.1871	525.5833	0.0828	-0.0241	0.2032	43.724	71.4019	3.9739	0.1700
52	7	53	0.1094	557.0000	0.0926	-0.1164	0.3000	47.454	79.8128	4.0340	0.1709
53	7	54	0.1764	592.0000	0.0779	-0.1592	0.2355	46.852	74.3965	3.7482	0.2177
54	7	55	0.1238	627.4333	0.0950	-0.1744	0.3000	48.414	104.1123	3.8196	0.0710
55	7	56	0.0981	664.7500	0.0901	-0.1527	0.2355	49.482	87.6464	3.4121	0.0583
56	7	57	0.0848	703.6667	0.1046	-0.2489	0.3484	47.382	104.5522	3.8645	0.1506
57	7	58	0.0848	744.2500	0.0803	-0.2653	0.1871	45.708	87.9331	3.9833	0.0510
58	7	59	0.1491	788.4667	0.1012	-0.2042	0.3000	49.576	108.1222	3.3816	0.0727
59	7	60	0.1680	834.2500	0.0742	-0.1463	0.2516	47.798	84.1479	3.5579	0.0399
60	7	61	0.2381	886.0000	0.0703	-0.2497	0.1710	49.778	83.5231	3.4252	0.0727
61	7	62	0.3425	938.3000	0.0606	-0.1103	0.1710	44.108	71.2774	3.6282	0.0341
62	7	63	0.0604	995.3333	0.0670	-0.0179	0.3484	46.946	87.9111	3.4541	0.0353
63	7	64	0.2004	1053.5833	0.0584	-0.0238	0.2355	49.160	67.5043	3.3861	0.0243
64	7	65	0.0576	1115.7500	0.0796	-0.0432	0.2677	51.122	109.1095	3.8351	0.0344
65	7	66	0.0392	1182.9333	0.0596	-0.0166	0.3645	51.408	83.3409	2.6778	0.0268
66	7	67	0.0728	1249.6667	0.0719	-0.1244	0.3323	47.544	96.8445	3.5650	0.0762
67	7	68	0.0806	1329.4167	0.0554	-0.1373	0.2839	50.556	83.7334	3.1573	0.0810
68	7	69	0.0797	1406.9000	0.0637	-0.1895	0.3000	52.770	87.4531	3.2488	0.0619
69	7	70	0.1061	1488.4000	0.0654	-0.2519	0.3484	49.920	99.4938	2.9511	0.0176
70	7	71	0.1105	1576.9833	0.0780	-0.2068	0.4290	50.176	103.2406	3.5063	0.0390
71	7	72	0.0965	1670.7167	0.0644	-0.2308	0.3323	52.084	94.7806	3.2130	0.0231
72	7	73	0.1488	1778.1500	0.0849	-0.2618	0.3484	52.946	117.6682	3.6723	0.0301
73	7	74	0.1045	1881.4167	0.0730	-0.0637	0.3645	51.356	98.5392	3.2654	0.0270
74	7	75	0.1737	1992.1167	0.0766	-0.1062	0.2839	52.846	135.5699	4.3327	0.0443
75	7	76	0.0506	2120.9167	0.0981	-0.1954	0.4452	55.116	148.4605	3.4747	0.0179

Table A.10.: Feature set for principal component analysis (continued from previous page).

	PROD	Key	AT/F	f_1	FCD/F	ILD/F	R/F	S/F	SC/F	SPL/F	T60/F
76	7	77	0.0925	2244.7833	0.1261	-0.1317	0.4613	51.168	162.1010	3.8992	0.0178
77	7	78	0.1327	2383.3333	0.0879	-0.1299	0.3806	52.206	127.4835	3.4882	0.0323
78	7	79	0.1723	2514.0833	0.0852	-0.2146	0.4774	50.554	133.1429	3.6383	0.0174
79	7	80	0.0827	2674.2833	0.0736	-0.0891	0.4452	50.808	144.7506	3.4769	0.0155
80	7	81	0.0577	2817.4000	0.0693	-0.1749	0.3806	53.240	149.2307	3.4665	0.0138
81	7	82	0.0881	2990.5833	0.0893	-0.2459	0.4774	53.422	156.9405	3.6516	0.0138
82	7	83	0.0628	3172.9333	0.0834	-0.3147	0.4290	53.152	164.7027	3.5087	0.0114
83	7	84	0.1665	3368.9667	0.0799	-0.0949	0.4613	60.778	155.0683	3.7638	0.0110
84	7	85	0.0938	3577.8833	0.0904	-0.2643	0.4613	59.500	173.8253	3.8459	0.0144
85	7	86	0.1597	3780.7167	0.0821	-0.1548	0.4290	51.166	159.0279	3.3239	0.0078
86	7	87	0.1592	4000.5667	0.0585	-0.1757	0.4290	54.290	132.9875	3.1231	0.0096
87	7	88	0.1307	4249.8500	0.0862	-0.0527	0.3968	56.874	183.4997	3.4532	0.0093
88	8	1	0.5202	27.5000	0.1744	0.0604	0.6548	34.336	89.5175	5.2159	0.2238
89	8	2	0.7770	29.2500	0.1866	0.0383	0.6710	33.388	82.6710	6.0853	0.2670
90	8	3	1.4249	31.0000	0.1401	0.0188	0.6548	36.540	77.0715	5.3641	0.2887
91	8	4	0.7826	32.7500	0.1660	-0.0378	0.7032	33.852	85.0857	4.9419	0.2916
92	8	5	0.5256	34.7500	0.1792	0.0198	0.7355	38.700	94.2458	5.6776	0.4335
93	8	6	0.7349	36.7500	0.2330	-0.0849	0.7194	35.456	103.5245	3.9869	0.3566
94	8	7	0.5518	39.0000	0.1940	-0.0402	0.7677	36.098	85.5666	4.9522	0.2727
95	8	8	0.7107	41.2500	0.2256	-0.0587	0.7677	35.542	106.3821	4.5579	0.5525
96	8	9	0.4720	43.7500	0.1498	-0.0513	0.7516	35.892	82.1550	4.0068	0.3531
97	8	10	0.5985	46.5000	0.2356	-0.0181	0.8000	37.746	119.0716	5.0612	0.5003
98	8	11	0.5673	49.0000	0.2610	-0.0248	0.7839	36.812	106.4573	5.1191	0.4456
99	8	12	1.4981	52.0000	0.2279	-0.0040	0.7516	37.914	97.0120	5.6626	0.3444
100	8	13	0.5519	55.2500	0.2332	0.0397	0.8161	38.584	118.4592	4.5686	0.5919

Table A.11.: Feature set for principal component analysis (continued from previous page).

	PROD	Key	AT/F	f_1	FCD/F	ILD/F	R/F	S/F	SC/F	SPL/F	T60/F
101	8	14	0.5775	58.5000	0.2182	0.0486	0.8000	35.958	119.7556	4.4353	0.3148
102	8	15	0.3631	61.7500	0.3683	0.0106	0.7677	36.222	118.4728	5.0283	0.4203
103	8	16	0.4645	65.7500	0.1987	-0.0387	0.7839	35.800	79.7692	4.4830	0.3783
104	8	17	0.4139	69.5000	0.1903	-0.0039	0.7194	35.904	77.1199	4.9741	0.3181
105	8	18	0.7512	74.2500	0.2059	-0.1529	0.7032	36.748	90.3322	5.2056	0.4030
106	8	19	0.4906	78.5000	0.2871	-0.0500	0.7355	35.888	99.1032	4.9132	0.2691
107	8	20	0.3323	83.0000	0.2346	-0.1161	0.7355	37.852	90.2755	4.9289	0.3531
108	8	21	0.4253	87.2500	0.3191	-0.0656	0.7516	39.422	99.7661	4.8417	0.2378
109	8	22	0.2501	92.5000	0.2414	-0.0151	0.7032	37.346	82.5438	4.9471	0.3525
110	8	23	1.0913	98.4500	0.1910	-0.0714	0.6226	38.908	86.1735	4.7876	0.2990
111	8	24	0.4126	104.5000	0.2501	-0.0140	0.6871	38.690	82.7301	4.8546	0.2432
112	8	25	0.2083	110.7500	0.2005	-0.0320	0.6710	40.362	84.4298	4.2749	0.1634
113	8	26	0.2263	117.2500	0.2891	-0.1085	0.6548	38.852	90.3563	4.5797	0.2718
114	8	27	0.1539	124.0000	0.2270	-0.0449	0.6387	39.072	77.1331	4.9601	0.1858
115	8	28	0.1593	131.2500	0.2589	-0.0539	0.5903	39.228	87.6584	4.5848	0.1734
116	8	29	0.3480	139.5000	0.1592	-0.0432	0.5258	38.788	93.0879	4.8958	0.1833
117	8	30	0.1864	148.0000	0.2011	0.0037	0.4935	38.392	69.0488	3.9433	0.1350
118	8	31	0.3694	156.5000	0.2139	-0.0843	0.5097	35.934	76.1876	4.4205	0.3726
119	8	32	0.1189	165.7500	0.2025	-0.0111	0.5581	38.926	90.0152	3.9401	0.2327
120	8	33	0.1743	175.5000	0.2640	-0.0510	0.5097	39.554	75.0242	4.6761	0.1661
121	8	34	0.0726	185.7500	0.1613	-0.0356	0.4613	38.792	61.7465	4.7908	0.1562
122	8	35	0.4145	196.7500	0.1241	0.0398	0.3968	36.684	70.1799	4.9424	0.1758
123	8	36	0.3419	208.2500	0.0858	0.0991	0.3806	39.982	68.9761	4.7416	0.1637
124	8	37	0.3532	221.5000	0.1402	-0.0707	0.3806	37.960	67.3996	4.2977	0.1762
125	8	38	0.1920	234.5000	0.1843	-0.1099	0.4452	36.936	72.9429	4.5345	0.2794

Table A.12.: Feature set for principal component analysis (continued from previous page).

	PROD	Key	AT/F	f_1	FCD/F	ILD/F	R/F	S/F	SC/F	SPL/F	T60/F
126	8	39	0.0864	248.5000	0.1776	-0.0737	0.4290	37.180	65.3559	4.8562	0.1970
127	8	40	0.3460	263.0000	0.1934	0.0387	0.3806	41.402	80.8502	4.8718	0.1216
128	8	41	0.1729	279.0000	0.0980	-0.0844	0.3484	39.682	66.2643	5.2358	0.1052
129	8	42	0.2000	295.2500	0.1060	-0.0717	0.3161	37.830	72.3448	5.9274	0.1827
130	8	43	0.1933	313.0000	0.1425	-0.0622	0.3645	43.886	75.6751	4.9166	0.0870
131	8	44	0.1661	331.5000	0.1141	-0.0152	0.3968	43.666	84.0842	4.5554	0.0963
132	8	45	0.2034	351.0000	0.1209	-0.0886	0.3645	43.162	88.4721	4.6036	0.1076
133	8	46	0.4138	372.5000	0.1386	-0.1105	0.3000	41.804	85.6986	4.6013	0.1301
134	8	47	0.2753	394.9000	0.1346	0.1314	0.3323	42.322	96.2651	4.7355	0.1130
135	8	48	0.2745	417.7000	0.1903	0.0551	0.3323	42.094	101.2204	4.3456	0.1394
136	8	49	0.1358	442.6667	0.1480	0.0340	0.3000	40.682	97.8504	4.4526	0.2224
137	8	50	0.1872	469.2500	0.1318	-0.0507	0.3000	47.450	98.3140	4.7102	0.0941
138	8	51	0.1974	496.7500	0.0931	-0.0750	0.2194	44.340	78.8527	2.9999	0.0999
139	8	52	0.2145	527.0833	0.0895	-0.0843	0.2032	45.406	81.0905	3.9906	0.0660
140	8	53	0.0988	558.2500	0.0966	-0.0877	0.3000	46.326	91.1092	4.0069	0.1696
141	8	54	0.0707	590.4500	0.0894	-0.1912	0.2355	46.820	88.7780	3.5777	0.0713
142	8	55	0.0593	627.5000	0.1045	-0.2101	0.3000	46.212	99.8013	3.8028	0.0645
143	8	56	0.0782	663.3333	0.0825	-0.1467	0.2355	45.532	88.2736	3.3298	0.2126
144	8	57	0.1048	702.5500	0.1166	-0.2254	0.3484	49.066	102.0225	3.8005	0.0712
145	8	58	0.0754	744.2500	0.0729	-0.2606	0.1871	43.856	74.6867	3.9253	0.0452
146	8	59	0.1355	790.2667	0.0894	-0.1766	0.3000	47.986	93.8789	3.3170	0.0663
147	8	60	0.1936	836.3333	0.0791	-0.1306	0.2516	45.352	96.2860	3.5140	0.0848
148	8	61	0.2520	886.9333	0.0765	-0.3059	0.1710	46.856	94.8783	3.3792	0.0304
149	8	62	0.2739	939.9333	0.0702	-0.0141	0.1710	44.042	89.0983	3.5512	0.0874
150	8	63	0.0551	995.0833	0.0780	-0.0693	0.3484	47.636	97.8521	3.4266	0.0305

Table A.13.: Feature set for principal component analysis (continued from previous page).

	PROD	Key	AT/F	f_1	FCD/F	ILD/F	R/F	S/F	SC/F	SPL/F	T60/F
151	8	64	0.0546	1053.5833	0.0700	0.0081	0.2355	46.852	71.2975	3.2811	0.0530
152	8	65	0.0305	1119.7167	0.0714	-0.1057	0.2677	48.724	80.7799	3.8337	0.0363
153	8	66	0.0290	1183.9000	0.0734	-0.1207	0.3645	50.244	91.5371	2.6659	0.0268
154	8	67	0.0444	1257.8333	0.0803	-0.1885	0.3323	45.560	99.3760	3.5788	0.0410
155	8	68	0.1317	1331.1333	0.0622	-0.0764	0.2839	47.942	75.3047	3.1733	0.0386
156	8	69	0.1036	1408.1667	0.0705	-0.2812	0.3000	49.684	88.7096	3.2190	0.0441
157	8	70	0.0864	1491.4333	0.0589	-0.2534	0.3484	49.868	83.0073	2.9825	0.0482
158	8	71	0.0784	1579.7333	0.0586	-0.2449	0.4290	49.430	94.1820	3.4725	0.0326
159	8	72	0.0880	1675.6833	0.0631	-0.1553	0.3323	49.334	91.9394	3.2198	0.0150
160	8	73	0.0982	1775.9167	0.0680	-0.1950	0.3484	52.136	103.3087	3.6253	0.0153
161	8	74	0.0791	1884.8333	0.0757	-0.1984	0.3645	50.138	118.7119	3.2065	0.0195
162	8	75	0.1219	1999.3667	0.0750	-0.0925	0.2839	56.258	107.8117	4.2567	0.0177
163	8	76	0.0920	2118.2500	0.0616	-0.1917	0.4452	50.468	117.1273	3.4938	0.0135
164	8	77	0.0993	2243.4167	0.0718	-0.2316	0.4613	56.602	120.4855	3.9068	0.0251
165	8	78	0.1454	2384.1833	0.0849	-0.1290	0.3806	52.122	136.6019	3.4812	0.0150
166	8	79	0.0918	2526.7667	0.0598	-0.1141	0.4774	53.994	102.1711	3.5547	0.0082
167	8	80	0.0870	2674.3667	0.0754	0.0098	0.4452	50.796	140.7719	3.4307	0.0109
168	8	81	0.0957	2842.1167	0.0750	-0.1337	0.3806	52.636	126.2015	3.4683	0.0133
169	8	82	0.0801	3019.1833	0.0681	-0.2003	0.4774	50.872	121.0537	3.5952	0.0147
170	8	83	0.1458	3208.2833	0.0762	-0.1771	0.4290	56.306	132.1793	3.4762	0.0174
171	8	84	0.1203	3386.2333	0.0637	-0.0891	0.4613	56.616	120.2509	3.7645	0.0152
172	8	85	0.1682	3606.1500	0.0732	-0.2292	0.4613	55.482	141.4005	3.8556	0.0120
173	8	86	0.1232	3808.0167	0.0609	-0.2011	0.4290	58.340	120.8157	3.2803	0.0093
174	8	87	0.1580	4045.2333	0.0860	-0.1533	0.4290	52.552	152.4230	3.1487	0.0110
175	8	88	0.1179	4276.0667	0.0891	-0.1143	0.3968	51.128	137.8440	3.5205	0.0137

Bibliography

Aramaki, M. et al. (2001). "Resynthesis of Coupled Piano String Vibrations Based on Physical Modeling." In: *Journal of New Music Research* 30.3, pp. 213–226. DOI: 10.1076/jnmr.30.3.213.7472 (cit. on p. 168).

Askenfelt, Anders and Erik V. Jansson (1990a). "From touch to string vibrations." In: *Five lectures on the Acoustics of the piano*. Ed. by Anders Askenfelt. Stockholm: Royal Swedish Academy of Music (cit. on pp. 11–13, 19).

– (1990b). "From touch to string vibrations. I: Timing in the grand piano action." In: *The Journal of the Acoustical Society of America* 88.1, pp. 52–63. DOI: 10.1121/1.399933 (cit. on pp. 11, 13, 15, 28, 174).

– (1991). "From touch to string vibrations. II: The motion of the key and hammer." In: *The Journal of the Acoustical Society of America* 90.5, pp. 2383–2393. DOI: 10.1121/1.402043 (cit. on p. 15).

– (1993). "From touch to string vibrations. III: String motion and spectra." In: *The Journal of the Acoustical Society of America* 93.4, pp. 2181–2196. DOI: 10.1121/1.406680 (cit. on pp. 16, 18, 19, 21).

Bader, Rolf (2002). "Fraktale Dimensionen, Informationsstrukturen und Mikrorhythmik der Einschwingvorgänge von Musikinstrumenten." PhD thesis (cit. on p. 156).

– (2010). "Reconstruction of radiating sound fields using minimum energy method." In: *The Journal of the Acoustical Society of America* 127.1, pp. 300–308. DOI: 10.1121/1.3271416 (cit. on pp. 66, 67).

– (2012a). "Outside-instrument coupling of resonance chambers in the New-Ireland friction instrument lounuet." In: *Proceedings of Meetings on Acoustics*. Vol. 15, p. 035007. DOI: 10.1121/2.0000167 (cit. on p. 66).

Bader, Rolf (2012b). "Radiation characteristics of multiple and single sound hole vihuelas and a classical guitar." In: *The Journal of the Acoustical Society of America* 131.1, pp. 819–828. DOI: 10.1121/1.3651096 (cit. on pp. 57, 66).

– (2013). *Nonlinearities and Synchronization in Musical Acoustics and Music Psychology*. Springer (cit. on p. 156).

– (2014). "Microphone Array." In: *Springer Handbook of Acoustics*. Ed. by Thomas D. Rossing. New York, NY: Springer New York. Chap. Microphone, pp. 1179–1207. DOI: 10.1007/978-1-4939-0755-7_29 (cit. on p. 66).

Bank, Balázs and Heidi-Maria Lehtonen (2010). "Perception of longitudinal components in piano string vibrations." In: *The Journal of the Acoustical Society of America* 128.3, EL117–23. DOI: 10.1121/1.3453420 (cit. on pp. 28, 136).

Bank, Balázs and László Sujbert (2005). "Generation of longitudinal vibrations in piano strings: From physics to sound synthesis." In: *The Journal of the Acoustical Society of America* 117.4, pp. 2268–2278. DOI: 10.1121/1.1868212 (cit. on p. 28).

Beauchamp, James W (1982). "Synthesis by Spectral Amplitude and Brightness Matching of Analyzed Musical Instrument Tones." In: *J. Audio Eng. Soc.* 30.6 (cit. on p. 155).

Beavitt, A. (1996). "Humidity cycling." In: *Strad* November, pp. 916–920 (cit. on pp. 5, 125).

Berthaut, J., M. N. Ichchou, and L. Jézéquel (2003). "Piano soundboard: Structural behavior, numerical and experimental study in the modal range." In: *Applied Acoustics* 64, pp. 1113–1136. DOI: 10.1016/S0003-682X(03)00065-3 (cit. on pp. 3, 38, 83, 89, 116).

Bilhuber, Paul H. (1936). *U.S. Patent No. 2,051,633: Soundboard for pianos and other instruments or devices using soundboards* (cit. on pp. 36, 191).

– (1937). *U.S. Patent No. 2,070,391: Soundboard for Pianos* (cit. on p. 31).

Bilhuber, Paul H. and C. A. Johnson (1940). "The Influence of the Soundboard on Piano Tone Quality." In: *The Journal of the Acoustical Society of America* 11.3, pp. 311–320. DOI: 10.1121/1.1916039 (cit. on pp. 1, 36).

Birkett, Stephen (2013). "Experimental investigation of the piano hammer-string interaction." In: *The Journal of the Acoustical Society of America* 133.4, pp. 2467–2478. DOI: 10.1121/1.4792357 (cit. on p. 15).

Bissinger, George (1995). "Modal Analysis Comparison of New Violin Before and After 250 Hours of Playing." In: *Proc.13th Intern. Modal Analysis Conf.-Soc. Exp. Mechanics* July, pp. 822–827 (cit. on p. 125).

– (n.d.). *Extracting Internal Damping From Total Damping And Radiation Efficiency Measurements*. Tech. rep. (cit. on p. 50).

Boley, Jon and Michael Lester (2009). "Statistical Analysis of ABX Results Using Signal Detection Theory." In: *Audio Engineering Society Convention 127* (cit. on p. 139).

Borland, M. J. (2014). "The Effect of Humidity and Moisture Content on the Tone of Musical Instruments." PhD thesis, pp. 1–146 (cit. on p. 48).

Boutillon, Xavier (1988). "Model for piano hammers: Experimental determination and digital simulation." In: *The Journal of the Acoustical Society of America* 83.February, pp. 746–754 (cit. on p. 15).

Brémaud, Iris and Joseph Gril (2015). "Effect of transitional moisture change on the vibrational properties of violin-making wood." In: *Cost FP1302 WoodMusICK annual conference "Effects of playing on early and modern musical instruments"* (cit. on pp. 5, 124).

Bucur, Voichita (2006). *Acoustics of Wood*. Springer Series in Wood Science. Berlin: Springer-Verlag. DOI: 10.1007/3-540-30594-7 (cit. on pp. 41, 48, 97, 124).

– (2016). *Handbook of Materials for String Musical Instruments*. Cham: Springer International Publishing. DOI: 10.1007/978-3-319-32080-9 (cit. on p. 48).

Burstein, Herman (1988). "Approximation Formulas for Error Risk and Sample Size in ABX Testing." In: *Journal of the Audio Engineering Society* 36.11, pp. 879–883 (cit. on p. 140).

– (1989). "Transformed Binomial Confidence Limits for Listening Tests." In: *Journal of the Audio Engineering Society* 37.5, pp. 363–367 (cit. on p. 140).

Chaigne, Antoine and Anders Askenfelt (1994). "Numerical simulations of piano strings. II. Comparisons with measurements and systematic exploration of some hammer-string parameters." In: *The Journal of the Acoustical Society of America* 95.3, pp. 1631–1640. DOI: 10.1121/1.408549 (cit. on p. 15).

Chaigne, Antoine, Benjamin Cotté, and Roberto Viggiano (2013). "Dynamical properties of piano soundboards." In: *The Journal of the Acoustical Society of America* 133.4, pp. 2456–2466. DOI: 10.1121/1.4794387 (cit. on pp. 35, 83, 84).

Cheng, Tian, Simon Dixon, and Matthias Mauch (2015). "Modelling the decay of piano sounds." In: *2015 IEEE International Conference on Acoustics, Speech and Signal Processing (ICASSP)*. IEEE, pp. 594–598. DOI: 10.1109/ICASSP.2015.7178038 (cit. on p. 168).

Clark, David (1982). "High-Resolution Subjective Testing Using a Double-Blind Comparator." In: *Journal of the Audio Engineering Society* 30.5, pp. 330–336 (cit. on p. 136).

Clemens, B M et al. (2014). "Effect of Vibration Treatment on Guitar Tone: A Comparative Study." In: *Savart Journal*, pp. 1–9 (cit. on pp. 125, 126).

Conklin, Harold A. (1973). *U.S. Patent No. US3866506 A: Soundboard construction for stringed musical instruments* (cit. on pp. 3, 35, 36, 38, 93).

– (1996a). "Design and tone in the mechanoacoustic piano. Part I. Piano hammers and tonal effects." In: *The Journal of the Acoustical Society of America* 99.6, pp. 3286–3296. DOI: 10.1121/1.414947 (cit. on pp. 21, 23, 28).

– (1996b). "Design and tone in the mechanoacoustic piano. Part II. Piano structure." In: *The Journal of the Acoustical Society of America* 100.2, pp. 695–708. DOI: 10.1121/1.416233 (cit. on pp. 15, 16, 19, 33, 34, 37, 39, 79, 91).

– (1996c). "Design and tone in the mechanoacoustic piano. Part III. Piano strings and scale design." In: *The Journal of the Acoustical Society of America* 100.3, pp. 1286–1298. DOI: 10.1121/1.416017 (cit. on pp. 23, 32, 39).

Conlon, Stephen C., John B. Fahnline, and Fabio Semperlotti (2015). "Numerical analysis of the vibroacoustic properties of plates with embedded grids of acoustic black holes." In: *The Journal of the Acoustical Society of America* 137.1, pp. 447–457. DOI: 10.1121/1.4904501 (cit. on p. 191).

Corradi, Roberto, Paolo Fazioli, and S. Marforio (2010). "Modal analysis of a grand piano soundboard." In: *Proceedings of ISMA2010*, pp. 59–72 (cit. on pp. 3, 81).

Corradi, Roberto et al. (2017). "Modal analysis of a grand piano soundboard at successive manufacturing stages." In: *Applied Acoustics* 125, pp. 113–127. DOI: 10.1016/j.apacoust.2017.04.010 (cit. on p. 4).

Cremer, L., M. Heckl, and B.A.T. Petersson (2005). *Structure-Borne Sound*. Berlin, Heidelberg: Springer Berlin Heidelberg, pp. 1–607. DOI: 10.1007/b137728 (cit. on pp. 38, 68).

Cuenca, Jacques et al. (2012). "Improving the acoustic black hole effect for vibration damping in one-dimensional structures." In: *Proceedings of Acoustics 2012*, pp. 2189–2191 (cit. on p. 191).

Ege, Kerem (2009). "La table d'harmonie du piano-Études modales en basses et moyennes fréquences." PhD thesis (cit. on pp. 3, 34, 63).

Ege, Kerem and Xavier Boutillon (2010a). "Synthetic description of the piano soundboard mechanical mobility." In: *arXiv preprint arXiv:1210.5688* August, pp. 25–31 (cit. on pp. 38, 39).

– (2010b). "Vibrational and acoustical characteristics of the piano soundboard." In: *Proceedings of 20th International Congress on Acoustics*, pp. 1–7 (cit. on pp. 83, 86, 93).

Ege, Kerem, Xavier Boutillon, and Marc Rébillat (2013). "Vibroacoustics of the piano soundboard: (Non)linearity and modal properties in the low- and mid-frequency ranges." In: *Journal of Sound and Vibration* 332.5, pp. 1288–1305. DOI: 10.1016/j.jsv.2012.10.012. arXiv: arXiv:1212.2323v1 (cit. on p. 65).

Ellermeier, Wolfgang et al. (2008). *Kompendium zur Durchführung von Hörversuchen in Wissenschaft und industrieller Praxis*. Tech. rep. Berlin: Deutsche Gesellschaft für Akustik e.V., pp. 1–56 (cit. on p. 136).

Farina, Angelo (2000). "Simultaneous measurement of impulse response and distortion with a swept-sine technique." In: *Audio Engineering Society Convention 108*, pp. 1–24. DOI: 10.1109/ASPAA.1999.810884 (cit. on p. 63).

Farina, Angelo (2007). "Advancements in Impulse Response Measurements by Sine Sweeps." In: *Audio Engineering Society Convention* 122, pp. 4–9 (cit. on p. 63).

Fastl, Hugo and Eberhard Zwicker (2007). *Psychoacoustics: Facts and models*. Springer, pp. 1–463. DOI: 10.1007/978-3-540-68888-4 (cit. on p. 170).

Fletcher, Harvey, E. Donnell Blackham, and Richard Stratton (1962). "Quality of Piano Tones." In: *The Journal of the Acoustical Society of America* 34.6, pp. 749–761. DOI: 10.1121/1.1918192 (cit. on pp. 21, 24).

Fletcher, Neville H. and Thomas D. Rossing (1998). *The Physics of Musical Instruments*. New York, NY: Springer New York, p. 756. DOI: 10.1007/978-0-387-21603-4 (cit. on pp. 9, 13, 16, 20, 22, 53, 166).

Franke, Bettina and Pierre Quenneville (Mar. 2011). "Numerical Modeling of the Failure Behavior of Dowel Connections in Wood." In: *Journal of Engineering Mechanics* 137.3, pp. 186–195. DOI: 10.1061/(ASCE)EM.1943-7889.0000217 (cit. on p. 45).

Fukada, Eiichi (1950). "The Vibrational Properties of Wood I." In: *Journal of the Physical Society of Japan* 5.5, pp. 321–327. DOI: 10.1143/JPSJ.5.321 (cit. on p. 52).

Galembo, Alexander and Anders Askenfelt (2004). "Perceptual relevance of inharmonicity and spectral envelope in the piano bass range." In: *Acta Acustica united with Acustica*, pp. 528–536 (cit. on p. 23).

Galembo, Alexander et al. (2001). "Effects of relative phases on pitch and timbre in the piano bass range." In: *The Journal of the Acoustical Society of America* 110.3, pp. 1649–1666. DOI: 10.1121/1.1391246 (cit. on p. 136).

Ghaznavi, Mohammadreza et al. (2013). "Traditional Varnishes and Acoustical Properties of Wooden Soundboards." In: *Science International* 1.12, pp. 401–407. DOI: 10.17311/sciintl.2013.401.407 (cit. on p. 49).

Giordano, Nicholas (1997). "Simple model of a piano soundboard." In: *The Journal of the Acoustical Society of America* 102.2, pp. 1159–1168. DOI: 10.1121/1.419868 (cit. on pp. 3, 81).

– (1998). "Mechanical impedance of a piano soundboard." In: *The Journal of the Acoustical Society of America* 103.4, pp. 2128–2133. DOI: 10.1121/1.421358 (cit. on pp. 3, 38, 89).

Giordano, Nicholas, Harvey Gould, and Jan Tobochnik (1998). "The physics of vibrating strings." In: *Computers in Physics* 12.2, p. 138. DOI: 10.1063/1.168621 (cit. on p. 35).

Giordano, Nicholas and M. Jiang (2004). "Physical Modeling of the Piano." In: *EURASIP Journal on Advances in Signal Processing* 2004.7, pp. 926–933. DOI: 10.1155/S111086570440105X (cit. on pp. 15, 17).

Giordano, Nicholas and A. J. Korty (1996). "Motion of a piano string: Longitudinal vibrations and the role of the bridge." In: *The Journal of the Acoustical Society of America* 100.6, pp. 3899–3908. DOI: 10.1121/1.417219 (cit. on p. 28).

Giordano, Nicholas and J. P. Winans (2000). "Piano hammers and their force compression characteristics: Does a power law make sense?" In: *The Journal of the Acoustical Society of America* 107.4, pp. 2248–2255. DOI: 10.1121/1.428505 (cit. on p. 17).

Goebl, Werner, Roberto Bresin, and Alexander Galembo (2003). "The piano action as the performer's interface: Timing properties, dynamic behaviour, and the performer's possibilities." In: *Proceedings of the Stockholm Music Acoustics Conference, August 6–9, 2003 (SMAC 03)*. Vol. 2003. Smac 03, pp. 159–162 (cit. on p. 13).

– (2005). "Touch and temporal behavior of grand piano actions." In: *The Journal of the Acoustical Society of America* 118.2, pp. 1154–1165. DOI: 10.1121/1.1944648 (cit. on p. 14).

Good, Edwin M. (2001). *Giraffes, Black Dragons, and Other Pianos*. Stanford University Press (cit. on pp. 49, 103).

Günther, W. (1959). *U.S. Patent No. 2,911,874: Means for adjusting the touch of keys in pianos and like musical instruments* (cit. on p. 12).

Haines, Daniel W. (1980). "On musical instrument wood - part 2." In: *Catgut Acoustical Society Journal* 1.31, pp. 19–23 (cit. on pp. 46, 97).

Hall, Donald E. (1986). "Piano string excitation in the case of small hammer mass." In: *The Journal of the Acoustical Society of America* 79.1, pp. 141–147. DOI: 10.1121/1.393637 (cit. on pp. 15, 19).

– (1987). "Piano string excitation II: General solution for a hard narrow hammer." In: *The Journal of the Acoustical Society of America* 81.2, pp. 535–546. DOI: 10.1121/1.394919 (cit. on p. 18).

Hall, Donald E. and Anders Askenfelt (1988). "Piano string excitation V: Spectra for real hammers and strings." In: *The Journal of the Acoustical Society of America* 83.4, pp. 1627–1638. DOI: 10.1121/1.395917 (cit. on p. 167).

Hall, Donald E. and Peter Clark (1987). "Piano string excitation IV: The question of missing modes." In: *The Journal of the Acoustical Society of America* 82.6, pp. 1913–1918. DOI: 10.1121/1.395686 (cit. on pp. 19, 20).

Hansing, S. (1950). *Das Pianoforte in seinen akustischen Anlagen*. 2. Auflage. Herausgegeben von Freunden Siegfried Hansings (cit. on pp. 1, 51).

Hearmon, Roy F. S. (1948). "Elasticity of Wood and Plywood." In: *Nature* 162.4125, pp. 826–826. DOI: 10.1038/162826a0 (cit. on p. 46).

Helmholtz, Hermann von (1863). *Die Lehre von den Tonempfindungen als physiologische Grundlage für die Theorie der Musik*. Braunschweig: Vieweg (cit. on pp. 159, 161).

Holz, Dietrich (1974). "On some important properties of non-modified coniferous and leaved woods in view of mechanical and acoustical data in piano soundboards." In: *Archiwum Akustyki* 9.1, pp. 37–57 (cit. on pp. 50–52).

Houtsma, Adrian J. M. (1982). "Inharmonicity of wound guitar strings." In: *The Journal of the Acoustical Society of America* 71.S1, S9. DOI: 10.1121/1.2019676 (cit. on p. 124).

Hundley, T. Chase, Hugo Benioff, and Daniel W. Martin (Nov. 1978). "Factors contributing to the multiple rate of piano tone decay." In: *The Journal of the Acoustical Society of America* 64.5, pp. 1303–1309. DOI: 10.1121/1.382116 (cit. on p. 168).

Hunt, D. G. and E. Balsan (1996). "Why old fiddles sound sweeter." In: *Nature* 379.6567, pp. 681–681. DOI: 10.1038/379681a0 (cit. on pp. 5, 125).

Hutchins, Carleen Maley (1998). "A Measurable Effect of Long-term Playing on Violin Family Instruments." In: *Catgut Acoustical Society Journal* 3.5, pp. 38–40 (cit. on pp. 5, 125).

Hutchins, Carleen Maley, K. A. Stetson, and P. A. Taylor (1971). "Clarification of "Free Plate Tap Tones" by Hologram Interferometry." In: *J. Catgut Acoust. Soc.* 16.2, pp. 15–23 (cit. on p. 2).

Hutchins, Morton A. (1991). "Effects on spruce test strips of four-year application on four different sealers plus oil varnish." In: *Catgut Acoustical Society Journal* 1.7, pp. 11–16 (cit. on p. 49).

International Telecommunication Union (2003). *ITU-R Recommendation BS.1284-1 General methods for the subjective assessment of sound quality*. Tech. rep., pp. 1–13 (cit. on p. 136).

Jansson, Erik V. (2002). *Acoustics for violin and guitar makers* (cit. on p. 2).

Jiang, Minghui and Nicholas Giordano (1999). "Sound production by a vibrating piano soundboard: Theory." In: *The Journal of the Acoustical Society of America* 106.4, pp. 2141–2141. DOI: 10.1121/1.427322 (cit. on pp. 32, 40).

Junghanns, Herbert (1984). *Der Piano- und Flügelbau*. Verlag Erwin Bochinsky (cit. on p. 122).

Kao, Anne and Stephen R. Poteet, eds. (2007). *Natural Language Processing and Text Mining*. London: Springer London. DOI: 10.1007/978-1-84628-754-1 (cit. on p. 147).

Keane, Martin (2006). "An evaluation of piano sound and vibration leading to improvements through modification of the material properties of the structure." PhD thesis. The University of Auckland (cit. on p. 51).

Kirk, Roger E. (1959). "Tuning Preferences for Piano Unison Groups." In: *The Journal of the Acoustical Society of America* 31.12, pp. 1644–1648. DOI: 10.1121/1.1907673 (cit. on pp. 127, 159).

Kob, Malte (2017). "Experimental Approaches to the Study of Damping in Musical Instruments." In: *Studies in Musical Acoustics and Psychoacoustics*. Ed. by Albrecht Schneider. Springer International Publishing, pp. 187–200. DOI: 10.1007/978-3-319-47292-8_6 (cit. on p. 51).

Kraft, Sebastian and Udo Zölzer (2014). "BeaqleJS : HTML5 and JavaScript based Framework for the Subjective Evaluation of Audio Quality." In: *Linux Audio Conference (LAC-2014)* May (cit. on p. 138).

Krylov, V. V. and F. J. B. S. Tilman (July 2004). "Acoustic 'black holes' for flexural waves as effective vibration dampers." In: *Journal of Sound and Vibration* 274.3-5, pp. 605–619. DOI: 10.1016/j.jsv.2003.05.010 (cit. on p. 191).

Laroche, Jean (1993). "The use of the matrix pencil method for the spectrum analysis of musical signals." In: *The Journal of the Acoustical Society of America* 1.4, pp. 1958–1965 (cit. on pp. 3, 86).

Le Moyne, Sylvie et al. (2012). "Restoration of a 17th-century harpsichord to playable condition: A numerical and experimental study." In: *The Journal of the Acoustical Society of America* 131.1, p. 888. DOI: 10.1121/1.3651092 (cit. on p. 66).

Lieber, E. (1979). "The influence of the soundboard on piano sound." In: *Das Musikinstrument* 20 (cit. on pp. 51, 93).

Lieberman, Richard K. (1995). *Steinway & Sons*. New Haven & London: Yale University Press, pp. 1–374 (cit. on p. 1).

Lottermoser, W. and F. J. Meyer (1960). "Impulsmethode zur Messung von Geigenresonanzen." In: *Gravesaner Blätter* 5.19/20, pp. 106–119 (cit. on p. 51).

Lyon, Richard H. and Richard G. DeJong (1995). *Theory and Application of Statistical Energy Analysis*. Elsevier. DOI: 10.1016/C2009-0-26747-X (cit. on p. 190).

Mamou-Mani, Adrien, Joël Frelat, and Charles Besnainou (2008). "Numerical simulation of a piano soundboard under downbearing." In: *The Journal of the Acoustical Society of America* 123.4, pp. 2401–2406. DOI: 10.1121/1.2836787 (cit. on pp. 40, 91).

Mamou-Mani, Adrien et al. (2012). "Prestress effects on the eigenfrequencies of the soundboards: Experimental results on a simplified string instrument." In: *The Journal of the Acoustical Society of America* 131.1, pp. 872–877. DOI: 10.1121/1.3651232 (cit. on pp. 39, 125).

Martin, D. W. and W. D. Ward (1961). "Subjective Evaluation of Musical Scale Temperament in Pianos." In: *The Journal of the Acoustical Society of America* 33.5, pp. 582–585. DOI: 10.1121/1.1908730 (cit. on pp. 24, 27, 127, 163).

Matthias, Max (1990). *Steinway Service Manual: Leitfaden zur Pflege eines Steinway*. Fachbuchre. Frankfurt am Main: Verlag Erwin Bochinsky (cit. on p. xxxiii).

Mironov, M. A. (1988). "Propagation of a flexural wave in a plate whose thickness decreases smoothly to zero in a finite interval." In: *Sov. Phys. Acoust.* 34.3, pp. 318–319 (cit. on p. 191).

Moore, Brian C. J. and Brian R. Glasberg (1990). "Frequency discrimination of complex tones with overlapping and non overlapping harmonics." In: *The Journal of the Acoustical Society of America* 87.5, pp. 2163–2177. DOI: 10.1121/1.399184 (cit. on p. 165).

Moore, Thomas R. (2018). "Measurement Techniques." In: *Springer Handbook of Systematic Musicology*. Ed. by Rolf Bader. Springer H. Springer. Chap. 5, pp. 81–103. DOI: 10.1007/978-3-662-55004-5 (cit. on p. 68).

Moore, Thomas R. and Sarah A. Zietlow (2006). "Interferometric studies of a piano soundboard." In: *The Journal of the Acoustical Society of America* 119.3, pp. 1783–1793. DOI: 10.1121/1.2164989 (cit. on pp. 32, 35, 38).

Morse, P. M. and K. U. Ingard (1986). *Theoretical Acoustics*. Internatio. Princeton University Press (cit. on p. 20).

Nakamura, Isao (1983). "The vibrational character of the piano soundboard." In: *Proceedings of the 11th ICA*, pp. 385–388 (cit. on pp. 3, 32, 38).

Norman, Eddie (2003). "Innovation in design and technology : the polymer acoustic guitar and the case for the relegation of ' the design process '." In: *DATA International Research Conference*, pp. 91–97 (cit. on p. 2).

Norton, M. P. and D. G. Karczub (2003). *Fundamentals of Noise and Vibration Analysis for Engineers*. Cambridge University Press, pp. 147–155. DOI: 10.3397/1.2721371 (cit. on p. 38).

Öberg, Fredrik and Anders Askenfelt (2012). "Acoustical and perceptual influence of duplex stringing in grand pianos." In: *The Journal of the Acoustical*

Society of America 131.1, pp. 856–871. DOI: 10.1121/1.3664049 (cit. on p. 136).

Ono, Teruaki (1981). "Relationship of the Selection of Wood Used for Piano Soundboards to the Dynamic Mechanical Properties." In: *Journal of the Society of Materials Science, Japan* 30.334, pp. 719–724 (cit. on p. 46).

– (1993). "Effects of varnishing on acoustical characteristics of wood used for musical instrument soundboards." In: *Journal of the Acoustical Society of Japan (E)* 14, pp. 397–407. DOI: 10.1250/ast.14.397 (cit. on p. 49).

Oxenham, A. J. (2012). "Pitch Perception." In: *Journal of Neuroscience* 32.39. DOI: 10.1523/JNEUROSCI.3815-12.2012 (cit. on p. 165).

Peeters, G. (2004). *A large set of audio features for sound description (similarity and classification) in the CUIDADO project*. Tech. rep. 0. IRCAM, pp. 1–25 (cit. on p. 166).

Petersen, Sonja (2011). *Vom "Schwachstarktastenkasten" und seinen Fabrikanten - Wissensräume im Klavierbau 1830 bis 1930*. Waxmann Verlag (cit. on pp. 1, 151).

Pfeifle, Florian (2013). "Acoustical measurements and finite difference simulation of the West-African "talking drum"." In: *The Journal of the Acoustical Society of America* 134.5, pp. 4158–4158. DOI: 10.1121/1.4831238 (cit. on p. 57).

Pierce, Allan D. (2010). "Intrinsic damping, relaxation processes, and internal friction in vibrating systems." In: *Proceedings of Meetings on Acoustics*. Vol. 9. May, pp. 065001–065001. DOI: 10.1121/1.3449319 (cit. on p. 50).

Plath, Niko and Katharina Preller (2018). "Early Development Process of the Steinway & Sons Grand Piano Duplex Scale." In: *Wooden Musical Instruments - Different Forms of Knowledge. Book of End of WoodMusICK COST Action FP1302*. Cité de la Musique - Philharmonie de Paris (cit. on p. 1).

Plomp, R. and W. J. M. Levelt (1965). "Tonal Consonance and Critical Bandwidth." In: *The Journal of the Acoustical Society of America* 38.4, pp. 548–560. DOI: 10.1121/1.1909741 (cit. on p. 161).

Poletti, P. (2000). "Steinway and the invention of the overstrung grand piano frame." In: *Matière et musique: The Cluny Encounter, Proc. European En-*

counter on Instrument Making and Restoration. Labo19, pp. 241–263 (cit. on p. 192).

Railsback, O. L. (Jan. 1938). "Scale Temperament as Applied to Piano Tuning." In: *The Journal of the Acoustical Society of America* 9.3, pp. 274–274. DOI: 10.1121/1.1902056 (cit. on pp. 24, 126).

Reblitz, Arthur A. (1993). *Piano Servicing, Tuning, and Rebuilding*. Vestal Press Inc. (cit. on p. 122).

Richardson, M. H. (1997). "Is it a mode shape, or an operating deflection shape?" In: *Sound and Vibration* 30th Anniversary Issue, pp. 1–8 (cit. on p. 83).

Rocaboy, F. and Voichita Bucur (1990). "About the physical properties of wood of twentieth century violins." In: *Catgut Acoustical Society Journal* 1.6 (cit. on p. 46).

Rosenbaum, Paul R. (2010). *Design of Observational Studies*. Vol. 27. Springer Series in Statistics 2. New York, NY: Springer New York, pp. 83–85. DOI: 10.1007/978-1-4419-1213-8 (cit. on p. 128).

Rossing, Thomas D., ed. (2010). *The Science of String Instruments*. New York, NY: Springer New York. DOI: 10.1007/978-1-4419-7110-4 (cit. on pp. 9, 20, 40).

Roy, Richard and Thomas Kailath (1989). "ESPRIT - Estimation of Signal Parameters via Rotational Invariance Techniques." In: *IEEE Transactions on Acoustics, Speech, and Signal Processing* 37.7, pp. 984–995. DOI: 10.1109/29.32276 (cit. on pp. 3, 86).

Schelleng, John C. (1968). "Acoustical Effects of Violin Varnish." In: *The Journal of the Acoustical Society of America* 44.5, pp. 1175–1183. DOI: 10.1121/1.1911243 (cit. on p. 49).

Schleske, Martin (1990). "Speed of sound and damping of spruce in relation to the direction of grains and rays." In: *Catgut Acoustical Society Journal* 1.6, pp. 16–20 (cit. on p. 45).

– (1996). "Eigenmodes of Vibration in the Working Process of a Violin." In: *J. Catgut Acoust. Soc.* 3.1 (cit. on p. 2).

Schleske, Martin (1998). "On the acoustical properties of violin varnish." In: *Catgut Acoustical Society Journal* 3.6, pp. 27–43 (cit. on p. 49).

– (2002). "Empirical Tools in Contemporary Violin Making: Part II. Psychoacoustic Analysis and Use of Acoustical Tools." In: *Catgut Acoustical Society Journal* 4.6, pp. 43–61 (cit. on p. 2).

Schneider, Albrecht, Arne von Ruschkowski, and Rolf Bader (2009). "Klangliche Rauhigkeit, ihre Wahrnehmung und Messung [Timbre roughness, its perception and measurement]." In: *Musical Acoustics, Neurocognition and Psychology of Music*. Ed. by Rolf Bader. Hamburger. Frankfurt am Main: Peter Lang, pp. 101–144 (cit. on pp. 160, 161).

Schroeder, M. R. (1965). "New Method of Measuring Reverberation Time." In: *Journal of the Acoustical Society of America* 37.3, p. 409. DOI: 10.1121/1.1909343 (cit. on pp. 102, 168).

Schuck, O. H. and R. W. Young (1943). "Observations on the Vibrations of Piano Strings." In: *The Journal of the Acoustical Society of America* 15.1, pp. 1–11. DOI: 10.1121/1.1916221 (cit. on pp. 21, 24–26).

Segerman, E. (2001). "Some aspects of wood structure and function." In: *Catgut Acoustical Society Journal* 4.3, pp. 5–9 (cit. on p. 125).

Sethares, William A. (1993). "Local consonance and the relationship between timbre and scale." In: *The Journal of the Acoustical Society of America* 94.3, pp. 1218–1228. DOI: 10.1121/1.408175 (cit. on p. 161).

Skudrzyk, Eugen (1980). "The mean value method of predicting the dynamic response of complex vibrators." In: *The Journal of the Acoustical Society of America* 67.4, pp. 1105–1135. DOI: 10.1121/1.384169 (cit. on p. 84).

Steinway, H. Jr. (1859). *U.S. Patent No. 26,300: Stringing Pianos* (cit. on p. 192).

Stulov, Anatoli (1995). "A simple grand piano hammer felt model." In: *Proc. Estonian Acad. Sci. Engin*, pp. 172–182 (cit. on p. 18).

– (2003). "Experimental and theoretical studies of piano hammer." In: *Proceedings of the Stockholm Music Acoustics …* 2003.Smac 03, pp. 6–9 (cit. on pp. 15, 18).

Suzuki, Hideo (1986). "Vibration and sound radiation of a piano soundboard." In: *The Journal of the Acoustical Society of America* 80.6, pp. 1573–1582. DOI: 10.1121/1.394321 (cit. on pp. 3, 40, 81, 89).

Suzuki, Hideo and Isao Nakamura (1990). "Acoustics of pianos." In: *Applied Acoustics* 30.2-3, pp. 147–205. DOI: 10.1016/0003-682X(90)90043-T (cit. on p. 9).

Tervaniemi, Mari et al. (2005). "Pitch discrimination accuracy in musicians vs nonmusicians: an event-related potential and behavioral study." In: *Experimental Brain Research* 161.1, pp. 1–10. DOI: 10.1007/s00221-004-2044-5 (cit. on p. 163).

Ventsel, Eduard and Theodor Krauthammer (2001). *Thin Plates and Shells*. Boca Raton: CRC Press. DOI: 10.1201/9780203908723. arXiv: 1401.5045 (cit. on p. 109).

Waltham, Chris and Shigeru Yoshikawa (2018). "Construction of Wooden Musical Instruments." In: *Springer Handbook of Systematic Musicology*. Ed. by Rolf Bader. Springer H. Springer, Berlin, Heidelberg, pp. 63–79. DOI: 10.1007/978-3-662-55004-5_4 (cit. on p. 46).

Waltham, Christopher et al. (2013). "Acoustic imaging of string instrument soundboxes." In: 19, pp. 035004–035004. DOI: 10.1121/1.4799438 (cit. on p. 66).

Wegst, Ulrike G. K. (2006). "Wood for sound." In: *American Journal of Botany* 93.10, pp. 1439–1448 (cit. on p. 46).

Weinreich, Gabriel (1977). "Coupled piano strings." In: *The Journal of the Acoustical Society of America* 62.6, p. 1474. DOI: 10.1121/1.381677 (cit. on p. 168).

Weldert, Gregor (2017). "Sound Enhancement of Musical Instruments by 'Playing them in': Fact or Fiction?" In: *Europiano* 3, pp. 41–43 (cit. on pp. 5, 121).

Williams, Earl G. (1999). *Fourier Acoustics - Sound Radiation and Nearfield Acoustical Holography*. London: Academic Press Inc. (cit. on p. 68).

Wogram, Klaus (1979). *Akustische Untersuchungen an Klavieren*. Tech. rep. Braunschweig: Phys.-Techn. Bundesanstalt, pp. 1–45 (cit. on pp. 3, 32, 35, 38, 40, 89).

– (1984). "Akustische Untersuchungen an Klavieren - Teil 1:Schwingungseigenschaften des Resonanzbodens." In: *Der Piano- und Flügelbau*, pp. 380–404 (cit. on p. 93).

Young, Robert W. (1952). "Inharmonicity of Plain Wire Piano Strings." In: *The Journal of the Acoustical Society of America* 24.3, pp. 267–273. DOI: 10.1121/1.1906888 (cit. on pp. 24, 163).

– (Jan. 1954). "Inharmonicity of Piano Bass Strings." In: *The Journal of the Acoustical Society of America* 26.1, pp. 144–144. DOI: 10.1121/1.1917803 (cit. on p. 23).

Ziemer, Tim (2014). "Sound Radiation Characteristic of a Shakuhachi with different Playing Techniques." In: *Proceedings of ISMA 2014*, pp. 549–555 (cit. on p. 58).

Zwick, William R. and Wayne F. Velicer (1986). "Comparison of five rules for determining the number of components to retain." In: *Psychological Bulletin* 99.3, pp. 432–442. DOI: 10.1037/0033-2909.99.3.432 (cit. on p. 177).

List of Publications Resulting from the Dissertation

2019

- Plath, Niko, “Influence of Playing on the Tonal Characteristics of a Concert Grand Piano - an Observational Study”, Proceedings of the 2019 International Symposium on Musical Acoustics (ISMA), 18–22 September, Detmold, Germany (2019)
- Plath, Niko, ”Influence of Playing on the Tonal Characteristics of a Concert Piano - Dataset (Version 1.0.1)” [Data set], Zenodo, `http://doi.org/10.5281/zenodo.3274772`

2017

- Plath, Niko and Pfeifle, Florian and Koehn, Christian and Bader, Rolf, “Radiation Characteristics of Grand Piano Soundboards in Different Stages of Production”, Proceedings of the 2017 International Symposium on Musical Acoustics (ISMA), 18–22 June, Montreal, Canada (2017)

2016

- Plath, Niko and Pfeifle, Florian and Koehn, Christian and Bader, Rolf (2016), “Vibrational Behaviour of Concert Grand Piano Soundboards in Different Stages of Production”, 5th Joint meeting of the Acoustical Society of America and the Acoustical Society of Japan - Honolulu, Hawaii (2016)

- Plath, Niko and Pfeifle, Florian and Koehn, Christian and Bader, Rolf, "Microphone Array Measurements of the Grand Piano", Musikalische Akustik zwischen Empirie und Theorie, Fachausschuss Musikalische Akustik in der DEGA, Hamburg, Germany (2016), 9:10
- Plath, Niko and Pfeifle, Florian and Koehn, Christian and Bader, Rolf, "Driving Point Mobilities of a Concert Grand Piano Soundboard in Different Stages of Production", Proceedings of the 3rd Annual COST FP1302 WoodMusICK Conference, Barcelona, Spain (2016), 117-123

2015

- Plath, Niko and Pfeifle, Florian and Koehn, Christian and Bader, Rolf, "Microphone Array Measurements of the Grand Piano", Proceedings of the Third Vienna Talk on Music Acoustics, Vienna, Austria (2015), p.161